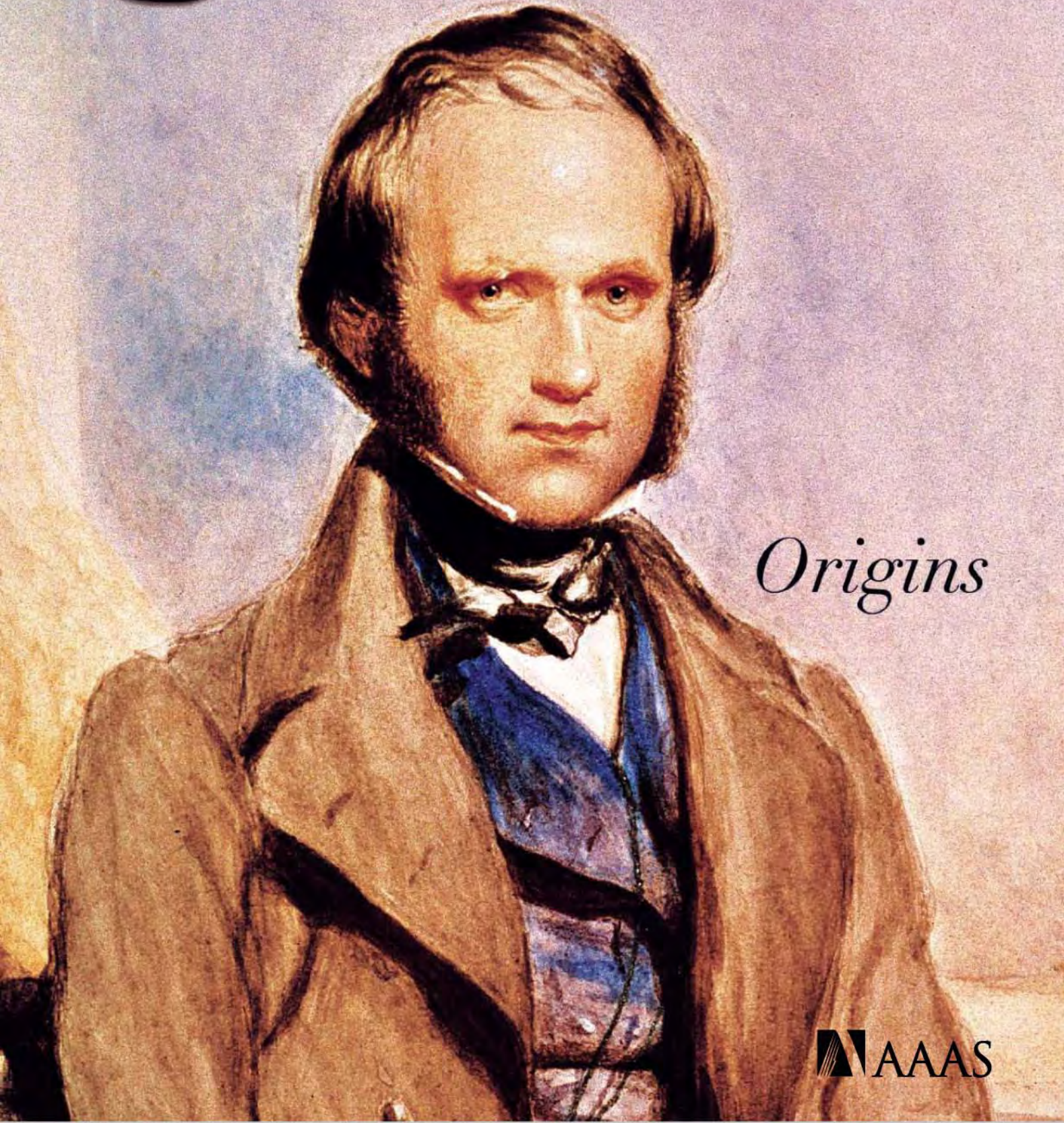


9 January 2009 | \$10

Science



Origins

 AAAS



Revolutionize life

From red hair to red blood cells.

Whether it's hair color or disease susceptibility, our unique genetic makeup plays a powerful role in determining who we are and shaping our lives. Our mission is to revolutionize how the world benefits from genetic information, which will enable people to make more informed decisions about their health.

Affymetrix GeneChip® technology has been pivotal in many landmark studies, including those named "Breakthrough of the Year" by *Science* magazine. Our technology offers the most complete view of the whole genome—to accelerate the development of diagnostics, help tailor treatments and ultimately cure the world's most critical diseases. Affymetrix is committed to developing innovative products that broaden our view of the human genome.

We are passionate about creating a world where everyone benefits from understanding their own DNA.

To learn more, visit www.affymetrix.com



Redefining the cell-based assay!

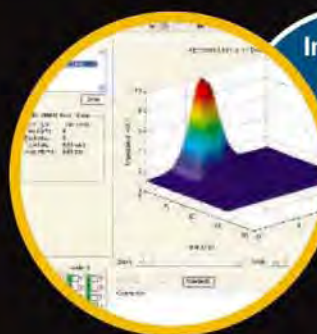
25 years of experience with impedance-based cell assays put into one instrument line!

Measurements are rapid, accurate and highly reproducible. ECIS monitors cell behavior in tissue culture quantitatively and in real time. The ECIS Z & Z θ are the new standard in life sciences for impedance-based quantification of cell behavior in vitro.

To learn more or to demo ECIS visit www.biophysics.com or call 1.866.301.ECIS (3247).



Quantifying Cell Behavior



Intuitive, versatile software runs on Mac or PC.



FREE
with registration

Science Alerts in Your Inbox

Get daily and weekly E-alerts on the latest news and research! Sign up for our e-alert services and you can know when the latest issue of *Science* or *Science Express* has been posted, peruse the latest table of contents for *Science* or *Science Signaling*, and read summaries of the journal's research, news content, or Editors' Choice column, all from your e-mail inbox. To start receiving e-mail updates, go to:

sciencemag.org/ema

Science Posting Notification
Alert when weekly issue is posted

ScienceNOW Weekly Alert
Weekly headline summary

Science News This Week
Brief summaries of the journal's news content

ScienceNOW Daily Alert
Daily headline summary

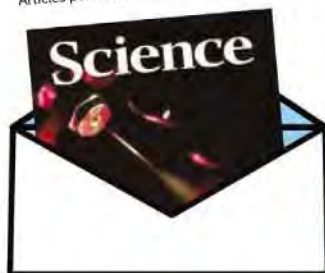
Science Magazine TOC
Weekly table of contents

Science Express Notification
Articles published in advance of print

Science Signaling TOC
Weekly table of contents

Editors' Choice
Highlights of the recent literature

This Week in Science
Summaries of research content



Genomics of Energy & Environment is the topic of the 2009 Department of Energy Joint Genome Institute (DOE JGI) User Meeting, which will be held March 25-27 in Walnut Creek, California. This year's meeting will specifically emphasize the **genomics of renewable energy strategies, biomass conversion to biofuels, environmental gene discovery, and engineering of fuel-producing organisms**. The meeting will feature presentations by leading scientists advancing these topics. The meeting will also include informatics workshops and tutorials for the analysis of prokaryotic and eukaryotic genomes, and the evaluation of new sequencing platforms and their applications. Poster submissions are encouraged. Pre-registration is required as interest is expected to exceed meeting capacity again this year. Registration and a preliminary agenda can be found at: www.jgi.doe.gov.

Biacore systems

from inspiration
...to publication

Highest quality, information-rich interaction data from Biacore™ systems deepen your understanding of molecular mechanisms and interaction pathways and enable you to add function to structure.

Select the perfect solution for your application and draw conclusions with confidence – from the company that continues to set the standard for label-free protein interaction analysis.



Biacore T100
unmatched performance



Biacore X100
ready to run research system



Biacore Flexchip
array-based comparative profiling

www.biacore.com



imagination at work



EDITORIAL

- 185 A Celebration and a Challenge
Andrew Sugden et al.
>> *Origins Essay* p. 198

NEWS OF THE WEEK

- 192 Scientists Laud Bush's Blue Legacy
But Want More
- 193 Higher Temperatures Seen Reducing
Global Harvests
>> *Report* p. 240
- 194 A New Spy Agency Asks Academics
for Help in Meeting Its Mission
- 195 Brain Scans of Pain Raise Questions
for the Law
- 196 TB Bacteria May Reign Over Cells Intended
to Bridle Them
- 197 Indian Neutrino Detector Hits Snag on
Environmental Concerns

NEWS FOCUS

- 198 EVOLUTIONARY ROOTS
On the Origin of Life on Earth
>> *Editorial* p. 185, *Review* p. 223
- 200 Seeking Africa's First Iron Men
- 203 A New View on—and Hope for—an Old
Disease
A Discriminating Killer

LETTERS

- 206 Unsung Hero Robert C. Gallo
G. Abbadessa et al.
An Award for Science Is an Obsolete Notion
M. Gozum
The Time to Demand Funding
C. C. Mello and J. V. Walsh
Autistic Phenotype from *MEF2C*
Knockout Cells
S. A. Lipton et al.
Science Should Stick to Science
A. M. Thro
Science Careers: Where Does Advocacy Fit?
J. Yang

Unintended Consequences at NIH
T. E. Decoursey

209 CORRECTIONS AND CLARIFICATIONS

BOOKS ET AL.

- 210 Science for Lawyers
E. Y. Drogin, Ed., reviewed by D. Greenbaum
and M. Gerstein

POLICY FORUM

- 211 Trade Liberalization and Economic
Development
J. K. Sundaram and R. von Arnim

PERSPECTIVES

- 213 When Infinity Does Not Count
V. V. Cheianov
>> *Report* p. 228
- 214 Unjamming a Polymer Glass
D. A. Weitz
>> *Report* p. 231
- 215 Surprising Emotions
E. R. Smith and D. M. Mackie
>> *Report* p. 276
- 216 Extending Polymer Conjugation into the
Second Dimension
D. F. Perepichka and F. Rosei
- 218 The Descent of Minerals
C. Vasconcelos and J. A. McKenzie
- 219 Old New Nitrogen
J. P. Montoya
>> *Report* p. 244
- 220 Pluripotent Chromatin State
A. S. Chi and B. E. Bernstein
- 221 Histone Cross-Talk in Stem Cells
E. Smith and A. Shilatifard
>> *Report* p. 248

REVIEW

- 223 Darwin's Originality
P. J. Bowler
>> *Origins Essay* p. 198

CONTENTS continued >>



page 198



page 211



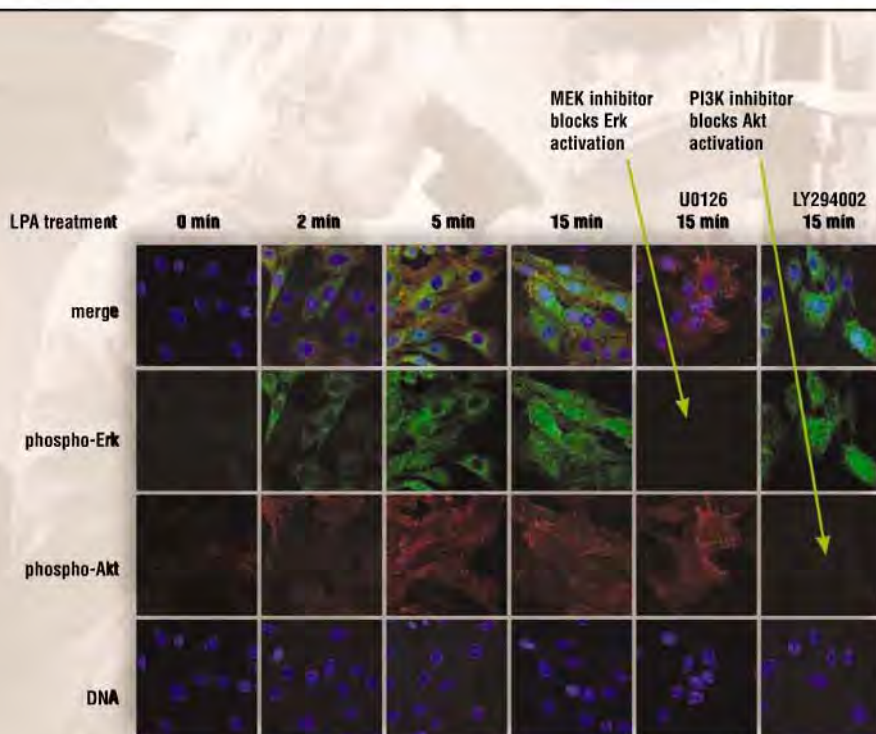
COVER

Charles Darwin, a few years after his *Beagle* voyage. *Science's* celebration of his 200th birthday and the 150th anniversary of the publication of *On the Origin of Species* begins with a Review by Bowler (p. 223) and an Essay on the origins of life (p. 198), the start of a monthly series exploring evolution. See also the Editorial (p. 185) for additional features and upcoming content.

Image: Chalk and watercolor portrait by George Richmond/
Bridgeman Art Library, London (SuperStock)

DEPARTMENTS

- 183 This Week in *Science*
186 Editors' Choice
188 *Science* Staff
189 Random Samples
191 Newsmakers
279 New Products
280 *Science* Careers



Treatment of C6 (rat glioma) cells with kinase-specific inhibitors to verify specificity using Phospho-p44/42 MAPK (Thr202/Tyr204) (E10) Mouse mAb #9106 (green) and Phospho-Akt (Ser473) (193H12) Rabbit mAb #4058 (red).

Side by side lot comparison using > Phospho-Akt (Ser473) Antibody #9271.

1: C2C12 cells +insulin (100 nM for 10 min.)
2: C2C12 cells, untreated



1	2	1	2	1	2	1	2	Lot
Lot 7	8/1/2002	Lot 8	7/23/2003	Lot 9	2/12/2004	Lot 10	4/7/2006	Lot
								release date

Antibody Validation

at Cell Signaling Technology®

Unparalleled product quality, validation and technical support.

Scientists at Cell Signaling Technology (CST) follow a stringent *validation protocol*, using a combination of several approaches and applications, to provide you with the highest quality antibodies. This ensures credible and reproducible results with the least expenditure of your costly time, samples and reagents.

- ✓ **Testing in a number of applications** – to help you choose the antibody that works in your application
- ✓ **Verifying specificity and reproducibility** – to make sure the antibody works each and every time in all applications specified
- ✓ **Identifying optimal conditions** – to save your precious time, samples and reagents

To learn more about what validation means at Cell Signaling Technology visit www.cellsignal.com

for quality products you can trust...

www.cellsignal.com



Cell Signaling

TECHNOLOGY®

BREVIA

227 Bat White-Nose Syndrome: An Emerging Fungal Pathogen?

D. S. Blehert et al.

Bats that died en masse in New York state while they were hibernating were infected with a cold-tolerant fungus.

REPORTS

228 Universal Theory of Nonlinear Luttinger Liquids

A. Imambekov and L. J. Glazman

A theory of one-dimensional quantum liquids is generalized from linear interactions among particles to nonlinear ones, affecting, for example, predicted tunneling dynamics.

>> Perspective p. 213

231 Direct Measurement of Molecular Mobility in Actively Deformed Polymer Glasses

H.-N. Lee et al.

Optical bleaching of a dilute molecular probe shows that when a rubbery polymer begins to flow, polymer chains become more mobile than predicted from a classical model.

>> Perspective p. 214

234 Suppression of Metallic Conductivity of Single-Walled Carbon Nanotubes by Cycloaddition Reactions

M. Kanungo et al.

Reacting carbon nanotubes with fluorinated olefins suppresses the conductivity of the metallic tubes without affecting semiconducting tubes.

237 Self-Organization of a Mesoscale Bristle into Ordered, Hierarchical Helical Assemblies

B. Pokroy et al.

Evaporating an organic liquid from the tips of polymer pillars can induce them to form helical structures.

240 Historical Warnings of Future Food Insecurity with Unprecedented Seasonal Heat

D. S. Battisti and R. L. Naylor

By analogy with past examples, higher growing season temperatures and extreme heat will cause major disruptions to global agriculture. >> News story p. 193

244 Foraminiferal Isotope Evidence of Reduced Nitrogen Fixation in the Ice Age Atlantic Ocean

H. Ren et al.

Nitrogen fixation in the tropical Atlantic increased during deglaciation and, along with increased denitrification, helped to stabilize the ocean nitrogen reservoir.

>> Perspective p. 219

248 *Drosophila* Stem Cells Share a Common Requirement for the Histone H2B Ubiquitin Protease Scrawny

M. Buszczak et al.

Stem cells in the germ line, epithelium, and intestine all require a particular modification of histone H2B to repress key differentiation genes and maintain pluripotency.

>> Perspective p. 221

251 The Aryl Hydrocarbon Nuclear Translocator Alters CD30-Mediated NF- κ B-Dependent Transcription

C. W. Wright and C. S. Duckett

Signals from a cancer-associated receptor that activate a key pathway in the immune system are modulated by its binding to a stress-responsive transcription factor.

256 HDAC4 Regulates Neuronal Survival in Normal and Diseased Retinas

B. Chen and C. L. Cepko

An enzyme that deacetylates histones in the nucleus also functions in the cytoplasm to promote the survival of retinal neurons in mice.

259 Genetic Code Supports Targeted Insertion of Two Amino Acids by One Codon

A. A. Turanov et al.

One codon can code for two different amino acids within the same gene, with the choice determined by an RNA structure in an untranslated region.

262 *tasselseed1* Is a Lipoyxygenase Affecting Jasmonic Acid Signaling in Sex Determination of Maize

I. F. Acosta et al.

A gene that controls male floral development in maize is involved in synthesis of a hormone that suppresses female organ development.

266 Structure of a Type IV Secretion System Core Complex

R. Fronzes et al.

The structure of a bacterial secretion complex suggests how Gram-negative bacteria might regulate the transfer of certain virulence factors.

269 AMPylation of Rho GTPases by *Vibrio* VopS Disrupts Effector Binding and Downstream Signaling

M. L. Yarbrough et al.

A G1-active pathogen destroys intestinal cells, in part by improperly modifying a host signaling protein, causing loss of cell shape and contributing to cell death.

272 Simpson's Paradox in a Synthetic Microbial System

J. S. Chuang et al.

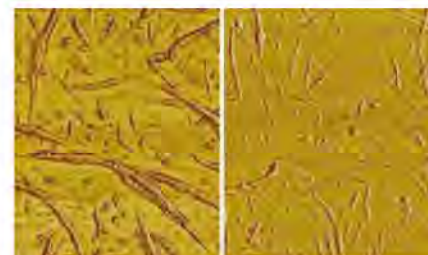
Stochastic fluctuations in the population structure of microorganisms can allow a disadvantaged subpopulation to be maintained.

276 Mispredicting Affective and Behavioral Responses to Racism

K. Kawakami et al.

People predict that they will feel worse after witnessing a racist comment than they actually do. >> Perspective p. 215

CONTENTS continued >>



page 234



page 227



SCIENCECAREERS
Making archaeology pay.



SCIENCE SIGNALING
Signaling advances in all kingdoms.

ScienceInsider

blogs.sciencemag.org/scienceinsider
Breaking news and analysis from the world of science policy.

SCIENCE (ISSN 0036-8075) is published weekly on Friday, except the last week in December, by the American Association for the Advancement of Science, 1200 New York Avenue, NW, Washington, DC 20005. Periodicals Mail postage (publication No. 484460) paid at Washington, DC, and additional mailing offices. Copyright © 2009 by the American Association for the Advancement of Science. The title **SCIENCE** is a registered trademark of the AAAS. Domestic individual membership and subscription (51 issues): \$146 (\$74 allocated to subscription). Domestic institutional subscription (51 issues): \$835; Foreign postage extra: Mexico, Caribbean (surface mail) \$55; other countries (air assist delivery) \$85. First class, airmail, student, and emeritus rates on request. Canadian rates with GST available upon request, GST #1254 88122. Publications Mail Agreement Number 1069624. **Printed in the U.S.A.**

Change of address: Allow 4 weeks, giving old and new addresses and 8-digit account number. **Postmaster:** Send change of address to AAAS, P.O. Box 96178, Washington, DC 20090-6178. **Single-copy sales:** \$10.00 current issue, \$15.00 back issue prepaid includes surface postage; bulk rates on request. **Authorization to photocopy** material for internal or personal use under circumstances not falling within the fair use provisions of the Copyright Act is granted by AAAS to libraries and other users registered with the Copyright Clearance Center (CCC) Transactional Reporting Service, provided that \$20.00 per article is paid directly to CCC, 222 Rosewood Drive, Danvers, MA 01923. The identification code for *Science* is 0036-8075. *Science* is indexed in the *Reader's Guide to Periodical Literature* and in several specialized indexes.



ADVANCING SCIENCE. SERVING SOCIETY

SCIENCEEXPRESS

www.sciencexpress.org

HIN-200 Proteins Regulate Caspase Activation in Response to Foreign Cytoplasmic DNA

T. L. Roberts et al.

A family of proteins is identified that binds to foreign cytoplasmic DNA in mammalian cells and regulates the immune response.

10.1126/science.1169841

Self-Sustained Replication of an RNA Enzyme

T. A. Lincoln and G. F. Joyce

Two ribozymes synthesize each other from oligonucleotide substrates to give a self-replicating system.

10.1126/science.1167856

Function of Mitochondrial Stat3 in Cellular Respiration

J. Wegrzyn et al.

A protein that has a nuclear function as a transcription factor also functions to support respiration in the mitochondria.

10.1126/science.1164551

Harmonic Convergence in the Love Songs of the Dengue Vector Mosquito

L. J. Cator et al.

Male and female mosquitos change their wing beat frequencies to match each other as a prelude to mating.

10.1126/science.1166541

SCIENCE NOW

www.sciencenow.org

Highlights From Our Daily News Coverage

How Twisters Get Their Spin

Simulations show tornadoes must have large water droplets to form.

Tougher Than a Black Hole

Dense clouds resist cosmic monster's violent pull.

Death of a Star Scientist Inflicts Long-Term Damage on Field

Collaborators experience dramatic drop in output that can last decades.

SCIENCE SIGNALING

www.sciencesignaling.org

The Signal Transduction Knowledge Environment

EDITORIAL GUIDE: 2008 Signaling Breakthroughs of the Year

E. M. Adler

The signaling breakthroughs of 2008 extended from protein crystals to cells and subcellular structures to whole genomes.

PERSPECTIVE: MicroRNAs—Opening a New Vein in Angiogenesis Research

J. E. Fish and D. Srivastava

MicroRNAs regulate angiogenic signaling in endothelial cells.

PERSPECTIVE: Computational Implications of Cooperative Plasticity Induction at Nearby Dendritic Sites

K. Morita

Cooperative interactions at nearby synapses may endow individual neurons with computational functions.

JOURNAL CLUB: *Drosophila* Toll Pathway—The New Model

Y. Ashok

New data has led to reevaluation of the proteolytic cascades that activate Toll in flies.

SCIENCECAREERS

www.sciencemag.org/career_development

Free Career Resources For Scientists

Opportunities: Career Advantages of Collaboration

P. Fiske

While the value of collaboration is widely acknowledged, the career advantages are rarely discussed.

Bilateral Training Opportunities in the United States and Portugal

S. Coelho

New programs between U.S. and Portuguese universities offer scientists unique training opportunities.

Archaeology for Fun and Profit

S. Coelho

Private companies provide career opportunities for archaeologists.

Science Careers Best of 2008

Science Careers Staff

Our editors choose the best career articles of the past year.

SCIENCEPODCAST

www.sciencemag.org/multimedia/podcast

Free Weekly Show

Download the 9 January *Science* Podcast to hear about responses to racism, love songs of the dengue vector mosquito, and a new series about evolution.

ORIGINSBLOG

blogs.sciencemag.org/origins

A History Of Beginnings

QUARTERLY AUTHOR INDEX

www.sciencemag.org/feature/data/aindex.dtl



Turn of the Screw >>

To make chiral superstructures, one usually needs to start with either chiral starting materials or a driving force, like stirring in one direction, that promotes a specific handedness to the helicity. **Pokroy et al.** (p. 237) show an exception to this with the agglomeration of soft polymeric pillars. The pillars are covered with droplets of an organic liquid, and, as the liquid evaporates, surface tension draws the pillars together. The process can be controlled to bias the helicity over large areas, and the drying process can be used to capture particles within a web of pillars.

Nonlinear Quantum Fluids

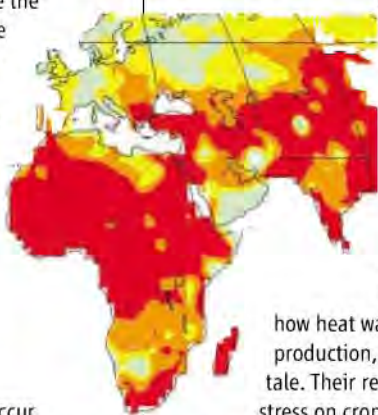
The quantum-level description of many-body electronic effects has generally been simplified to include only a linear degree of interaction between the particles. Recent measurements, however, reveal that this linearization is an oversimplification and fails to describe the complex interparticle effects that may arise at low temperatures. **Imambekov and Glazman** (p. 228, published online 27 November; see the Perspective by **Cheianov**) introduce a nonlinear theoretical description of correlation effects in a one-dimensional quantum system. The nonlinear description may represent a universal description of many-body phenomena in condensed-matter quantum systems.

for developing more general theoretical treatments of plastic flow.

What We Will Reap

Global warming is making growing seasons longer, but higher growing season temperatures, and the episodes of extreme heat that are expected to accompany them, could cause serious damage

to agriculture worldwide. **Battisti and Naylor** (p. 240; see the news story by **Holden**) use the outputs of 23 climate models to predict how temperatures will change by the end of the 21st century, and historical examples of



how heat waves have affected crop production, to weave a cautionary tale. Their results suggest that heat stress on crops could cause profound negative impacts on global agriculture and food security in the absence of adequate adaptation.

Evolution of Darwin's Thinking

The principal sources of Darwin's originality in the formulation of his theory of evolution by natural selection are reviewed by **Bowler** (p. 223), who focuses on Darwin's recognition that the evolution of life must be represented as an irregularly branching tree. The author contrasts this idea with other models available at the time and identifies the source of Darwin's idea in his work on bio-

geography. The role of artificial selection in Darwin's thinking and his appeal to the metaphor of the "struggle for existence" are also analyzed.

Chromatin and Stemness

Ubiquitination of one of the histones, H2B, has consequences for modifications such as methylation of other histones. These interactions cascade down to control the general activity of the genes bound up with these histones. **Buszczak et al.** (p. 248, published online 27 November; see the Perspective by **Smith and Shilatifard**) now show that in *Drosophila* a ubiquitin protease, *scrawny*, helps keep genes silent. *Scrawny*'s functions seem particularly important for stem cells in the germline, in epithelia, and in the intestine. In various types of stem cells, the balance between stem and differentiated fates might be tipped by a common chromatin modification route.

Retinal Protection

Mechanisms controlling apoptosis or cell death in photoreceptor cells are of importance because loss of these cells can result in blindness. **Chen and Cepko** (p. 256) report that histone deacetylase (HDAC) 4 functions in mouse retina to support survival of retinal neurons. Depletion of HDAC4 increased cell death. Overexpression of HDAC4, on the other hand, supported retinal cell survival. HDACs produce some of their effects by modifying histones associated with DNA, which alters transcription. However, in this case, HDAC4 was predominantly found in the cytoplasm, and mutation of HDAC4 to promote its exclusion from the nucleus did not prevent its protective effects on the

Follow the Moving Polymer Chains

When materials deform, changes occur within them all the way down to the atomic and molecular level. When rubbery polymers begin to be pulled apart, the classic model put forward by Eyring predicts that the molecular chains will become more mobile. **Lee et al.** (p. 231, published online 27 November; see the Perspective by **Weitz**) have measured chain mobilities in a rubbery polymer, poly(methyl methacrylate), using an optical photobleaching method. They find that while the Eyring model works at low stress, once the material starts to flow, mobility values jump up and the distribution of values narrows. Mobility decreases when even greater stresses are applied that induce strain hardening. These results provide a guide

2009

SARDINIA

for Plant Enthusiasts!

April 17-29, 2009

Explore Capo Caccia, a hotspot for endemic plants and the Gallura region. Cross to the unspoiled island of Caprera, and explore the island's prehistoric Nuragic culture. Visit the Sinis peninsula, the remarkable Phoenician and Roman site of Tharros, and the basalt plateau of Giara di Gesturi. \$3,850 + air.



AEGEAN HERITAGE by Yacht May 1-9, 2009

Explore the heritage of the Aegean, including the Cyclades Islands and the Aegean Coast of Turkey, on board the 170-passenger sailing yacht, *Star Clipper*. See Rhodes, Bodrum Castle, Caunos, Santorini, and Hydra. From \$3,295 + air.

Wild & Prehistoric FRANCE

May 22-June 4, 2009

Join **Mark Walters** and discover wild areas and prehistoric sites in Haute Provence, the Massif Central, and the Dordogne. See images of the greatest cave paintings in Europe at Lascaux II. See the cave art by train at Rouffignac. Visit the Vézère Valley, Font de Gaume, Arles, and Les Baux. \$3,895 + air.

ALASKA

May 31-June 7, 2009

Explore Southeast Alaska's coastal wilderness aboard the *National Geographic Sea Lion*. From \$5,390 plus free air from Seattle.

For a detailed brochure,
please call (800) 252-4910

AAAS Travels

17050 Montebello Road
Cupertino, California 95014

Email: AAASInfo@betchartexpeditions.com

This Week in Science

Continued from page 183

retinal cells. Cytoplasmic HDAC4 may act by interacting with the transcription factor hypoxia-inducible factor 1 α (HIF1 α); deacetylation of HIF1 α promotes its stability and accumulation in the nucleus.

Tassel Tussle

Sex expression in the maize tassel (which only has male flowers) results from the halting of female organ development, but the genetic regulation of this process is unknown. **Acosta et al.** (p. 262) identify a major gene involved in male floral specificity by mapping and identifying the function of the *Tasselseed1* gene. Surprisingly, the gene is not a standard transcription factor but rather appears to be plastid localized and involved in the jasmonic acid pathway. The *ts1* mutants have reduced jasmonate level, and its flowers contain both pistils and stamens, instead of male tassels. Exogenous jasmonate can rescue the mutant phenotype. Thus, jasmonate (or its metabolites) is required to suppress female development in male flowers in maize.

Hole in Two

Type IV secretion systems (T4SS) are used by many Gram-negative bacteria to inject toxin or effector molecules into host cells or transfer plasmids harboring antibiotic resistance genes between bacteria.

Fronzes et al. (p. 266) report a cryoelectron microscopy structure of the core complex of a T4SS. The double-walled structure spans the bacterial inner and outer membranes and is open on the cytoplasmic side and constricted on the extracellular side. These details may provide insights into how secretion might be regulated.



Paradoxical Producers

It is still not clear why certain cooperative behaviors persist when the benefit to nonparticipants appears to outweigh the advantage to the cooperators. In exploring a synthetic microbial system, **Chuang et al.** (p. 272) contend that although cooperators might be disadvantaged locally because of structural heterogeneities in the population, across the entire population, cooperation has a selective advantage. This study shows how entangled the parameters of natural populations can be and why statistical outcomes might be ambiguous or misleading.

Black and White Reaction?

Researchers have demonstrated that humans are stupendously poor at forecasting how they will feel in emotionally challenging situations. Usually and happily for our innate dispositions, our estimate of how bad we expect to feel is much worse than the actual feelings we experience. **Kawakami et al.** (p. 276; see the Perspective by **Smith and Mackie**) have applied this insight to the question of why prejudicial attitudes and behavior (assessed in the context of white-black relations) persist even though publicly expressed reactions toward prejudicial actions are overwhelmingly censorious. In a series of studies, they show that witnesses of a racist remark made by a white subject toward a black subject consistently predict that they would feel worse than they actually do and that they would shun the white subject (in a partnership task) more than they actually do.

Fixing Nitrogen

Nitrate is an essential macronutrient for marine algae, the availability of which could help explain glacial-interglacial changes in the concentration of atmospheric CO₂ through its effects on marine photosynthetic productivity. The largest source of nitrate in the oceans comes from nitrogen fixation by bacteria. **Ren et al.** (p. 244, published online 18 December) report measurements of the nitrogen isotopic composition of planktonic foraminifera from Caribbean marine sediments, which indicate that there was less nitrogen fixation in the Atlantic during the last Ice Age than afterward. These data support a long-suspected, but poorly documented, feedback between denitrification and nitrogen fixation across the global ocean.

CREDIT: FRONZES ET AL.

A Celebration and a Challenge

Andrew Sugden is the International Managing Editor at *Science*.

Brooks Hanson is Deputy Editor for physical sciences at *Science*.

Elizabeth Pennisi is a News Writer at *Science*.

Elizabeth Culotta is a Contributing News Editor at *Science*.

THIS ISSUE MARKS THE BEGINNING OF *SCIENCE*'S COVERAGE OF TWO PROMINENT ANNIVERSARIES. Charles Robert Darwin, originator of modern evolutionary theory, was born 200 years ago next month. His book setting forth this theory, *On the Origin of Species by Means of Natural Selection, or the Preservation of Favoured Races in the Struggle for Life*, was published 150 years ago in November. These anniversaries have special resonance for scientists worldwide, and the general public too, in that Darwin wrote specifically for a broad audience. As *The Times* (London) wrote in 1909 in honor of his first centenary, "To no other man has it been given to effect a revolution in human thought so large, so pervading, so sudden, and yet so enduring. Darwin taught mankind to see all things in a new light, not only the mysteries of nature, great and small, the mysteries of existence and the innumerable objects of research, but the common things of everyday life."

Darwin's gift was to sense the mystery of the diversification of living organisms, and his achievement was to make sense of it. Remarkably, he revealed the mechanism and process of evolution without having a clue about how variation was generated. He developed his arguments based on painstaking examination of paleontological and biological evidence, and the emergent properties of organisms, but with no knowledge of the underlying genetics. Evolutionary biology has been much transformed and enhanced since his time, but at its core remains Darwin's electrifying idea: natural selection and descent with modification as the agent and manifestation, respectively, of evolutionary change.

The first centenary was marked in 1909 with an enthusiasm unprecedented for a figure so recently departed. Delegates from 20 countries attended a 3-day festival in Cambridge, UK (where Darwin studied), featuring garden parties, lectures, receptions, and the award of doctorates to many foreign visitors. In the United States, the pioneering geneticist T. H. Morgan spoke on "Darwin's Influence on Zoology" at Columbia University, and there were events at the University of Georgia, the Massachusetts Institute of Technology, and many more.

We begin *Science*'s own celebration of Darwin's bicentenary with a review article by Peter Bowler (see page 223), who analyzes the originality of Darwin's contribution. We also feature an essay by Carl Zimmer (see page 198) on how life might have begun, the first in a monthly series about "Origins" that takes a broad look at key developments in evolution and in human culture. In February, we will feature a special issue on speciation and diversification, still major themes in evolutionary science. You will also find additional content online (www.sciencemag.org/darwin/), as well as an Origins blog (<http://blogs.sciencemag.org/origins/>), throughout the year.

Evolution is also woven into the theme of the AAAS annual meeting (www.aaas.org/meetings), which starts in February, on Darwin's birthday. In July, the AAAS will be supporting the Darwin Festival in Cambridge, UK (www.darwin2009.cam.ac.uk/festival), which will echo, on a grander scale and with more public outreach, the prominent festival of 1909.

Beyond laying the foundations for evolutionary biology, Darwin built a home that biology could furnish with the concepts and findings from paleontology, ecology, and population genetics, and more recently molecular biology, developmental biology, and genomics. In marking his bicentenary, we reaffirm the values and practice of science, and the generous spirit of inquiry, observation, experiment, and discussion that Darwin himself exemplified.

These values, and their fruits, need continued public promulgation. In 1909, *The Times* also wrote that "[Darwin's] achievement has, in a sense, become so familiar, its indirect influence has so closely interpenetrated the general consciousness of mankind that we can hardly see it plain or measure its proportions. It is not a matter for the learned only, but for all of us." A century later, it is still a matter for all of us. In today's society, where science is broadly integrated in enhancing human welfare, such a broad public understanding is required of not just new discoveries, but of their deep and enduring roots. This year's bicentennial celebrations will only be a success if they meet this challenge.

—Andrew Sugden, Brooks Hanson, Elizabeth Pennisi, Elizabeth Culotta



VIROLOGY

Vaccine Takes a Toll

Respiratory syncytial virus (RSV) is a common cause of lower respiratory tract infections in infants, and early exposure to the virus is thought to confer an increased risk of wheezing and asthma later in life. Efforts to develop a protective vaccine suffered a major setback in the 1960s when a formalin-inactivated vaccine against RSV (FIRSV) not only failed to protect against viral infection, but severely exacerbated lung disease in vaccinated infants and children, many of whom required hospitalization. Forty years later, Delgado *et al.* offer a fresh perspective on why the FIRSV vaccine may have failed. Studying the immune responses in mice treated with wild-type RSV or with either of two inactivated vaccines [FIRSV or a vaccine inactivated by ultraviolet light (UVRSV)], they found that both inactivated vaccines elicited short-lived antibodies that were nonprotective. Further experiments with UVRSV revealed that these antibodies had a low affinity for crucial viral antigens and that this was due to deficient activation of Toll-like receptor (TLR) signaling in B cells. Mice that had been treated with both UVRSV and TLR agonists and then infected with RSV had lower levels of virus and milder lung disease than mice treated with the vaccine alone. These results cast doubt on an earlier hypothesis attributing the vaccine failure to formalin-mediated disruption of viral antigens, and they raise the possibility that agents stimulating the TLR pathway may enhance the efficacy of future candidate vaccines. — PAK

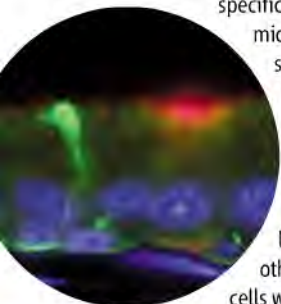
Nat. Med. 10.1038/nm.1894 (2008).

CELL BIOLOGY

Reaching Out to the Other Side

Epithelial cells line the surfaces of the body, either in monolayers (simple) or in multiple layers (stratified). A third type of arrangement, referred to as pseudostratified, contains only a single layer of cells, but with their nuclei dispersed so as to give a laminated appearance. Shum *et al.* have used cell-specific labeling, confocal

microscopy, and three-dimensional reconstruction to show that in pseudostratified epithelia, basal cells (on which the epithelium sits) extend projections that infiltrate the epithelial cell layer to make contact with the other (luminal) surface. Such cells were observed in epididymis



Osedax (shown above) is a recently discovered annelid worm that, with a little help from endosymbiotic bacteria called *Oceanospirillales*, feeds on the bones of whales. However, whale carcasses are rare, and the diversity of *Osedax* species astonishing, so how these organisms persist and scatter is a conundrum. Rouse *et al.* have set out to elucidate the life-history peculiarities of worms feasting on whale carcasses planted at defined depths in Monterey Bay, California.

Male worms are parasitic on females, and thus fertilization is guaranteed. Moreover the animals are highly fecund, with females devoting a large proportion of their body mass to ovary, whereas the male's somatic development is sidetracked into sperm production, possibly by signals from the females; under laboratory conditions, they seem to reproduce continuously. It appears that the metamorphosis of females from a swimming trochophore only occurs when the larvae encounter a carcass and have been infected with the endosymbiont. These tactics concur with the obvious ecological needs of these strange worms, but how long the larvae live, whether they have searching strategies, and how far they disperse are interesting questions that still await answers. — CA

Mar. Biol. 10.1007/s00227-008-1091-z (2008).

(both rat and human), rat coagulating gland (similar to the prostate), and rat trachea. Detailed analysis of the rat epididymis revealed that the frequency of these projections varied, with less than 10% of basal cells exhibiting this trait in proximal vas deferens and about 60% extending toward the lumen in more distal regions. The morphology of these projections varied, with some appearing just beneath tight junctions and some passing through the tight junctions

at which three epithelial cells met. The authors detected angiotensin type 2 receptors (the renin-angiotensin system regulates male fertility) only in the basal cells (shown at left, green), and not in the clear cells (red) that acidify the lumen and keep sperm dormant during maturation and storage. Perfusion of rat epididymis with angiotensin II triggered the extension

*Nancy R. Gough is Editor of *Science Signaling*.

CREDITS (TOP TO BOTTOM): ROUSE ET AL., MAR. BIOL. 10.1007/S00227-008-1091-Z (2008); SHUM ET AL., CELL 135, 1108 (2008)

sion of proton pump–enriched microvilli from the clear cells and stimulated proton secretion. Thus, the authors suggest that the luminal projections of the basal cells serve as sensors of hormones and transmit signals to neighboring cells within the epithelium. — NRG*

Cell **135**, 1108 (2008).

CHEMISTRY

Reactive Channels

Coordination polymers consist of metal centers strung together by multiple ligands, often to form a porous framework material that can encapsulate molecular guests. For many coordination polymers, a change in the oxidation state of the metal leads to a collapse of the framework structure. One exception is a layered material based on $[\text{Fe}^{\text{III}}(\text{CN})_6]^{3-}$ units, which is structurally stable to reduction because the reduced $[\text{Fe}^{\text{II}}(\text{CN})_6]^{4-}$ groups retain a similar coordination geometry. Yanai *et al.* have exploited this property by infiltrating the framework with pyrrole monomers, which are then oxidized and polymerized by the iron within well-defined channels. Addition of the



chelator ethylenediamine tetraacetic acid cleanly dismantles the framework to liberate the polypyrrole. Whereas bulk polypyrrole has a granular morphology, the

polypyrrole grown inside the coordination polymer (shown above) exhibited an overlapping plate structure made up of discernible stacks of thin layers. After the product was doped with iodine, the conductivity along the direction parallel to the plates was 20 times as high as that perpendicular to the plates, confirming the orienting impact of the iron host and catalyst framework. — MSL

Angew. Chem. Int. Ed. **47**, 9883 (2008).

DEVELOPMENT

Budding Blood Cells

Arguably the best-understood stem cells are those that generate the body's blood cells—hematopoietic stem cells (HSCs). Although the place of origin, the aortic-gonado-mesonephric (AGM) columns, is known, the specific cell type responsible for their emergence is not. By labeling cell populations *in vivo* either with the adhesion molecule VE cadherin or the transcription factor myocardin, Zovein *et al.* were able to follow endothelial and mesenchymal progeny, respectively. Their data point to an endothelial origin of

HSCs for subsequent long-term, multilineage adult hematopoiesis. Further, the HSC endothelial progeny could be monitored as they traveled first to the fetal liver and then to the bone marrow for subsequent expansion and multilineage differentiation. Besides the AGM region, the authors also identified the placental vasculature and yolk sac as endothelial sources of HSCs. Hence, the origin of hematopoietic stem cells is endothelium, which itself comes from a transient mesenchymal population of cells. — BAP

Cell Stem Cell **3**, 625 (2008).

ANIMAL BEHAVIOR

Bee Raves

Cocaine triggers reward pathways in the human brain and is toxic at high doses; it is postulated to have evolved as an insecticide that protects the coca plant. Barron *et al.* have tested the response of honey bees to cocaine and find suggestive evidence of a reward effect at low doses. By examining the honey bee dance—the means by which bees signal the availability of resources to their hive-mates—they found that dosing the bees with cocaine increased both the likelihood and rate of dance after foraging; furthermore, the bees exhibited behavior consistent with a withdrawal effect when the drug was withheld after chronic treatment. The authors conclude that responsiveness and signaling in the appropriate settings were increased by the treatment with cocaine, suggesting that the response to the drug may be similar in humans and bees. — LMZ

J. Exp. Biol. **212**, 163 (2009).

APPLIED PHYSICS

Holey Different Films

Surface plasmon-polaritons (SPPs) are generally studied in noble metals. The problem in observing coupling of SPPs to the magnetic field effects in ferromagnetic metals is that absorption broadens out the anticipated magneto-optical signatures. Cistis *et al.* prepared cobalt films (50 to 100 nm thick) that contained a hexagonal array of nanoholes (diameters between 220 and 330 nm and with a spacing of 470 nm). The presence of the holes changed the magnetic properties of the film in two ways—it increased the coercive field in the in-plane directions and created magnetization components out-of-plane. Light transmission through these films depended on the external magnetic field through the excitation of SPPs. The films showed higher polarization rotation than a continuous cobalt film, and the enhancement occurred at the wavelength maxima of the SPPs. — PDS

Nano Lett. **10**.1021/nl801811t (2008).

Bicentennial of Darwin's birth!

Galapagos

May 30–June 8, 2009



This is as close as you can get to the extraordinary! With an *optional extension to Peru*, June 7-17, 2009 also available.

There is something very special about Galapagos... the archipelago provides enchantment, surprise and delight. It is one of the world's great remaining natural areas, full of wonder, beauty, and unusual wildlife. You will have the unique opportunity for close encounters with sea lions, penguins, tortoises, fur seals and seabirds.

With 97% of the Galapagos Islands protected as national park land, this amazing place is also one of the world's most important laboratories for the future of conservation, sustainable tourism, and wildlife management.

Travel aboard the 48-guest *National Geographic Islander...* an extremely comfortable expedition ship noted for excellent personal service with a fleet of



sturdy Zodiac landing craft providing access to virtually anywhere. Also available are kayaks, wet suits, snorkeling gear and underwater video equipment, making the vibrant undersea world accessible to all. From \$5,120 + air.

For a detailed brochure, please call (800) 252-4910

AAAS Travels

17050 Montebello Road
Cupertino, California 95014

Email: AAASInfo@betchartexpeditions.com

1200 New York Avenue, NW
Washington, DC 20005

Editorial: 202-326-6550, FAX 202-289-7562

News: 202-326-6581, FAX 202-371-9227

Bateman House, 82-88 Hills Road
Cambridge, UK CB2 1LQ

+44 (0) 1223 326500, FAX +44 (0) 1223 326501

SUBSCRIPTION SERVICES For change of address, missing issues, new orders and renewals, and payment questions: 866-434-AAAS (2227) or 202-326-6417, FAX 202-842-1065. Mailing addresses: AAAS, P.O. Box 96178, Washington, DC 20090-6178 or AAAS Member Services, 1200 New York Avenue, NW, Washington, DC 20005

INSTITUTIONAL SITE LICENSES please call 202-326-6755 for any questions or information

REPRINTS: Author Inquiries 800-635-7181

Commercial Inquiries 803-359-4578

PERMISSIONS 202-326-7074, FAX 202-682-0816

MEMBER BENEFITS AAAS/Barnes&Noble.com bookstore www.aaas.org/bn; AAAS Online Store www.apisource.com/aaas/; Apple Store www.apple.com/store/aaas; Bank of America MasterCard 1-800-833-6262 priority code FAA3YU; Cold Spring Harbor Laboratory Press Publications www.cshlpress.com/affiliates/aaas.htm; GEICO Auto Insurance www.geico.com/landingpage/go51.htm?logo=17624; Hertz 800-654-2200 CDP#343457; Office Depot <http://hsd.officedepot.com/portalLogin.do>; Seabury & Smith Life Insurance 800-424-9883; Subaru VIP Program 202-326-6417; VIP Moving Services www.vipmayflower.com/domestic/index.html; Other Benefits: AAAS Member Services 202-326-6417 or www.aaasmember.org.

science_editors@aaas.org (for general editorial queries)

science_letters@aaas.org (for queries about letters)

science_reviews@aaas.org (for returning manuscript reviews)

science_bookrevs@aaas.org (for book review queries)

Published by the American Association for the Advancement of Science (AAAS), *Science* serves its readers as a forum for the presentation and discussion of important issues related to the advancement of science, including the presentation of minority or conflicting points of view, rather than by publishing only material on which a consensus has been reached. Accordingly, all articles published in *Science*—including editorials, news and comment, and book reviews—are signed and reflect the individual views of the authors and not official points of view adopted by AAAS or the institutions with which the authors are affiliated.

AAAS was founded in 1848 and incorporated in 1874. Its mission is to advance science, engineering, and innovation throughout the world for the benefit of all people. The goals of the association are to: enhance communication among scientists, engineers, and the public; promote and defend the integrity of science and its use; strengthen support for the science and technology enterprise; provide a voice for science on societal issues; promote the responsible use of science in public policy; strengthen and diversify the science and technology workforce; foster education in science and technology for everyone; increase public engagement with science and technology; and advance international cooperation in science.

INFORMATION FOR AUTHORS

See pages 634 and 635 of the 1 February 2008 issue or access www.sciencemag.org/about/authors

EDITOR-IN-CHIEF **Bruce Alberts**

EXECUTIVE EDITOR **Monica M. Bradford**

DEPUTY EDITORS

R. Brooks Hanson, Barbara R. Jasny,

Katrina L. Kelner

NEWS EDITOR

Colin Norman

EDITORIAL SUPERVISORY SENIOR EDITOR Phillip D. Szurmi; **SENIOR EDITOR/PERSPECTIVES** Lisa D. Chong; **SENIOR EDITORS** Gilbert J. Chin, Pamela J. Hines, Paula A. Kiberstis (Boston), Marc S. Lavine (Toronto), Beverly A. Purnell, L. Bryan Ray, Guy Riddihough, H. Jesse Smith, Valda Vinson; **ASSOCIATE EDITORS** Kristen L. Mueller, Jake S. Yeston, Laura M. Zahn; **ONLINE EDITOR** Stewart Wills; **ASSOCIATE ONLINE EDITORS** Robert Frederick, Tara S. Marathe; **WEB CONTENT DEVELOPER** Martyn Green; **BOOK REVIEW EDITOR** Sherman J. Suter; **ASSOCIATE LETTERS EDITOR** Jennifer Sills; **EDITORIAL MANAGER** Cara Tate; **SENIOR COPY EDITORS** Jeffrey E. Cook, Cynthia Howe, Harry Jach, Barbara P. Ordway, Trista Wagoner; **COPY EDITORS** Chris Filatreau, Lauren Kmeck; **EDITORIAL COORDINATORS** Carolyn Kyle, Beverly Shields; **PUBLICATIONS ASSISTANTS** Ramatoulaye Diop, Joi S. Granger, Jeffrey Hearn, Lisa Johnson, Scott Miller, Jerry Richardson, Jennifer A. Seibert, Brian White, Anita Wynn; **EDITORIAL ASSISTANTS** Carlos L. Durham, Emily Guise, Patricia M. Moore; **EXECUTIVE ASSISTANT** Sylvia S. Kihara; **ADMINISTRATIVE SUPPORT** Maryrose Madrid

NEWS DEPUTY NEWS EDITORS Robert Coontz, Eliot Marshall, Jeffrey Mervis, Leslie Roberts; **CONTRIBUTING EDITORS** Elizabeth Colutta, Polly Shulman; **NEWS WRITERS** Yudhijit Bhattacharjee, Adrian Cho, Jennifer Couzin, David Grimm, Constance Holden, Jocelyn Kaiser, Richard A. Kerr, Eli Kintisch, Andrew Lawler (New England), Greg Miller, Elizabeth Pennisi, Robert F. Service (Pacific NW), Erik Stokstad; **INTERN** Rachel Zerkowicz; **CONTRIBUTING CORRESPONDENTS** Jon Cohen (San Diego, CA), Daniel Ferber, Ann Gibbons, Robert Koenig, Matt Leslie, Charles C. Mann, Virginia Morell, Evelyn Strauss, Gary Taubes; **COPY EDITORS** Linda B. Felaco, Melvin Gatling, Melissa Raimondi; **ADMINISTRATIVE SUPPORT** Scherraine Mack, Fannie Groom; **BUREAU NEW ENGLAND:** 207-549-7755, San Diego, CA: 760-942-3252, FAX 760-942-4979, Pacific Northwest: 503-963-1940

PRODUCTION DIRECTOR James Landry; **SENIOR MANAGER** Wendy K. Shank; **ASSISTANT MANAGER** Rebecca Doshi; **SENIOR SPECIALISTS** Steve Forrester, Chris Redwood; **SPECIALIST** Anthony Rosen; **PREFLIGHT DIRECTOR** David M. Tompkins; **MANAGER** Marcus Spiegler

ART DIRECTOR Yael Kats; **ASSOCIATE ART DIRECTOR** Laura Creveling;

ILLUSTRATORS Chris Bickel, Katharine Suttiff; **SENIOR ART ASSOCIATES** Holly Bishop, Preston Huey, Nayomi Kevitigalaga; **ART ASSOCIATE** Jessica Newfield; **PHOTO EDITOR** Leslie Blizard

SCIENCE INTERNATIONAL

EUROPE (science-int@aaas.org) **EDITORIAL:** INTERNATIONAL MANAGING EDITOR Andrew M. Sugden; **SENIOR EDITOR/PERSPECTIVES** Julia Fahrenkamp-Uppenbrink; **SENIOR EDITORS** Caroline Ash, Stella M. Hurlley, Ian S. Osborne, Peter Stern; **ASSOCIATE EDITOR** Maria Cruz; **EDITORIAL SUPPORT** Deborah Dennison, Rachel Roberts, Alice Whaley; **ADMINISTRATIVE SUPPORT** John Cannell, Janet Clements; **NEWS:** EUROPE NEWS EDITOR John Travis; **DEPUTY NEWS EDITOR** Daniel Cleary; **CONTRIBUTING CORRESPONDENTS** Michael Balter (Paris), John Bohannon (Vienna), Martin Enserink (Amsterdam and Paris), Gretchen Vogel (Berlin); **INTERN** Sara Coelho

ASIA Japan Office: Asca Corporation, Eiko Ishioka, Fusako Tamura, 1-8-13, Hirano-cho, Chuo-ku, Osaka-shi, Osaka, 541-0046 Japan; +81 (0) 6 6202 6272, FAX +81 (0) 6 6202 6271; asca@os.gulf.or.jp; **ASIA NEWS EDITOR** Richard Stone (Beijing: rstone@aaas.org); **CONTRIBUTING CORRESPONDENTS** Dennis Normile (Japan: +81 (0) 3 3391 0630, FAX +81 (0) 3 5936 3531; dnormile@gol.com); Hao Xin (China: +86 (0) 10 6307 4439 or 6307 3676, FAX +86 (0) 10 6307 4358; cindyhao@gmail.com); Pallava Bagla (South Asia: +91 (0) 11 2271 2896; pbagla@vsnl.com)

EXECUTIVE PUBLISHER **Alan I. Leshner**

PUBLISHER **Beth Rosner**

FULFILLMENT SYSTEMS AND OPERATIONS (membership@aaas.org); **DIRECTOR** Waylon Butler; **SENIOR SYSTEMS ANALYST** Jonny Blaker; **CUSTOMER SERVICE SUPERVISOR** Pat Butler; **SPECIALISTS** Latoya Casteel, LaVonda Crawford, Vicki Linton, April Marshall; **DATA ENTRY SUPERVISOR** Cynthia Johnson; **SPECIALISTS** Eintou Bowden, Tarrika Hill, William Jones

BUSINESS OPERATIONS AND ADMINISTRATION DIRECTOR Deborah Rivera-Wienhold; **ASSISTANT DIRECTOR, BUSINESS OPERATIONS** Randy Yi; **MANAGER, BUSINESS ANALYSIS** Michael LoBue; **MANAGER, BUSINESS OPERATIONS** Jessica Tierney; **FINANCIAL ANALYSTS** Priti Pamnani, Celeste Troxler; **RIGHTS AND PERMISSIONS:** ADMINISTRATOR Emilie Dabed; **ASSOCIATE** Elizabeth Sandler; **MARKETING DIRECTOR** Ian King; **MARKETING MANAGER** Allison Pritchard; **MARKETING ASSOCIATES** Aimee Aponte, Alison Chandler, Mary Ellen Crowley, Julianne Wielga, Wendy Wise; **INTERNATIONAL MARKETING MANAGER** Wendy Sturley; **MARKETING EXECUTIVE** Jennifer Reeves; **MARKETING/MEMBER SERVICES EXECUTIVE** Linda Rusk; **DIRECTOR, SITE LICENSING** Tom Ryan; **DIRECTOR, CORPORATE RELATIONS** Eileen Bernadette Moran; **PUBLISHER RELATIONS, eResources SPECIALIST** Kiki Forsythe; **SENIOR PUBLISHER RELATIONS SPECIALIST** Catherine Holland; **PUBLISHER RELATIONS, EAST COAST** Phillip Smith; **PUBLISHER RELATIONS, WEST COAST** Philip Tsolakis; **FULFILLMENT SUPERVISOR** Iquo Edim; **FULFILLMENT COORDINATOR** Laura Clemens; **ELECTRONIC MEDIA MANAGER** Elizabeth Harman; **PROJECT MANAGER** Trista Snyder; **ASSISTANT MANAGER** Lisa Stanford; **SENIOR PRODUCTION SPECIALISTS** Christopher Coleman, Walter Jones; **PRODUCTION SPECIALISTS** Nichole Johnston, Kimberly Oster

ADVERTISING DIRECTOR, WORLDWIDE AD SALES Bill Moran

PRODUCT (science_advertising@aaas.org); **MIDWEST/WEST COAST/W. CANADA** Rick Bongiovanni: 330-405-7080, FAX 330-405-7081; **EAST COAST/E. CANADA** Laurie Faraday: 508-747-9395, FAX 617-507-8189; **UK/EUROPE/ASIA** Roger Goncalves: TEL/FAX +41 43 234 1358; **JAPAN** Masahiko Yoshikawa: +81 (0) 3 3235 5961, FAX +81 (0) 3 3235 5852; **SENIOR TRAFFIC ASSOCIATE** Delandra Simms

COMMERCIAL EDITOR Sean Sanders: 202-326-6430

PROJECT DIRECTOR, OUTREACH Brianna Blaser

CLASSIFIED (advertise@sciencecareers.org); **INSIDE SALES MANAGER:** MIDWEST/CANADA Daryl Anderson: 202-326-6543; **INSIDE SALES REPRESENTATIVE** Karen Foote: 202-326-6740; **KEY ACCOUNT MANAGER** Jorihab Able; **NORTHEAST** Alexis Fleming: 202-326-6578; **SOUTHEAST** Tina Burks: 202-326-6577; **WEST** Nicholas Hintibidze: 202-326-6533; **SALES COORDINATORS** Rohan Edmonson, Shirley Young; **INTERNATIONAL SALES MANAGER** Tracy Holmes: +44 (0) 1223 326525, FAX +44 (0) 1223 326532; **SALES** Susanne Kharras, Dan Pennington, Alex Palmer; **SALES ASSISTANT** Louise Moore; **JAPAN** Masahiko Yoshikawa: +81 (0) 3 3235 5961, FAX +81 (0) 3 3235 5852; **ADVERTISING PRODUCTION OPERATIONS MANAGER** Deborah Tompkins; **SENIOR PRODUCTION SPECIALIST/GRAPHIC DESIGNER** Amy Hardcastle; **SENIOR PRODUCTION SPECIALIST** Robert Buck; **SENIOR TRAFFIC ASSISTANT** Christine Hall; **PUBLICATIONS ASSISTANT** Mary Lagnaoui

AAAS BOARD OF DIRECTORS RETIRING PRESIDENT, CHAIR David Baltimore; PRESIDENT James J. McCarthy; PRESIDENT-ELECT Peter C. Agre; TREASURER David E. Shaw; CHIEF EXECUTIVE OFFICER Alan I. Leshner; BOARD LYNN W. Enquist, Susan M. Fitzpatrick, Alice Gast, Linda P. B. Katehi, Nancy Knowlton, Cherry A. Murray, Thomas D. Pollard, Thomas A. Woolsey



ADVANCING SCIENCE, SERVING SOCIETY

SENIOR EDITORIAL BOARD

John I. Brauman, *Chair, Stanford Univ.*
Richard Losick, *Harvard Univ.*
Robert May, *Univ. of Oxford*
Marcia McNutt, *Monterey Bay Aquarium Research Inst.*
Linda Partridge, *Univ. College London*
Pera C. Rubin, *Carnegie Institution*
Christopher R. Somerville, *Univ. of California, Berkeley*

BOARD OF REVIEWING EDITORS

Joanna Aizenberg, *Harvard Univ.*
R. McNeill Alexander, *Leeds Univ.*
David Altshuler, *Broad Institute*
Arturo Alvarez-Buylla, *Univ. of California, San Francisco*
Ricardo Amasino, *Univ. of Wisconsin, Madison*
Angelika Amon, *MIT*
Meinrat O. Andreae, *Max Planck Inst., Mainz*
Kristi S. Anseth, *Univ. of Colorado*
John A. Bargh, *Yale Univ.*
Cornelia I. Bargmann, *Rockefeller Univ.*
Ben Barres, *Stanford Medical School*
Marisa Bartolomei, *Univ. of Penn. School of Med.*
Ray H. Baughman, *Univ. of Texas, Dallas*
Stephen J. Benkovic, *Penn State Univ.*
Michael J. Bevan, *Univ. of Washington*
Tom Bisseling, *Wageningen Univ.*
Mina Bissell, *Lawrence Berkeley National Lab*
Peer Bork, *EMBL*
Dianna Bowles, *Univ. of York*
Robert W. Boyd, *Univ. of Rochester*
Paul M. Brakenhoff, *Leiden Univ.*
Dennis Bray, *Univ. of Cambridge*
Stephen Buratowski, *Harvard Medical School*
Joseph A. Burns, *Cornell Univ.*
William P. Butz, *Population Reference Bureau*
Peter Carmeliet, *Univ. of Leuven, VIB*
Gerbrand Ceder, *MIT*
Mildred Cho, *Stanford Univ.*
David Clapham, *Children's Hospital, Boston*
David Clary, *Oxford University*
J. M. Claverie, *CNRS, Marseille*

Jonathan D. Cohen, *Princeton Univ.*
Stephen M. Cohen, *Tennessee Life Sciences Lab, Singapore*
Robert H. Crabtree, *Yale Univ.*
F. Fleming Crim, *Univ. of Wisconsin*
William Cumberland, *Univ. of California, Los Angeles*
George O. Daley, *Children's Hospital, Boston*
Jeff L. Dangl, *Univ. of North Carolina*
Stanislav Dehaene, *Collège de France*
Edward DeLong, *MIT*
Emmanouil T. Dermizakis, *Wellcome Trust Sanger Inst.*
Robert Desimone, *MIT*
Dennis Discher, *Univ. of Pennsylvania*
Scott C. Doney, *Woods Hole Oceanographic Inst.*
Peter J. Donovan, *Univ. of California, Irvine*
W. Ford Doolittle, *Dalhousie Univ.*
Jennifer A. Doudna, *Univ. of California, Berkeley*
Julian Downward, *Cancer Research UK*
Denis Duboule, *Univ. of Geneva/EPFL Lausanne*
Christopher Dye, *WHO*
Richard Ellis, *Cal Tech*
Gerhard Ertl, *Fritz-Haber-Institut, Berlin*
Douglas H. Erwin, *Smithsonian Institution*
Mae Estelle, *Indiana Univ.*
Barry Everitt, *Univ. of Cambridge*
Paul G. Falkowski, *Rutgers Univ.*
Ernst Fehr, *Univ. of Zurich*
Tom Fenchel, *Univ. of Copenhagen*
Alain Fischer, *INSERM*
Scott E. Fraser, *Cal Tech*
Chris D. Frith, *Univ. College London*
Wulfraut Gerstner, *EPFL Lausanne*
Charles Godfray, *Univ. of Oxford*
Diane Griffin, *Johns Hopkins Bloomberg School of Public Health*
Christoph Haass, *Ludwig Maximilians Univ.*
Niels Hansen, *Technical Univ. of Denmark*
Dennis L. Hartmann, *Univ. of Washington*
Chris Hawkesworth, *Univ. of Bristol*
Martin Heimann, *Max Planck Inst., Jena*
James A. Hendler, *Rensselaer Polytechnic Inst.*
Ray Hilborn, *Univ. of Washington*
Ove Hoegh-Guldberg, *Univ. of Queensland*
Ronald R. Hoy, *Cornell Univ.*
Olli Ikkala, *Helsinki Univ. of Technology*
Meyer B. Jackson, *Univ. of Wisconsin Med. School*

Stephen Jackson, *Univ. of Cambridge*
Steven Jacobson, *Univ. of California, Los Angeles*
Peter Jonas, *Universität Freiburg*
Barbara B. Kahn, *Harvard Medical School*
Daniel Kahne, *Harvard Univ.*
Gerard Karsenty, *Columbia Univ. College of P&S*
Bernhard Kellmer, *Max Planck Inst., Stuttgart*
Elizabeth A. Kellig, *Univ. of Missouri, St. Louis*
Alan B. Krueger, *Princeton Univ.*
Lee Kump, *Penn State Univ.*
Mitchell A. Lazar, *Univ. of Pennsylvania*
Virginia Lee, *Univ. of Pennsylvania*
Norman L. Letwin, *Beth Israel Deaconess Medical Center*
Olle Lindvall, *Univ. Hospital, Lund*
John Lis, *Cornell Univ.*
Richard Losick, *Harvard Univ.*
Ke Lu, *Chinese Acad. of Sciences*
Andrew P. MacKenzie, *Univ. of St Andrews*
Anne Magurran, *Univ. of St Andrews*
Virginia Miller, *Washington Univ.*
Yasushi Miyashita, *Univ. of Tokyo*
Richard Morris, *Univ. of Edinburgh*
Edward Moser, *Norwegian Univ. of Science and Technology*
Naoto Nagaoka, *Univ. of Tokyo*
James Nelson, *Stanford Univ. School of Med.*
Timothy W. Nilsen, *Case Western Reserve Univ.*
Roeland Nolte, *Univ. of Nijmegen*
Helga Nowotny, *European Research Advisory Board*
Eric N. Olson, *Univ. of Texas, SW*
Eria O'Shea, *Harvard Univ.*
Elinor Ostrom, *Indiana Univ.*
Jonathan T. Overpeck, *Univ. of Arizona*
John Pendry, *Imperial College*
Philippe Poulin, *CNRS*
Mary Power, *Univ. of California, Berkeley*
Molly Przeworski, *Univ. of Chicago*
David J. Read, *Univ. of Sheffield*
Les Real, *Emory Univ.*
Colin Renfrew, *Univ. of Cambridge*
Trevor Robbins, *Univ. of California, Berkeley*
Barbara A. Romanowicz, *Univ. of California, Berkeley*
Edward M. Rubin, *Lawrence Berkeley National Lab*
Jürgen Sandkühler, *Medical Univ. of Vienna*
David S. Schimel, *National Center for Atmospheric Research*

David W. Schindler, *Univ. of Alberta*
Georg Schulz, *Albert-Ludwigs-Universität*
Paul Schulze-Lefert, *Max Planck Inst., Cologne*
Christine Seidman, *Harvard Medical School*
Terrence J. Sejnowski, *The Salk Institute*
David Sibley, *Washington Univ.*
Montgomery Slatkin, *Univ. of California, Berkeley*
George Somero, *Stanford Univ.*
Joan Steitz, *Yale Univ.*
Elisbeth Stern, *ETH Zürich*
Jerome Strauss, *Virginia Commonwealth Univ.*
Glenn Telling, *Univ. of Kentucky*
Marc Tessier-Lavigne, *Genentech*
Jurg Tschopp, *Univ. of Lausanne*
Michiel van der Klis, *Astronomical Inst. of Amsterdam*
Derek van der Kooy, *Univ. of Toronto*
Bert Vogelstein, *Johns Hopkins Univ.*
Ulrich H. von Andrian, *Harvard Medical School*
Bruce D. Walker, *Harvard Medical School*
Christopher A. Walsh, *Harvard Medical School*
Graham Warren, *Univ. School of Med.*
Clint Watts, *Univ. of Dundee*
Detlef Weigel, *Max Planck Inst., Tübingen*
Jonathan Weissman, *Univ. of California, San Francisco*
Ellen D. Williams, *Univ. of Maryland*
Ian A. Wilson, *The Scripps Res. Inst.*
Jerry Workman, *Stowers Inst. for Medical Research*
John R. Yates III, *The Scripps Res. Inst.*
Jan Zaanen, *Leiden Univ.*
Martin Zatz, *NIMH, NIH*
Huda Zoghbi, *Baylor College of Medicine*
Maria Zuber, *MIT*

BOOK REVIEW BOARD

John Aldrich, *Duke Univ.*
David Bloom, *Harvard Univ.*
Angela Creager, *Princeton Univ.*
Richard Schweder, *Univ. of Chicago*
Ed Wasserman, *DuPont*
Lewis Wolpert, *Univ. College London*

Giving Wallace His Due

Tiny Ternate, Indonesia, hopes to spotlight its role in the history of evolutionary theory by memorializing the site where Alfred Russel Wallace penned *On the Tendency of Varieties to Depart Indefinitely from the Original Type*. The paper, read at a meeting of the Linnean Society in London in July 1858 while Wallace was still abroad, described concepts such as survival of the fittest and natural selection. At the same meeting, Charles Darwin presented his hastily assembled notes on evolution, published 16 months later in *On the Origin of Species*.

Last year, the 150th anniversary of the meeting, Wallace boosters located the site of the long-vanished house where the naturalist lived for 3 of the 8 years he spent collecting specimens in Southeast Asia, says Sangkot Marzuki, director of the Eijkman Institute for Molecular Biology in Jakarta. Among other things, the observations defined the "Wallace Line"—the boundary between Asian and Australian fauna.



Ternate plans to erect a monument, rebuild the house following a floor plan outlined in Wallace's writings, and rename the street for Wallace. Endang Sukara, an official at the Indonesian Institute of Sciences, says it's hoped that publicizing the area's role in understanding evolution will spur efforts to preserve the region's biodiversity.

Science and the City

Teachers complain of trouble getting their students interested in science. Try getting a whole city pumped on the subject.

That's the goal of Science Chicago, a year-long series of events launched in September 2008 to increase kids' interest in science, math, and technology.



THE PRIESTESS'S TALE

More than 4800 years since death stilled her voice, an Egyptian singer-priestess named Meresamun stars in a new exhibit at the University of Chicago's Oriental Institute. The detailed view of her life and times boasts the most technically advanced mummy reconstruction ever achieved, based on scans by a 256-channel "Intelligent CT" (above) conducted at the University of Chicago Medical Center.

In life, Meresamun would have accompanied a High Priest as he performed rituals before the god Amun, says curator Emily Teeter. At 168 centimeters, she was tall for her time. She had wide-set eyes and an overbite; her bones and teeth were in good shape. She died around the age of 30 and was mummified and buried in Luxor. The institute's founder, James Henry Breasted, bought her coffin in Egypt in 1920.

The exhibit, which opens 10 February, recreates Meresamun's life on the basis of scenes from tombs and temple walls and from ancient texts. It includes musical instruments, ritual objects, pottery, jewelry, and documents, including a marriage contract.



At Mayor Richard Daley's 9th Annual Holiday Sports Fest last month, about 80,000 people got a science lesson along with their sports fix. Teachers from the University of Illinois set up workstations next to basketball courts, indoor biking tracks, golf links, and other sports arenas, where visitors could study questions such as how geometry affects a billiard ball's trajectory or how the heart reacts to running a 50-yard dash.

"We're using sports and everyday activities to show that everything we do has scientific underpinnings," says former National Science Foundation Director Walter Massey. Massey co-chairs the initiative, driven by the MacArthur Foundation and Chicago's Museum of Science and Industry, with Foundation Vice President Arthur Sussman.

The Sports Fest was the biggest event so far for the program, which features smaller, weekly events such as nature walks and demonstrations at local universities and research sites such as Fermilab.

Go, Yankee Physics

Pacific Rim countries now produce almost as many scientific papers, but the United States still holds an across-the-board edge in relative citation impact, according to the latest tally of 21 scientific fields by the ScienceWatch tracking service (www.sciencewatch.com). U.S. physics papers lead the field with an average of 6.15 cites each, compared with the world average of 3.96.

TOP 10 FIELDS IN RELATIVE CITATION IMPACT, 2003–07

	U.S. world share (%)	U.S. citation impact	Relative impact v. world (%)
Physics	23.26	6.15	+55
Chemistry	20.70	7.33	+52
Materials science	18.10	4.23	+47
Geosciences	34.62	5.40	+42
Computer science	35.27	2.10	+40
Microbiology	34.01	9.90	+39
Clinical medicine	36.92	7.84	+36
Biology/biochemistry	37.10	10.33	+35
Space science	49.17	10.48	+34
Pharmacology	30.84	7.23	+34

Coming Fall 2009



Integrating clinical medicine and science

AAAS, publisher of the world's leading general science journal, *Science*, is launching a new journal of translational medicine in the fall of 2009.

The journal's mission is to facilitate communication and cooperation among basic and preclinical researchers, physician scientists, regulators, policy makers, industry, and funding agencies in order to improve health around the world. It will present original, science-based peer-reviewed research that successfully moves the field closer to helping patients. Perspectives and reviews from basic and clinical viewpoints along with discussions about research funding and regulatory issues will be included.

With *Science Translational Medicine*, you can expect the same level of breakthrough research that is the hallmark of the journal *Science*. The journal will be edited by Katrina L. Kelner, Ph.D., and an international advisory group of clinician scientists and other experts.

The monthly print edition, to be published 12 times a year, will be a compilation of the weekly online edition and sold exclusively to subscribers of the online edition. The print issues will include a selection of the online content and all primary peer-reviewed research. More subscription details will be available as the launch date approaches. For more information contact the editor and product manager at scitranslationalmed@aaas.org. For information on site licenses and subscriptions to print, please contact sciencemedicine@aaas.org.





Three Q's >>

George Csicsery, a filmmaker in Oakland, California, has won this year's communications award from the American Mathematical Society. Csicsery has directed several independent films with mathematical themes, including *Julia Robinson and Hilbert's Tenth Problem* (2008)—a biographical documentary about one of the first American women to

rise to prominence in mathematics and her role in solving a famous problem—and *Hard Problems:*

The Road to the World's Toughest Math Contest (2008), a documentary about high school students competing in the 2006 International Mathematical Olympiad.

Q: What do you find so interesting about math?

Principally, I'm interested in the mathematicians. I consider myself a cultural anthropologist.

Q: What's interesting about mathematicians?

I'm interested in groups of people who find a way to negotiate their own terms with reality. [Mathematicians] are able to work in a universe that they construct themselves.

Q: How do you try to capture that on film?

They're perfectly happy to explain what it is that attracts them to the work, what it is that's beautiful about mathematics. In almost every instance, I've found something that is on the boundary between aesthetics and religion.

TWO CULTURES

GAME CHANGER. A self-taught designer of low-voltage electrical devices has helped a team from the University of Washington (UW), Seattle, win an international protein-folding contest.

Steven Pletsch of Mesa, Arizona, got into the field of protein structure prediction by becoming an ace at a computer game, Foldit, that the UW researchers created and distributed on the Web. The team, led by biologist David Baker



and computer scientist Zoran Popović, recruited him to compete last spring in the Critical Assessment of Techniques for Protein Structure Prediction (CASP), a biannual academic contest between hundreds of scientists trying to predict the structure of 300 proteins based on their amino acid sequences.

Pletsch, 32, spent up to 30 hours a week, his newborn daughter Lydia cradled in one arm, folding a subset of the CASP puzzles. Pletsch's Foldit team, "Another Hour Another Point," provided Baker's team with several winning proteins.

Popović flew Pletsch to Seattle in September to share his insights, which the Foldit developers are now using to improve

the game. "What impressed me the most," says doctoral student Robert Vernon, is that Pletsch has no background in chemical physics but has learned "the same science by experimentation." Pletsch says his folding future is uncertain. He wants to make time to get an undergraduate degree and, perhaps more problematic, "Lydia has lost interest in watching Foldit."

ON CAMPUS

TALK CIRCUIT, SHORT CIRCUIT. Emory University has banned psychiatrist Charles Nemeroff from collecting industry money at certain speaking engagements after investigating his ties to a major pharmaceutical company. The Atlanta, Georgia, university conducted the investigation after U.S. Senator Charles Grassley (R-IA) accused Nemeroff of failing to report at least \$1.2 million of the more than \$2.4 million he earned from various companies. Emory focused on GlaxoSmithKline and found that Nemeroff received more than \$800,000 that he did not report to Emory.

In a statement late last month, Emory said that Nemeroff must "seek review and approval" before accepting any paid speaking engagements, and that he can't apply for National Institutes of Health grants for 2 years. He will be permitted to accept payment for talks only at continuing medical education events that are "sponsored by academic institutions or professional societies." Nemeroff, who has resigned from the chairmanship of his department following the investigation, said in the statement that he had misunderstood the disclosure rules and thought he was following them properly.

Science and Society >>

A NEW LENS. On the eve of the 400th anniversary of Galileo's first telescopic observations, the Vatican has launched a new effort to atone for the way it treated him.

In an address on 21 December 2008, Pope Benedict XVI pointed out how Galileo and other scientists have helped to explain the laws of nature. He extended a greeting to astronomers involved in celebrating 2009 as the International Year of Astronomy and touched on the role of astronomical calculations in determining times for prayer.

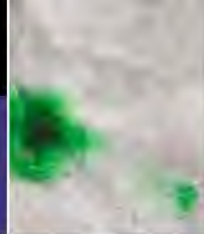
In May, representatives from the Vatican Observatory, the Pontifical Academy of Sciences, and other scientific and religious institutions will gather in Florence, Italy, to take a fresh look at the circumstances that led the Catholic Church to accuse Galileo of heresy and put him under house arrest. The conference is aimed at fostering "a climate of collaboration" between religion and science, "partly in view of the increasingly complex problems arising from recent developments in biotechnology," says Father Ennio Brovedani, director of the Stensen Institute in Florence. The Vatican officially rehabilitated Galileo in 1992, following a reexamination of documents related to his trial in 1633.



Got a tip for this page? E-mail people@aaas.org

Neuroscience
meets the law

195

How TB bacteria
co-opt immune cells

196

CONSERVATION

Scientists Laud Bush's Blue Legacy But Want More



Setting a middle course between the wishes of marine biologists and the concerns of the Pentagon and recreational fishers, President George W. Bush this week dusted off a little-used law for the second time in his Administration to protect swaths of ocean totaling an area the size of Spain.

On 6 January, using the 1906 Antiquities Act, which gives the president unfettered authority to protect any place of scientific or historical interest—and scientists say intact island ecosystems constitute such places—Bush created three separate national monuments spread out over eight remote patches of the Pacific totaling 505,000 square kilometers. Although short of the 2.2 million square kilometers many marine scientists had advocated, the monuments consolidate Bush's legacy as the president who has preserved far more ocean than any other: more than 850,000 square kilometers.

"It's terrific," says Jay Nelson, director of Ocean Legacy at the Pew Environment Group, who lobbied for the Marianas monument. "It's the single largest marine conservation act in history."

The action culminated a yearlong effort that started following Bush's much-praised creation of the 362,000-square-kilometer Papahānaumokuākea Marine National Monument around the Northwestern Hawaiian Islands. Next, Bush asked James L. Connaughton, chair

of the White House Council on Environmental Quality, whether other U.S. waters could be named national monuments. Connaughton met with representatives from a handful of marine conservation organizations, who then submitted proposals for a dozen sites. Fishing and mining groups knocked off those involving the protection of seamounts and canyons off California's coast; the waters off the island of Navassa between Haiti and Jamaica; and deep-sea coral beds off the Atlantic coast of South Carolina to Florida.

In August, the White House announced the finalists: the waters around 11 remote, tiny, and uninhabited islands that were either lightly fished or not fished. This week, Bush disclosed

Beneficiaries. Along with tuna, sharks, dolphins, turtles, and birds should profit from the new Pacific marine protected areas.

the size of the monuments—they extend 92 kilometers from shore—and the degree of protection: generally no-take fishing, under a management system to be fine-tuned later.

The first monument, and perhaps the most interesting scientifically, consists of 246,000 square kilometers of ocean around the Mariana Islands, already nature reserves, just south of Japan. It includes the islands of Maug, Asunción, and Uracus and is rich in submerged volcanoes with an exceptional diversity of life forms. The monument also stretches east and south to include the Marianas Trench, the oceanic equivalent of the Grand Canyon—only five times longer—and a group of seamounts with more hydrothermal life than anywhere else, teeming with the oldest living things on Earth: bacteria. Asunción erupts so often that it provides a unique platform to observe the rapid birth, death, and rebirth of coral and other marine life. Maug's water is so acidic in places that "it's the only place where you can look at the effects of ocean acidification on a shallow reef in a natural way," says Rusty Brainard, chief of the Coral Reef Ecosystem Division of the National Oceanic and Atmospheric Administration (NOAA) in Honolulu.

The second and smallest monument surrounds Rose in American Samoa, the world's smallest atoll, which has some of the densest coral cover in the world and hosts several seabird rookeries.

For the third, Bush designated five separate areas in the Central Pacific, totaling 225,000 square kilometers. Wake Island and Johnston Atoll host military bases; the rest are National Wildlife Refuges: Howland and Baker in the Phoenix Islands; Jarvis, in the Line Islands; and Kingman Reef and Palmyra, ▶



CREDIT: NOAA/PACIFIC ISLAND FISHERIES SCIENCE CENTER/CORAL REEF ECOSYSTEM DIVISION; SOURCE: COUNCIL ON ENVIRONMENTAL QUALITY



also in the Line Islands. They have some of the greatest densities of fish in the world because the waters around them are unusually full of nutrients brought by upwelling currents. There, with the reefs already protected, the main beneficiaries are expected to be declining populations of tuna as well as the sharks, birds, turtles, and dolphins that are accidentally caught by longline fishing.

The most significant opposition to making the monuments bigger came from the Pentagon. Nelson says several senior officials there expressed concern to him "that the designation of a monument over a big area could lead to future restrictions on their ability to operate

effectively." He said the officials cited lawsuits stemming from Bush's designation of the Northwestern Hawaiian Islands monument that restricted the use of sonar in war games.

Eight groups of recreational fishers also expressed their displeasure in a letter to Connaughton, as did some politicians in the Commonwealth of the Northern Marianas. The Marianas Hotel Association and the Chamber of Commerce, on the other hand, enthusiastically endorsed the proposal as a way to "boost the local economy in promoting ecotourism."

Although scientists and conservationists are delighted with the new sanctuaries, they say bigger no-take areas are needed to counter

increased fishing pressure in the Pacific. As a board member of Environmental Defense, marine biologist Jane Lubchenco of Oregon State University in Corvallis lobbied hard for Bush to protect the entire Exclusive Economic Zone around each island, which would have quadrupled the area protected. If confirmed as President-elect Barack Obama's choice to head NOAA, Lubchenco, also a past president of AAAS, which publishes *Science*, will oversee how all these monuments are managed. "We will continue to work with the next Administration to see if they can extend the area," says Nelson.

—CHRISTOPHER PALA

Christopher Pala is a writer based in Hawaii.

CLIMATE CHANGE

Higher Temperatures Seen Reducing Global Harvests

Thousands of people died from the heat that baked western Europe in the summer of 2003. The heat wave also devastated the region's agricultural sector: In France, where temperatures were 3.6°C above normal, the country's corn and fruit harvests fell more than 25%. Thirty-one years earlier, another very hot summer shrank harvests in southwest Russia and Ukraine and led to a tripling in world grain prices.

By the end of the century, two researchers predict, those summers may seem like cool ones, and the impact on agriculture will be even greater.

In a paper appearing on page 240, atmospheric scientist David Battisti of the University of Washington, Seattle, and economist Rosamond Naylor of Stanford University in Palo Alto, California, apply 23 global climate models used by the Intergovernmental Panel on Climate Change to estimate end-of-century temperatures. Their conclusions with regard to agriculture are sobering. "In the past, heat waves, drought, and food shortages have hit particular regions," says Battisti. But the future will be different: "Yields are going to be down every place." Heat will be the main culprit. "If you look at extreme high temperatures so far observed—basically since agriculture started—the worst summers on record have been mostly because of heat," not drought, he says.

The models predict that by 2090, the average summer temperature in France will be



Brownout. These wilting sunflowers in southwestern France show the effects of the exceptionally hot summer of 2003 that devastated agriculture.

3.7°C above the 20th century average. Elevated temperatures not only cause excess evaporation but also speed up plant growth with consequent reductions in crop yields, the authors note. Although rising temperatures may initially boost food production in temperate latitudes by prolonging the growing season, Battisti and Naylor say crops will eventu-

ally suffer unless growers develop heat-resistant versions that don't need a lot of water. "You have to go back at least several million years before you find ... temperatures" comparable to those being predicted, Battisti says.

Just as France offered a glimpse of the future in temperate regions, says Naylor, the Sahel in Africa shows what life could be like in the tropics and subtropics, home to half the world's population. A generation-long drought in the region lifted in the early 1990s, but higher temperatures have remained, depressing crop and livestock production. The authors predict future production reductions of 20% to 40%, while the population in tropical regions is expected to double to 6 billion.

The conclusions of the paper seem "reasonable," says plant and soil scientist Peter Smith of the University of Aberdeen in the United Kingdom, who also does greenhouse gas modeling. Smith adds that future pressures on food supplies come not only from steadily growing populations but also from changes in food preferences, in particular, more people eating meat. "Demand for livestock products in developing countries will greatly increase over the next few decades," says Smith. That trend, he says, represents "a switch to less efficient ways of feeding ourselves."

So developing heat-tolerant crops won't be enough to solve the problem of rising temperatures, he says. "We humans also need to change our behavior." —CONSTANCE HOLDEN

U.S. NATIONAL SECURITY

A New Spy Agency Asks Academics For Help in Meeting Its Mission

One year ago, applied physicist Lisa Porter took over a new government agency charged with developing the next generation of spy craft technologies. In a rare interview, Porter, the director of the Intelligence Advanced Research Projects Agency (IARPA), discussed the agency's progress and plans with *Science*.

Temporarily housed with the Center for Advanced Study of Language at the University of Maryland, College Park, IARPA expects by the end of the year to move into its own building on campus and double its size to 30 program managers. The academic location is no accident: The agency wants to build strong ties with academia through a continuing flow of grant solicitations. "The intelligence community likes to keep its business in the family—Lisa is trying to go beyond," says Steve Nixon, former director for science and technology within the office of the Director of National Intelligence (DNI), which was created in 2004 and oversees IARPA.

Porter was working at a national security think tank in northern Virginia when the terrorist strikes of 11 September 2001 made her "look in the mirror" and ask what more she could do to defend the country. Her answer was to join the Defense Advanced Research Projects Agency, a model for IARPA. There she ran classified and unclassified programs, including one aimed at making helicopter blades less noisy. A few years later, she went to NASA to head its aeronautics program.

Porter's first task was to soothe concerns that IARPA was part of a power grab by DNI to take over the research portfolios of the Central Intelligence Agency, National Security Agency, and a dozen other entities (*Science*, 22 June 2007, p. 1693). An effective communicator, Porter erased those fears by providing lawmakers with budget numbers showing that those agencies would retain most of their programs, says one congressional aide. (IARPA's budget is classified but believed to be well in excess of \$100 million.) She's expected to retain her job in the Obama Administration.

Here are some highlights from her recent conversation with *Science*.

—YUDHIJIT BHATTACHARJEE



Less cloak. Lisa Porter hopes most of IARPA's research will be unclassified.

the nuggets of true value. We need to be smarter up front in figuring out where to collect and what to collect. We also need to develop new sensors and new ways of deploying sensors to collect the data we want. Historically, we have relied on satellites and spy planes to look at big targets [such as airfields] that are fairly fixed in space. Today, we're looking for things that could be much smaller and could be moving around [like small weapons].

Even after smart collection, we're going to end up with a lot of data in different forms. Let's say you've got an image of something, you've also got sensor measurements that give you temperature and humidity. How do you fuse all of the information together? How do you line up different pieces of information in time so that you understand what's going on? This is really, really hard and requires new tools of analysis. The third area, safe and secure operations, has to do with addressing future vulnerabilities in cyberspace.

Q: How do you plan to solve these problems?

Part of IARPA's approach is to engage [people] outside the intelligence community as well as within who are working on problems that are analogous. For example, there's research being supported by NASA on how to combine data from airline pilots, the maintenance crew, and the flight recorder to make predictions about future safety risks.

That may be the kind of stuff that we can leverage.

Q: Will researchers be free to publish their results?

There will be programs where the program manager says, "I anticipate this will be fully unclassified, and everything will be publishable."

But sometimes you don't know where the research is going to take you. In those cases, we would have a caveat that although we anticipate the work to be openly publishable, there may be some results coming out of the research that will require a review because it may release sensitive intelligence information.

Q: How will you measure IARPA's success?

If I start rolling out widgets in 6 months, then you need to fire me because I've abandoned the principle of long-term research. In the near term, I'd say the quality of the program managers would be a good metric. Building a reputation for technical integrity is important.

Q: What will IARPA do that's new?

Each of the [intelligence community's] agencies focuses on its particular mission. They are driven by today's challenges. We are forward-looking: Our time horizon is not months but years. We want to ensure that we have the technological advantage to stay ahead of our adversaries.

Q: What are these challenges?

We have divided them into three thrust areas: smart collection, incisive analysis, and safe and secure operations. The problem with the current approach to intelligence gathering is that we are collecting lots and lots and lots of data and then relying on people down the chain to somehow sift through it all and find

NEUROSCIENCE

Brain Scans of Pain Raise Questions for the Law

PALO ALTO, CALIFORNIA—Ready or not, neuroimaging is knocking on the courthouse door. Last summer, Sean Mackey, a neurologist who directs Stanford University's Pain Management Center, was asked by defense lawyers in a workers' compensation case to serve as an expert witness. A man who received chemical burns in a workplace accident was seeking compensation from his employer, claiming that the accident had left him with chronic pain. The evidence his lawyers assembled included functional magnetic resonance imaging (fMRI) scans of his brain that showed heightened activity in the "pain matrix," a network of brain regions implicated in dozens of studies on the neural basis of pain.

But do those scans, taken while technicians gently brushed his afflicted arm or asked him to squeeze a rubber ball, prove that the man was experiencing the agony he claimed? Hardly, says Mackey, who uses fMRI in his own research. The worker may well have had a valid case, Mackey says, but the fMRI findings weren't relevant. Although certain brain regions consistently rev up when people experience pain, neuroscientists have yet to demonstrate that the converse is true: that any particular pattern of brain activity necessarily indicates the presence of pain. "I'm of the strong opinion that in 2008, we cannot use fMRI to detect pain, and we should not be using it in a legal setting," he said here last month.

This particular case did not go to trial: The two sides reached a settlement, says Mackey, who spoke at a Stanford Law School event that brought together neuroscientists and legal scholars to discuss how the neuroimaging of pain potentially could be used—or abused—in the legal system. The general consensus seemed to be that although the science is still emerging, the possibility of legal applications is very real, as Mackey's experience shows.

The intersection of neuroscience and the law has generated a buzz recently, both

among experts and in the popular media. Much of the attention has focused on using fMRI and other methods for lie detection. But Adam Kolber, a law professor at the University of San Diego in California, argued here that pain detection is more likely to be the first fMRI application to find widespread use in the courtroom, in part because the neuroscience of pain is better understood. Kolber estimates that pain is an issue in about half of all tort cases, which include personal injury cases. Billions of dollars are at stake. Yet people with real pain are sometimes unable to prove it, and malingerers sometimes win cases by faking it.

Using fMRI as a painometer isn't straightforward, however. For starters, said Katja Wiech, a cognitive neuroscientist at University College London, pain sensitivity varies considerably from one person to the next. It's also influenced by psychological factors such as anxiety (which tends to make pain worse) and attention (focusing on pain makes it worse; distractions take the edge off). Such influences also show up in fMRI scans, Wiech said. Moreover, she and others noted that several studies have found broad overlap in the brain regions activated by real and imagined pain—something that could be exploited by plaintiffs with bogus claims.

A. Vania Apkarian, a neuroscientist at Northwestern University in Evanston, Illinois, was more optimistic. His group has found that activity in the medial prefrontal cortex and the right insula correlates well with pain intensity and the duration of chronic pain, respectively, in people with chronic back pain. "This is an objective measure of pain in these patients," Apkarian said. Based on these and other findings, he predicted that fMRI will be courtroom-ready sooner than others had suggested. "Maybe not in 2008, maybe in 2012," he said. "It's inevitable."

Apkarian's data looked promising to several legal experts in attendance. "You

scientists care more about causation than we do in the law," said Stanford law professor Henry "Hank" Greely. "If the correlation is high enough, ... we would see that as a useful tool." Indeed, Greely and others noted, even if fMRI can't provide a perfectly objective measure of pain, it may still be better than the alternatives. "We let people get on the stand ... and say all kinds of things that may or may not be true," said William Fletcher, a judge on the U.S. Court of Appeals for the Ninth Circuit.

"There's absolutely no doubt that lawyers will become aware of this [neuroimaging evidence] and push for it," said Stephen Easton, a former trial lawyer and professor at the University of Missouri School of Law. Easton is concerned that fMRI images, like other types of visual evidence, could unduly sway juries. "Pictures can have an aura of objectivity beyond which is justified," he said. Indeed, a handful of recent studies have hinted that non-experts rate articles about human behavior as being more convincing when they're accompanied by irrelevant images of the brain (*Science*, 13 June 2008, p. 1413).

That's an important consideration, said law professor David Faigman of the University of California Hastings College of the Law in San Francisco. According to rule 403 of the Federal Rules of Evidence, judges can disallow relevant evidence if they deem it likely to mislead or prejudice the jury. Rule 403 has been invoked to exclude evidence from polygraph tests, Faigman said, on the grounds that the general public sees the tests as a more valid means of lie detection than they really are. He thinks the same logic could apply to neuroimaging evidence as well.

The verdict is still out, then, on how and to what extent the neuroimaging of pain will enter the legal system. But the opening arguments are already being heard. —GREG MILLER



Pain in the brain. Scholars are wrestling with the legal implications of the neuroimaging of pain.

MICROBIOLOGY

TB Bacteria May Reign Over Cells Intended to Bridle Them

Even before scientists identified the agent that causes tuberculosis (TB), they could tell when it had invaded a person's body from the presence of hallmark lesions called granulomas. These nodules wall off the trouble-making microbe *Mycobacterium tuberculosis* and contain immune cells called macrophages. Conventional wisdom holds that granulomas protect the host, but some work has hinted that they promote bacterial multiplication early in infection. Now, Lalita Ramakrishnan of the University of Washington, Seattle, and graduate student Muse Davis report in the 9 January issue of *Cell* that mycobacteria harness granuloma formation, recruiting new macrophages to the structures and then manipulating the cells into offering the bacteria new quarters in which to reproduce.

Although scientists already realized that granulomas help the TB microbe in the sense that they enable it to hide away and break out decades later, "the belief was that the granuloma is part of a good immune response; it benefits the host," says microbiologist William Bishai of the Johns Hopkins School of Medicine in Baltimore, Maryland. Ramakrishnan "turned the central dogma on its head." Andrea Cooper, an infectious disease immunologist at the Trudeau Institute in Saranac Lake, New York, says the new study "redirects our thinking" to considering how the TB bacterium interacts with macrophages early in infection. The work, she and others say, might open new therapeutic avenues and yield clues about why 90% to 95% of infected humans remain symptom-free for life.

The Seattle pair studied *M. marinum*, a relative of *M. tuberculosis*, in zebrafish embryos, an experimental organism whose power derives in part from its transparency. This attribute allows researchers to literally see how bacteria and immune cells behave, even immediately after exposure, when few microbes are present. The study's medical relevance isn't fully known, as *M. marinum* is not *M. tuberculosis*, and zebrafish are not humans, but "the work raises the question of

whether we've been thinking the wrong way" about granulomas, says microbiologist Eric Rubin of Harvard School of Public Health in Boston.

Davis and Ramakrishnan injected fluorescent *M. marinum* into a cavity above the brain, a site that lacks macrophages in the absence of bacteria, and then recorded video of what happened. Macrophages rapidly arrived, ingested bacteria, and traveled into brain tissue. Within 4 days, collections of infected macrophages—early granulomas—appeared. To distinguish whether these structures form when infected macrophages recruit fresh, uninfected ones or when collections of infected macrophages amass, the researchers waited for an initial group of macrophages to engulf

show up consume chunks of the infected cells, thereby ingesting the bacteria inside. "The key point is that one dying cell is infecting a lot of other cells," says Cooper.

As uninfected macrophages home to the granulomas, they display characteristics of cells that are swimming toward chemical attractants, the researchers observed. The team also discovered that *M. marinum* without a particular region of its genome—RD1—fails to spur key events associated with granuloma formation. RD1 was known to enhance virulence, but no one knew exactly how. The new results suggest that this stretch of mycobacterial DNA somehow triggers granulomas to release a chemical signal that attracts uninfected macrophages. "Here's a clear indication of what RD1

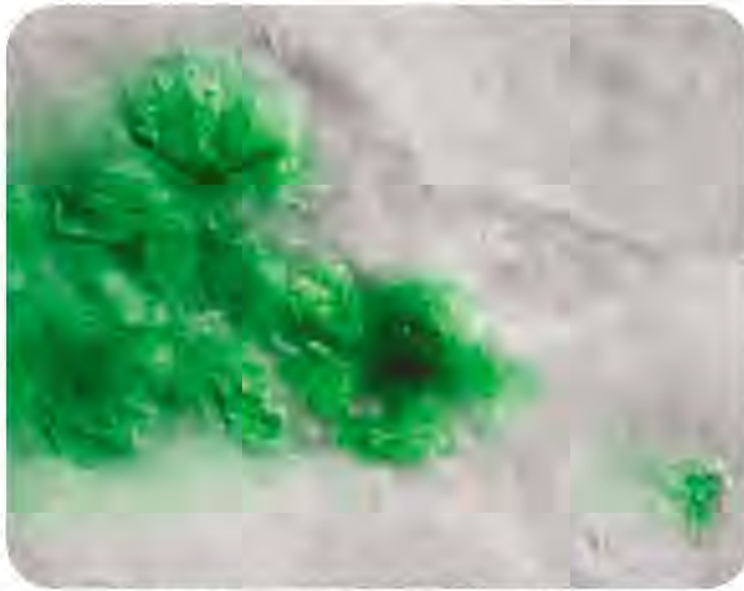
does early in an intact animal," says Cooper.

Additional experiments revealed that macrophages can escape from early granulomas and seed new ones. "Some macrophages serve as taxicabs to bring [bacteria] to locations where new granulomas can form," says Bishai. Further analysis revealed that this process accounts for most, if not all, granulomas that appear elsewhere. This observation contradicts a popular theory, which posits that the bloodstream carries free mycobacteria around the body. Whether the strategy operates in other tuberculosis models is unknown, but preliminary results from monkeys are consistent with the dissemination scheme outlined in the zebra-

fish work, says JoAnne Flynn, an immunologist at the University of Pittsburgh School of Medicine in Pennsylvania.

Studying the RD1 system could generate insights about why most people infected with *M. tuberculosis* don't get sick, suggests Ramakrishnan. Individuals who resist disease may, for example, not respond to RD1's influence. The work might also point toward clinical interventions that quash infection before it takes hold, she says. "If you could intercept the pathway that RD1 uses to lure macrophages, you would have a whole new approach to treating TB."

—EVELYN STRAUSS



Hitching a ride. Infected macrophages (green) can leave established granulomas (left) and seed new ones at other sites in the body.

microbes and then injected a blue compound that marks macrophages into the bloodstream. Because this substance does not cross the blood-brain barrier, any dye found in the brain must have been carried by cells that came from elsewhere. Uninfected animals' brains remained largely colorless, whereas brains of infected animals held numerous blue, infected macrophages within multiple granulomas, indicating that those cells had been recruited by the first responders.

When infected cells in early granulomas die, they retain their contents, the researchers found. The uninfected macrophages that then

PARTICLE PHYSICS

Indian Neutrino Detector Hits Snag on Environmental Concerns



Waiting game. Naba Mondal at INO's proposed site.

team led by B. V. Sreekantan and M. G. K. Menon, using an iron calorimeter in a gold mine shaft, were the first in the world to detect neutrinos created in the atmosphere. The facility was shuttered in 1992 when Kolar Gold Fields closed and the experiment became too costly to maintain. "Many of us in the international community grieved over the termination of that line of work," says John Learned, a physicist at the University of Hawaii, Manoa.

India hopes INO will help it secure a leading position in the next generation of neu-

MASINAGUDI, INDIA—The rosewood and teak forest here in southern India's Nilgiri Biosphere Reserve is prime elephant habitat. It's also where Indian particle physicists hope to install a massive detector to stalk a more exotic quarry: neutrinos. But concerns about the well-being of the heaviest land animals have so far blocked plans to tune in to the lightest known fundamental particles.

The \$167 million India-based Neutrino Observatory (INO), slated for completion in 2012, is the country's most expensive science facility ever. The magnetized iron detector would be nestled in a cavern 2 kilometers deep inside a granite mountain in Tamil Nadu state, some 250 kilometers southeast of Bangalore. Neutrinos are produced in stars as well as on Earth, in nuclear reactors and when cosmic rays smash into the upper atmosphere. They have the slightest mass and are elusive because they interact with other particles only by means of the weak nuclear force. The granite in Nilgiri would absorb most cosmic rays that at the surface would swamp any neutrino signal, but neutrinos will readily pass through to the detector.

A 100-strong team of physicists has conducted site surveys and has begun fabricating detector components at Tata Institute of Fundamental Research (TIFR) in Mumbai and at collaborating institutions. The initiative is "unique and important," says Maury Goodman, a neutrino specialist at Argonne National Laboratory in Illinois. INO, adds Anil Kakodkar, chair of the Atomic Energy Commission, is a "perfect launching pad" for attracting fresh blood into basic sciences in India.

Before work at Nilgiri can begin, INO must obtain a permit from Tamil Nadu's

forestry department. State officials say the physicists have not yet made a convincing case. "INO would be detrimental to the ecological balance of the area," says a senior forestry official, who cites two chief concerns: damage to fragile habitat as equipment and materials are hauled through the forest, and debris from tunneling choking the watershed. The World Wide Fund for Nature-India also opposes the facility, arguing that Nilgiri "is already under pressure, and INO will lead to permanent detrimental impacts on wildlife."

Last month, forestry officials and INO scientists met in Chennai, capital of Tamil Nadu, to seek common ground. Kakodkar and project staff outlined their strategy for minimizing INO's environmental impact. The discussions were "positive," says INO spokesperson Naba K. Mondal, a particle physicist at TIFR. But as *Science* went to press, it was unclear whether the state government would issue a permit.

A few decades ago, India was at the forefront of neutrino research. In 1964, a TIFR

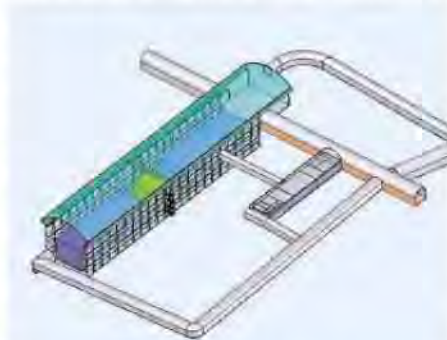
team led by B. V. Sreekantan and M. G. K. Menon, using an iron calorimeter in a gold mine shaft, were the first in the world to detect neutrinos created in the atmosphere. The facility was shuttered in 1992 when Kolar Gold Fields closed and the experiment became too costly to maintain. "Many of us in the international community grieved over the termination of that line of work," says John Learned, a physicist at the University of Hawaii, Manoa.

India hopes INO will help it secure a leading position in the next generation of neutrino research. For instance, more robust estimates of neutrino mass could shed light on an enduring mystery: why there is more matter than antimatter in the universe. The project entails delving an underground laboratory and installing a 50,000-ton detector for studying atmospheric neutrinos and anti-neutrinos. Down the road, the detector could be doubled in size to study neutrinos beamed through the planet from particle accelerators in Europe or Japan. Both experiments aim to yield more precise calculations of neutrino masses. "No large dedicated experiment to study atmospheric neutrinos has ever been built," Goodman says. "The INO design is certainly a better way to study atmospheric neutrinos than has been done before."

According to Mondal, the Nilgiri site is ideal in part because the geology was well-characterized during preparation for a hydroelectric project at the mountain. (The waterworks were built a decade ago, when India's environmental movement was weaker than it is today.) Mondal acknowledges that excavating the tunnel will require hauling huge amounts of materials and rubble through elephant habitat. "No doubt there will be some pain," says Raman Sukumar, an elephant biologist at the Indian Institute of Science in Bangalore who has worked in the area for 3 decades. But he argues that "INO can also be converted into an opportunity" if the project funds conservation efforts in Nilgiri. INO plans to create just such a fund, Mondal says.

In that case, Sukumar says, "both neutrinos and elephants can be winners." Mondal and his colleagues are anxiously waiting to see if Tamil Nadu officials agree.

—PALLAVA BAGLA



Taking the measure. INO aims to make precise calculations of neutrino mass.

On the Origin of Life on Earth



AN AMAZON OF WORDS FLOWED FROM Charles Darwin's pen. His books covered the gamut from barnacles to orchids, from geology to domestication. At the same time, he filled notebooks with his ruminations and scribbled thousands of letters packed with observations and speculations on nature. Yet Darwin dedicated only a few words of his great verbal flood to one of the biggest questions in all of biology: how life began.

The only words he published in a book appeared near the end of *On the Origin of Species*: "Probably all the organic beings which have ever lived on this earth have descended from some one primordial form, into which life was first breathed," Darwin wrote.

Darwin believed that life likely emerged spontaneously from the chemicals it is made of today, such as carbon, nitrogen, and phosphorus. But he did not publish these musings. The English naturalist had built his argument for evolution, in large part, on the processes he could observe around him. He did not think it would be possible to see life originating now because the life that's already here would prevent it from emerging.

In 1871, he outlined the problem in a letter to his friend, botanist Joseph Hooker: "But if (and Oh! what a big if!) we could conceive

in some warm little pond, with all sorts of ammonia and phosphoric salts, light, heat, electricity, etc., present, that a protein compound was chemically formed ready to undergo still more complex changes, at the present day such matter would be instantly devoured or absorbed, which would not have been the case before living creatures were formed."

Scientists today who study the origin of life do not share Darwin's pessimism about our ability to reconstruct those early moments. "Now is a good time to be doing this research, because the prospects for success are greater than they have ever been," says John Sutherland, a chemist at the University of Manchester in the United Kingdom. He and others are addressing each of the steps involved in the transition to life: where the raw materials came from, how complex organic molecules such as RNA formed, and how the first cells arose. In doing so, they are inching their way toward making life from scratch. "When I was in graduate school, people thought investigating the origin of life was something old scientists did at the end of their career, when they could sit in an armchair and speculate," says Henderson James Cleaves of the Carnegie Institution for Science in Washington, D.C. "Now making an artificial cell doesn't sound like science fiction any more. It's a reasonable pursuit."

Raw ingredients

Life—or at least life as we know it—appears to have emerged on Earth only once. Just about all organisms use double-stranded DNA to encode genetic information, for example. They copy their genes into RNA and then translate RNA into proteins. The genetic code they use to translate DNA into proteins is identical, whether they are emus or bread mold. The simplest explanation for this shared biology is that all living things inherited it from a common ancestor—namely, DNA-based microbes that lived more than 3.5 billion years ago. That common ancestor was already fairly complex, and many scientists have wondered how it might have evolved from a simpler predecessor. Some now argue that membrane-bound cells with only RNA inside predated both DNA

and proteins. Later, RNA-based life may have evolved the ability to assemble amino acids into proteins. It's a small step, biochemically, for DNA to evolve from RNA.

In modern cells, RNA is remarkably versatile. It can sense the levels of various compounds inside a cell and switch genes on and off to adjust these concentrations, for example. It can also join together amino acids, the building blocks of proteins. Thus, the first cells might have tapped RNA for all the tasks on which life depends.

For 60 years, researchers have been honing theories about the sources of the amino acids and RNA's building blocks. Over time, they have had to refine their ideas to take into account an ever-clearer understanding of what early Earth was like.

In an iconic experiment in 1953, Stanley Miller, then at the University of Chicago, ignited a spark that zapped through a chamber filled with ammonia, methane, and other gases. The spark created a goo rich in amino acids, and, based on his results, Miller suggested that lightning on the early Earth could have created many compounds that would later be assembled into living things.

By the 1990s, however, the accumulated evidence indicated that the early Earth was dominated by carbon dioxide, with a pinch of nitrogen—two gases not found in Miller's flask. When scientists tried to replicate Miller's experiments with carbon dioxide in the mix, their sparks seemed to make almost no amino acids. The raw materials for life would have had to come from elsewhere, they concluded.

In 2008, however, lightning began to look promising once again. Cleaves and his colleagues suspected that the failed experiments were flawed because the sparks might have produced nitrogen compounds that destroyed any newly formed amino acids. When they added buffering chemicals that could take up these nitrogen compounds, the experiments generated hundreds of times more amino acids than scientists had previously found.

Cleaves suspects that lightning was only one of several ways in which organic compounds built up on Earth. Meteorites that fall to Earth contain amino acids and organic carbon molecules such as formaldehyde. Hydrothermal vents spew out other compounds that could have been incorporated into the first life forms. Raw materials were not an issue, he says: "The real hurdle is how you put together organic compounds into a living system."

Step 1: Make RNA

An RNA molecule is a chain of linked nucleotides. Each nucleotide in turn consists of three parts: a base (which functions as a

THE YEAR OF DARWIN



This essay is the first in a monthly series, with more on evolutionary roots online at blogs.sciencemag.org/origins

“letter” in a gene’s recipe), a sugar molecule, and a cluster of phosphorus and oxygen atoms, which link one sugar to the next. For years, researchers have tried in vain to synthesize RNA by producing sugars and bases, joining them together, and then adding phosphates. “It just doesn’t work,” says Sutherland.

This failure has led scientists to consider two other hypotheses about how RNA came to be. Cleaves and others think RNA-based life may have evolved from organisms that used a different genetic material—one no longer found in nature. Chemists have been able to use other compounds to build backbones for nucleotides (*Science*, 17 November 2000, p. 1306). They’re now investigating whether these humanmade genetic molecules, called PNA and TNA, could have emerged on their own on the early Earth more easily than RNA. According to this hypothesis, RNA evolved later and replaced the earlier molecule.

But it could also be that RNA wasn’t put together the way scientists have thought. “If you want to get from Boston to New York, there is an obvious way to go. But if you can’t get there that way, there are other ways you could go,” says Sutherland. He and his colleagues have been trying to build RNA from simple organic compounds, such as formaldehyde, that existed on Earth before life began. They find they make better progress toward producing RNA if they combine the components of sugars and the components of bases together instead of separately making complete sugars and bases first.

Over the past few years, they have documented almost an entire route from prebiotic molecules to RNA and are preparing to publish even more details of their success. Discovering these new reactions makes Sutherland suspect it wouldn’t have been that hard for RNA to emerge directly from an organic

soup. “We’ve got the molecules in our sights,” he says.

Sutherland can’t say for sure where these reactions took place on the early Earth, but he notes that they work well at the temperatures and pH levels found in ponds. If those ponds dried up temporarily, they would concentrate the nucleotides, making conditions for life even more favorable.

Were these Darwin’s warm little ponds? “It might just be that he wasn’t too far off,” says Sutherland.

Step 2: The cell

If life did start out with RNA alone, that RNA

would need to make copies of itself without help from proteins. Online in *Science* this week (www.sciencemag.org/cgi/content/abstract/1167856), Tracey Lincoln and Gerald Joyce of the Scripps Research Institute in San Diego, California, have shown how that might have been possible. They designed a pair of RNA molecules that join together and assemble loose nucleotides to match their partner. Once the replication is complete, old and new RNA molecules separate and join with new partners to form new RNA. In 30 hours, Lincoln and Joyce found, a population of RNA molecules could grow 100 million times bigger.

Lincoln and Joyce kept their RNA molecules in beakers. On the early Earth, however, replicating RNA might have been packed in the first cells. Jack Szostak and his colleagues at Harvard Medical School in Boston have been investigating how fatty acids and other molecules on the early Earth might have trapped

RNA, producing the first protocells. “The goal is to have something that can replicate by itself, using just chemistry,” says Szostak.

After 2 decades, he and his colleagues have come up with RNA molecules that can build copies of other short RNA molecules.

They have been able to mix RNA and fatty acids together in such a way that the RNA gets trapped in vesicles. The vesicles are able to add fatty acids to their membranes and grow. In July 2008, Szostak reported that he had figured out how protocells could “eat” and bring in nucleotides to build the RNA.

“Now making an artificial cell doesn’t sound like science fiction any more. It’s a reasonable pursuit.”

—HENDERSON JAMES CLEAVES,
CARNEGIE INSTITUTION FOR SCIENCE

All living cells depend on complicated channels to draw nucleotides across their membranes, raising the question of how a primitive protocell membrane brought in these molecules. By experimenting with different recipes for membranes, Szostak and his colleagues have come up with protocells leaky enough to let nucleic acids slip inside, where they could be assembled into RNA, but not so porous that the large RNA could slip out.

Their experiments also show that these vesicles survive over a 100°C range. At high temperatures, protocells take in nucleotides quickly, and at lower temperatures, Szostak found, they build RNA molecules faster.

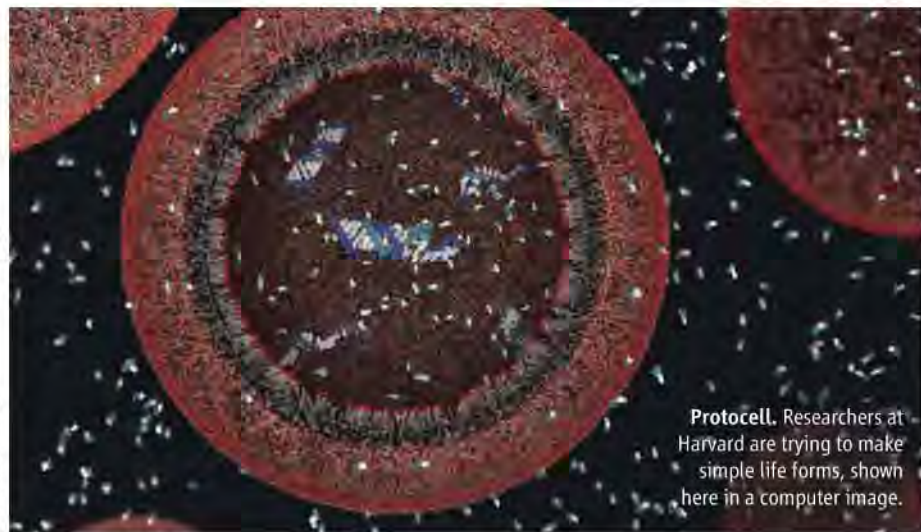
He speculates that regular temperature cycles could have helped simple protocells survive on the early Earth. They could draw in nucleotides when they were warm and then use them to build RNA when the temperature dropped. In Szostak’s protocells, nucleotides are arranged along a template of RNA. Strands of RNA tend to stick together at low temperatures. When the protocell warmed up again, the heat might cause the two strands to pull apart, allowing the new RNA molecule to function.

Now Szostak is running experiments to bring his protocells closer to life. He is developing new forms of RNA that may be able to replicate longer molecules faster. For him, the true test of his experiments will be whether his protocells not only grow and reproduce, but evolve.

“To me, the origin of life and the origin of Darwinian evolution are essentially the same thing,” says Szostak. And if Darwin was alive today, he might well be willing to write a lot more about how life began.

—CARL ZIMMER

Carl Zimmer is the author of *Microcosm: E. coli and the New Science of Life*.



Protocell. Researchers at Harvard are trying to make simple life forms, shown here in a computer image.

CREDIT: JANET IWASA



Seeking Africa's First Iron Men

Archaeologists are battling over when—and how—ancient African cultures entered the Iron Age

According to myth, Rwanda's ancient line of kings descended from a man with secret knowledge: He could transform chunks of ordinary rock into smooth, gleaming iron. With this new technology, he taught his people to make hard, durable weapons for defeating their enemies and sharp axes for cutting the forest to make fields. By the time the first Europeans arrived in the 19th century, iron had become power in the kingdom of Rwanda. Its kings had taken the blacksmith's hammer and anvil for their royal regalia, and at least one Rwandan ruler was buried with his head resting on two iron anvils.

Other traditional African societies tell stories of mythical ironworkers who descended from heaven or came from other lands. The prevalence of such legends underlines the importance of ironworking in these cultures, and archaeologists have long wondered if the arrival of iron metallurgy spurred the growth of complex early societies. Did foreigners in fact bring ironworking to

Africa, or did Africans invent it themselves?

Entering the Iron Age was not easy. Metalworkers had to smelt ore at precise temperatures and then repeatedly hammer and reheat the spongy metal, known as a bloom, that first emerged from their furnaces. The traditional view is that metallurgists in Anatolia, the

Asian part of Turkey, were the first to smelt iron ore deliberately, beginning around 1800 B.C.E. Initially, they reserved the new metal for precious ornaments or ritual objects. But by 1200 B.C.E., workers in the Levant were churning out considerable amounts of iron.

The metal had a major impact on societies. "Iron was a transformative metal," says archaeologist Scott MacEachern of Bowdoin College in Brunswick, Maine. Iron ores are much more abundant than copper or the tin needed to make bronze. Bronze was therefore costly and largely limited to use in ritual objects and goods for elites. But once cultures learned to smelt iron, they could put iron tools into the hands of ordinary people for clearing forests and tilling the soils. According to some models, this boosted agricultural yields, increased the numbers of villages, and triggered ever more social complexity.

A long debate has raged, however, about the origin of ironmaking in Africa. According to traditional thinking, iron metallurgy diffused slowly from one society to the next in the Old World, reaching northern Africa by 750 B.C.E. but not crossing the barrier of



First iron? Controversial sites from some countries in sub-Saharan Africa suggest that iron smelting was developed there 4000 years ago.

CREDIT: DAVID KILICK

Smiths at work. Demonstrating old methods, Cameroonian men forge iron with a stone hammer.

the Sahara Desert until 500 B.C.E. or later.

Now controversial findings from a French team working at the site of Ôbouï in the Central African Republic challenge the diffusion model. Artifacts there suggest that sub-Saharan Africans were making iron by at least 2000 B.C.E. and possibly much earlier—well before Middle Easterners, says team member Philippe Fluzin, an archaeometallurgist at the University of Technology of Belfort-Montbéliard in Belfort, France. The team unearthed a blacksmith's forge and copious iron artifacts, including pieces of iron bloom and two needles, as they describe in a recent monograph, *Les Ateliers d'Ôbouï*, published in Paris. "Effectively, the oldest known sites for iron metallurgy are in Africa," Fluzin says.

Some researchers are impressed, particularly by a cluster of consistent radiocarbon dates. The new finds should prompt researchers to explore how sub-Saharan metal smiths could have worked out iron production without the benefit of an earlier Copper or Bronze Age, says archaeologist Augustin F. C. Holl of the University of Michigan, Ann Arbor. "We are in a situation where we have to rethink how technology evolves," he says.

Others, however, raise serious questions about the new claims. Archaeometallurgist David Killick at the University of Arizona in Tucson says the Ôbouï iron artifacts are far too well preserved for the dates given: "There is simply no way that they have been sitting in the ground for 3800 radiocarbon years in acidic soils and a seasonally moist environment like the western Central African Republic."

An invisible equation

The idea that iron metallurgy diffused to Africa from the Middle East, rather than being invented independently, receives its strongest support from the sheer complexity of iron smelting. Working meteoritic iron is fairly straightforward, but to extract iron from hematite and other common ores, early metalworkers had to bring the ore to a precise range of temperatures, so the iron could fuse with carbon released from the burning of charcoal. To pull off this feat, smelters had to master an invisible equation, placing the ore out of sight in a clay furnace fueled with the

correct amount of charcoal and fed with just the right amount of air for combustion. According to the diffusion theory, only people who possessed millennia of experience working copper, such as the Anatolians, would have had sufficient knowledge to begin experimenting with iron.

The archaeological data on early ironworking in northern Africa are frustratingly spotty, but current evidence suggests that Phoenician traders carried the technology to their colony of Carthage in northern Africa around 750 B.C.E. Other travelers brought iron technology to Egypt, which already possessed copper, by 660 B.C.E., if not earlier. The wealthy Nubian kingdom just to the south possessed bronze and began smelting iron between 800 and 500 B.C.E. In

ently as early as 3600 B.C.E. Their analyses were strongly criticized by prominent researchers in the United States, who argued that the early radiocarbon dates likely came from wood older than the iron artifacts. In reviewing the debate in a 2005 paper in the journal *History in Africa*, independent scholar Stanley Alpern suggested that Francophone researchers had fallen under the influence of African nationalism and pride, which blinded them to problems in their data. The critiques persuaded many researchers outside France that the earliest good evidence for sub-Saharan African ironworking came from carefully excavated sites dated between 800 and 400 B.C.E., such as Walalde in Senegal, where a complex society of pastoralists and craft specialists may



Digging for iron. Nine field seasons at Ôbouï revealed an ancient iron workshop and artifacts such as this iron needle (left).

the Nubian city of Meroë, workers created an iron industry that one writer dubbed "the Birmingham of Africa," because as with the British town, iron was the source of Meroë's wealth. The city produced an estimated 5 to 20 tons of the metal annually for hoes, knives, spears, and other everyday goods, as Thilo Rehren, an archaeometallurgist at University College London, wrote in a 2001 article in *Mitteilungen der Sudanarchäologischen Gesellschaft*. From North Africa, the technology was thought to have crossed the Sahara Desert around 500 B.C.E., spreading to southern lands that lacked both copper and bronze-working traditions.

Evidence contradictory to this model has cropped up since the 1960s, however. Several French and Belgian archaeologists have pointed to evidence from sites in Niger, Rwanda, and Burundi suggesting that Africans invented ironworking independ-

have developed a trading system using precious iron bars for exchange.

Meanwhile, French proponents of the very early dates dismissed such charges as the last gasp of scientists wedded to the diffusion model. A frosty impasse ensued: Many Francophone Africanists stopped attending Anglophone meetings and informally sharing their research results. "There is a taboo there," fumes Holl. "People just have this conception that iron technology in sub-Saharan Africa has to be later than 500 B.C.E., and when it is earlier than that, they start looking for [alternative] explanations."

The deep chill lasted until the fall of 2008, when Anglophone researchers learned that a French team led by archaeologist Étienne Zangato of the University of Paris X had published the Ôbouï monograph a year earlier with sensational new evidence for ancient African ironworking. Now the controversy has fired up again.



Forging ahead. Excavator Étienne Zangato claims early dates from Ôbouï's forge (left) show that Africans were the first ironsmiths.



An ancient forge

Zangato's most important data come from Ôbouï, a site where horticulturists and fishers lived for millennia; by 800 B.C.E., people in the region were erecting megaliths and burying important people in impressive tombs.

Zangato began excavations at the site after a violent storm struck in 1992, sweeping away part of the capping sediments and exposing a layer of metallic objects, potsherds, and stone tools. Zangato and his team spent nine field seasons at the site, opening more than 800 square meters. They recovered 339 stone artifacts and a host of evidence for ironsmithing: a blacksmith's forge, consisting of a clay-lined furnace, stone anvil, and part of a ceramic pot that likely held water for cooling or possibly tempering red-hot iron. They also found charcoal storage pits, 1450 pieces of slag, 181 pieces of iron bloom, and 280 small iron lumps and objects, including two needles.

Fluzin detected none of the telltale waste produced by the first stage of smelting, implying that Ôbouï's smiths imported iron bloom from elsewhere or that excavators have yet to find the site's smelting area. But microscopic examination of thin slices from iron samples collected near the anvil demonstrates that people at Ôbouï purified the bloom by repeatedly heating and hammering it. Some lumps contained as much as 85% iron and revealed visible traces of hammering, such as deformations caused by crushing, under the microscope. "It is undeniable that these samples correspond to metalworking, already quite advanced, of fragments of bloom," concludes Fluzin. His comparative studies of minerals in the ore suggest that the most likely source was an ancient mine located 12 kilometers away.

To date the site, seven charcoal samples were taken from inside and outside the furnace. They were radiocarbon dated by Jean-François Saliège in the Laboratory of Dynamic Oceanography and Climatology at the University of Paris VI to between 2343 and

1900 B.C.E.—long before the Anatolians were working iron.

Those dates are early, but they fit well with a newly emerging pattern, says Zangato. Excavations he directed between 1989 and 2000 at the three nearby sites of Balimbé, Bétumé, and Bouboun each un-

covered layers containing ironworking debris, he says. Those layers were radiocarbon dated by Zangato, Saliège, and Magloire Mandeng-Yogo of the Institute of Research for Development in Bondy, France, to between 1612 and 2135 B.C.E. at Balimbé and Bouboun, and to sometime between 2930 and 3490 B.C.E. at Bétumé. "There is no longer any reason to cling to the diffusionist theory for iron metallurgy in Africa," says Zangato. "I believe more and more in local development [of the technology]."

The evidence is very convincing, says Patrick Pion, a University of Paris X archaeologist who specializes in the European Iron Age. The metallographic analysis is clear proof of ironworking at Ôbouï, he says, and "the series of C^{14} dates obtained are coherent, done by a laboratory and a specialist recognized for C^{14} dating in Africa. I see no reason intrinsically to question them." MacEachern agrees that the seven consistently early dates from the forge are persuasive. "This is not the common situation that we've had in the past in African metallurgy, where we've had isolated dates from debatable contexts," he says.

But Killick and others are completely



Tools of power. In the ancient Nubian city of Meroë, iron used for durable tools, like this small tool kit, became the source of great wealth.

unconvinced by the dates, though they agree that the forge is real. "Although it seems that the seven oldest radiocarbon dates form a coherent group, they are all coming from a few square meters in a very disturbed archaeological site," says Bernard Clist, an archaeologist at the Institute of Research for Development in Grasse, France. "They are closely bounded by pits and structures well dated to around 2000 B.P. and later." This means that later ironworkers could have dug into ground laced with charcoal from an earlier occupation or forest fire, giving dates that are far too old. To push back the dates convincingly, say critics, the team needs to publish more detailed stratigraphic data and charcoal studies. They also need several consistent lines of chronological evidence, such as thermoluminescence (TL) dates on clay furnaces, accelerator mass spectrometry (AMS) dates on short-lived plant remains, and indirect dates from sequences of ceramic styles.

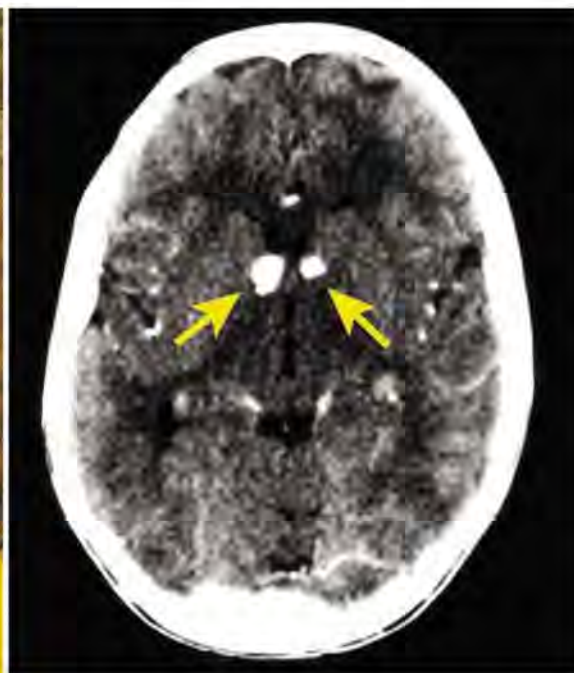
Zangato concedes that the team's case would have benefited from more dating. But he says that the €500,000 he received for the 15-year project from France's Ministry of Foreign Affairs was insufficient to cover expensive TL and AMS dates; he opted for additional radiocarbon dates instead. He and Fluzin dismiss the charge that the iron artifacts are too pristine for their age, saying that a dense, difficult-to-excavate upper layer of sandy clay at Ôbouï prevented the diffusion of water and oxygen, and so reduced corrosion. Killick counters that the high soil temperatures at the site should in fact speed corrosion. If Ôbouï's iron bloom really dates back to 2000 B.C.E., then its open pores "ought to be completely full of corrosion products, leaving small islands of metal in a sea of corrosion," says Killick. There is no sign of this in the published photos. Even MacEachern finds the relative lack of corrosion puzzling. "I'd certainly like to know more about the preservation of the iron tools," he says.

Neither Zangato nor Fluzin is backing away from their claims, however. Zangato and Holl are working on a paper for the World of Iron conference in London from 16 to 20 February. Expect lively sessions, says conference organizer and archaeometallurgist Xander Veldhuijzen of University College London: "The earliest iron debate is currently in a very interesting phase, as a lot of new evidence is just appearing."

—HEATHER PRINGLE

Heather Pringle is a contributing editor at *Archaeology* magazine.

CREDITS: COURTESY OF ÉTIENNE ZANGATO; COURTESY OF THE ORIENTAL INSTITUTE



BIOMEDICINE

A New View on—and Hope for—an Old Disease

Researchers are debating whether growths called tubers cause the mental problems in many people with tuberous sclerosis. Regardless, an organ-transplant drug may offer a treatment for the rare disease

It can start so subtly that most parents don't even notice the telltale signs. A baby's arms and upper body may jerk, or the eyes may dart to the side; the seizure is brief, with muscles momentarily stiffening and then relaxing. It's usually only when their baby gets a bit older that parents notice that the child is having problems with walking or talking. But even then, they will hardly suspect what's behind the symptoms: growths called tubers, sometimes hundreds of them, which have sprouted throughout their child's body.

In Laura Jensen's case, the mother from California thought her baby boy's gagging spells were caused by teething, until one episode, when he was 9 months old, made it clear something much more serious was going on. "He made a choking noise, his face turned blue, and his mouth started to pull to one side," she recalls. "I didn't know it was a seizure, but I sure knew it wasn't teething."

When Jensen was finally referred to a neurologist, who diagnosed her son with a rare condition called tuberous sclerosis complex (TSC), she had no clue what it was. She soon learned that her son would likely be

plagued with crippling seizures for the first few years of his life. In addition, children with TSC can end up severely mentally handicapped, autistic, or nonverbal. The disease is sometimes disfiguring, as tubers may erupt on the face or elsewhere under the skin. It can also kill in several ways, by causing kidney failure or destroying lung function, for example (see sidebar, p. 204). Fortunately, Jensen's son, now 16 years old, is one of the lucky ones; his symptoms have turned out to be comparatively benign.

The mental disabilities that accompany TSC have traditionally been tied to the tubers that form in the brain. Researchers have assumed that the growths, lodged in areas critical for cognition, disrupt and impair normal brain functioning. Scientists have, therefore, tried to attack the disease by thwarting tuber growth. After connecting TSC to a signaling cascade already implicated in cancers, they have begun clinical trials with rapamycin, an organ-transplant drug approved by the U.S. Food and Drug Administration. At a conference this fall on TSC in Brighton, U.K., several groups presented results from

Growth problem. In tuberous sclerosis, growths can appear under the skin and freckle a face (left) or disrupt a brain (right, arrows).

rapamycin trials showing dramatic tuber shrinkage in various organs, including the brain. "There's tremendous excitement about it," says Elisabeth Henske, an oncologist who also works on TSC at Brigham and Women's Hospital in Boston.

Yet along with this enthusiasm comes a new debate about what exactly is causing the mental problems of some people with TSC. Petrus J. de Vries, a pediatric psychologist at the University of Cambridge in the United Kingdom, has recently tried to convince his colleagues that their focus on tubers as the source of the condition's cognitive impairment is too narrow. De Vries has studied young tuberous sclerosis patients for decades, and he believes that the growths in the brain are not the sole culprits. If his controversial theory is right, tuberous sclerosis researchers will have to significantly rethink what they know about this strange disease. "I like stirring things up a little bit," says De Vries. "I think it's important to make people question their assumptions."

Decoding the disease

TSC was first documented in 1880 by Désiré-Magloire Bourneville, a French neurologist who treated a 15-year-old boy with severe retardation and epilepsy. After the patient died, Bourneville found clusters of tuberlike growths throughout the boy's brain. These noncancerous growths, the

A Discriminating Killer

One of tuberous sclerosis complex's (TSC's) most mysterious manifestations is lymphangioleiomyomatosis (LAM), a progressive lung disease that is decidedly sexist. The disease affects only women, usually in their childbearing years, and typically proves fatal within a decade or two of its diagnosis.

Surprisingly, the tuberous growths that are a hallmark of TSC aren't the problem. Instead, LAM is caused by smooth muscle cells that invade the lungs. Researchers don't know where these invaders come from, nor what makes the cells spread to the lungs, where their accumulation slowly impairs breathing. "We don't know why the [cells] metastasize; ... they look benign under the microscope," says Elisabeth Henske, an oncologist at Brigham and Women's Hospital in Boston who specializes in LAM. She notes that the disease can come back even after a patient has had a lung transplant, confirming that the source of the smooth muscle cells is somewhere other than the lungs.

The disease's gender preference also remains inexplicable. "We're trying to address why this happens only in women," says Henske. "We're looking to see whether there is something in estrogen that would be involved in a metastatic process." Despite these mysteries, a new treatment could be on the horizon: A small study done at the Cincinnati Children's Hospital Medical Center in January 2008 found that the organ-transplant drug rapamycin improved lung function in some LAM patients. Now, a larger, phase II trial on 120 LAM patients is under way as scientists seek to confirm that the drug can truly keep the disease at bay.

—L.C.



Out of breath. A CT scan (above) can reveal how lymphangioleiomyomatosis obstructs lungs.

hallmark of the disease, can show up not only in the brain but also in the heart, eyes, skin, kidneys, and lungs.

The disease is rare, striking just 1 in 6000 births, so researchers typically have difficulty finding large populations of patients to study. However, a few decades ago, scientists identified several large families in which TSC showed up several times, indicating it was a genetic disease. Researchers began looking at the genes of these families and in 1993, a European consortium of TSC investigators linked mutations in a gene on chromosome 16 to the disease in some of the families. Five years later, a group led by Marjon van Slegtenhorst at Erasmus University in Rotterdam, the Netherlands, located a gene on chromosome 11 that when mutated also leads to the disease (*Science*, 8 August 1997, p. 805).

That gene encodes a protein called harmatin, whereas the chromosome 16 gene encodes one called tuberlin. Both proteins are located inside cells throughout all tissues of the body. Scientists found that either the tuberlin or harmatin gene was not functioning in the tuber growths of people with TSC, suggesting that the proteins were somehow involved in suppressing cell growth.

Mutant fruit flies helped confirm this. Scientists genetically engineered strains of the insect lacking either tuberlin, harmatin, or

both proteins. All three kinds of mutants developed the same abnormalities—grossly large eyes, organs, and wings—indicating that their cell growth and proliferation had gone unchecked.

In 1998, the Van Slegtenhorst group had shown that harmatin and tuberlin bind together and function as a unit inside cells. With more fruit fly and mammalian studies, a number of research teams then independently determined that this molecular complex crucial to TSC participated in a signal cascade known as the mTOR pathway. This pathway is the main molecular switchboard for cellular growth: The protein mTOR, short for molecular target of rapamycin, directly activates a protein called S6K, thus driving cell growth. Depending on the energy state of the cell, upstream proteins, such as PI3Kinase, AKT, and insulin, will signal mTOR to increase or decrease cell growth.

Researchers have learned that tuberlin and harmatin act as the primary upstream brake on mTOR's drive for cell growth. The pair does this by inhibiting the protein Rheb, the direct activator for mTOR and cell proliferation. Consequently, if the tuberlin-harmatin complex malfunctions, say as a result of a mutation in one of the genes for the proteins, mTOR's brake is released. Unbridled, mTOR is thought to cause not only the tubers in TSC

but also tumor formation in most types of cancer. The realization that the tuberous sclerosis proteins were connected to mTOR "dumped us right in the center of a topical and hot regulatory pathway," says Julian Sampson, a medical geneticist and TSC researcher at Cardiff University in the United Kingdom. "So then another heap of people got interested in these genes and proteins."

De Vries agrees that the study of TSC took off once it was connected to the mTOR pathway. "That's when things started to explode," he says.

Brain debates

With the disrupted molecular pathway in TSC finally delineated, researchers are now trying to resolve how that leads to the disease's most severe manifestations, the problems in the brain. "The most devastating things about tuberous sclerosis are the cognitive deficits and the intractable epilepsy," says Vicky Holets Whittemore, vice president of the Tuberous Sclerosis Alliance. Roughly 70% of TSC patients have epilepsy, 25% develop autism, and 25% have severe mental disabilities. Although 40% to 50% of people with TSC will score normally on IQ tests, even they seem to have very specific problems with certain key memory and attention-related tasks.

Perhaps one of the most difficult aspects of the disease is the uncertain prognosis once a child is diagnosed. "You can't predict how severely affected a child is going to be after they're born," says John Yates, a retired medical geneticist at the University of Cambridge. "You can't tell if a child [will have] huge mental problems or a few blemishes on the skin."

Studies have shown that the frequency of seizures can affect a child's ultimate cognitive ability; thus, antiepileptic medication is often the first line of defense when a child receives a TSC diagnosis. Still, although several medications are effective at stopping seizures, some people develop severe mental disabilities anyway. That's one reason many scientists have blamed the tubers in the brain, not the seizures they cause, for a person's mental problems. Indeed, several case studies show that the number and size of tubers correlate with more severe cognitive deficits.

Yet De Vries, and a growing number of other researchers, contend that neither seizures nor tubers are responsible. "People thought that more tubers equals more brain problems," says De Vries. "But the more data we collected, the less clear it became to me. We've had adult patients with Ph.D.s,

who have 20 to 30 tubers [in their brains], and people with severe [mental] problems with one or two tubers—so there were lots of exceptions to the rule.”

If the tubers aren’t causing mental dysfunction, what is? De Vries suggests that mutations in the genes for tuberin and harmatin directly sabotage neurons by disrupting the mTOR pathway. He notes that the mTOR pathway helps control formation of the cytoskeleton within neurons and the synapses that provide connections between neurons, as well as the brain’s production of myelin, which insulates nerve fibers. Defects in any or all of these functions, he suggests, could explain TSC’s severe cognition problems. Additionally, the mTOR pathway is necessary for long-term potentiation, the process by which neurons in the brain retain memories; that may explain the memory problems many people with TSC experience. “All you need is a disruption of [this] pathway,” says De Vries.

De Vries’s theory is relatively new—he published the idea in the summer of 2007—but it’s gaining influence. Several studies on mouse and rat models of TSC have shown that even the animals without seizures or tubers in the brain have cognitive problems. “I think the tubers sort of distracted everybody for a long time,” says Whittemore. “Everyone’s beginning to understand that there’s an underlying molecular issue.”

Still, not everyone is convinced. After De Vries’s presentation in Brighton, scientists in the audience expressed their doubts. In gen-

eral, Yates says, most people with extreme cognitive deficits usually have a history of severe seizures or several tubers in the brain or both. Yates also argued that if the mTOR pathway disruption in neurons was the real culprit, then family members with TSC would have very similar manifestations of the disease, rather than the wildly different presentations that can happen between parents and children or between siblings

Wonder drug?

While researchers in Brighton debated the roots of TSC’s mental dysfunction, they also discussed the merits of the disease’s most promising treatment: rapamycin. Like the molecular complex naturally formed by the tuberin and harmatin proteins, this drug blocks mTOR activity and thus prevents cell proliferation. Currently, it’s used as an immunosuppressant for organ transplant patients—the drug prevents the proliferation of immune cells that target a donor organ—and is being tested in clinical trials as a treatment for renal cancers. Scientists and doctors have theorized that the drug’s restraint of mTOR could compensate for TSC patients’ defective genes, stopping the abnormal cell growth behind tubers. Bolstering this hypothesis, several research groups at the Bristol meeting presented initial results from phase II trials that showed rapamycin significantly shrinks tubers in both the brain and the kidney, on average.

Perhaps even more tantalizing is the possibility that rapamycin could address TSC’s epilepsy and cognitive problems. If de Vries is right, and the disruption of the mTOR pathway in neurons indeed causes the mental problems in TSC, rapamycin should be able to treat the condition’s actual molecular dysfunction.

Researchers have recently proved the concept in animal models; Michael Wong, a neurologist at Washington University School of Medicine in St. Louis, has found that in a mouse model of TSC that includes epilepsy, daily doses of rapamycin will prevent the seizures. A research group at the University of California, Los Angeles, led by neuroscientist Dan Ehninger, also looked at rapamycin’s effect on a strain of mice with mutations in the tuberin gene that develop learning and memory problems but that didn’t have tuber growths or seizures. Ehninger’s team found that rapamycin completely rescued adults of



“I think it’s important to make people question their assumptions.”

—PETRUS J. DE VRIES,
CAMBRIDGE UNIVERSITY

this strain from their cognitive problems, making them just like wild-type mice. These studies have some TSC scientists more hopeful than they’ve ever been. “I think that’s truly one of the more exciting things to evolve over the years I’ve been involved in TSC research,” says Henske. “It’s paradigm-shifting—precedent-setting.”

In people with TSC, however, evidence for rapamycin’s effect on cognition and seizures remains largely anecdotal; doctors have mentioned that the drug seems to improve mental functions of some patients. In the United Kingdom, an ongoing phase II trial

of rapamycin’s effects on kidney tubers and lung functioning is also measuring how the participants’ memory is affected by the drug. At the conference, De Vries announced that eight out of 13 people taking the drug have so far showed a memory improvement, but two have seen their memory worsen.

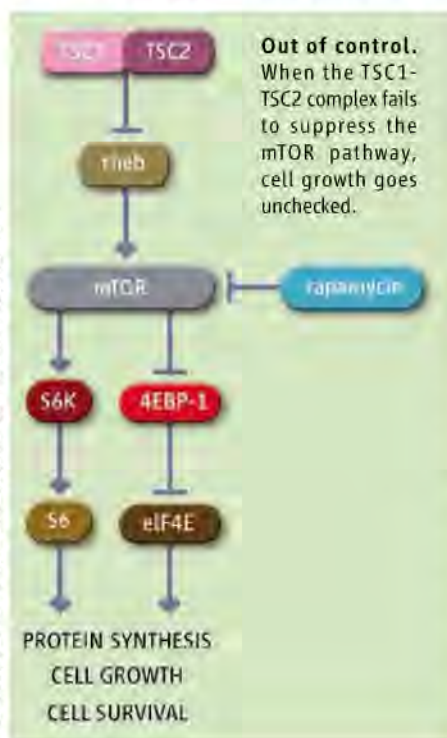
Even in terms of restraining tubers, rapamycin is far from a silver bullet. In the phase II trials, the moment a patient went off the drug, his or her tubers began to grow back, researchers reported at the meeting. Wong had a similar outcome with his experiments in epileptic TSC mice. “They were normal as long as they were on the rapamycin,” he says. “If you take them off of it—the symptoms happen again.”

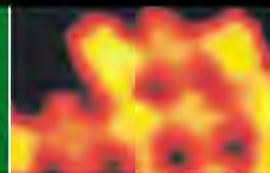
That distresses Sampson. Chronic use of rapamycin is not advisable, he notes, because of its immunosuppressive properties. “It’s controlling [tubers], not curing them,” he says. “If you’re thinking of a therapy that’s going to be long term, ... this isn’t a cure for tuberous sclerosis.”

Still, many TSC scientists are pleased at the progress and hopeful that rapamycin can be fine-tuned into a safe and effective treatment. At the conference in Brighton, De Vries noted how far the understanding of this odd and rare disease has come. “It is very exciting to see how we have moved on in the field. My first TSC conference was in 1998, and the second gene had just been cloned—we had no idea about all the events, including drug trials, awaiting us 10 years later,” he says. “It will be very interesting to see where the field will be at in 2018.”

—LAUREN CAHOON

Lauren Cahoon is a freelance writer based in Ithaca, New York.





LETTERS

edited by Jennifer Sills

Unsung Hero Robert C. Gallo

AWARDING THE NOBEL PRIZE IN PHYSIOLOGY OR MEDICINE TO FRANCOISE BARRÉ-SINOUSSE and Luc Montagnier for the discovery of HIV-1, the causative agent of AIDS (1), is timely given the harm that the virus continues to inflict on the people of the world.

While these awardees fully deserve the award, it is equally important to recognize the contributions of Robert C. Gallo. Gallo definitively proved HIV-1 as the cause of AIDS through the successful isolation and long-term cultivation of HIV-1 and developed a diagnostic kit that prevented new infections and saved thousands of lives. These contributions, together with Gallo's earlier discovery of interleukin-2 (fundamental for growing HIV-1 *in vitro*) and of HTLV-1, the first human pathogenic retrovirus, warrant equal recognition.

Previously, the Nobel committee acknowledged similar pioneering contributions. Karl Landsteiner and Erwin Popper identified the poliovirus in 1908, establishing the link with poliomyelitis, but the 1954 Nobel Prize was given to John Enders, Frederick Robbins, and Thomas Weller for learning to grow poliovirus, which was pivotal for Jonas Salk and Albert B. Sabin to develop vaccines. Like Landsteiner and Popper, Barré-Sinoussi and Montagnier isolated a virus but, unlike them, could not establish whether it was the AIDS virus (2), an achievement accomplished by Gallo and colleagues

just one year later (3–6). Gallo—like Enders, Robbins, and Weller—learned to grow the virus and, furthermore, discovered its role, saved the blood supply, and opened the way for drug and vaccine development. Without Gallo's contributions, the relevance of this virus to AIDS might not have been recognized for years, and many thousands more lives would have been lost.

Given the enormous impact of these developments on the lives of countless thousands globally, Gallo's contributions should not go unrecognized.

GIOVANNI ABBADESSA,¹ ROBERTO ACCOLLA,² FERNANDO AIUTI,³ ADRIANA ALBINI,⁴ ANNA ALDOVINI,⁵ MASSIMO ALFANO,⁶ GUIDO ANTONELLI,³ COURTENAY BARTHOLOMEW,⁷ ZVI BENTWICH,⁸ UMBERTO BERTAZZONI,⁹ JAY A. BERZOFKY,¹⁰ PETER BIBERFELD,¹¹ ENZO BOERI,⁶ LUIGI BUONAGURO,¹² FRANCO M. BUONAGURO,¹² MICHAEL BUKRINSKY,¹³ ARSÈNE BURNY,¹⁴ ARNALDO CARUSO,¹⁵ SHARON CASSOL,¹⁶ PRAKASH CHANDRA,¹⁷ LUCA CECCHERINI-NELLI,¹⁸ LUIGI CHIECO-BIANCHI,¹⁹ MARIO CLERICI,²⁰ SANDRA COLOMBINI-HATCH,²¹ CARLO DE GIULI MORGHEN,²⁰ ANDREA DE MARIA,²² ANITA DE ROSSI,¹⁹ MANFRED DIERICH,²³ RICCARDO DELLA-FAVERA,²⁴ ANTONINA DOLEI,¹⁵ DANIEL DOUEK,²⁶ VOLKER ERFLE,²⁷ BARBARA FELBER,²⁸ SIMONA FIORENTINI,¹⁵ GENOVEFFA FRANCHINI,¹⁰ JONATHAN M. GERSHONI,²⁹ FRANCES GOTCH,³⁰ PATRICK GREEN,³¹ WARNER C. GREENE,³² WILLIAM HALL,³³ WILLIAM HASELTINE,³⁴ STEPHENS JACOBSON,³⁵ LARS O. KALLINGS,³⁶ VANIAMBADI S. KALYANARAMAN,³⁷ HERMANN KATINGER,³⁸ KAMEL KHALILI,³⁹

GEORGE KLEIN,¹¹ EVA KLEIN,¹¹ MARY KLOTMAN,⁴⁰ PAUL KLOTMAN,⁴⁰ MOSHE KOTLER,⁴¹ REINHARD KURTH,⁴² ALAIN LAFEUILLADE,⁴³ MICHELANGELO LA PLACA,⁴⁴ JONATHAN LEWIS,¹ FLAVIA LILLO,⁴⁵ JULIANNA LISZIEWICZ,⁴⁶ ANITA LOMONICO,¹⁰ LUCIA LOPALCO,⁶ FRANCO LORI,⁴⁶ PAOLO LUSSO,²⁶ BEATRICE MACCHI,⁴⁷ MICHAEL MALIM,⁴⁸ LEONID MARGOLIS,⁴⁹ PHILLIP D. MARKHAM,³⁷ MYRA MCCLURE,⁵⁰ NANCY MILLER,²⁶ MARIA C. MINGARI,²² LORENZO MORETTA,⁵¹ DOUGLAS NOONAN,² STEVE O'BRIEN,²⁸ TAKASHI OKAMOTO,⁵² RANAJIT PAL,³⁷ PETER PALESE,⁴⁰ AMOS PANET,⁴¹ GIUSEPPE PANTALEO,⁵³ GEORGE PAVLAKIS,²⁸ MAURO PISTELLO,¹⁸ STANLEY PLOTKIN,⁵⁴ GUIDO POLI,^{6*} ROGER POMERANTZ,⁵⁵ ANTONIA RADAELLI,²⁰ MARJORIE ROBERT-GUROFF,¹⁰ MARIO ROEDERER,²⁶ MANGALASSERIL G. SARNGADHARAN,³⁷ DOMINIQUE SCHOLS,⁵⁶ PAOLA SECCHIERO,⁵⁷ GENE SHEARER,¹⁰ ANTONIO SICCARDI,²⁰ MARIO STEVENSON,⁵⁸ JAN SVOBODA,⁵⁹ JIM TARTAGLIA,⁶⁰ GIUSEPPE TORELLI,⁶¹ MARIA LINA TORNESELLO,¹² ERWIN TSCHACHLER,⁶² MAURO VACCAREZZA,⁶³ ANGELIKA VALLBRACHT,⁶⁴ JAN VAN LUNZEN,⁶⁵ OLIVIERO VARNIER,²² ELISA VICENZI,⁶ HARALD VON MELCHNER,¹⁷ ISAAC WITZ,²⁹ DANIEL ZAGURY,⁶⁶ JEAN-FRANÇOIS ZAGURY,⁶⁷ GIORGIO ZAULI,⁵⁷ DONATO ZIPETO⁹

¹ZIOPHARM Oncology Inc., Boston, MA, USA. ²University of Insubria, Varese, Italy. ³La Sapienza University, Roma, Italy. ⁴IRCCS Multimedica, Milano, Italy. ⁵Children's Hospital and Harvard Medical School, Boston, MA, USA. ⁶San Raffaele University and Scientific Institute, Milano, Italy. ⁷The Medical Research Foundation of Trinidad and Tobago, Port of Spain, Trinidad and Tobago. ⁸Ben Gurion University, Beer Sheva, Israel. ⁹University of Verona, Verona, Italy. ¹⁰National Cancer Institute, Bethesda, MD, USA. ¹¹Karolinska Institute, Stockholm, Sweden. ¹²Istituto Nazionale Tumori "Fond. G. Pascali," Napoli, Italy. ¹³The George Washington University, Washington, DC, USA. ¹⁴Center for Cellular and Molecular Biology, Gembloux, Belgium. ¹⁵University of Brescia, Brescia, Italy. ¹⁶University of Pretoria, Pretoria, South Africa. ¹⁷University of Frankfurt Medical School, Frankfurt, Germany. ¹⁸University of Pisa, Pisa, Italy. ¹⁹University of Padova, Padova, Italy. ²⁰University of Milano, Milano, Italy. ²¹National Heart, Lung and Blood Institute, Bethesda, MD, USA. ²²University of Genova, Genova, Italy. ²³Innsbruck Medical University, Innsbruck, Austria. ²⁴Columbia University, New York, NY, USA. ²⁵University of Sassari, Sassari, Italy. ²⁶National Institute of Allergy and Infectious Diseases, Bethesda, MD, USA. ²⁷GSF-Institut fuer Molekulare Virologie, Munich, Germany. ²⁸National Cancer Institute, Frederick, MD, USA. ²⁹Tel Aviv University, Tel Aviv, Israel. ³⁰Imperial College London, London, UK. ³¹Ohio State University, Columbus, OH, USA. ³²Gladstone Institute of Virology and Immunology, San Francisco, CA, USA. ³³University College Dublin, Dublin, Ireland. ³⁴The William A. Haseltine Foundation for Medical Sciences and the Arts, Rockville, MD,



Mineral evolution

218



Marine nitrogen cycle

219

USA. ³⁵National Institute of Neurological Disorders and Stroke, Bethesda, MD, USA. ³⁶UN-Secretariat General, New York, NY, USA, and Djursholm, Sweden. ³⁷Advanced Bioscience Laboratories, Kensington, MD, USA. ³⁸University of Natural Resources and Applied Life, Vienna, Austria. ³⁹Temple University School of Medicine, Philadelphia, PA, USA. ⁴⁰Mt. Sinai School of Medicine, New York, NY, USA. ⁴¹The Hebrew University Hadassah Medical School, Jerusalem, Israel. ⁴²Robert Koch-Institut, Berlin, Germany. ⁴³Hospital "Font Pre," Toulon, France. ⁴⁴University of Bologna, Bologna, Italy. ⁴⁵Fondazione San Raffaele G. Giglio, Cefalù, Italy. ⁴⁶Genetic Immunity, Budapest, Hungary. ⁴⁷University of Roma-2, Roma, Italy. ⁴⁸King's College London School of Medicine, London, UK. ⁴⁹National Institute of Child Health and Human Development, Bethesda, MD, USA. ⁵⁰Imperial College London, Norfolk Place, UK. ⁵¹Istituto Giannina Gaslini, Genova, Italy. ⁵²Nagoya City University, Nagoya, Japan. ⁵³Centre Hospitalier Universitaire Vaudois, Lausanne, Switzerland. ⁵⁴Sanofi Pasteur, Doylestown, PA, USA. ⁵⁵Tibotec Pharmaceuticals Ltd., Yardley, PA, USA. ⁵⁶Rega Institute, Katholieke Universiteit Leuven, Leuven, Belgium. ⁵⁷University of Ferrara, Ferrara, Italy. ⁵⁸University of Massachusetts Medical School, Worcester, MA, USA. ⁵⁹Institute of Molecular Genetics, Prague, Czechoslovakia. ⁶⁰Sanofi Pasteur, Toronto, Canada. ⁶¹University of Modena,

Modena, Italy. ⁶²Medical University of Vienna, Vienna, Austria. ⁶³University of Cassino, Cassino, Italy. ⁶⁴Universitaet Bremen, Bremen, Germany. ⁶⁵University Medical Center Hamburg-Eppendorf, Hamburg, Germany. ⁶⁶Neovscs SA, Paris, France. ⁶⁷Conservatoire National des Arts et Metiers, Paris, France.

*To whom correspondence should be addressed. E-mail: poli.guido@hsr.it

References and Notes

1. Francoise Barré-Sinoussi and Luc Montagnier received the award along with Harald zur Hausen for discovery of HPV causing cervical cancer.
2. F. Barré-Sinoussi *et al.*, *Science* **220**, 868 (1983).
3. M. Popovic, M. G. Sarngadharan, E. Read, R. C. Gallo, *Science* **224**, 497 (1984).
4. R. C. Gallo *et al.*, *Science* **224**, 500 (1984).
5. J. Schupbach *et al.*, *Science* **224**, 503 (1984).
6. M. G. Sarngadharan, M. Popovic, L. Bruch, J. Schupbach, R. C. Gallo, *Science* **224**, 506 (1984).
7. This initiative was taken independently of Robert Gallo's influence. The authors are signing the letter as private citizens; this opinion does not necessarily reflect that of the authors' own respective institutions.

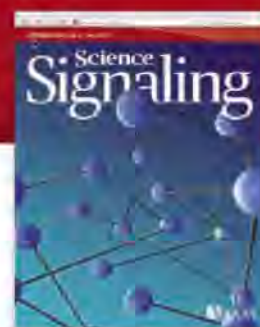
An Award for Science Is an Obsolete Notion

THE EXCLUSION OF ROBERT GALLO FROM THE Nobel prize this year ("HIV, HPV researchers honored, but one scientist is left out," J. Cohen and M. Enserink, 10 October 2008, p. 174) may appear controversial, but his situation is not unique. Any prize awarded for scientific discoveries is bound to overlook important contributors. Discoveries are built on the backs of many workers, and no matter the contribution, all contribute to the whole. Recognizing any one worker as seminal implies that the supporting work is less vital. Prizes would better serve the community by driving science forward. For example, a prize could be awarded prospectively for a particular goal, such as the X Prize (1), instead of retrospectively reviewing an accomplishment and naming one person crucial to its success. As illustrated by the vital yet overlooked contributions of Rosalind Franklin, Nicola Tesla, and Thomas Edison, the Nobel science prizes send the wrong message to the public and would-be scientists. **MARVIN GOZUM**

Division of Internal Medicine, Jefferson Medical College, Thomas Jefferson University, Philadelphia, PA 19107, USA. Email: gozum@computer.org

Call for Papers

Science Signaling



From the publishers of *Science*, *Science Signaling*, formerly known as *Science's* STKE, now features top-notch, peer

reviewed, original research. Each week the journal will publish leading-edge findings in cellular regulation including:

- Molecular Biology
- Development
- Physiology and Medicine
- Immunology
- Neuroscience
- Microbiology
- Pharmacology
- Biochemistry
- Cell Biology
- Bioinformatics
- Systems Biology

Subscribing to *Science Signaling* ensures that you and your lab have the latest cell signaling resources. For more information visit sciencesignaling.org

Announcing Chief Scientific Editor for *Science Signaling* –

Michael B. Yaffe, M.D., Ph.D.

Associate Professor, Department of Biology
Massachusetts Institute of Technology

Now accepting original research submissions at:
sciencesignaling.org/about/help/research.dtl

Science Signaling



Reference

1. X Prize Foundation (www.xprize.org).

The Time to Demand Funding

THE FUNDING CRISIS FOR SCIENCE MAY FIND its solution, however unfortunately, in the recession at hand. There will be a need for federal spending on real infrastructure projects to rescue the economy. NIH and NSF should be among the foremost beneficiaries. In the 1930s, cultural and artistic endeavors were among the beneficiaries of economic stimulus programs through the Works Progress Administration. That was before the existence of NIH or NSF. Surely, science is among the highest achievements of human culture. Spending on NIH and NSF can rescue our endangered scientific infrastructure and save the scientific careers of what will otherwise be a lost generation. The proposals are ready to go in the form of thousands of unfunded but worthy grants, thus meeting the criterion of immediate implementation necessary for a stimulus package. And the public should welcome this. Increased spending on research is virtually certain to benefit us, our children, and their children.

Disappointingly, despite unprecedented opportunities for research in diverse areas that promise transformative and life-saving advances, we scientists seem rather quiet these days. We seem to be begging for scraps of funding that will keep us alive, rather than advocating for the steady diet of research support necessary to ensure that the engines of innovation keep running. If the United States can spend \$700 billion on a Wall Street bailout and another \$700 billion on the military and wars this year, can it not spend \$10 to 20 billion more annually on research? This would be an investment in knowledge and life, not war and accumulation of personal wealth. It is time for the scientific community to speak out boldly and loudly for such funding.

CRAIG C. MELLO¹ AND JOHN V. WALSH^{2*}

¹Department of Molecular Medicine, University of Massachusetts Medical School, Worcester, MA 01655-0127, USA.
²Department of Physiology, University of Massachusetts Medical School, Worcester, MA 01655-0127, USA.

*To whom correspondence should be addressed. E-mail: john.walsh@umassmed.edu

Autistic Phenotype from MEF2C Knockout Cells

IN THEIR RESEARCH ARTICLE ("IDENTIFYING autism loci and genes by tracing recent shared ancestry," 11 July 2008, p. 218), E. M. Morrow *et al.* showed that gene expression associated with autism-spectrum disorders (ASD) is controlled by MEF2 transcription factors and hypothesized that autistic phenotypes result from abnormal activity-dependent regulation of synapse development caused by altered MEF2 signaling.

However, other studies suggest that the defects in MEF2 activity may be important even earlier in development, in embryonic neural progenitor/stem cells (NSCs). We recently showed that knockout of *MEF2C* in NSCs produces neurodevelopmental defects similar to ASD (1). In adulthood, these mice displayed autistic phenotypes resembling Rett syndrome in that they manifested altered anxiety and increased stereotypy (purposeless movements) on neurobehavioral testing, representing key characteristics of ASD. Coupled with our report that activated MEF2C drives the formation of neurons from NSCs (2), this work indicates that MEF2C plays a pivotal role in early neuronal differentiation. Additionally, mice with *MEF2C* conditionally knocked out at the NSC stage exhibited fewer, smaller, and more compacted neurons (1), similar to findings in Rett syndrome (3). When *MEF2C* was knocked out later in development, although synapse formation was altered, neurogenesis was not affected and no autistic behaviors resulted (4). Taken together, these reports are consistent with the idea that ASD may be initiated at the NSC stage and thus represent a defect in neurogenesis, of which one aspect is synapse formation. This suggests a broader role for MEF2 in neurogenesis and ASD than was previously appreciated.

STUART A. LIPTON,* HAO LI,
 JEFFREY D. ZAREMBA, SCOTT R. MCKERCHER,
 JIANKUN CUI, YEON-JOO KANG, ZHIGUO NIE,
 WALID SOUSSOU, MARIA TALANTOVA,
 SHU-ICHI OKAMOTO, NOBUKI NAKANISHI

Del E. Webb Center for Neuroscience, Aging, and Stem Cell Research, Burnham Institute for Medical Research, La Jolla, CA 92037, USA.

*To whom correspondence should be addressed. E-mail: slipton@burnham.org

References

1. H. Li *et al.*, *Proc. Natl. Acad. Sci. U.S.A.* **105**, 9397 (2008).
2. Z. Li *et al.*, *J. Neurosci.* **28**, 6557 (2008).
3. R. Z. Chen *et al.*, *Nat. Genet.* **27**, 327 (2001).
4. A. C. Barbosa *et al.*, *Proc. Natl. Acad. Sci. U.S.A.* **105**, 9391 (2008).

Science Should Stick to Science

THE NEWS OF THE WEEK STORY "SCIENTISTS plant grass-roots effort for Obama in final days of contest" by E. Kintisch (31 October 2008, p. 658) would have been fine in a newspaper, where we expect to find campaign articles. It was surprising and unwise in a magazine that reports on science.

Science did attempt to represent both candidates. Kintisch states that little or no grass-roots scientist effort for McCain was found. An objective piece about the observed differences in the parties' degree of support among scientists would have been more appropriate than the partisan tone of the piece as written.

There is a risk in publishing articles suggesting that only the politically like-minded are welcome readers of *Science*. It is in the long-term interest of the scientific enterprise that scientists do not make those who identify with other political parties uncomfortable in their midst. It is important to continue to judge scientists by their work in science. Likewise, it is important to keep *Science* about science.

ANN MARIE THRO

21298 Steptoe Hill Road, Middleburg, VA 20117, USA.

Science Careers: Where Does Advocacy Fit?

IN HIS PRESIDENTIAL ADDRESS ("A GLOBAL perspective on science and technology," 24 October 2008, p. 544), D. Baltimore warned against erosion of U.S. leadership in the biological sciences, acknowledging the entire scientific community's lack of involvement and personal responsibility in our government.

As a graduate student training for a career in the academe, I wonder at what point in my career it will be most appropriate to begin thinking about exercising responsibility for my nation's actions. Clearly, there are good reasons why scientists and engineers need to consider stepping outside our laboratories to serve our nation (1). Yet, there are few moments on the road to tenure where it would be wise

Letters to the Editor

Letters (~300 words) discuss material published in *Science* in the previous 3 months or issues of general interest. They can be submitted through the Web (www.submit2science.org) or by regular mail (1200 New York Ave., NW, Washington, DC 20005, USA). Letters are not acknowledged upon receipt, nor are authors generally consulted before publication. Whether published in full or in part, letters are subject to editing for clarity and space.

to step from the bench to engage in advocacy or policy.

More generally, how do scientists and engineers understand our scientific/technological citizenship? Does our employment by taxpayers or nonprofit organizations necessarily endow a specific role or responsibility in the larger global community? Or should action be taken only by those who sense a specific calling to act as representatives on behalf of the entire scientific community?

Moreover, in the training of graduate students who are still in the early stages of developing their personal scientific identities and personalities, how and when is it most appropriate to lead them in such self-discovery? How do we train students to consider the broader social impact of their work and livelihoods?

As I begin to form my own scientific identity, I wonder what it will mean for my fellow socially conscious students and me to exercise our voices in the world we'll inherit. I wonder if there will be meaningful opportunities for us to participate without having to first get inducted into the National Academies, or if we really have as

much potential to shape our world as we want to believe.

JASON YANG

Department of Biomedical Engineering, University of Virginia, Charlottesville, VA 22908, USA. E-mail: jhyang@virginia.edu

Reference

1. W. A. Wulf, A. K. Jones, *Science* **322**, 1025 (2008).

Unintended Consequences at NIH

FORMER NIH DIRECTOR ELIAS ZERHOUNI HAS done his level best to destroy biomedical basic research in the United States ("Zerhouni's parting message: Make room for young scientists," J. Kaiser, *News of the Week*, 7 November 2008, p. 834). Zerhouni's parting shot is a devastating quota system that requires funding disproportionate numbers of new investigators.

The consequence will be a brutal "Darwinian" scenario in which hundreds of bright-eyed new assistant professors will sail through receiving their first R01. When they come to their competitive renewal,


they will no longer be in the favored group, and most will fail (especially if the R01 pay-line stays at 10%). Their chances for promotion and tenure will vanish, and they may continue on their now severely crippled academic careers or they will branch into industry or a completely different career path. Many established investigators, in the peak of their careers and highly productive, will be forced out of science, to make room for the steady influx of new lambs to the slaughter. The best and brightest will avoid biomedical research because they will see a vicious and corrupt system in which tremendous intellect, work, and dedication produce little reward and no security. Obviously, this is a recipe for disaster.

THOMAS E. DECOURSEY


Department of Molecular Biophysics and Physiology, Rush University Medical Center, Chicago, IL 60612, USA. E-mail: tdecours@rush.edu

CORRECTIONS AND CLARIFICATIONS


AAAS News and Notes: "AAAS members elected as Fellows" (19 December 2008, p. 1808). In the Section on General Interest in Science and Engineering, Joseph J. Romm's affiliation should have been the Center for American Progress.



U.S. DEPARTMENT OF
ENERGY
Office of Science



JGI
DOE JOINT GENOME INSTITUTE



U.S. Department of Energy
Joint Genome Institute (DOE JGI)

COMMUNITY SEQUENCING PROGRAM (CSP)

is soliciting genome proposals related to DOE missions of bioenergy, global carbon cycling and biogeochemical processes influencing contaminant transport for:

Bacterial Resequencing: Bacterial isolates related to DOE missions, for which a reference genome exists, may be proposed; proposals may focus on community structure and dynamics, understanding gene function under selective pressure, or of mutagenized strains.

Metagenomes: Microbial communities involved in DOE relevant activities or specific mission-driven gene or pathway discovery.


Eukaryotic Resequencing: Large-scale (> 20 gigabases) efforts that exploit next-gen sequencing technologies may be proposed: e.g., biomass feedstocks, plant models, biomass-degrading fungi and plant pathogens for which a reference genome exists or is currently planned.

Eukaryotic Reference Genomes: DOE mission-relevant genomes of < 250 megabases appropriate for

next-gen sequencers—ideally inbred with minimal polymorphism and repeat content. For larger sequencing projects, applicants may apply for pilot-scale sequencing to acquire this basic information.

Bacterial & Archaeal Isolates: Beginning January 2009, brief proposals will be accepted on a continuous basis and reviewed every three months for organisms that participate in processes directly relevant to DOE missions or that enable sequence-based comparisons to illuminate gene function(s). Successful proposals will be prioritized and approved for sequencing when DNA prepared according to DOE JGI's standards is received.

Letters of intent are due Jan 30, 2009 and should be filed electronically online at www.JGI.DOE.gov.



NASA Space Radiation Summer School

Call for Applications

Applications are now being accepted for the 2009 NASA Space Radiation Summer School, a three-week course designed to offer graduate students, postdoctoral fellows, and faculty an integrated curriculum of radiation biology, radiation chemistry, and physics culminating in hands-on accelerator-based experiments using the synchrotron facility at the NASA Space Radiation Laboratory. Up to 15 students will be selected for the course, tentatively scheduled for **May 27 – June 19, 2009** at the Brookhaven National Laboratory (BNL) on Long Island, New York. Topics will include DNA damage and repair, genotoxicity measurements, cell cycle checkpoints and apoptosis, the bystander effect, genomic instability, neurodegeneration, tissue remodeling, and the relationships of these processes to carcinogenesis and late degenerative effects following exposure to space radiation, as well as the space radiation environment, physics and biochemistry of charged particle interaction with condensed matter, ionizing radiation dosimetry, and accelerator operations. Course faculty consists of leading university and national laboratory biologists and physicists actively engaged in NASA space radiation research and BNL experts in heavy ion experimentation and methods.

Application instructions are available online at
www.dsls.usra.edu/spacerad/2009/

Application Deadline - 11:59 p.m. CT, February 28, 2009

U.S. citizens and foreign nationals may apply. All selected students must satisfy BNL/DOE safety and security requirements in order to be admitted. Selected students must also demonstrate oral and written proficiency in the English language. Travel expenses in the U.S. and room and board will be covered for selected participants. Successful applicants from outside the U.S. must provide for their travel to/from New York/Long Island. Course sponsors are the NASA Space Radiation Program, Pacific Northwest National Lab, U.S. Dept of Energy, Loma Linda University, Brookhaven National Lab, and Universities Space Research Association.

SCIENCE AND THE LAW

Grappling with the Gulf

Dov Greenbaum¹ and Mark Gerstein²

We expect intellectual property attorneys to regularly confront scientific matters, and policy-makers (who often have a legal education) to incorporate complex technical issues into their decisions. Surprisingly though, general practice lawyers also increasingly engage science on many levels: they may need to understand the science underlying a contentious patent litigation, identify an expert witness for a criminal defense, prepare to sue a dentist for malpractice, mull over how to retrieve deleted e-mails for a trial, confirm the alleged science in a toxic tort case, or value a company's intellectual property portfolio in preparation for a merger. With less than 10% of all lawyers having an undergraduate or graduate degree in science (1), these can be daunting tasks for the majority of attorneys.

Science for Lawyers, edited by lawyer and psychologist Eric Drogin, offers a useful starting place for these and other situations that result from the collision of science, technology, and law. Written to be easily understood by readers who lack even a rudimentary understanding of science, the volume is intended to help lawyers "absorb a basic working knowledge of a particular applied scientific discipline."

The 13 chapters are designed "to reacquaint counsel ... with dimly recalled undergraduate survey topics." To this end, the contributors present their respective scientific fields in a variety of ways.

Some chapters, like the one on dentistry, speak mostly to the accreditation process and the division of subspecialties. Others, like those on genetics or statistics, present the basic fundamentals of the science, accompanied by case studies that show the interaction of the field with the law. The genetics chapter, for instance, starts with an overview of DNA and then progresses to more complicated issues surrounding genetic counseling. The

chapters on computer forensics and ballistics provide a less theoretical and more practical overview of their respective specialties, equipping lawyers with actual details that they may encounter. The chapter on psychology seems to combine all of these aspects, offering the reader an overview, a discussion of the fundamental science, and some practical applications relevant to lawyers.

Still, a concern in any broad survey of current technical topics is that parts will rapidly become obsolete. This is particularly the case for the book's sections with a practical bent. For example, we envision future chapters on computer forensics to be substantially differ-



ent given that computing is shifting away from storing files locally on an individual personal computer to saving information in centralized data centers in distributed "cloud computing" (2).

Overall, the contributors are far from agreeing on the types of information that lawyers need or the level at which the necessary technical knowledge should be presented. This reflects the currently apprehensive interface between science and law. The book's varied presentation accurately depicts the wide gulf between them and the many different perspectives on how to bridge it.

Fundamentally, the gulf stems from scientists and lawyers having very different mindsets with which they view the world—a manifestation of the societal divide epitomized in C. P. Snow's "two cultures." We might concretize this vague concept of different mindsets through a quick look at three distinctive aspects

of communicative writing in each profession.

Jargon: From early on, scientists are typically channeled into narrow disciplines that have specialized terminology. Research papers are often accessible only to a few initiates of the sub-field, which creates a strong linguistic barrier to bridging the gulf with lawyers. Law students, in contrast, are urged to be generalists and to use a "universal" legal vocabulary—although, in practice, law has its own, albeit not as daunting, jargon.

Time scale: In scientific writing, there is a premium placed on being right and being accurate as opposed to producing an answer quickly. Granted there are races to discoveries, but research continues until it meets the required standards of rigor. In contrast, law toils mostly under tight, unsympathetic deadlines, providing the best advocacy it can within the limitations of resources and time. If you are late, you are useless or irrelevant: justice delayed is justice denied.

The story: Most scientific writing stems from the desire to explain novel concepts or new experimental observations; it endeavors to describe universal truths that are independent of context. Fundamentally, these efforts use language to transform complex ideas, visual observations, and mathematical concepts into textual representations. Papers are often built around figures and tables, with the exact wording only a secondary consideration. In contrast, legal writing uses only the known facts—as established by the relevant burdens of proof—in analyses; no new factual discoveries lurk in their pages. To the lay observer, it often seems that the attorney's goal is simply to construct and transmit a persuasive narrative, within a social context, and that the exact rendition of the facts and observations may be secondary to the way those facts fit the requisite precedential case law and the goals of justice.

Given these points, one can begin to understand the root of many disagreements: lawyers may perceive scientists as unable to see the bigger picture, whereas scientists may unfairly view attorneys as willing to bend the truth for an alternative good. In this context, Drogin's volume makes an ambitious and important step toward bridging the gap between law and science.

References

1. K. Craft, J. G. Baker, *J. Econ. Educ.* **34**, 263 (2003).
2. www.cs.hku.hk/research/techreps/document/TR-2008-14.pdf.

Science for Lawyers

Eric York Drogin, Ed.

Section of Science and Technology Law, American Bar Association, Chicago, 2008. 364 pp. Paper, \$129.95. ISBN 9781590319260.

¹Mcdermott, Will, and Emory LLP, 3150 Porter Drive, Palo Alto, CA 94304, USA. ²Department of Molecular Biophysics and Biochemistry, Program in Computational Biology and Bioinformatics, and Department of Computer Science, Yale University, New Haven, CT 06520, USA. E-mail: dov.greenbaum@aya.yale.edu

ECONOMICS

Trade Liberalization and Economic Development

Jomo Kwame Sundaram¹ and Rudiger von Arnim²

Over the past year and a half, a crisis beginning in the U.S. subprime mortgage market segment has triggered a global financial crisis of historic proportions, leading to a global economic slowdown that may rival the Great Depression. Contagion across sectors and borders in increasingly interdependent goods and money markets underscores the importance of international cooperation to contain the crisis, accelerate recovery, and avoid future crises. Proponents of free trade have argued that completion of the Doha Development Round of international trade negotiations would serve these goals, particularly in poor countries (1). Pascal Lamy, World Trade Organization (WTO) director-general, called—and then, given significant remaining differences, called off—a meeting to conclude Doha at the end of December 2008, suggesting that an agreement “would give a shot of confidence to a world economy reeling from the financial crisis” (2). Still, the calls for further liberalization continue to trickle in, and a ministerial meeting during the first half of 2009 is likely. But will trade liberalization generally, and possible outcomes of a Doha agreement particularly, promote development in poor countries?



Getting hit by free trade.

A Brief History of Free Trade Theory

The case for free trade rests on Ricardo's theory of comparative advantage (3). In the early 19th century, he argued that England and Portugal could engage in mutually beneficial exchange of cloth and wine—regardless of the respective industries' prices and productivities. However, his argument assumed a world of flexible

exchange rates responsive to changes in the market for goods, continuous full employment, and costless factor mobility, meaning that no barriers exist to seeking and finding employment anywhere in the world. Especially in developing

Across-the-board trade liberalization often impedes, rather than fosters, development in the poorest countries.

not only provide greater explanatory power but also justify policy interventions (i.e., tariffs and subsidies) to support strategically important, but uncompetitive, industries in developing countries. Paul Krugman, Nobel laureate in economics for 2008, played a crucial role in the development of these models (6, 7). Recent efforts have focused on the heterogeneity of corporate firms to explain why exporting firms tend to be a lot more productive than firms servicing only the domestic market (7, 8). Integration of this exciting research into policy models is the next step.

Large-scale policy models have focused on configurations that emphasize gains from trade—despite a large and growing chorus of prominent economists [including Nobelists Paul Samuelson (7) and Joseph Stiglitz (10, 11)] arguing that across-the-board liberalization can be harmful. For example, Alan Blinder (12), vice chair of the board of governors of the Federal Reserve System in the mid-1990s, has rejected the view that “offshore outsourcing” is business as usual and suggests it can be a threat to the long-term welfare of developed countries. Still other models (13, 14), derived from Keynesian theories, consider trade to be the result of differences in growth rates of incomes. Such models often allow for unemployment and also show fewer gains from trade liberalization than the H-O-S variants.

The fundamental difference between economies of the developed and developing world is another crucial dimension of trade theory. Suppose that countries specialize in sectors for which the production factors are relatively abundant, as is recommended by traditional models. Exports of developing countries tend to be concentrated in primary products, which offer little added value. However, over time the prices of primary products will tend to decrease relative to manufactured goods. The role manufacturing plays for development has been recognized (15). Gains

countries with chronic underemployment and volatile, cyclical capital flows, the last two assumptions are generally not satisfied.

The 20th century “Heckscher-Ohlin-Samuelson” (H-O-S) variant of Ricardo's theory states that countries export products based on inputs they have in abundance and import products based on inputs that are scarce. Unfortunately, trade patterns do not confirm this view, as the overwhelming majority of trade occurs among countries that are similar (4).

To explain such realities, economists introduced the idea of a love of variety and, subsequently, theories of “new” trade (5, 6), which

¹Assistant Secretary General for Economic Development, United Nations Department of Economic and Social Affairs, Two UN Plaza DC2-2324, New York, NY 10017, USA. E-mail: jomoks@yahoo.com. ²Assistant Professor, Department of Economics, University of Denver, Denver, CO 80208, USA. E-mail: rudiarnim@gmail.com

from trade then do not derive from Ricardian specialization but from expansion of dynamic sectors. From this perspective, the potential gains from trade liberalization are large, but they will materialize only if complemented by policies promoting development of industry (16, 17).

Where Are the Gains from Trade?

The World Bank has generally supported the WTO in pursuing trade liberalization, and its arguments often invoke the results of simulations based on computable general equilibrium (CGE) models. However, there are many problems with these models and their use.

In an influential World Bank study, several scenarios of trade liberalization were considered (18). The most realistic scenario projected welfare gains in 2015 of only \$96 billion [roughly one-fifth of 1% of world gross domestic product (GDP)]. Rich countries stand to gain \$80 billion (82%), compared with \$16 billion (18%) for developing countries. A major portion of the gains for developing nations benefits large countries such as Brazil and China, whereas sub-Saharan African countries are expected to be net losers. A CGE model-based agricultural trade scenario concluded that rich countries would gain \$19 billion; China and South Asia, \$1 billion each; while other developing countries would lose \$3 billion (19).

Polaski (20) introduced unemployment and separated agricultural labor markets from urban unskilled labor markets in a CGE model. The analysis suggested that global gains from further trade liberalization are, at 0.2% of world GDP, similarly modest, but—in sharp contrast to the World Bank's full employment models—developing countries' gains stem largely from increased market access for their manufactures. Again, the largest gains accrue to countries such as China, whereas the poorest (in sub-Saharan Africa) are net losers.

Other investigators, including Ackerman (21), have also criticized the theory and methodology in CGE-based estimates. Taylor and von Arnim (22) and Kraev (23) showed the problematic effects of underlying assumptions, particularly full employment. Whatever the right assumptions are, all the different models come to essentially the same conclusion: Global gains of a Doha trade agreement are minuscule relative to world GDP and mostly accrue in large and more developed countries. The poorest countries might very well lose.

This insight was belatedly invoked in 2005 to generate support for "aid for trade" as a sop to induce developing countries to accept further trade liberalization. Bhagwati (24) has argued that aid for trade needs to be ramped up to maintain global support for further liberaliza-

tion. First, governments need to be compensated for loss of tariff revenue, which can account for up to half of total tax revenue in the poorest countries. Second, producers, workers, and others have to be compensated for loss of "uncompetitive" production capacities in agriculture, industry, and even services. Third, funds are needed to help develop new internationally competitive capacities and capabilities. Such recognition of the need to compensate for the loss of revenue and economic capacities, as well as the high and uncertain costs of developing alternative economic capacities, underscores the limitations of traditional trade theory.

The Reality of Trade Negotiations

By 1994, the WTO replaced the General Agreement on Tariffs and Trade (GATT), which gave the WTO enhanced powers and significantly broadened scope. The WTO trade agenda now includes services and gives greater attention to agriculture. The broadening of the scope of multilateral negotiations has made it even harder for developing countries to be represented by expert negotiators.

Perhaps most important, membership in the WTO involves a single undertaking, requiring compliance with all WTO agreements—unlike the previous option under GATT of signing up on an agreement-by-agreement basis. The WTO has also created and strengthened processes and mechanisms for dispute settlement that have tended to favor corporate interests and rich-country governments, which can better afford the legal and lobbying resources to pursue their interests. Similarly, liberalization of services has mainly involved financial services, rather than construction or maritime services where developing countries are better able to compete. Also, the Agreement on Trade-Related Aspects of Intellectual Property Rights (TRIPs) has given transnational corporations greater powers than provided by the World Intellectual Property Organization (WIPO) and has limited developing countries' abilities to adapt and to imitate.

The Latest Doha Round

In July 2008, negotiations for a Doha Round trade deal collapsed again, this time over provisions to allow developing countries to protect the livelihoods of subsistence farmers. Premature trade liberalization undermines the policy space necessary for investment and technology policies for development. Further agricultural trade liberalization will undermine food security in most developing countries, many of which have been transformed from net food exporters into net food importers. Contrary to the claims of advocates of agricultural trade liberalization, eliminating agricultural and export subsidies in the Organisation for Economic Co-operation and Development would, at least

temporarily, increase food prices in food-importing countries! The supposed gains from agricultural trade liberalization are likely to bring greater benefits to a few rich agriculture-exporting countries, rather than to most of the developing world, let alone the bulk of the poor.

The current multilateral negotiations, the Doha Development Agenda, were conceived in the spirit of promoting global cooperation and under the banner of helping developing countries do just that—develop. A return to these principles is of utmost importance for successful conclusion of the round.

References

1. R. B. Zoellick, *A Challenge of Economic Statecraft*, 2 April 2008, Center for Global Development, Washington, DC [speech].
2. International Centre for Trade and Sustainable Development, "Lamy leaning towards calling mid-December mini-ministerial," *Bridges* 12(41) (3 December 2008); <http://ictsd.net/i/news/bridgesweekly/35168/>.
3. D. Ricardo, *Principles of Political Economy and Taxation* (John Murray, London, 1817).
4. H. G. Grubel, P. J. Lloyd, *Econ. J.* **35**, 646 (1975).
5. A. K. Dixit, J. E. Stiglitz, *Am. Econ. Rev.* **67**, 297 (1977).
6. P. R. Krugman, *J. Int. Econ.* **9**, 469 (1979).
7. P. R. Krugman, Ed., *Strategic Trade Policy and the New International Economics* (The MIT Press, Cambridge, MA, 1990).
8. A. B. Bernard, J. B. Jensen, S. J. Redding, P. K. Schott, *J. Econ. Perspect.* **21**, 105 (2007).
9. P. Samuelson, *J. Econ. Perspect.* **18**, 135 (2004).
10. J. E. Stiglitz, *Globalization and Its Discontents* (Norton, New York, 2003).
11. J. E. Stiglitz, A. Charlton, *A Development-Friendly Prioritization of Doha Round Proposals* (IPD working paper, Initiative for Policy Dialogue, Columbia University, New York, 2004).
12. A. S. Blinder, *Foreign Aff.* **85**, 113 (2006).
13. C. W. M. Naastepad, *Camb. J. Econ.* **30**, 403 (2006).
14. R. Frenkel, L. Taylor, Real Exchange Rate, Monetary Policy, and Employment (DESA working paper 19, Department of Economic and Social Affairs, United Nations, New York, 2006); www.un.org/esa/desa/papers/2006/wp19_2006.pdf.
15. J. A. Ocampo, in *Beyond Reforms* (Stanford Univ. Press, Stanford, CA, 2005), chap. 1.
16. H.-J. Chang, *Bad Samaritans: The Myth of Free Trade and the Secret History of Capitalism* (Random House, New York, 2007).
17. E. Reinert, *How Rich Countries Got Rich and Why Poor Countries Stay Poor* (Constable & Robinson, London, 2007).
18. K. Anderson, W. Martin, Eds., *Agricultural Trade Reform and the Doha Development Agenda* (World Bank, Washington, DC, 2005).
19. A. Bonet, J. C. Bureau, Y. Decreux, S. Jean, *Multilateral Agricultural Trade Liberalization: The Contrasting Fortunes of Developing Countries in the Doha Round* [Centre d'Etudes Prospectives et d'Informations Internationales (CEPII), Paris, 2004].
20. S. Polaski, *Winners and Losers: Impact of the Doha Round on Developing Countries* (Carnegie Endowment for International Peace, Washington, DC, 2006).
21. F. Ackerman, *The Shrinking Gains from Trade: A Critical Assessment of Doha Round Projection* (GDAE working paper no. 05-01, Global Development and Environment Institute, Tufts University, Medford, MA, 2005).
22. L. Taylor, R. von Arnim, *Modelling the Impact of Trade Liberalisation: A Critique of Computable General Equilibrium Models* (Oxford, 2006).
23. E. Kraev, *Estimating GDP Effects of Trade Liberalization on Developing Countries* (Christian Aid, London, 2005).
24. J. Bhagwati, *Financial Times*, 26 September 2005 [letter].

PHYSICS

When Infinity Does Not Count

Vadim V. Cheianov

Classical fluid dynamics is an incredibly flexible mathematical tool that can describe fluids as diverse as water and the dense nuclear matter of neutron stars. However, when a fluid is cooled to temperatures close to 0 K and exhibits quantum effects, a more fundamental theory must be used. Yet, attempts to introduce quantum effects as perturbations to the classical theory have not been successful: The solutions diverge and give meaningless, infinitely large answers. On page 228 of this issue, Imambekov and Glazman (1) consider a quantum fluid that moves in one spatial dimension and investigate how quantum effects influence the decay of elementary excitations caused by the nonlinearity of fluid dynamics. The authors apply a universal, nonperturbative transformation of variables, and the new theoretical formulation generates finite results.

The problem of divergent quantum corrections is not unique to fluid dynamics. Initially encountered in the early 1930s at the interface of quantum mechanics and Maxwell's theory of light, it is inherent to quantum field theory. Infinities encountered in perturbation theory can be cured with a procedure called renormalization (2). This procedure has been highly successful in both high-energy and condensed-matter physics, but it fails in some important nonlinear theories. The most notorious example is Einstein's theory of gravity (3), which has interesting parallels with the quantum theory of fluids (4). Whether there exists a meaningful quantum formulation of nonlinear theories that do not lend themselves to renormalization is an open question.

Some simplification of quantum fluid dynamics is achieved by considering the problem in one spatial dimension. A few decades ago, this exercise would have been regarded as a mathematical abstraction with no physical examples. Today, several examples of one-dimensional quantum fluids are known, including electron liquids in carbon nanotubes (5) and cold atomic gases in elongated traps (6). Small

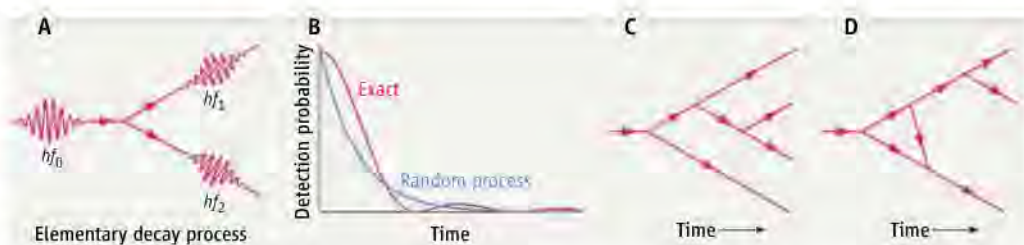
perturbations of a one-dimensional quantum fluid are captured by the Luttinger liquid theory (7), which describes how sound waves move through the fluid (for example, their velocity). Each sound wave of frequency f can accommodate an integer multiple of the energy quantum, $E = hf$, where h is Planck's constant. Such energy quanta constitute elementary particles of the system and are called phonons.

The price to pay for the simplicity of the Luttinger model is that it neglects all of the nonlinear terms in the equations of fluid dynamics, which leaves out a lot of interesting physics. For instance, in a nonlinear system, a phonon could decay into several other

A transformation of variables overcomes fundamental difficulties in formulating a unified theory of one-dimensional quantum fluids.

gas (an ideal gas not of classical particles but of fermions) (8). In this case, the exact result does not correspond to what one would expect from a rare-event random process (see the figure, panel B). As time passes, the phonon disappears, but then continues to reappear and disappear. This result suggests that the description of phonon decay in terms of rare events is wrong. The disagreement cannot be blamed on the particular model used; if quantum hydrodynamics is a universal theory, it should be insensitive to the exact microscopic nature of the system.

The lack of agreement with the exact phonon decay pattern indicates that more



Following the fate of phonons. One measure of a quantum fluid system is how sound waves, or phonons, decay as they move through it. (A) A diagram illustrating the simple case of a phonon of frequency f_0 decaying into two weaker phonons of frequencies f_1 and f_2 . (B) The probability of detecting a phonon in a model system, the one-dimensional Fermi gas, changes as a function of time. The exact result from the model (pink curve) does not match the prediction of the theory that includes only the lowest-order decay process as a rare random event (blue curve). This mismatch lies in ignoring higher-order decay processes. For example, a cascade of events (C) causes a phonon to decay into four weaker phonons. In a "bad" process (D), phonons created in the decay process exchange a virtual phonon. The contribution of this process diverges to infinity.

phonons. This decay process illustrates how divergences enter into the quantum description of this fluid. Consider, for example, a phonon decaying into two others (illustrated in the figure, panel A). If the theory is weakly nonlinear—that is, nonlinearity can be described as small corrections to the linear theory—such processes would be expected to be random rare events, like radioactive decay. If this is true, then the probability P for detecting a phonon after a time t would decay exponentially as $e^{-t/\tau}$, where τ is the phonon life time (see the figure, panel B).

How can we tell if this is what actually happens? Fortunately, there are models of many-particle systems that have a complete quantum solution and whose large-scale physics is governed by fluid dynamics. For example, the probability of detecting a phonon can be calculated exactly for a one-dimensional Fermi

complex phonon decay patterns must be taken into consideration; in fact, there are infinitely many higher-order processes (one example is shown in panel C of the figure). In perturbative field theory, there are well-developed methods for summing up all of these contributions, but in nonlinear fluid dynamics, this is where the real trouble starts. Phonons born by the decay of the initial phonon may exchange a virtual phonon (see the figure, panel D), and the contribution of each such process is infinite (9). This infinity is similar to the short-distance infinity encountered in quantum electrodynamics, except that it is much stronger and cannot be cured by means of renormalization.

Rather than trying to make sense out of meaningless infinities in phonon processes, Imambekov and Glazman make a change of variables. The nonlinear quantum transforma-

Department of Physics, Lancaster University, Bailrigg, Lancaster LA1 4YB, UK. E-mail: v.cheianov@lancaster.ac.uk

tion they use was initially proposed for the analysis of a model describing interacting relativistic particles in two-dimensional space-time (10). The theory now operates in a different world of particles: Phonons, which are normal modes of the entire system, are replaced by weakly interacting soliton-like particles that are fermions traveling through the system. The new theory cannot be renormalized, which should be expected given that it is the old one in disguise. However, if residual weak interactions between the new soliton-like particles are neglected, the theory can be treated exactly, and the interactions between the prototype particles—the

phonons—remain practically unchanged. These interactions are encoded in the nonlinear transformation rules from one theory to the other and allow any hydrodynamic observable to be calculated explicitly.

The beauty of Imambekov and Glazman's work is that it provides an example of a meaningful quantum field theory for a problem lacking a consistent perturbative formulation. The mathematics of this theory is not only interesting—it describes real systems with rich phenomenology, and should allow for further explorations. For example, it should be possible to develop a theory of quantum wave breaking and quantum shock waves.

References

1. A. Imambekov, L. I. Glazman, *Science* **323**, 228 (2009); published online 27 November 2008 (10.1126/science.1165403).
2. R. P. Feynman, *QED: The Strange Theory of Light and Matter* (Princeton Univ. Press, Princeton, NJ, 1985).
3. D. Kleppner, R. Jackiw, *Science* **289**, 893 (2000).
4. G. Volovik, *JETP Lett.* **82**, 319 (2005).
5. S. J. Tans *et al.*, *Nature* **386**, 474 (1997).
6. H. Moritz, T. Sifert, M. Köhl, T. Esslinger, *Phys. Rev. Lett.* **91**, 250402 (2003).
7. T. Giamarchi, *Quantum Physics in One Dimension* (Oxford Univ. Press, Oxford, UK, 2003).
8. M. Pustilnik, M. Khodas, A. Kamenev, L. I. Glazman, *Phys. Rev. Lett.* **96**, 196405 (2006).
9. D. N. Aristov, *Phys. Rev. B* **76**, 085327 (2007).
10. D. Mattis, E. Lieb, *J. Math. Phys.* **6**, 304 (1965).

10.1126/science.1168389

MATERIALS SCIENCE

Unjamming a Polymer Glass

David A. Weitz

When a glass is heated, it melts and begins to flow. This transition from an elastic solid to a flowing fluid is a distinguishing feature of the glass transition, one of the most widely studied, yet incompletely understood, phase transitions (1). The application of stress can also make a glass flow; softer glasses, including many polymers, yield when subjected to sufficiently large stresses (2). The equivalence of these two routes to flow is a basic tenet of jamming, a conceptual means of unifying glassy behavior with that of granular materials such as sand (3). The shear-induced flow of sand, or other granular materials, is well studied. On page 231 of this issue, Lee *et al.* (4) show that the nature of shear-induced flow in molecular glasses can now be probed. By measuring the motion of small probe molecules in a polymer glass, they find fluidlike properties when the glass is sheared; however, the route to melting the glass is different from that followed when it is heated.

Lee *et al.* use an optical method to measure the rate of rotation of small dye molecules embedded within thin slabs of lightly cross-linked poly(methyl methacrylate) (PMMA). These probe molecules provide a direct, local measure of the fluidity of the polymer. As the temperature is increased and the polymer glass starts to flow, the structural relaxation rate of the polymer, as determined by the



Shear flow. Schematics comparing shear-induced flow in a granular material (left) and a glassy polymer (right).

motion of the probe molecules, becomes measurable and begins to increase with temperature, adopting the characteristic stretched exponential form of a fluid very close to the glass transition (5). Moreover, the structural relaxation exhibits the strong spatial heterogeneity commonly observed in a fluid very close to the glass transition (5, 6). The new experiments investigate the behavior of the probe molecules when the polymer is subjected to an external uniaxial tension; the sample is pulled apart by its two ends. Initially, when the strain is small, the structural relaxation rate increases slightly, and can be described by a theory that incorporates the effects of the induced strain energy, which lowers the activation barriers for the relaxation of the probe molecules due to their shear-induced rotation (7). The shape of the decay retains the characteristic stretched exponential form. However, as both the strain and strain rate increase, the relaxation rate of the probe molecules increases by several orders of magnitude, and the shape of the relaxation becomes nearly exponential. At this point, the sample undergoes plastic flow, and

at the molecular scale, the glass melts due to the induced strain.

This shear-induced melting is exactly what is expected within the jamming picture. The basic concepts of jamming can be understood from the perspective of a granular material, such as a bucket of sand. Normally, the sand in the bucket is a solid; it does not flow and it supports a stress, as easily proven by stepping on it—the sand supports your weight. However, if you tip the bucket, the sand flows, much like a fluid. Here, gravity provides the shear stress that causes the sand to change from a solid to a fluid. To make the analogy between granular sand and a glass requires a second route to fluidizing the sand—by increasing its effective temperature. This can be accomplished by gently shaking it, or by blowing air slowly up through the sand, to slightly suspend all the grains in the flow of air (8). In this case, the grains are rapidly moving, but are trapped in place by all their neighbors. This rapid random motion of the grains is akin to an increased effective temperature. To complete the jamming picture, there is a third means of fluidizing a solid, and that is to

Department of Physics and School of Engineering and Applied Sciences, Harvard University, Cambridge, MA 02138, USA. E-mail: weitz@seas.harvard.edu

decrease the volume fraction. This may be difficult to comprehend for sand in air, so imagine instead immersing the sand in a fluid to provide buoyancy. Then, if you decrease the number of grains per unit volume, you will eventually have so few grains that they will no longer be self-supporting, and thus the solid will be fluidized. Any of these three routes can take the system through the solid-to-fluid transition, and much work has been devoted to explore the generality of this concept for granular systems. By contrast, there have been fewer attempts to explore the same concept of jamming for molecular glasses.

The importance of the experiments by Lee *et al.* is that they establish that shear does induce melting of the glass, and that the resultant flowing material has many features of a liquid, particularly as evidenced by the relaxation of the probe molecules. However, these experiments also establish that the nature of the solid-to-fluid transition is different when it is shear-induced as compared with thermally

induced melting. The sheared sample lacks the large spatial heterogeneities that characterize a melting sample.

Moreover, in a sheared sample, there is a narrower distribution of barriers to relaxation than in a sample that has melted. Instead, it is tempting to think that the imposed shear rate sets the scale for all the relaxations, resulting in a much narrower range of rates. Moreover, flow occurs in localized regions, in agreement with the picture of shear transformation zones (9), and the volume of these regions is consistent with that found in computer simulations (9) and in measurements of a colloidal glass (10), a material that straddles a granular system and a molecular glass.

The comparison between a granular system and a molecular glass, as originally postulated by the jamming concept, remains an intriguing and appealing hypothesis. These experiments provide strong evidence for the merit of this perspective, suggesting that computer simulations of jammed granular systems

under shear may also provide new insight into the behavior of sheared molecular glasses. However, a detailed understanding of the true extent of the analogy must await confirmation by further studies. The approach of Lee *et al.* should help make this possible.

References and Notes

1. C. A. Angell, *Science* **267**, 1924 (1995).
2. H. E. H. Meijer, L. E. Govaert, *Prog. Polym. Sci.* **30**, 915 (2005).
3. A. J. Liu, S. R. Nagel, *Nature* **396**, 21 (1998).
4. H.-N. Lee, K. Paeng, S. F. Swallen, M. D. Ediger, *Science* **323**, 231 (2009).
5. M. D. Ediger, *Annu. Rev. Phys. Chem.* **51**, 99 (2000).
6. E. R. Weeks, J. C. Crocker, A. C. Levitt, A. Schofield, D. A. Weitz, *Science* **287**, 627 (2000).
7. H. Eyring, *J. Chem. Phys.* **4**, 283 (1936).
8. N. Menon, D. J. Durian, *Phys. Rev. Lett.* **79**, 3407 (1997).
9. M. L. Falk, J. S. Langer, *Phys. Rev. E* **57**, 7192 (1998).
10. P. Schall, D. A. Weitz, F. Spaepen, *Science* **318**, 1895 (2007).
11. This work was supported by the NSF (grant DMR-0602684) and the Harvard Materials Science Research and Engineering Center (grant DMR-0820484).

10.1126/science.1168304

BEHAVIOR

Surprising Emotions

Eliot R. Smith¹ and Diane M. Mackie²

Imagine that you are a white student waiting with two other students, one black and one white, for a psychology experiment to begin. The black student steps out of the room for a moment, lightly bumping against the white student on his way out. While he is out of earshot, the white student comments, "Typical, I hate it when black people do that." How would you feel? And if you later had the choice, with which of the other students would you prefer to work? If you anticipate being upset and avoiding the fellow who made the racist remark, you are like most "forecaster" participants in a study by Kawakami *et al.* (1) on page 276 in this issue. These were students, self-identified as members of racial groups other than black, who predicted how they would react after reading about or viewing a videotaped enactment of these events.

Other participants in the study, from the same student population as the forecasters, actually experienced this event, with actors portraying the white and black students in the scenario. Surprisingly, when asked during the

experiment how they felt, these "experiencers" did not report feeling any more upset when the racist comment was made than when the same event occurred without any comment being made at all. Nor did the experiencers tend to avoid the originator of the racist comment.

These findings are an example of what social psychologists call a failure of affective forecasting: People often mispredict how they would feel (and therefore act) in imagined or future situations (2, 3). In other words, our emotional reactions (or lack of them) often



Who would be in this situation? Depending on the identity (such as egalitarian or racist) that is activated in a given situation, people can experience different emotions and behave in different ways. But people often fail to predict accurately their identity and emotions in a future or imagined situation.

Why are our predictions of how we'll feel or act sometimes wrong?

surprise us. Indeed, if our emotions never surprised us, they would fail to perform one of their most important functions: to call our attention to important aspects of a situation that we otherwise might not have consciously noted. For example, one reason for poor emotion forecasting is that experiencers react to a much wider range of cues in a situation, whereas forecasters focus more narrowly on its most salient features (such as the racist remark in the study by Kawakami *et al.*) (4).

One thing emotions can inform us about, sometimes to our surprise, is who we are in a given situation. This happens because emotions can arise from our identification with social groups and not only from our individual self (5, 6). For example, imagine you are a woman in an organization, learning that a female colleague has won promotion to upper management. You may feel disappointment and envy if you are taking an individual perspective. But if you are thinking of yourself instead primarily as a woman, you may feel pride and happiness at this blow to the "glass ceiling" (7). Thus, feeling happy rather than envious may tell you, perhaps to your surprise, what group membership defines you in the specific situation.

What identities and corresponding emotional and behavioral reactions are possible in

¹Department of Psychological and Brain Sciences, Indiana University, Bloomington, IN 47405, USA. E-mail: esmith4@indiana.edu ²Department of Psychology, University of California, Santa Barbara, CA 93106, USA. E-mail: mackie@psych.ucsb.edu

the experiment of Kawakami *et al.*? Some participants hearing the racist comment might identify with their own racial group, feeling emotions of pride and smug superiority to blacks. (Such an identification is no doubt what a real-life originator of a racist comment would be trying to elicit.) A second possibility, predicted by most forecasters, involves identification as a liberal, egalitarian person and perception of the racist as a violator of important norms of tolerance (or, at the very least, suppression of inappropriate speech). Such identification triggers distress and outrage and may also result in feelings of empathy toward the innocent black target of the comment (8).

A third potential identity, not tied to membership in any particular social group, is simply that of an experimental participant. The “research participant” identity in experimental situations is highly constraining. In the famous obedience study by psychologist Stanley Milgram, for example, people hated delivering presumed electric shocks to the “learner” as they were instructed, but most found it impossible to tell the experimenter that they refused to do so (9). The constraints of being in an experiment are very real to people experiencing the situation but are much less salient for forecasters, who therefore mis-

predict their reactions (4). From the perspective of an experimental participant, the racist comment is merely an unusual occurrence in the experimental context, able to be reinterpreted or minimized, and so eliciting little negative emotion or action. This appears to be the identity taken on by most experiencers in the study of Kawakami *et al.* Thus, it is not so much that forecasters mispredicted the emotional reactions that experiencers would feel, as that they mispredicted the identity that would be most salient in the actual situation. This represents a failure of identity forecasting rather than affective forecasting.

These results illustrate the flexibility of our social identities in the face of fluid social contexts. The Kawakami *et al.* study results suggest that the racist remark becomes the focal feature of the situation for some people, but it is easily dismissed as an oddity for individuals who categorize themselves in a different way. The results also show the power of categorization to determine whether someone takes on a proud racial identity that derives esteem from seeing blacks as inferior or a more egalitarian identity that leads to distress at a racist comment. We are not prisoners of our group memberships, inevitably drawn to ethnocentric thinking that glorifies our own racial or other

ingroups and derogates outgroups. Instead, our flexible social categorizations can lead us to reject fellow group members who violate norms of tolerance and egalitarianism, and to avoid—and perhaps, in an ideal world, even to confront—those individuals (10). And it is often our emotional reactions that first clue us in, sometimes to our surprise, to the identity that is guiding our perceptions and reactions in a given situation.

References and Notes

1. K. Kawakami, E. Dunn, F. Karmali, J. F. Dovidio, *Science* **323**, 276 (2009).
2. D. T. Gilbert, E. C. Pinel, T. D. Wilson, S. J. Blumberg, T. P. Wheatley, *J. Pers. Soc. Psychol.* **75**, 617 (1998).
3. T. D. Wilson, D. T. Gilbert, in *Advances in Experimental Social Psychology*, M. Zanna, Ed. (Elsevier, San Diego, CA, 2003), pp. 345–411.
4. E. W. Dunn, T. D. Wilson, D. T. Gilbert, *Pers. Soc. Psychol. Bull.* **29**, 1421 (2003).
5. D. M. Mackie, E. R. Smith, D. G. Ray, *Soc. Pers. Psychol. Compass* **2**, 1866 (2008).
6. E. R. Smith, C. R. Seger, D. M. Mackie, *J. Pers. Soc. Psychol.* **93**, 431 (2007).
7. M. B. Brewer, J. G. Weber, *J. Pers. Soc. Psychol.* **66**, 268 (1994).
8. E. Subasic, K. J. Reynolds, J. C. Turner, *Pers. Soc. Psychol. Rev.* **12**, 330 (2008).
9. S. Milgram, *J. Abnorm. Soc. Psychol.* **67**, 371 (1963).
10. C. W. Leach, A. Iyer, A. Pedersen, *Pers. Soc. Psychol. Bull.* **32**, 1232 (2006).
11. Supported by NSF (grant BCS-0719876).

10.1126/science.1168650

CHEMISTRY

Extending Polymer Conjugation into the Second Dimension

Dmitrii F. Perepichka^{1,2} and Federico Rosei^{2,3}

Organic materials are typically insulators, but polymers with backbones containing extended networks of conjugated π bonds can exhibit semiconducting behavior. Conjugated polymer semiconductors are used as active materials in optoelectronic devices, particularly in applications in which high speed is not critical. Their advantages versus traditional inorganic materials include simpler and cheaper processing and tunable properties. Yet the trade-off is a lower mobility of charge carriers in these more disordered systems. Conjugated polymers are

one-dimensional (1D) chains, so the charge carriers are slowed down as they hop between chains and across disordered chain fragments. Efforts are under way to create polymers with conjugation in two dimensions, because they may have enhanced carrier mobility or other favorable properties.

The extremely high carrier mobility of graphene—a completely conjugated single sheet of graphite (1, 2)—suggests that high mobilities might be achieved in 2D organic polymers. Although their carrier mobilities would likely be lower than for graphene, the greater variety of possible structures could allow for tuning of electronic properties and may confer advantages in processing. For 1D polymers, mobilities can be comparable to that of amorphous silicon [~ 1 square centimeter per volt per second ($\text{cm}^2 \text{V}^{-1} \text{s}^{-1}$)] but are still well below that of surface-bound graphene (which can be as high as 20,000

Crystal surface templates may improve the electronic properties of conjugated polymers by linking them into two-dimensional networks.

$\text{cm}^2 \text{V}^{-1} \text{s}^{-1}$). Some 2D polymers might also have zero band gap and potentially exhibit metallic conductivity.

The properties of 2D conjugated polymers have been explored theoretically for more than two decades (3–5). However, experimental efforts aimed at creating and characterizing such materials are more recent. The challenges include the design of properly functionalized monomers that can react in two independent directions without sterically hindering each other, and identifying a suitable template to guide the formation of a continuous 2D network. Because rigid and planar 2D conjugated polymers will certainly be insoluble, classical solution polymerization and characterization techniques are not likely to be suitable. Atomically flat single-crystal surfaces can act as templates to confine polymerization reactions epitaxially in two dimensions and enable in situ characterization

¹Department of Chemistry, McGill University, 801 Sherbrooke Street West, H3A 2K6 Montréal, Québec, Canada. ²Centre for Self-Assembled Chemical Structures, ³Institut National de la Recherche Scientifique, Énergie, Matériaux et Télécommunications, Université du Québec, 1650 Boulevard Lionel Boulet, J3X 1S2 Varennes, Québec, Canada. E-mail: dmitrii.perepichka@mcgill.ca; rosei@emt.inrs.ca

with methods such as scanning tunneling microscopy (STM).

Epitaxial surface polymerization was initially used to create 1D polymers. Building on pioneering studies from the 1970s (6), Okawa and Aono (7) and Miura *et al.* (8) reported the topological polymerization of self-assembled molecular networks of diacetylene monomers on graphite. They used either voltage pulses from the STM tip or ultraviolet light to create 1D polydiacetylene lines that were held together laterally by nonconjugated linkages.

monomers (13, 14), but the resulting 2D polymers were not conjugated.

Adapting solution polymerization reactions to single-crystal surfaces poses many challenges; the monomer reactivity can be affected, and reactions are more limited by diffusion. Indeed, surface-confined polymerizations have yielded oligomers that were at most several tens of units large. The “chain-end” effects that limit the properties of shorter 1D conjugated oligomers are likely to be even more detrimental for 2D structures.

The formation of defect-free continuous polymer sheets will require either a topological polymerization reaction in a preordered monomer or a self-repair mechanism, in which the mislinked units can dissociate and reconnect to converge into the most thermodynamically stable structure. However, reactions that reversibly form a covalent bond are rare. One possibility is linking an aldehyde (–CHO) and an amine (–NH₂) with an imine bond (–CH=N–). The by-product of the reaction (water) can hydrolyze the imine bond, driving the reaction backward and facilitating self-repair.

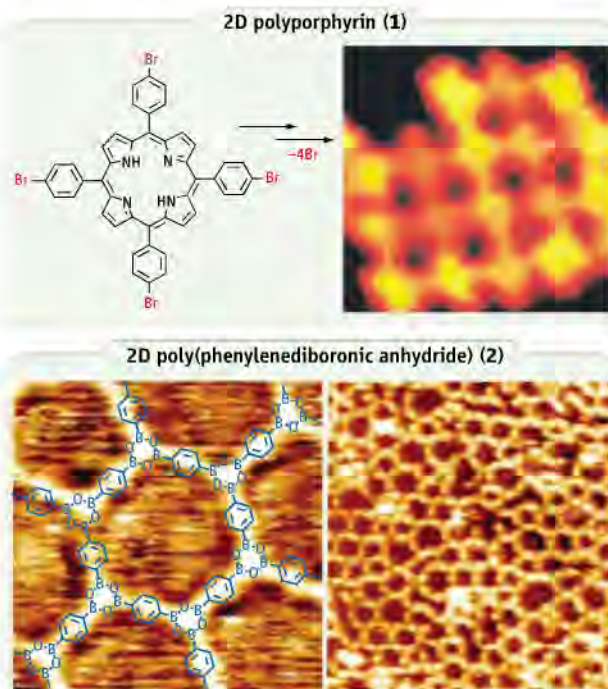
Using this approach, Weigelt *et al.* have linked aromatic trialdehydes with aliphatic diamines into a 2D imine polymer (15). In this case, aliphatic chains break the conjugation and

ties of 2D conjugated polymers would mainly be exploited on insulating surfaces (for example, gate dielectrics in transistors). It might be possible to use insulating surfaces directly as templates. Alternatively, exfoliation of the 2D polymer from a substrate or sacrificial oxidation of the top layer of a substrate (to create an insulating oxide interlayer) can be explored.

The use of 2D polymers as active components in devices will require new strategies for their synthesis over large areas and subsequent manipulation. If these efforts are successful, 2D conjugated polymers could have improved functionalities over conventional conjugated polymers, for example, by achieving true metallic behavior (zero band gap), ambipolarity of charge carriers, and higher carrier mobility. Their application in current technologies could lead to faster and less dissipative organic transistors and more efficient sensors. In the future, 2D polymerization on surfaces could enable the bottom-up construction of nanoelectronic circuits that are “one molecule” in size.

References and Notes

1. D. Li, R. B. Kaner, *Science* **320**, 1170 (2008).
2. Large polyaromatic hydrocarbons synthesized by conventional solution methods as well-defined oligomers can be considered nanographene sheets (19).
3. F. K. Abraham, D. R. Nelson, *Science* **249**, 393 (1990).
4. R. H. Baughman, H. Eckardt, M. Kertesz, *J. Chem. Phys.* **87**, 6687 (1987).
5. K. Tanaka, N. Kosai, H. Maruyama, H. Kobayashi, *Synth. Met.* **92**, 253 (1998).
6. B. Tieke, G. Wegner, D. Naegle, H. Ringsdorf, *Angew. Chem. Int. Ed.* **15**, 764 (1976).
7. Y. Okawa, M. Aono, *Nature* **409**, 683 (2001).
8. A. Miura *et al.*, *Langmuir* **19**, 6474 (2003).
9. H. Sakaguchi, H. Matsumura, H. Gong, *Nat. Mater.* **3**, 551 (2004).
10. H. Sakaguchi, H. Matsumura, H. Gong, A. M. Aboulwafa, *Science* **310**, 1002 (2005).
11. M. Matena, T. Riehm, M. Stöhr, T. A. Jung, L. H. Gade, *Angew. Chem. Int. Ed.* **47**, 2414 (2008).
12. L. Grill *et al.*, *Nat. Nanotechnol.* **2**, 687 (2007).
13. J. Michl, T. F. Magnera, *Proc. Natl. Acad. Sci. U.S.A.* **99**, 4788 (2002).
14. M. I. Veld, P. Iavicoli, S. Haq, D. B. Amabilino, R. Raval, *Chem. Commun.* **2008**, 1536 (2008).
15. S. Weigelt *et al.*, *Angew. Chem. Int. Ed.* **47**, 4406 (2008).
16. A. P. Côté *et al.*, *Science* **310**, 1166 (2005).
17. Although the conjugation can formally extend through boronic anhydride (via the $>B^{(3-)}O^{(1-)}<$ resonance structure), it will be quite weak.
18. N. A. A. Zwaneveld *et al.*, *J. Am. Chem. Soc.* **130**, 6678 (2008).
19. K. Müllen, J. P. Rabé, *Acc. Chem. Res.* **41**, 511 (2008).
20. We acknowledge funding from le Ministère du Développement Économique, de l'Innovation et de l'Exportation (Quebec), the Natural Sciences and Engineering Research Council (Canada), the Petroleum Research Fund (American Chemical Society), the Air Force Office of Scientific Research, and the Asian Office of Aerospace Research and Development (U.S.A.). D.F.P. is a Dupont Young Professor. F.R. is grateful to the Canada Research Chairs program for partial salary support.



Conjugated polymers in the plane. Chemical structures and STM images of (top) polyporphyrin **1** [reproduced from (12), with permission] and (bottom) poly(phenylenediboronic anhydride) **2** [reproduced from (18), with permission] formed on gold surfaces.

More recent studies include the electro-oxidative epitaxial polymerization of thiophene units on iodine-covered gold surfaces (9, 10) and the addition polymerization of tetra-azapyropyrene on copper (11).

Grill *et al.* (12) extended surface reactions to synthesize 2D conjugated networks by annealing tetrakis(bromophenyl)porphyrin on a gold single crystal, which acts as a passive template. The exceptionally high stability of the porphyrin core allows the monomer to be heated above 330°C, where the dissociation of the weakest C–Br bonds results in reactive phenyl radicals. Under ultrahigh-vacuum conditions, these radicals couple to each other to form a square-lattice 2D poly(tetrakisphenyleneporphyrin) **1** (see the figure, top panel). Other groups have polymerized structurally similar porphyrin

yield flexible and poorly ordered polymers. Côté *et al.* (16) have shown that heating phenylene-1,4-diboronic acid in a closed container leads to a crystalline boronic anhydride polymer consisting of layers of 2D covalent networks (17). Zwaneveld *et al.* performed the same reaction in monolayers on the Au(111) surface and imaged the resulting 2D “honeycomb” networks by STM (see the figure, bottom panel) (18). However, under the ultrahigh-vacuum conditions used in (15) and (18), the water by-product immediately desorbs, disabling the reverse self-repair reactions and leading to high defect densities. Performing such reactions at a solid-liquid interface might yield better ordered structures.

The surface polymerization reactions described above have all been performed on conducting substrates, but the useful proper-

GEOCHEMISTRY

The Descent of Minerals

Crisogono Vasconcelos and Judith A. McKenzie

Evolutionary theory states that some differences between individuals in a population are heritable, so that, when the environment changes, individuals bearing traits that provide the best adaptation to the new environment have the greatest chance for reproductive success. In a recent article in the *American Mineralogist* (1), Hazen *et al.* apply the term “evolution” to minerals in a similar manner, because new mineral patterns will adapt or evolve with changing environmental conditions throughout geologic time. The authors argue that the vast increase in the number of discrete mineral phases—from a sparse ~60 at the time of Earth’s formation to the more than 4300 known mineral species found on the modern Earth’s surface—requires an evolutionary explanation that goes beyond pure physical and chemical considerations.

Hazen *et al.* define three eras comprising 10 stages, which relate mineral evolution to the chronological divisions of Earth’s history. The eras of Earth’s mineral evolution arise from three basic mechanisms: first, the gradual change in the concentration and distribution of elements from the presolar nebula homogeneity to an expanded mineralogical diversity through physical processes during the era of planetary accretion (over 4550 million years ago); second, the introduction of new physicochemical conditions on the Earth’s surface, such as variable pressures and temperatures, as well as the increased activities of H_2O , CO_2 , and O_2 , led to a marked diversification of minerals in the terrestrial realm during the era of crust and mantle reworking (4550 to 2500 million years ago); and third, the development of widespread non-equilibrium conditions with the rising influence of life on the environment during the era of biologically mediated mineralogy (2500 million years ago to the present).

This process of mineral evolution is irreversible, advancing from sparse diversity to increasingly more variable and complex mineral assemblages. With the establishment of these chronological divisions, the authors present the scientific community with a new way to visualize the origin and evolution of Earth in a logical systematic fashion through its evolving mineralogy.

Geomicrobiology Laboratory of the Geological Institute, ETH-Zürich, 8092 Zürich, Switzerland. E-mail: cris.vasconcelos@erdw.ethz.ch



Examples of biogeochemical laminae. (Left) A 3500-million-year-old stromatolite sample collected from the Apex Chert Formation in the Pilbara region of Western Australia. The wavy laminae and small digit structures are thought to have been produced by the metabolic activity of primitive microorganisms on early Earth. (Right) Microbial mat cultured under hypersaline conditions in the Geomicrobiology Laboratory, ETH Zürich. In the uppermost green layer, the primary producers, cyanobacteria, photosynthesize the biomass and release free oxygen. The underlying pinkish-brown layers contain other microorganisms, which consume and decompose the primary organic matter. The white layers consist of calcium-magnesium carbonate precipitated in situ as a by-product of the microbes’ metabolism; they will eventually amalgamate to form distinct laminae.

Despite their complexity, the history of the planet and the history of life on Earth are profoundly linked. Science and technology have advanced to the point where this relationship can now be explored. Indeed, Hazen *et al.* relate surface geochemistry and life evolution to mineral diversity. When the Earth’s surface achieved a geochemical state that allowed life to flourish, geomicrobiological processes began to form biominerals, probably via biologically induced precipitation. These processes led to the production of large mineral deposits, such as giant banded iron formations (BIFs), which are a major economic source of iron ore. The deposition of the iron minerals in BIFs is thought to require the presence of microorganisms that can photosynthetically produce O_2 and/or oxidize Fe^{2+} ions (2).

Another example of the early association of minerals and life is exemplified by fossil stromatolites, which are considered to be the oldest evidence for microbial life on Earth. In the rock record, these remarkable structures appear as wavy laminated, lithified sedimentary growth structures, which accrete away from an initiation point or surface (3) (see the figure, left panel). The laminae comprise biominerals, such as carbonates, silica, and phosphates, and represent the former presence of a viable microbial community. This ancient microcosm contained the essential trophic groups needed to maintain life—primary producers, consumers, and decomposers—organized into specific communities that interacted with each other (4). These biological interactions induced mineral precipitation, which may have bene-

The appearance of minerals during Earth history is closely linked to biological evolution.



fited the microorganisms by providing a mechanism for generating energy.

The biochemical process of lamina formation can be observed in modern microbial mats cultured in the laboratory. The microbial community produces discrete carbonate laminae in an organic matrix, or biofilm, as a by-product of distinct metabolic activity, such as photosynthesis or sulfate reduction (5) (see the figure, right panel). Over time, the organic matrix decomposes, allowing the intercalated laminae to coalesce and eventually become amalgamated into lithified layers, which can potentially be preserved in the rock record.

Thus, the study of modern microbial mats suggests that the oldest evidence for life represents the record of a primitive minimal ecosystem, which is, however, a very complex system evolved from a cooperative and sustainable association of organisms. Indeed, the appearance of stromatolites in the early Archean (~3500 million years ago) implies that life and the associated biominerals most likely coevolved on the primitive planet. This early but complex biogeochemical phenomenon directly links biological evolution with mineral evolution.

With the introduction of mineral evolution, Hazen *et al.* provide a new perspective on the study of Earth history. Combining inorganic and organic processes in a chronological association allows scientists to calibrate geologic events in the context of the 10 stages of mineral evolution, from the simplicity of the presolar dust particles to the biomineral explosion in the past 545 million years. Understanding the formation sequence and the interactions of

PHOTO CREDITS: (LEFT TO RIGHT) C. VASCONCELOS; R. WARTHMANN

minerals associated with life on Earth could be a new proxy or tracer to evaluate the occurrence of life on other planets, that is, associating specific minerals with the physical, chemical, and biological evolution of the planet. Using mineral evolution to interpret planetary evolution has the potential to energize the field of mineralogy, placing mineralogic processes firmly in a geologic time frame.

OCEAN SCIENCE

Old New Nitrogen

Joseph P. Montoya

During the last glacial period, both nitrogen fixation and denitrification rates are likely to have been much lower than they are today.

The availability of nitrogen limits primary production in many parts of the ocean, creating a tight link between the fluxes of nitrogen and carbon through marine ecosystems. This coupling between the nitrogen and carbon cycles is often quantified in terms of “new nitrogen,” or nitrogen added to the biologically active pools in the upper ocean by processes such as vertical mixing, river runoff, atmospheric deposition, and nitrogen fixation. On page 244 of this issue, Ren *et al.* (1) introduce a powerful approach for characterizing the history of the oceanic nitrogen cycle and the role of new nitrogen in supporting primary production by measuring the nitrogen isotopic composition of the shells of planktonic foraminifera.

Recent studies have demonstrated the key role currently played by nitrogen fixation in supplying new nitrogen to nutrient-poor regions of the open ocean (2), but the overall magnitude of this key biological flux and the identity and distribution of the organisms responsible remain unclear. It is also uncertain how nitrogen fixation relates to other nitrogen-cycle processes, although stoichiometric considerations suggest that nitrogen fixation and denitrification may act together to control, and perhaps stabilize, the oceanic content of NO_3^- and other forms of combined nitrogen (3). Any global-scale decoupling of denitrification and nitrogen fixation can potentially affect marine primary production; at least one recent effort (4) suggests that the oceanic nitrogen budget is currently far from balanced, with a large excess of losses relative to inputs.

Nitrogen isotope studies have been used to

References and Notes

1. R. Hazen *et al.*, *Am. Mineral.* **93**, 1693 (2008).
2. K. O. Konhauser *et al.*, *Geobiology* **3**, 167 (2005).
3. M. A. Semikhatov *et al.*, *Can. J. Earth Sci.* **16**, 992 (1979).
4. P. T. Visscher, J. F. Stolz, *Palaeo* **219**, 87 (2005).
5. C. Vasconcelos *et al.*, *Sediment. Geol.* **185**, 175 (2006).
6. Stromatolite culture experiments were supported by grants from ETH Zürich and ESF Research Network ArchEnviron.

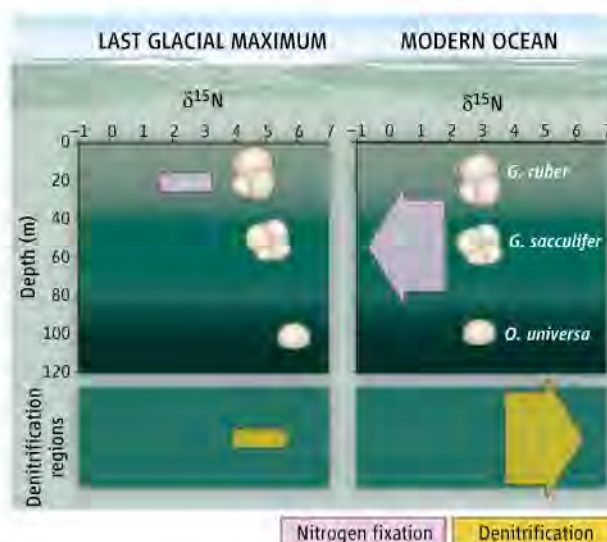
10.1126/science.1168807

both the quantity and isotopic composition of nitrogen in the ocean (6). In essence, nitrogen fixation adds new nitrogen with a low $\delta^{15}\text{N}$ to the ocean, whereas denitrification removes combined nitrogen from the ocean and increases the $\delta^{15}\text{N}$ of the nitrogen that remains.

The isotopic composition of bulk sedimentary organic matter is relatively easy to measure, but sedimentary nitrogen may undergo alteration after deposition (diagenesis). Ren *et al.* avoid this complication by measuring the isotopic composition of nitrogen in the shells of planktonic foraminifera, which live and grow in the upper water column. This approach is not novel; others have recognized that the nitrogen in the shell matrix is protected from most diagenetic processes (7). However, the small quantities of nitrogen available and the potential for contamination required careful development and testing of methods before the approach could be used profitably on real sediment samples.

Ren *et al.* first confirmed that recently deposited (core-top) foraminifera from various locations in the Atlantic and Pacific basins faithfully reflect the $\delta^{15}\text{N}$ of the inorganic nitrogen in those regions. They then investigated the $\delta^{15}\text{N}$ of nitrogen laid down by foraminifera as they fed and grew over the past 30,000 years at a site in the western Caribbean (ODP Site 999) that provides a record of conditions in the Caribbean and North Atlantic Basins.

The results reveal interesting differences between the glacial and interglacial parts of the record. First, the foraminifera shells record a clear decrease in $\delta^{15}\text{N}$ from the Last Glacial Maximum to the present (see the figure). This shift mirrors changes previously measured in bulk sedimentary nitrogen from the Cariaco Basin (an anoxic environment in the Eastern Caribbean) (8) and implies a fundamental change in the workings of the oceanic nitrogen cycle. The simplest interpretation is that oceanic nitrogen fixation supported a smaller fraction of total biological production during the glacial period than it does today. Using a simple isotopic mixing model, Ren *et al.* estimate that inputs of new nitrogen by nitrogen fixation in the glacial North Atlantic were roughly 20% of the present-day rate. Nitrogen isotope measurements of



Nitrogen past and present. The nitrogen isotopic composition ($\delta^{15}\text{N}$) of foraminifera shells was different under glacial conditions (left) than in the contemporary ocean (right). Nitrogen fixation adds ^{15}N -depleted (low- $\delta^{15}\text{N}$) nitrogen to the ocean, whereas denitrification removes nitrogen from the ocean and increases the $\delta^{15}\text{N}$ of the remainder. Under glacial conditions, new nitrogen was added to the upper water column at lower rates and at shallower depths than in the contemporary ocean.

resolve some of these uncertainties. The natural abundance ($\delta^{15}\text{N}$) of the stable isotope ^{15}N varies as a result of biologically mediated isotopic discrimination. Therefore, measurements of the $\delta^{15}\text{N}$ of plankton and dissolved inorganic nitrogen can be used to quantify the sources of nitrogen that support production in contemporary pelagic ecosystems (5). The isotopic signature of plankton in the upper water column propagates to the seafloor through sedimentation of organic matter, and the $\delta^{15}\text{N}$ of sedimentary organic matter records the relative importance of nitrogen fixation and denitrification, which have opposing effects on

sediment cores from the major regions of water column denitrification (Arabian Sea and eastern tropical Pacific) provide strong evidence for reduced denitrification during the last glacial period (6), suggesting that the major input (nitrogen fixation) and output (denitrification) terms of the oceanic nitrogen budget were both much lower under glacial conditions. This suggests a close coupling between these fluxes and feedback stabilization of oceanic nitrogen content, perhaps mediated by competition for nutrients between nitrogen fixers and other plankton (3).

Second, the results provide evidence of subtle but intriguing differences in the vertical distribution of nitrogen fixation through time. Many foraminiferal species have restricted depth ranges. Ren *et al.* used these species-specific characteristics to investigate the vertical distribution of nitrogen isotopes. The data show a clear isotopic separation of three foraminifera species during the last glacial period. In contrast, modern samples of the same three species have very similar $\delta^{15}\text{N}$ values, despite occupying different depth ranges of the upper water

column. This difference could arise through behavioral changes through time, but a more likely explanation is that these amoebae recorded a real change in the isotopic gradient of the upper water column. This shift appears to reflect both a reduced overall rate of nitrogen fixation in the North Atlantic and an upward shift in the vertical distribution of nitrogen fixation during the glacial period. In contrast, in today's ocean, nitrogen fixation is carried out by various organisms distributed throughout the upper water column of warm, nutrient-depleted waters (9–11).

Ren *et al.* have shown that foraminifera shells can be used to elucidate the past nitrogen cycle. The apparent reduction of both the denitrification and the nitrogen fixation rate in the glacial ocean suggests that these processes may be linked in a way that makes substantial imbalances in the nitrogen budget unlikely, at least on millennial time scales. The nature of these linkages remains unclear, but the old new nitrogen trapped in foraminifera shells provides an important record of the

oceanic nitrogen cycle and a valuable tool for investigating the controls on nitrogen fixation in the ocean.

References

1. H. Ren *et al.*, *Science* **323**, 244 (2009); published online 18 December 2008 (10.1126/science.1165787).
2. J. P. Zehr, H. W. Paerl, in *Microbial Ecology of the Oceans*, D. Kirchman, R. Mitchell, Eds. (Wiley, New York, ed. 2, 2008), pp. 481–526.
3. N. Gruber, in *Carbon-Climate Interactions*, M. Follows, T. Oguz, Eds. (Kluwer Academic, Dordrecht, Netherlands, 2004), pp. 97–148.
4. L. A. Codispoti, *Biogeosciences* **4**, 233 (2007).
5. J. P. Montoya, in *Nitrogen in the Marine Environment*, D. G. Capone, E. J. Carpenter, M. R. Mulholland, D. A. Bronk, Eds. (Academic Press, Burlington, MA, ed. 2, 2008), pp. 1277–1302.
6. E. D. Galbraith, D. M. Sigman, R. S. Robinson, T. Pedersen, in *Nitrogen in the Marine Environment*, D. G. Capone, E. J. Carpenter, M. R. Mulholland, D. A. Bronk, Eds. (Academic Press, Burlington, MA, ed. 2, 2008), pp. 1497–1535.
7. M. A. Altabet, W. B. Curry, *Global Biogeochem. Cycles* **3**, 107 (1989).
8. A. N. Meckler *et al.*, *Global Biogeochem. Cycles* **21**, GB4019 (2007).
9. M. J. Church *et al.*, *Limnol. Oceanogr.* **53**, 63 (2008).
10. J. P. Zehr *et al.*, *Limnol. Oceanogr.* **52**, 169 (2007).
11. R. J. Langlois, D. Hummer, J. LaRoche, *Appl. Environ. Microbiol.* **74**, 1922 (2008).

10.1126/science.1168246

DEVELOPMENTAL BIOLOGY

Pluripotent Chromatin State

Andrew S. Chi^{1,2,3} and Bradley E. Bernstein^{1,2,4}

Embryonic stem cells have the unique ability to self-renew and to develop into any cell type, making them an essential model for developmental biology and a promising source for cell transplantation therapy. How embryonic stem cells maintain this suspended state of pluripotency is the subject of intense investigation.

Embryonic stem cell identity is specified by a network that principally involves the transcription factors Oct4, Sox2, and Nanog. Adult somatic cells can be reprogrammed to pluripotent embryonic stemlike cells by overexpressing certain transcription factors in this network (1). It has been suggested that embryonic stem cells represent a “ground state” for a mammalian cell based solely on the activities of these transcription factors and a “freedom” from extrinsic signals for cell differentiation (2).

Chromatin—the DNA and proteins that comprise chromosomes—might also affect this ground state as its components include fundamental regulators of development. Indeed, chromatin in embryonic stem cells differs from that in lineage-restricted cells in several respects. Embryonic stem cell chromatin is decondensed, such that major structural proteins, such as histone H1, are loosely bound and exhibit hyperdynamic binding kinetics (3). High expression levels of Polycomb-group repressor proteins and methylation of histone 3 (H3) on a specific lysine (K27) are present, most notably associated with silenced developmental gene loci (4, 5). These target loci also exhibit features of active chromatin (regions where DNA is being transcribed into RNA), including histone 3 methylation on lysine 4, which may ready genes for subsequent expression (6, 7).

Despite its unique properties, the function of chromatin in embryonic stem cells remains uncertain. Embryonic stem cell lines that lack critical chromatin regulators, including DNA methyltransferases, histone methyltransferases, chromatin-remodeling proteins, and Polycomb-group proteins (8), tend to exhibit defective differentiation, which may reflect roles for these components in differentiation-

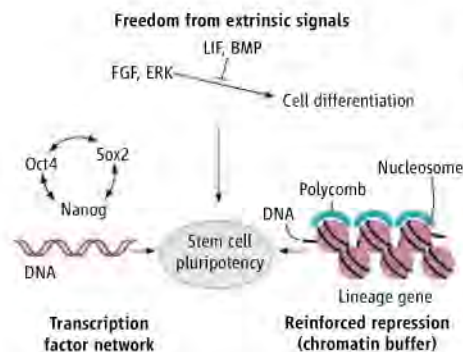
Chromatin in pluripotent embryonic stem cells may act as a buffer to transcriptional noise.

associated remodeling and/or the subsequent engagement of lineage-specifying epigenetic controls. Yet, the viability of these mutant embryonic stem cells implies that chromatin regulation may paradoxically be dispensable for maintaining embryonic stem cell identity.

Nonetheless, a growing body of research highlights an essential function for chromatin in buffering variability in transcription, a control of “noise” that is almost certainly an indispensable feature of the embryonic stem cell ground state. An embryonic stem cell occupies a precarious position—ready to respond to differentiation signals with extensive transcriptional changes. To maintain a pluripotent state, it must minimize stochastic extrinsic and intrinsic signals that create noise in gene expression and may initiate differentiation (see the figure).

Biochemical, genetic, and computational studies indicate that chromatin can buffer transcriptional noise (9–13). Chromatin consists of nucleosomes, which contain DNA wrapped around histone proteins. Transcription factors compete with histones for access to DNA, and the binding energy of several factors is typically required to displace one nucleosome. This “collaborative competition” between transcription factors and chromatin has profound

¹Molecular Pathology Unit and Center for Cancer Research, Massachusetts General Hospital, Charlestown, MA 02129, USA. ²Broad Institute of Harvard and Massachusetts Institute of Technology, Cambridge, MA 02139, USA. ³Stephen E. and Catherine Pappas Center for Neuro-Oncology, Department of Neurology, Massachusetts General Hospital, Boston, MA 02114, USA. ⁴Department of Pathology, Harvard Medical School, Boston, MA 02115, USA. E-mail: bernstein.bradley@mgh.harvard.edu



Recipe for pluripotency. Hallmark requirements of the embryonic stem cell ground state include the transcription factor network (1) and neutralization of extrinsic perturbations by signaling pathway inhibitors (2, 17) and chromatin. BMP, bone morphogenetic protein; ERK, extracellular signal-related kinase; FGF, fibroblast growth factor; and LIF, leukemia inhibitory factor.

consequences at the level of gene regulation, including threshold responses and combinatorial control (9, 10). By setting thresholds, nucleosomes may help prevent inappropriate gene expression due to weak activating signals and limit noise-induced errors.

In addition, nucleosome remodeling can directly affect noise in gene expression. For example, noise in the expression of the gene *PHO5* in yeast is due to stochastic remodeling events that remove and re-form nucleosomes on the gene's promoter region (11, 12). Remarkably, the extent of noise fluctuation can be altered in cis by mutations affecting nucleosome stability at the *PHO5* promoter or in trans by mutations affecting chromatin-remodeling complexes.

The basic elements of transcriptional noise and buffering are likely common to all eukaryotes. Mammalian cell models exhibit stochastic bursts of gene expression that can underlie large variations within a population (14). The nucleosomal buffering mechanisms established in yeast may be particularly applicable to embryonic stem cells, whose dynamic chromatin environment and relative lack of restrictive heterochromatin are reminiscent of the model organism. Their accessible chromatin state appears to render embryonic stem cells prone to transcriptional leakiness (15). This may confer a greater dependency on buffering, especially at lineage-specifying developmental genes whose promoters must integrate many signals and whose inappropriate expression risks triggering cell differentiation.

How might embryonic stem cells achieve a higher level of transcriptional safeguarding without compromising their plasticity? Noise buffering can be tuned by varying the activities of chromatin complexes. Polycomb-group repressors are attractive candidates for such a role

because they are highly expressed in embryonic stem cells and target many developmental genes. Although the functional importance of Polycomb-group proteins in pluripotency has been called into question by the viability of embryonic stem cell lines that lack these repressors (8), the propensity of these cells to differentiate, and their weak up-regulation of target gene expression (4, 16), are consistent with a role in minimizing transcriptional fluctuations.

Hence, by reinforcing the repression of critical gene targets, Polycomb proteins filter noise and neutralize extrinsic perturbations—a hallmark requirement of the embryonic stem cell ground state (2). Other chromatin components, such as nucleosome-remodeling complexes whose expression is disproportionately increased (15), may also contribute to a specialized network that stabilizes the pluripotent state by minimizing extrinsic signals, yet remains permissive to appropriate differentiation programs.

The compelling implication is that chromatin may play distinct regulatory roles that vary during development. Its buffering function, perhaps most essential in early development, is distinct from the epigenetic functions typically ascribed to chromatin in lineage-committed cells. The latter is associated with

stable chromatin compaction and silencing of nonutilized genomic loci. The widespread changes in chromatin dynamics and the expression of key chromatin components during differentiation may reflect a functional reprioritization of chromatin, from a buffer to a preserver of lineage fidelity.

References and Notes

1. R. Jaenisch, R. Young, *Cell* **132**, 567 (2008).
2. J. Silva, A. Smith, *Cell* **132**, 532 (2008).
3. E. Meshorer et al., *Dev. Cell* **10**, 105 (2006).
4. L. A. Boyer et al., *Nature* **441**, 349 (2006).
5. T. I. Lee et al., *Cell* **125**, 301 (2006).
6. V. Azuara et al., *Nat. Cell Biol.* **8**, 532 (2006).
7. B. E. Bernstein et al., *Cell* **125**, 315 (2006).
8. H. Niwa, *Development* **134**, 635 (2007).
9. J. A. Miller, J. Widom, *Mol. Cell Biol.* **23**, 1623 (2003).
10. F. H. Lam, D. J. Steger, E. K. O'Shea, *Nature* **453**, 246 (2008).
11. J. M. Raser, E. K. O'Shea, *Science* **304**, 1811 (2004).
12. H. Boeger, J. Griesenbeck, R. D. Kornberg, *Cell* **133**, 716 (2008).
13. I. B. Dodd, M. A. Micheelsen, K. Sneppen, G. Thon, *Cell* **129**, 813 (2007).
14. A. Raj, C. S. Peskin, D. Tranchina, D. Y. Vargas, S. Tyagi, *PLoS Biol.* **4**, e309 (2006).
15. S. Efroni et al., *Cell Stem Cell* **2**, 437 (2008).
16. D. Pasini, A. P. Bracken, J. B. Hansen, M. Capillo, K. Helin, *Mol. Cell Biol.* **27**, 3769 (2007).
17. Q. L. Ying et al., *Nature* **453**, 519 (2008).
18. We thank J. Widom, L. Gaffney, A. Meissner, and E. Mendenhall for comments and discussion.

10.1126/science.1166261

DEVELOPMENTAL BIOLOGY

Histone Cross-Talk in Stem Cells

Edwin Smith and Ali Shilatifard

Specificity of gene regulation in stem cells may occur at the level of ubiquitin signaling to chromatin.

Stem cells have garnered substantial interest for their role in development, as a potential source of cell-based therapy in a number of diseases, and for the possibility that cells with stem cell properties are a common factor in tumorigenesis (1). The defining feature of all stem cells is the ability to both self-renew and give rise to other cell types. Beyond that, however, commonalities in stem cell biology are exceptional. The fruit fly *Drosophila melanogaster* has been a major source of our knowledge of stem cell biology, with several different types of adult stem cells having been identified in different tissues. On page 248 of this issue (2), Buszczak et al. have identified Scrawny (SCNY), a ubiquitin-specific protease, that targets a histone protein (H2B) as a common

requirement for maintaining multiple types of adult stem cells in *Drosophila*.

Ubiquitin-specific proteases form a large family of enzymes that remove ubiquitin molecules from proteins, either to rescue them from destruction (in the case of polyubiquitination) or to reverse the monoubiquitination of proteins, a posttranslational modification involved in cellular signal transduction. Recently, several members of this family have been shown to act on histones, proteins that package DNA into either open and active chromatin or more repressed chromatin (3). Buszczak et al. have identified SCNY as a ubiquitin-specific protease enriched in male and female germline stem cells. They show that it deubiquitinates monoubiquitinated H2B in vitro and that the amount of monoubiquitinated H2B increases in mutant larvae that lack the functional enzyme. Loss of SCNY function leads to premature differentiation and stem cell loss in at least four adult stem cell types: male and

Stowers Institute for Medical Research, 1000 East 50th Street, Kansas City, MO 64110, USA. E-mail: ash@stowers-institute.org

female germline stem cells, follicle stem cells, and intestinal stem cells. Thus, SCNY could be part of a common mechanism for regulating stem cell renewal and differentiation.

Cell identity is in large part regulated at the level of chromatin structure, with several key developmental regulators acting as modifiers of histones (4). Numerous histone modifications can be correlated with particular transcriptional states of a gene, at different regions of a gene, and in distinct areas within the genome. Two of the best-characterized modifications are the methylation of histone H3 on lysines 4 and 27 (H3K4 and H3K27), carried out respectively by the methyltransferases Trithorax and Enhancer of zeste, and their

increases the amount of H2B ubiquitination and H3K4 methylation through a conserved trans-histone cross-talk pathway (see the figure). Such cross-talk was first described in budding yeast, in which H3K4 methylation requires that the H2B histone first be ubiquitinated by the enzymes Rad6 and Bre1 (7–9). Although there is only one H3K4 methylase in budding yeast, called COMPASS, there are several COMPASS-related complexes found in metazoans (including Set1 and MLL1–4) that can methylate H3K4 (10). In budding yeast, interaction of COMPASS (via its Cps35 subunit) with chromatin depends on the monoubiquitination of histone H2B, and this may facilitate monoubiquitination-methylation cross-talk (11). Indeed,

in mammals, Wdr82, the homolog of Cps35, also interacts with chromatin in a histone H2B monoubiquitination-dependent manner, indicating that this mechanism for cross-talk could be conserved from yeast to humans (12). Because Wdr82 specifically associates with the COMPASS-related complex Set1, the latter is likely the H3K4 methyltransferase that is regulated by the monoubiquitinated form of H2B.

SCNY may function as a transcriptional repressor in adult stem cells by continually removing ubiquitin from histone H2B at the promoters of genes, thereby preventing H3K4 methylation. This is similar to Ubp10, the ubiquitin protease in budding yeast that removes ubiquitin from histone H2B to silence gene expression

(13, 14). This scenario implies that the Rad6-Bre1 ubiquitination complex is already present at the SCNY-repressed genes. These genes may be in a poised state, waiting for a developmental signal to quickly activate gene expression. This is in contrast to the poised state of genes in embryonic stem cells, which are already methylated on H3K4.

It is becoming increasingly clear that ubiquitin signaling to chromatin is pervasive in gene regulation. For example, ubiquitination of H2A is associated with silencing of genes by Polycomb repressor proteins, and a histone acetyltransferase complex uses an H2A-deubiquitinating enzyme to activate Polycomb-repressed genes (15). Polycomb group proteins play a major role in stem cell biology and may be misregulated in cancer stem cells as well (16). In addition to the gene-silencing properties of Ubp10 and SCNY, other H2B-deubiquitinating enzymes are associated with gene activation. A human

GCN5 histone acetyltransferase complex contains an H2B deubiquitinase needed for activation of genes by the proto-oncogene Myc and is required for Myc-mediated cellular transformation (17). Even though H2B ubiquitination is required for H3K4 methylation, failure to subsequently remove ubiquitin interferes with transcription. Furthermore, histones with mutations that increase H2B ubiquitination display reduced H3K4 methylation, which suggests that H2B ubiquitination and deubiquitination are dynamic and highly regulated processes (18). To complicate matters even further, loss of H2B monoubiquitination in fission yeast is more severe than loss of H3K4 methylation, which suggests that H2B monoubiquitination has more roles than currently realized (19).

Identifying proteins that associate with SCNY could provide insight into how SCNY activity is regulated, including how it is targeted to stem cell-repressed genes. It will also be worth considering whether SCNY deubiquitinates nonhistone targets. SCNY is a member of a large family of ubiquitin-specific proteases, with 16 members in budding yeast, 18 in *Drosophila*, and more than 50 in mammals. At least two enzymes in yeast and three in *Drosophila* have been demonstrated to be H2B-deubiquitinating enzymes. This is in contrast to a single Rad6-Bre1 ubiquitin ligase complex in these species (8). This may indicate that implementation of monoubiquitinated H2B by Rad6-Bre1 is a general process and that specificity in gene regulation may occur at the level of histone deubiquitination. Because this is a relatively new field of study, more ubiquitin-specific proteases that can deubiquitinate H2B and regulate gene expression are likely to be identified.

References

1. J. B. Sneddon, Z. Werb, *Cell Stem Cell* **1**, 607 (2007).
2. M. Buszczak, S. Paterno, A. C. Spradling, *Science* **323**, 248 (2009).
3. V. M. Weake, J. L. Workman, *Mol. Cell* **29**, 653 (2008).
4. S. R. Bhaumik, E. Smith, A. Shilatifard, *Nat. Struct. Mol. Biol.* **14**, 1008 (2007).
5. B. E. Bernstein et al., *Cell* **125**, 315 (2006).
6. M. G. Guenther, S. S. Levine, L. A. Boyer, R. Jaenisch, R. A. Young, *Cell* **130**, 77 (2007).
7. J. Dover et al., *J. Biol. Chem.* **277**, 28368 (2002).
8. A. Shilatifard, *Annu. Rev. Biochem.* **75**, 243 (2006).
9. Z. W. Sun, C. D. Allis, *Nature* **418**, 104 (2002).
10. A. Shilatifard, *Curr. Opin. Cell Biol.* **20**, 341 (2008).
11. J. S. Lee et al., *Cell* **131**, 1084 (2007).
12. M. Wu et al., *Mol. Cell Biol.* **28**, 7337 (2008).
13. N. C. Emre et al., *Mol. Cell* **17**, 585 (2005).
14. R. G. Gardner, Z. W. Nelson, D. E. Gottschling, *Mol. Cell Biol.* **25**, 6123 (2005).
15. P. Zhu et al., *Mol. Cell* **27**, 609 (2007).
16. A. Sparmann, M. van Lohuizen, *Nat. Rev. Cancer* **6**, 846 (2006).
17. X. Y. Zhang et al., *Mol. Cell* **29**, 102 (2008).
18. S. Nakanishi et al., *Nat. Struct. Mol. Biol.* **15**, 881 (2008).
19. J. C. Tanny, H. Erdjument-Bromage, P. Tempst, C. D. Allis, *Genes Dev.* **21**, 835 (2007).

Cross-talk in stem cell maintenance. In certain adult *Drosophila* stem cells, SCNY removes ubiquitin (Ub) from histone H2B at promoters of genes that need to stay silent to maintain stem cell identity. During stem cell differentiation, SCNY is inactivated to allow Rad6-Bre1 to monoubiquitinate histone H2B. This modification is required for recruitment and activation of the COMPASS histone methylase complex, which methylates (Me) histone H3 (H3K4).

related protein complexes (4). H3K4 methylation occurs at the promoters of actively expressed genes, whereas H3K27 methylation is associated with the silencing of genes during development. Interestingly, both modifications can coexist on promoters of genes in embryonic stem cells, which suggests that genes in pluripotent cells could be poised to choose either an active or a repressed fate for genes as appropriate to the developmental context (5). Many genes, despite being quiescent in embryonic stem cells, may be poised for activation, with RNA polymerase II already waiting at the promoter for activation (6).

In this context, it is remarkable that Buszczak et al. find that an enzyme that removes ubiquitin from H2B is required to prevent premature stem cell differentiation in adult stem cells. Repression of a subset of genes within stem cells is required to maintain stem cell identity, and their premature activation results in stem cell loss. Loss of SCNY in-

Darwin's Originality

Peter J. Bowler

Charles Darwin's theory of natural selection has been hailed as one of the most innovative contributions to modern science. When first proposed in 1859, however, it was widely rejected by his contemporaries, even by those who accepted the general idea of evolution. This article identifies those aspects of Darwin's work that led him to develop this revolutionary theory, including his studies of biogeography and animal breeding, and his recognition of the role played by the struggle for existence.

The publication of Charles Darwin's *On the Origin of Species* in 1859 is widely supposed to have initiated a revolution both in science and in Western culture. Yet there have been frequent claims that Darwinism was somehow "in the air" at the time, merely waiting for someone to put a few readily available points together in the right way [for instance (1)]. The fact that Alfred Russel Wallace (Fig. 1) independently formulated a theory of natural selection in 1858 is taken as evidence for this position. But Darwin had created the outlines of the theory 20 years earlier, and there were significant dif-

ferences between the ways in which he and Wallace formulated their ideas. In this essay, I argue that Darwin was truly original in his thinking, and I support this claim by addressing the related issue of defining just why the theory was so disturbing to his contemporaries.

pre-existing ones in a progressive sequence leading up to humans (5). But if the general idea of evolution was not entirely new, Darwin's vision of how the process worked certainly was. Although the theory was eventually paralleled by Wallace, Darwin had conceived its basic outline in the late 1830s, after his return from the voyage of H.M.S. *Beagle*. He worked on it in relative isolation over the next 20 years, until the arrival of Wallace's paper in 1858 precipitated the flurry of activity leading to the publication of the *Origin*.

Historians have quarried Darwin's notebooks and letters to establish the complex process by

opments that would push other naturalists toward an evolutionary vision during the years he worked in isolation. By the late 1850s, the idea of progressive evolution was widely recognized, and the positive role of individual competition was being articulated by thinkers such as Herbert Spencer (Fig. 1). But key aspects of the Darwinian vision were truly original and would not have occurred to any other naturalist at the time. Here, Wallace provides a good comparison: He too moved toward the idea of branching evolution driven by local adaptation, but even he did not share Darwin's insight that the work of the animal breeders throws light on the process of natural selection.

The theory was both original and disturbing. It was not just that the idea of natural selection challenged the belief that the world was designed by a wise and benevolent God. There was a wider element of teleology or goal-directedness almost universally accepted at the time. Most thinkers—including Jean-Baptiste Lamarck and Chambers—took it for granted that the development of life on earth represents the unfolding of a coherent plan aimed at a predetermined goal. (This assumption is still preserved in the very term "evolution"; the Latin *evolutio* refers to the unrolling of a scroll.) The explanatory framework centered on the



Fig. 1. Charles Darwin, Alfred Russel Wallace, and Herbert Spencer.

ferences between the ways in which he and Wallace formulated their ideas. In this essay, I argue that Darwin was truly original in his thinking, and I support this claim by addressing the related issue of defining just why the theory was so disturbing to his contemporaries.

Darwin was certainly not the first to suggest the idea of evolution as an alternative to the creation of species by God. J. B. Lamarck's theory, published in 1809, had been widely discussed, although generally rejected (2–4). Robert Chambers's *Vestiges of the Natural History of Creation* of 1844 sparked a debate over the possibility that new species were produced from

which he developed his theory (6–9). Darwin was a highly creative thinker who synthesized a number of key insights, some derived from his scientific work and others from currents circulating in his cultural environment. Few would now accept the claim that evolution by natural selection was in the air. Darwin approached the subject in a way that was significantly different from any of the other efforts being made to explain the history of life on earth. He had a unique combination of scientific interests that alerted him to topics ignored by other naturalists. He certainly drew on ideas widely discussed at the time, but was forced by his scientific interests to use those sources of inspiration in a highly original way.

To some extent, Darwin may have been merely "ahead of his time," anticipating devel-

theory of natural selection challenged this vision of nature as an orderly pattern of relations.

Darwin's world view was profoundly different because he argued that the adaptation of populations to their local environment was the sole cause of transmutation. Many people found it hard to see natural selection as the agent of either divine benevolence or of a rationally structured cosmic teleology. Selection adapted species to an ever-changing environment, and it did so by killing off "useless" variations in a ruthless "struggle for existence." This did not seem the kind of process that would be instituted by a benevolent God, especially because its essentially "selfish" nature meant that a parasitic way of life was a perfectly natural adaptive response in some circumstances.

More seriously for the idea of cosmic teleology, Darwin's supposition that the production

of the individual variants in a population was essentially undirected ruled out any possibility that evolution could be shaped by a predetermined developmental trend. There was no obvious goal toward which it was aimed, and it did not produce an orderly pattern of relations between species. The accusation that the theory depended on "random" variation indicated the concerns of his opponents on this score. As Darwin himself made clear, variation was certainly caused by something (later identified as genetic mutations), but it was not aimed in any one direction and, thus, left adaptive evolution essentially open-ended. He allowed a limited role for variation shaped by the organisms' own activities (the so-called Lamarckian effect), but this too permitted multiple vectors of change. Evolution had to be depicted as a branching tree in which each act of branching was the result of a more or less unpredictable migration of organisms to a new location. At the same time, Darwin's theory undermined the old idea that species were idealized types, fixed elements in a clearly defined natural order. Species had to be treated as populations of varying individuals, with no fixed limit on the range of possible variation.

The Tree of Life

One innovation at the heart of Darwin's theory seems so obvious today that it is hard for us to appreciate just how new and how radical it was at the time. Lamarck had proposed that there might be natural processes adapting species to changes in their environment. But Darwin was perhaps the first to realize that if adaptation to the local environment was the only mechanism of evolution, there would be major implications for the whole system by which species are classified into groups. Darwin's mentor in geology, Charles Lyell, had shown how his uniformitarian theory would allow the biogeographer to reconstruct the migrations of species on an ever-changing earth. Populations could sometimes become divided by geographical barriers, so that what was once a single species could split into multiple branches adapting to separate environments (10). Evolution would become a divergent process, with some branches splitting over and over again, whereas others came to a dead end through extinction.

The image of the tree of life had appeared in Darwin's notebooks of the late 1830s (Fig. 2) and was proposed independently by Wallace in a paper published in 1855. Both realized that it explained why naturalists were able to arrange species into groups within groups, using descent from a common ancestor to explain the underlying similarities. Closely related species have diverged recently from a common ancestor, whereas the ancestry of more distantly related forms must be traced further back down the family tree to find the common point of origin.

The idea of common descent now seems so obvious that we might wonder what alternative models could have been proposed to account for

the relations among species. Several proposals available in the 1830s deflected attention away from the model of the branching tree (11). William Sharp Macleay's quinary or circular system of classification supposed that every genus contained five species that could be arranged in a circle; each family five genera, and so on through the taxonomic hierarchy. Chambers's *Vestiges of the Natural History of Creation* depicted evolution in terms of parallel lines advancing through a predetermined sequence of stages within each family, driven by force derived from individual development.



Fig. 2. Tree of Life, from Darwin's notebooks (22).

These rigidly structured models of taxonomic relations and evolution made good sense to anyone embedded in a vision of nature as a predictable, orderly system governed by a divine plan. Such a world view made it difficult to accept that the history of life on earth might be essentially irregular and unpredictable, dependant on the hazards of migration, isolation, and local adaptation. Darwin was led toward his alternative model in part because he was more interested in adaptation than cosmic teleology, thanks to the influence of William Paley's natural theology. Natural selection replaced divine benevolence as an explanation of adaptation. Unlike Macleay and Chambers, Darwin did not expect

his theory to predict an orderly pattern of relations.

It has been argued that Darwin's move to a more historical viewpoint was inspired by German romanticism [e.g. (12)], but a more practical incentive was provided by the biogeographical insights gained on the *Beagle* voyage (1831–36). The Galapagos species provided the most obvious example of how the relations within a group can be explained by supposing that an original population became divided up, in this case by independent acts of migration to oceanic islands. Here, Darwin followed Lyell in seeing that bio-

geography must become a historical science, explaining present distributions in terms of past migrations, extinctions and (for Darwin but not for Lyell) evolutionary adaptations. Populations divided by geographical barriers will develop independently as each adapts to its new environment in its own way, and the possibility that barriers can be crossed occasionally allows for the branching process of evolution that Darwin conceived in the late 1830s. It was by approaching the problem of the origin of new species through a study of biogeography that Darwin was led to construct his model of open-ended, divergent evolution. Wallace developed a similar model and tested it during his explorations in South America and the Malay Archipelago (modern Indonesia).

Adrian Desmond and James Moore have recently proposed that Darwin's hatred of slavery prompted his move toward evolutionism (13). Because many slaveholders argued that the black race was separately created from the white, Darwin wanted to show that all races share a common ancestry, and he realized that this claim could be defended by extending the idea throughout the animal kingdom. As a basis for his thinking, this thesis is sure to generate much controversy, but if accepted it would emphasize the crucial role played by his move toward a model of branching evolution based on geographical diversity.

This model was so radical that many late 19th-century evolutionists were unable to accept it in full. Ernst Mayr argued that the theory of common descent was one of Darwin's greatest achievements, in addition to natural selection itself (14). So it was, but I think Mayr overestimated the rapidity with which other naturalists were converted to the theory. Many of the non-Darwinian theories of evolution proposed during the "eclipse of Darwinism" in the late 19th century were introduced with the aim of subverting the implications of the principle of common

descent (15). The American neo-Lamarckians Edward Drinker Cope and Alpheus Hyatt proposed that the evolution of each group should be seen as a series of parallel lines moved through the same hierarchy of developmental stages, an updated version of the idea suggested in Chambers's *Vestiges*. The similarities linking the species in a genus were due not to a recent common ancestry, but to parallel trends independently reaching the same stage of development. Like Chambers, they endorsed the recapitulation theory (ontogeny recapitulates phylogeny, in the terminology introduced by Ernst Haeckel) and saw evolution as the addition of preordained stages to ontogeny. Adaptation was not crucial once the basic character of the group was established, and the linear, orthogenetic evolution of the group might eventually generate bizarre nonadaptive characters as a prelude to extinction—the theory of “racial senility.” Darwin could make no sense of the theory proposed by Cope and Hyatt, because he could not imagine an evolutionary process driven by predetermined trends. But the fact that such theories flourished in the late 19th century demonstrates just how radical the theory of open-ended, divergent evolution was to the naturalists of the time.

Artificial Selection

These non-Darwinian models were ultimately marginalized by the synthesis of the selection theory and genetics in the early 20th century. Genetic mutations seemed to be essentially pluralistic and undirected, providing just the source of “random” variation that Darwin’s mechanism required as its raw material. This later development highlights the importance of another insight gained by Darwin in the late 1830s, his decision to investigate the work of the animal breeders (Fig. 3) and his recognition that their method of artificial selection offered a useful way of understanding how the equivalent natural process operated. The exact role played by Darwin’s study of breeding in the formulation of his theory is much debated by historians (16–17), but there can be little doubt of how important the analogy between artificial and natural selection became in his later thinking. In this case, Darwin was truly unique, because even Wallace did not take this step and dissociated himself from the link with artificial selection expressed in Darwin’s later writings.

Darwin turned to the breeders in search of a clue as to how a population could be changed—here at least was a situation where modifications were actually being produced on a human time

scale and that could be investigated directly. There was a well-developed network of breeders by this time, and although their ideas about heredity and variation were distinctly pregenetical (like Darwin’s own), they had a very clear appreciation of how they produced changes in their artificially small populations. The insight that they worked by selection may have been important (this is the point of contention among experts studying Darwin’s notebooks), but the breeders certainly taught him one thing. He realized that in a domesticated population there is always a fund of apparently purposeless and undirected variation among individual organisms. Although convinced that the degree of variability was artificially enhanced under domestication, Darwin, nevertheless, accepted that there must be some equivalent variability in every wild population. The analogy with artificial selection then allowed him to depict natural selection as a parallel process in which a few variant individuals, in this case with characters useful to the species rather than the human breeder, survive and reproduce. Those with harmful characters are eliminated by the struggle for existence, just as the breeder will not permit any animal to reproduce if it does not have the character he wants. It was the breeders who taught Darwin that variation is not directed toward some preordained goal, allowing him to build on his existing conviction that adaptive evolution must be an open-ended, branching process.

At the same time, the breeders’ attitude toward variation pushed Darwin toward the view that the species is just a population of

interbreeding individuals. Traditionally, species were treated as idealized types with a fixed essence, any variation from the norm being trivial and impermanent. The breeders knew that they could produce huge changes in structure by accumulating normal variations over a number of generations. When Darwin linked this information with his conviction that species could change indefinitely over time, he was driven toward a new form of species concept in which the population becomes paramount. The natural range of variability becomes part of the species’ character, not the result of accidental deviations from a fixed norm. This is what Mayr called the transition from typological thinking to population thinking, and although he may have exaggerated the extent to which Darwin himself made the conceptual transition, the subsequent development of the selection theory brought this implication out more clearly.

In the debates that followed the publication of *On the Origin of Species*, the analogy with artificial selection continued to play a key role by forcing even Darwin’s critics to think about the problems of heredity and variation in a new way (18). Opponents such as Fleeming Jenkin, who saw selection working on large variations or “sports of nature,” were, nevertheless, still working within the framework defined by this analogy. For supporters such as Francis Galton, artificial selection helped to clarify the nature of both heredity and selection, paving the way for the revolutionary impact of Mendelian genetics. The notion of “hard” heredity was introduced in opposition to the “soft” form of



Fig. 3. Pigeons (23).

inheritance implied by the Lamarckian process. The undirected nature of variation was clarified both through the study of large populations by Galton and through the breeding studies of the geneticists. Although it took some time for the geneticists to accept the situation, their studies of mutation ultimately endorsed Darwin's claim that the only way the environment could affect the population was by selection. Modern evolutionary developmental biology has reopened the question of whether variation and evolution can be quite as open-ended as Darwin and his followers believed. But the non-Darwinian vision of evolution unfolding to an orderly, predictable plan has been essentially marginalized by acceptance of the key insights on which Darwin based his theory of natural selection.

The Struggle for Existence

One of the most disturbing aspects of Darwin's theory was its appeal to the struggle for existence as the natural process that equates with the breeder's activity as a selecting agent. This very harsh vision of nature certainly threatened the traditional belief in a benevolent Creator. The term "struggle for existence" occurs in Thomas Robert Malthus's *An Essay on the Principle of Population*, although used in the context of tribal groups competing for limited resources. Darwin saw that population pressure would lead to competition between individuals and was perhaps the first to realize that it might represent a means by which the population could change through time (19, 20). The process worked by eliminating the least fit variants within the population and allowing the better adapted to survive and breed. This was what the philosopher Herbert Spencer would later refer to as the "survival of the fittest." Strictly speaking, natural selection requires only differential reproduction among variants, but Darwin thought that the pressure of competition was necessary to make it effective. It seems that without the input from Malthus, he would not have come up with the theory.

The idea of struggle was pervasive in the literature of the period, but could be exploited in many different ways. In the 1850s, Spencer had already seen how competition could be turned into a very different, and in some respects less disturbing, mechanism of progress (21). For Spencer, the interaction between individuals stimulated their efforts to adapt to the changing social and physical environment. He then invoked Lamarck's concept of the "inheritance of acquired characteristics" to explain how these self-improvements accumulated over many generations, leading to biological evolution and social progress. Spencer's self-improvement model of progress became immensely popular in the later 19th century, and because it too seemed to rely on struggle as the motor of change, it was often confused with the Darwinian mechanism. In fact, Spencer thought that all humans will eventually acquire the faculties needed to interact harmoniously with one another.

But his occasional use of highly individualistic language allowed him to be perceived as the apostle of free enterprise. Much of what later became known as "social Darwinism" was, in fact, Spencerian social Lamarckism expressed in the terminology of struggle popularized by Darwin.

This point is important in the context of the charge raised by modern opponents of Darwinism that the theory is responsible for the appearance of a whole range of unpleasant social policies based on struggle. Darwin exploited the idea of the struggle for existence in a way that was unique until paralleled by Wallace nearly 20 years later. Their theory certainly fed into the movements that led toward various kinds of social Darwinism, but it was not the only vehicle for that transition in the late 19th century. It did, however, highlight the harsher aspects of the consequences of struggle. The potential implications were drawn out even more clearly when Galton argued that it would be necessary to apply artificial selection to the human race in order to prevent "unfit" individuals from reproducing and undermining the biological health of the population. This was the eugenics program, and in its most extreme manifestation at the hands of the Nazis, it led not just to the sterilization but also to the actual elimination of those unfortunates deemed unfit by the state. Did Darwin's emphasis on the natural elimination of maladaptive variants help to create a climate of opinion in which such atrocities became possible?

It has to be admitted that, by making death itself a creative force in nature, Darwin introduced a new and profoundly disturbing insight into the world, an insight that seems to have resonated with the thinking of many who did not understand or accept the details of his theory. Darwinism was not "responsible" for social Darwinism or eugenics in any simple way. After all, some early geneticists endorsed eugenics by analogy with animal breeding even while dismissing natural selection as the mechanism of evolution. And the Nazis wanted to purify a fixed racial type, which they certainly did not want to admit had evolved gradually from an ape ancestry. But by proposing that evolution worked primarily through the elimination of useless variants, Darwin created an image that could all too easily be exploited by those who wanted the human race to conform to their own pre-existing ideals. In the same way, his popularization of the struggle metaphor focused attention onto the individualistic aspects of Spencer's philosophy.

Modern science recognizes the importance of Darwin's key insights when used as a way of explaining countless otherwise mysterious aspects of the natural world. But some of those insights came from sources with profoundly disturbing implications, and many historians now recognize that the theory, in turn, played into the way those implications were developed by later generations. This is not a simple

matter of science being "misused" by social commentators, because Darwin's theorizing would almost certainly have been different had he not drawn inspiration from social, as well as scientific, influences. We may well feel uncomfortable with those aspects of his theory today, especially in light of their subsequent applications to human affairs. But if we accept science's power to upset the traditional foundations of how we think about the world, we should also accept its potential to interact with moral values.

References

1. L. Eiseley, *Darwin's Century: Evolution and the Men Who Discovered It* (Doubleday, New York, 1958).
2. P. Corsi, *The Age of Lamarck: Evolutionary Theories in France, 1790–1830* (Univ. of California Press, Berkeley, 1988).
3. A. Desmond, *The Politics of Evolution: Morphology, Medicine and Reform in Radical London* (Univ. of Chicago Press, Chicago, 1989).
4. P. J. Bowler, *Evolution: The History of an Idea* (Univ. of California Press, Berkeley, ed. 3, 2003).
5. J. A. Secord, *Victorian Sensation: The Extraordinary Publication, Reception, and Secret Authorship of Vestiges of the Natural History of Creation* (Univ. of Chicago Press, Chicago, 2000).
6. D. Kohn, Ed., *The Darwinian Heritage: A Centennial Retrospect* (Princeton Univ. Press, Princeton, NJ, 1985).
7. J. Browne, *Charles Darwin: Voyaging* (Jonathan Cape, London, 1985).
8. C. Darwin, *The Power of Place* (Jonathan Cape, London, 2002).
9. M. J. S. Hodge, G. Radick, Eds., *The Cambridge Companion to Darwin* (Cambridge Univ. Press, Cambridge, 2003).
10. M. J. S. Hodge, *Stud. Hist. Biol.* **6**, 1 (1982).
11. P. F. Rehbock, *The Philosophical Naturalists: Themes in Early Nineteenth-Century British Biology* (Univ. of Wisconsin Press, Madison, 1983).
12. R. J. Richards, *The Meaning of Evolution: The Morphological Construction and Ideological Reconstruction of Darwin's Theory* (Univ. of Chicago Press, Chicago, 1992).
13. A. Desmond, J. R. Moore, *Darwin's Sacred Cause: Race, Slavery and the Quest for Human Origins* (Allen Lane, London, 2009).
14. E. Mayr, *One Long Argument: Charles Darwin and the Genesis of Evolutionary Thought* (Harvard Univ. Press, Cambridge, MA, 1991).
15. P. J. Bowler, *The Eclipse of Darwinism: Anti-Darwinian Evolution Theories in the Decades Around 1900* (Johns Hopkins Univ. Press, Baltimore, MD, 1983).
16. R. J. Richards, *Stud. Hist. Philos. Sci.* **28**, 75 (1997).
17. M. Ruse, *J. Hist. Ideas* **36**, 339 (1975).
18. J. Gayon, *Darwinism's Struggle for Survival: Heredity and the Hypothesis of Natural Selection* (Cambridge Univ. Press, New York, 1998).
19. P. J. Bowler, *J. Hist. Ideas* **37**, 631 (1976).
20. A. Desmond, J. R. Moore, *Darwin* (Michael Joseph, London, 1991).
21. M. Francis, *Herbert Spencer and the Invention of Modern Life* (Acumen, Stocksfield, UK, 2007).
22. C. Darwin, *Transmutation Notebook D*, from *Natural Selection* portfolio (Cambridge Univ. Library, Cambridge, 1838); P. H. Barrett, P. J. Gautrey, S. Herbert, D. Kohn, S. Smith, transcribers and Eds., *Charles Darwin's Notebooks* (British Museum of Natural History, Cornell Univ. Press, Ithaca, NY, 1987); available at the Darwin Digital Library, <http://darwinlibrary.amnh.org/>.
23. G. Neumeister, *Das Ganze der Taubenzucht* (B. F. Voigt, Weimar, 1876).

10.1126/science.1160332

Bat White-Nose Syndrome: An Emerging Fungal Pathogen?

David S. Blehert,^{1*} Alan C. Hicks,² Melissa Behr,^{3†} Carol U. Meteyer,¹ Brenda M. Berlowski-Zier,¹ Elizabeth L. Buckles,⁴ Jeremy T. H. Coleman,⁵ Scott R. Darling,⁶ Andrea Gargas,⁷ Robyn Niver,⁵ Joseph C. Okoniewski,² Robert J. Rudd,³ Ward B. Stone²

The first evidence of bat white-nose syndrome (WNS) was documented in a photograph taken at Howes Cave, 52 km west of Albany, New York, on 16 February 2006. Since emerging in the northeastern United States, WNS has been confirmed by gross and histologic examinations of bats at 33 sites in Connecticut, Massachusetts, New York, and Vermont (fig. S1). Current bat population surveys suggest a 2-year population decline in excess of 75% [see supporting online material (SOM) text for further details].

WNS has been characterized as a condition of hibernating bats and was named for the visually striking white fungal growth on muzzles, ears, and/or wing membranes of affected bats (Fig. 1A). Detailed postmortem evaluations were completed for 97 little brown myotis (*Myotis lucifugus*; Mylu), nine northern long-eared myotis (*M. septentrionalis*; Myse), five big brown bats (*Eptesicus fuscus*; Epfu), three tricolored bats (*Perimyotis subflavus*; Pesu), and three unidentified bats from 18 sites within the WNS-affected region. Distinct cutaneous fungal infection was observed in histologic sections from 105 of the 117 necropsied bats [91 Mylu (94%), eight Myse (89%), zero Epfu (0%), three Pesu (100%), and three unidentified (100%)]. Fungal hyphae replaced hair follicles and associated sebaceous and sweat glands, breaching the

basement membrane and invading regional tissue. Hyphae also eroded the epidermis of ears and wings (Fig. 1B). Additionally, 69 of the 105 bats [62 Mylu (64%), six Myse (67%), zero Epfu (0%), one Pesu (33%), and zero unidentified (0%)] with cutaneous fungal infection had little or no identifiable fat reserves, crucial for successful hibernation [see SOM text for additional mortality investigation details].

A fungus with a previously undescribed morphology was isolated from 10 bats (table S1) with histologic evidence of WNS-associated cutaneous fungal infection. These bats were collected between 1 February and 1 April 2008 from all states within the confirmed WNS-affected region (fig. S1). The distinctive curved conidia (Fig. 1C) of the isolates were identical to conidia scraped directly from the muzzles of WNS-affected little brown myotis collected at Graphite Mine (New York) and to conidia observed histologically on the surface of infected bat skin (Fig. 1B, inset). Isolates were initially cultured at 3°C, grew optimally between 5°C and 10°C, but grew marginally above 15°C. The upper growth limit was about 20°C. Temperatures in WNS-affected hibernacula seasonally range between 2° and 14°C, permitting year-round growth and reservoir maintenance of the psychrophilic fungus.

Phylogenetic analysis of the identical internal transcribed spacer region (fig. S2) and small subunit (fig. S3) ribosomal RNA gene sequences from the 10 psychrophilic fungal isolates placed them within the inoperculate ascomycetes (Order Helotiales) near representatives of the anamorphic genus *Geomyces* (teleomorph *Pseudogymnoascus*) (1). In contrast to the genetic data, morphology of the psychrophilic fungal isolates differed from that known for *Geomyces* species. The bat isolates produced single, curved conidia (Fig. 1C) morphologically distinct from clavate and arthroconidia characteristic of *Geomyces* (2). Species of *Geomyces* are terrestrial saprophytes that grow at cold temperatures (3). Placement of the WNS fungal isolates within *Geomyces*, members of which colonize the skin of animals in cold climates (4), is consistent with properties predicted for a causative agent of WNS-associated cutaneous infection.

Worldwide, bats play critical ecological roles in insect control, plant pollination, and seed dissemination (5), and the decline of North American bat populations would likely have far-reaching ecological consequences. Parallels can be drawn between the threat posed by WNS and that from chytridiomycosis, a lethal fungal skin infection that has recently caused precipitous global amphibian population declines (6). A comprehensive understanding of the etiology, ecology, and epidemiology of WNS is essential to develop a strategy to manage this current devastating threat to bats of the northeastern United States.

References

1. A. V. Rice, R. S. Currah, *Mycologia* **98**, 307 (2006).
2. L. Sigler, J. W. Carmichael, *Mycotaxon* **4**, 349 (1976).
3. S. M. Duncan et al., *Antarct. Sci.* **10**, 1017/50954102008001314 (2008).
4. W. A. Marshall, *Microb. Ecol.* **36**, 212 (1998).
5. T. H. Kunz, M. B. Fenton, *Bat Ecology* (Univ. Chicago Press, Chicago, 2003).
6. L. F. Skerratt et al., *EcoHealth* **4**, 125 (2007).

Supporting Online Material

www.sciencemag.org/cgi/content/full/1163874/DC1

Materials and Methods

SOM Text

Figs. S1 to S4

Table S1

References

28 July 2008; accepted 30 September 2008

Published online 30 October 2008;

10.1126/science.1163874

Include this information when citing this paper.

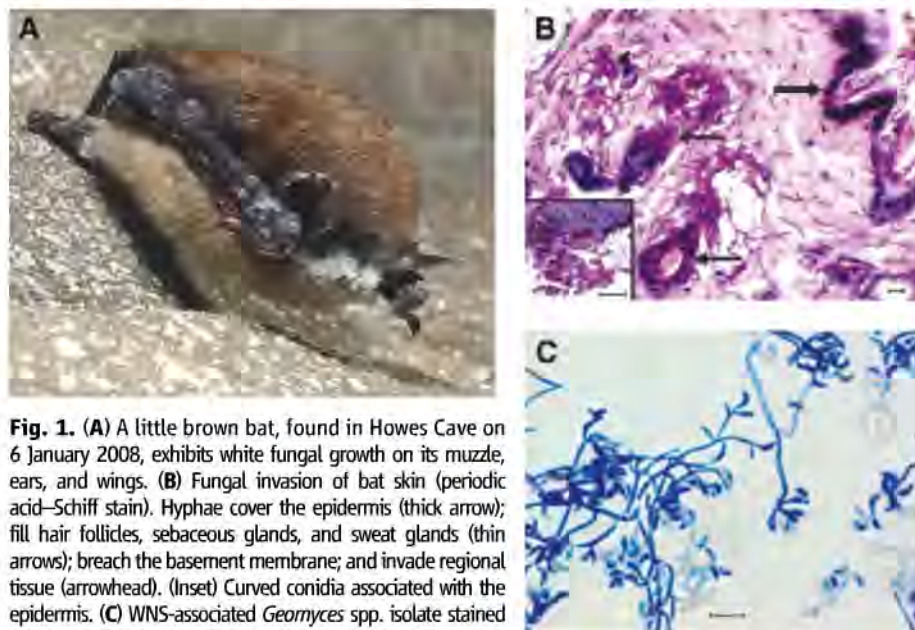


Fig. 1. (A) A little brown bat, found in Howes Cave on 6 January 2008, exhibits white fungal growth on its muzzle, ears, and wings. (B) Fungal invasion of bat skin (periodic acid-Schiff stain). Hyphae cover the epidermis (thick arrow); fill hair follicles, sebaceous glands, and sweat glands (thin arrows); breach the basement membrane; and invade regional tissue (arrowhead). (Inset) Curved conidia associated with the epidermis. (C) WNS-associated *Geomyces* spp. isolate stained with lactophenol cotton blue. Scale bars indicate 10 μ m.

¹National Wildlife Health Center, U.S. Geological Survey (USGS), 6006 Schroeder Road, Madison, WI 53711, USA. ²New York Department of Environmental Conservation, 625 Broadway, Albany, NY 12233, USA. ³New York Department of Health, Post Office Box 22002, Albany, NY 12201, USA. ⁴Cornell University, VRT T6008, Ithaca, NY 14853, USA. ⁵U.S. Fish and Wildlife Service, 3817 Luker Road, Cortland, NY 13045, USA. ⁶Vermont Fish and Wildlife Department, 271 North Main Street, Rutland, VT 05701, USA. ⁷Symbiology Limited Liability Corporation, Middleton, WI 53562, USA.

*To whom correspondence should be addressed. E-mail: dblehert@usgs.gov

†Present address: Wisconsin Veterinary Diagnostic Laboratory, 445 Easterday Lane, Madison, WI 53706, USA.

Universal Theory of Nonlinear Luttinger Liquids

Adilet Imambekov and Leonid I. Glazman*

One-dimensional quantum fluids are conventionally described by using an effective hydrodynamic approach known as Luttinger liquid theory. As the principal simplification, a generic spectrum of the constituent particles is replaced by a linear one, which leads to a linear hydrodynamic theory. We show that to describe the measurable dynamic response functions one needs to take into account the nonlinearity of the generic spectrum and thus of the resulting quantum hydrodynamic theory. This nonlinearity leads, for example, to a qualitative change in the behavior of the spectral function. The universal theory developed in this article is applicable to a wide class of one-dimensional fermionic, bosonic, and spin systems.

The development of the universal effective description of many-body phenomena is a central problem of the condensed matter theory. The hydrodynamic approach known as Luttinger liquid (LL) theory (1–3) is routinely applied to one-dimensional (1D) interacting systems. As a crucial simplification, a generic spectrum of the constituent particles is replaced by a linear one, leading to a linear hydrodynamic theory, which is nothing but a collection of non-interacting oscillators. However, to understand a variety of phenomena, such as Coulomb drag between quantum wires (4), momentum-resolved tunneling of electrons in nanowires (5), and neutron scattering off spin chains (3), one needs to take into account the nonlinearity of the spectrum. From classical physics, it is known that the existence of nonlinearities may result in qualitatively new phenomena, such as propagation of solitons and appearance of shock waves. These phenomena take place in a variety of experimental situations because classical nonlinear hydrodynamics is universal: It is phenomenologically derived from simple assumptions, which do not rely on microscopic details. Although description of linear quantum hydrodynamic theory requires only quantum mechanical treatment of non-interacting oscillators, formulation of nonlinear quantum hydrodynamics remains a challenging task because of divergences typical of nonlinear quantum field theories. In this article, we develop a universal theory of 1D quantum liquids that includes nonlinear hydrodynamic effects, leading to qualitative changes in predictions for dynamic response functions (e.g., spectral function).

If the 1D quantum many-body problem for fermions is simplified by replacing a generic spectrum of particles by a linear one [the Tomonaga-Luttinger (TL) model (6–8)], it becomes solvable at any interaction strength. The Lorentz invariance

introduced by this simplification protects the existence of well-defined elementary excitations with linear dispersion relation. These excitations are quantized waves of density propagating with a velocity v . Adding a fermion to a 1D system described by the TL model requires creation of multiple elementary excitations (9, 10). This can be seen from the form of the fermionic single-particle spectral function $A(p, \omega)$, which describes the probability of tunneling a fermion with given momentum p and energy ω into the system [see Supporting Online Material (SOM) for the precise definition (11)]. The spectral function has a power-

law singularity at the energy of collective excitation $\omega = vp$ (see eq. S4). The corresponding exponent is determined only by the universal LL parameter K [the latter is expressed in terms of the density, compressibility, and sound velocity v , the three low-energy properties of 1D liquid (3)].

In the phenomenological LL approach, energy scale $p^2/(2m^*)$ is fully dispensed with (the effective mass m^* characterizes spectrum nonlinearity at $p = 0$ and is defined below). The conventional justification for such simplification is irrelevance, in the renormalization group sense, of the nonlinearity (2). Indeed, the irrelevant terms hardly affect the fermion propagator away from the singular lines in space-time, $x \pm vt \gg \sqrt{t/m^*}$. However, it is the vicinity of these lines that defines the nature of singular behavior of the spectral function. We show here that for all spinless 1D fermionic models with short range interactions the single-particle spectral function at $p \ll k_f$ is universal. In the vicinity of Fermi wave vector $+k_f$ and $p, \omega > 0$, for example, $A(p, \omega)$ is a universal function of a single argument

$$A(p, \omega) \propto A(\epsilon), \quad \epsilon = \frac{\omega - vp}{p^2/2m^*} \quad (1)$$

(hereinafter p is measured from the closest Fermi point, and we use units with $\hbar = 1$). The new nontrivial function $A(\epsilon)$ is very different from the LL theory predictions, yet it depends only on the LL parameter K . The asymptote of $A(\epsilon)$ at $\epsilon \gg$

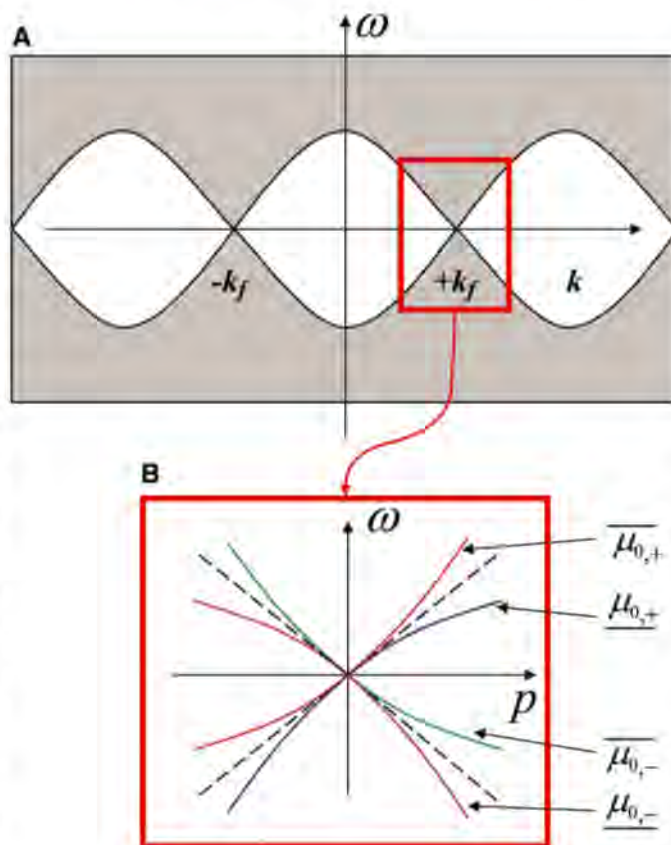


Fig. 1. Spectral function. **(A)** Spectral function $A(k, \omega)$ in momentum-energy plane. Shaded areas indicate the regions where $A(k, \omega) \neq 0$. The region with $\omega > 0$ corresponds to the particle part of the spectrum, and the region with $\omega < 0$ corresponds to the hole part of the spectrum. **(B)** Close-up view of the vicinity of $k \approx +k_f$, where $p = k - k_f$. Notations of μ indicate which exponents presented in Table 1 should be used in Eq. 6. Notations for exponents near $k \approx (2n + 1)k_f$ are obtained by substituting corresponding n instead of $n = 0$.

Department of Physics, Yale University, New Haven, CT 06520, USA.

*To whom correspondence should be addressed. E-mail: Leonid.Glazman@yale.edu

1 does reproduce the LL theory predictions, eq. S4, but at $|e \pm 1| \ll 1$ the spectral function is described by power-law asymptotes with new exponents. The exponents are different from the predictions of the LL theory but can still be analytically expressed in terms of K . We find numerically the universal single-variable crossover function $A(\epsilon)$, by relating it to the nonlinear dynamics in nonequilibrium Fermi gases (12–15). We also briefly discuss applications of our results for bosonic and spin systems.

The spectral function could be measured in tunneling experiments with electrons in nanowires (5) and cold atoms in elongated traps (16, 17). A closely related object, transverse dynamic spin structure factor, is measurable by neutron scattering off 1D spin liquids placed in a magnetic field (3). The universal crossover function and its analytically obtained asymptotes also provide one with a test for numerical methods to evaluate many-body dynamics of 1D models, for example, using density-matrix renormalization group algorithms (18, 19).

Within a LL approach, fermionic field Ψ is expanded by using its components near Fermi points as $\Psi(x, t) \approx \Psi_R(x, t)e^{ik_F x} + \Psi_L(x, t)e^{-ik_F x}$, and the kinetic energy term in the Hamiltonian is linearized. Solution of the linearized model can be described by using free bosonic fields with linear dispersion. Fermionic operators are expressed as exponentials of free bosonic fields, and their correlations are easily evaluated. Including the nonlinearity of the spectrum of constituent fermions leads to interactions between bosonic fields (2, 20). One cannot treat such interactions perturbatively in bosonic language in the vicinity of the line $\omega = v p$ because even in the second order of perturbation theory corrections diverge there (21). Physically this happens because conservation laws of energy and momentum are satisfied simultaneously for waves with linear dispersion. Thus, two wave packets spend an infinite amount of time near each other, leading to an ill-defined perturbation theory. To understand the effects of nonlinear

spectrum, it is more convenient to work in the fermionic representation. Recently a connection between dynamic response functions of 1D quantum liquids and well-known Fermi edge singularity was elucidated (22, 23). It allowed one to evaluate dynamic structure factor $S(p, \omega)$ and spectral function perturbatively in the interaction between fermions. Moreover, it established the form of the effective Hamiltonian defining the true low-energy behavior of a liquid composed of generic particles with nonlinear dispersion relation. For some integrable 1D models, it is possible to determine the parameters of the effective Hamiltonian nonperturbatively by means of Bethe ansatz (24–26).

The Hamiltonian of the TL model may be recast into the Hamiltonian of free fermionic quasiparticles (27–29) having a linear spectrum:

$$\hat{H}_1 = iv \int dx [\tilde{\Psi}_L^\dagger(x) \nabla \tilde{\Psi}_L(x) - \tilde{\Psi}_R^\dagger(x) \nabla \tilde{\Psi}_R(x)] \quad (2)$$

Here $\tilde{\Psi}_{R(L)}^\dagger(x)$ and $\tilde{\Psi}_{R(L)}(x)$ are creation and annihilation operators for quasiparticles on the right (left) branch, satisfying usual fermionic commutation relations. Colons indicate the normal ordering with respect to filled Fermi seas: for right (left) branch all states with negative (positive) momenta are occupied. The density of quasiparticles $\tilde{\rho}_{R(L)}(x) = \tilde{\Psi}_{R(L)}^\dagger(x) \tilde{\Psi}_{R(L)}(x)$ is simply related to the density of fermions in the TL model $\rho_{R(L)}(x) = \Psi_{R(L)}^\dagger(x) \Psi_{R(L)}(x)$. Because the canonical transformation that diagonalizes the TL Hamiltonian is a Bogoliubov rotation in the space of particle-hole excitations, such a relation is linear, $\rho_R(x) + \rho_L(x) = K[\tilde{\rho}_R(x) + \tilde{\rho}_L(x)]$. Fermionic operators are related to fermionic quasiparticles using “string” operators $\tilde{F}_{R(L)}^\dagger(x)$ as (e.g., for right-movers)

$$\begin{aligned} \Psi_R^\dagger(x) &= \tilde{F}_R^\dagger(x) \tilde{\Psi}_R^\dagger(x), \tilde{F}_R^\dagger(x) \\ &= \exp \left\{ i \int^x dy [\delta_+ \tilde{\rho}_R(y) + \delta_- \tilde{\rho}_L(y)] \right\} \end{aligned} \quad (3)$$

Here we have introduced parameters

$$\begin{aligned} \frac{\delta_+}{2\pi} &= 1 - \frac{1}{2\sqrt{K}} - \frac{\sqrt{K}}{2} < 0, \\ \frac{\delta_-}{2\pi} &= \frac{1}{2\sqrt{K}} - \frac{\sqrt{K}}{2} \end{aligned} \quad (4)$$

Using Eqs. 3 and 4 together with Eq. 2, one can obtain the usual results for Green's function of the TL model (27).

If one wants to consider effects of nonlinearity, one has to include terms that are less relevant in the renormalization group sense into quasiparticle Hamiltonian. One such term is the nonlinearity of the spectrum of quasiparticles:

$$\begin{aligned} \hat{H}_2 &= \frac{1}{2m_*} \int dx [(\nabla \tilde{\Psi}_L^\dagger)(\nabla \tilde{\Psi}_L) + \\ &+ (\nabla \tilde{\Psi}_R^\dagger)(\nabla \tilde{\Psi}_R)] \end{aligned} \quad (5)$$

Here m_* is the effective mass, which can be related (20) to low-energy properties as $1/m_* = v/K^{1/2} \partial v / \partial h + v^2 / (2K^{3/2}) \partial K / \partial h$, where h is the chemical potential.

In principle, there is another term that needs to be included together with Eq. 5: It amounts to interaction between quasiparticles created by operators $\tilde{\Psi}_{L,R}^\dagger$. It can be shown (28), however, that in the limit of small p interactions between quasiparticles are weak and can be treated perturbatively, along the lines of (22, 23). Perturbation theory is valid as long as the interaction between the original fermions (created by Ψ^\dagger) is short-ranged. Interactions between quasiparticles are responsible for weak singularities in $S(p, \omega)$ near $\omega = v p \pm p^2 / (2m_*)$, large- ω tails of $S(p, \omega)$ (22), and for possible finite $\propto p^8$ smearing (23) of some of the singularities of $A(p, \omega)$. All these effects vanish as long as one is interested in the scaling limit $p \rightarrow 0, \epsilon \rightarrow \text{const}$; see SOM (11) for more detailed discussion. For models with interactions decaying as $\propto 1/\lambda^2$ or slower, nonanalytic dependence of interactions on momentum be-

Table 1. Universal exponents for spectral function. Notations are indicated in Fig. 1, and parameters δ_\pm defined by Eq. 4 are functions of K only. Note that $\mu_{n,+} = \mu_{-n-1,-}$, which follows from the $k \leftrightarrow -k$ symmetry.

$$\begin{aligned} \overline{\mu_{n,+}} &= 1 - \frac{1}{2} \left[2n - (2n+1) \frac{\delta_+ + \delta_-}{2\pi} \right]^2 - \frac{1}{2} \left(\frac{\delta_+ - \delta_-}{2\pi} \right)^2 \\ \mu_{n,+} &= 1 - \frac{1}{2} \left[2n + 2 - (2n+1) \frac{\delta_+ + \delta_-}{2\pi} \right]^2 - \frac{1}{2} \left(2 - \frac{\delta_+ - \delta_-}{2\pi} \right)^2 \\ \overline{\mu_{n,-}} &= 1 - \frac{1}{2} \left[2n + 2 - (2n+1) \frac{\delta_+ + \delta_-}{2\pi} \right]^2 - \frac{1}{2} \left(\frac{\delta_+ - \delta_-}{2\pi} \right)^2 \\ \mu_{n,-} &= 1 - \frac{1}{2} \left[2n - (2n+1) \frac{\delta_+ + \delta_-}{2\pi} \right]^2 - \frac{1}{2} \left(2 - \frac{\delta_+ - \delta_-}{2\pi} \right)^2 \end{aligned}$$

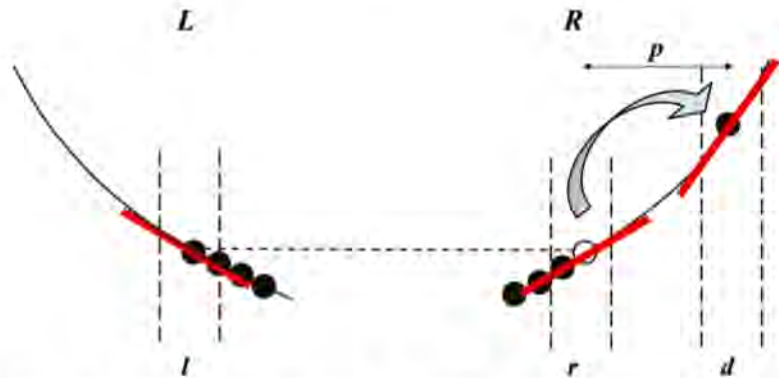


Fig. 2. Reduction to the effective Hamiltonian. We show excitations contributing to the singularity at $|\omega - (vp + \frac{p^2}{2m_*})| \ll \frac{p^2}{2m_*}$. The Hamiltonian given by Eqs. 2 and 5 is reduced to the three-subband model in Eqs. 7 and 8.

comes possible, and one cannot neglect interactions between quasiparticles. This can be already seen from perturbative calculations (23).

The spectral function $A(p, \omega)$ gets modified by the spectrum nonlinearity in a profound way because the dynamics of the string operators $\tilde{F}_{R(L)}^\dagger(x, t)$ in Eq. 3 becomes nonlinear. Effective mass m_* defines the energy scale $\sim p^2/(2m_*)$ near $\omega = v p$ where modifications from the TL model take place. Because parameters δ_\pm defining $\tilde{F}_{R(L)}^\dagger(x, t)$ are universally related to K , full form of the crossover written in terms of a variable ε is a universal function of K . Investigation of the properties of crossover function $A(\varepsilon)$ is the main subject of the present article.

Before proceeding to discuss the form of the universal crossover, let us consider the main new features of $A(p, \omega)$ that arise because of nonlinear spectrum. We find that in the vicinity of each low-energy region $k \approx (2n+1)k_f$ spectral function $A(p, \omega)$ has a power-law behavior near frequencies $\pm[vp \pm p^2/(2m_*)]$, which is related to orthogonality catastrophe phenomenon (22, 23):

$$A(p, \omega) \propto \text{const} + \left| \frac{1}{\omega \pm \left(vp \pm \frac{p^2}{2m_*}\right)} \right|^\mu \quad (6)$$

and notations for μ are shown in Fig. 1. Such power-law behavior results from multiple low-energy particle-hole excitations near left and right Fermi points, which are created when “high energy” fermion tunnels into the system.

To be specific, let us focus on the vicinity of $+k_f$ for $p > 0$ and $\omega > 0$. Because the fermion that tunnels into the system has a momentum near $+k_f$ and energy of the system increases for $\omega > 0$, we need to consider only the correlator $\langle \Psi_R(x, t) \Psi_R^\dagger(0, 0) \rangle$.

Let us first discuss the exponent $\mu_{0,+}$ at the edge $\left| \omega - \left(vp + \frac{p^2}{2m_*}\right) \right| \ll \frac{p^2}{2m_*}$. To understand its origin, one has to understand the states that can be created by Ψ_R^\dagger , when the energy of the tunneling fermion is in the vicinity of the edge. From energy and momentum conservation, such state is given by a single fermionic quasiparticle with “large” momentum $\approx p$ and multiple low-energy particle-hole excitations with momenta much smaller than p , as indicated in Fig. 2. Then one can neglect all other states (22, 23) and project quasiparticle operators $\tilde{\Psi}_R(x)$ and $\tilde{\Psi}_L(x)$ onto narrow (of the width much smaller than p) subbands r, d , and l as $\tilde{\Psi}_R(x) \approx \tilde{\Psi}_r(x) + e^{ipx} \tilde{d}(x)$, $\tilde{\Psi}_L(x) \approx \tilde{\Psi}_l(x)$.

The effective Hamiltonian determining the evolution of these states is obtained by projecting $\tilde{H}_1 + \tilde{H}_2$ onto subbands r, l , and d and linearizing the corresponding spectra:

$$\tilde{H}_{r,l} = i v \int dx [\tilde{\Psi}_l^\dagger(x) \nabla \tilde{\Psi}_l(x) - \tilde{\Psi}_r^\dagger(x) \nabla \tilde{\Psi}_r(x)] \quad (7)$$

$$\tilde{H}_d = \int dx \tilde{d}^\dagger(x) \left[vp + \frac{p^2}{2m_*} - i \left(v + \frac{p}{m_*} \right) \nabla \right] \tilde{d}(x) \quad (8)$$

The Green's function factorizes as $\propto e^{ipx} \langle \tilde{d}(x, t) \tilde{d}^\dagger(0, 0) \rangle_{\tilde{H}_d} \langle \tilde{F}_r(x, t) \tilde{F}_r^\dagger(0, 0) \rangle_{\tilde{H}_{r,l}}$. To obtain string operators \tilde{F}_r, \tilde{F}_l from Eq. 3, one should keep only r and l components of the density there. The free-particle correlator $\langle \tilde{d}(x, t) \tilde{d}^\dagger(0, 0) \rangle_{\tilde{H}_d}$ equals $\propto e^{-i \left(vp + \frac{p^2}{2m_*} \right) t} \delta \left[x - \left(v + \frac{p}{m_*} \right) t \right]$, and string correlator can be bosonized and evaluated (3) in a usual way as $\langle \tilde{F}_r(x, t) \tilde{F}_r^\dagger(0, 0) \rangle_{\tilde{H}_{r,l}}|_{x=(v+\frac{p}{m_*})t} \propto t^{-[\delta_-/(2\pi)]^2 - [\delta_+/(2\pi)]^2}$. Taking Fourier transform of $\langle \Psi_R(x, t) \Psi_R^\dagger(0, 0) \rangle$, we obtain the universal exponent

$$\mu_{0,+} = 1 - \left(\frac{\delta_-}{2\pi} \right)^2 - \left(\frac{\delta_+}{2\pi} \right)^2 \quad (9)$$

Analogously, exponent $\mu_{0,-}$ for $\omega - \left(vp - \frac{p^2}{2m_*}\right) \ll$

$\frac{p^2}{2m_*}$ is determined by configurations with one quasihole with the momentum $\approx -p$, two quasiparticles near right Fermi point, and low-energy particle-hole excitations. One can again reduce the problem to three-subband model and bosonize states near right and left Fermi points. This way, one obtains the exponent

$$\mu_{0,-} = 1 - \left(\frac{\delta_-}{2\pi} \right)^2 - \left(2 - \frac{\delta_+}{2\pi} \right)^2 < -3 \quad (10)$$

New exponents given by Eqs. 9 and 10 are clearly different from the result for the TL model in eq. S4, which corresponds to the exponent $1 - [\delta_-/(2\pi)]^2$.

Configurations responsible for the remaining exponents $\mu_{0,-}, \mu_{0,+}$ consist of “high energy” particle-hole excitation on the left branch, particle at the right Fermi point, and low-energy excitations on left and right branches. Singularities near $k \approx (2n+1)k_f$ also include n low-energy particle-hole pairs with momentum $\approx 2nk_f$. All exponents can be obtained by using projections onto three-subband models, and the results are summarized in Table 1.

We now discuss the results for the universal crossover function $A(\varepsilon)$ in the vicinity of $+k_f$ for $p, \omega > 0$ [details of the derivations are available in SOM (11)]. The answer is defined by a universal function $D(y)$, determined only by δ_\pm and normalized as $\int_{-1}^1 D(y) dy = 1$. By using $D(y)$,

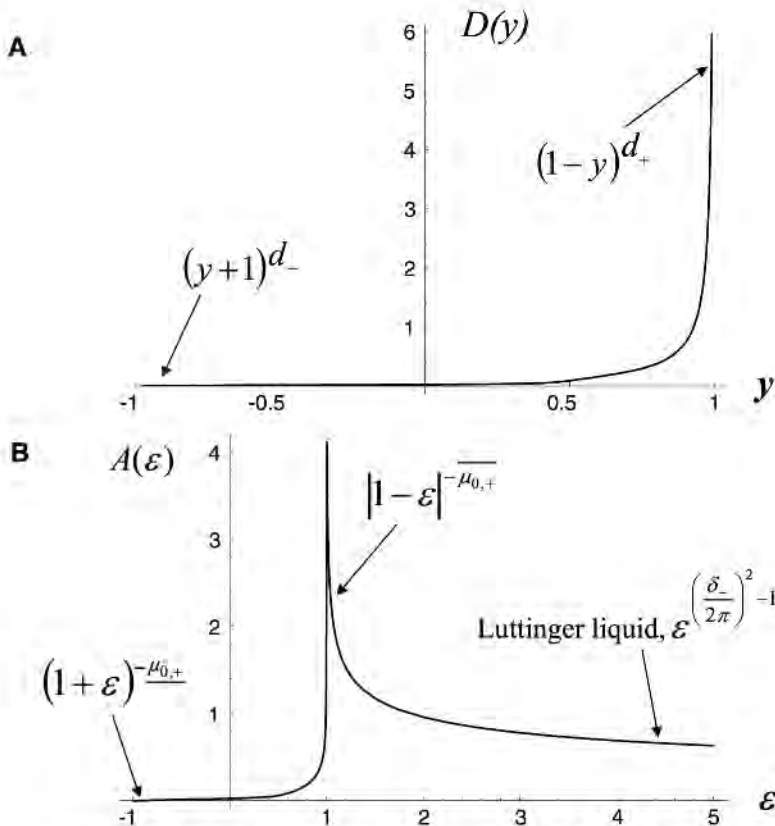


Fig. 3. Universal crossover. **(A)** Universal crossover function $D(y)$ for $K = 4.54$ and the corresponding values $\delta_+/(2\pi) = -0.3$ and $\delta_-/(2\pi) = -0.83$; see Eq. 4. Exponents d_\pm defining the asymptotic behavior at $y \rightarrow \pm 1$ are given by Eq. 12. **(B)** Universal function $A(\varepsilon)$ for $K = 4.54$. Exponents $\mu_{0,-}$ and $\mu_{0,+}$ defining the asymptotic behavior at $\varepsilon \rightarrow \pm 1$ are given by Eqs. 9 and 10. The ratio of prefactors determining the asymmetry of the singularity at $\varepsilon = 1$, see Eq. 13, equals 2.96 for $K = 4.54$.

spectral function can be written as a convolution of contributions from the left and right branches. Universal function $A(\epsilon)$ in Eq. 1 is related to $D(y)$ as

$$A(\epsilon) = \int_{-1}^1 dy D(y) \theta(\epsilon - y) (\epsilon - y)^{\left(\frac{\delta_+}{2\pi}\right)^2 - 1} \quad (11)$$

One can analytically obtain limiting behavior of $D(y)$ for $y \rightarrow \pm 1$ from Eqs. 9 to 11 as $D(y) \propto (1 \mp y)^{d_{\pm}}$ for $y \rightarrow \pm 1$, where

$$d_+ = \left(\frac{\delta_+}{2\pi}\right)^2 - 1, \quad d_- = \left(2 - \frac{\delta_+}{2\pi}\right)^2 - 1 > 3 \quad (12)$$

At moderate interaction strength, $\bar{\mu}_{0,+} > 0$, function $A(\epsilon)$ diverges at $\epsilon = 1$. Then the ratio of the prefactors above and below the singular line is universal,

$$\lim_{|\delta\epsilon| \rightarrow 0} \frac{A(1 + |\delta\epsilon|)}{A(1 - |\delta\epsilon|)} = \frac{\Gamma\left[\left(\frac{\delta_+}{2\pi}\right)^2\right] \Gamma\left[1 - \left(\frac{\delta_+}{2\pi}\right)^2\right]}{\Gamma\left[\left(\frac{\delta_-}{2\pi}\right)^2\right] \Gamma\left[1 - \left(\frac{\delta_-}{2\pi}\right)^2\right]} \quad (13)$$

To evaluate $D(y)$ away from the edges, one should be able to calculate the dynamics of chiral vertex operators (11). For a nonlinear spectrum, this is a very nontrivial problem, the analytic solution of which is not known. Similar correlators have attracted attention recently (12, 13), and their connection to the nonlinear quantum shock wave dynamics and nonlinear differential equations has been discussed. Although it might be possible to proceed similarly for the evaluation of $D(y)$, it is not clear whether nonlinear differential equations obtained this way will have an analytic solution. We use an alternative approach of (14, 15), which allows us to develop a representation of $D(y)$ in terms of certain determinants built of single-particle (rather than many-body) states. These determinants can be evaluated numerically, which practically solves the problem of finding $D(y)$. Representative results for $D(y)$ and $A(\epsilon)$ for $K = 4.54$ are shown in Fig. 3.

The universal Hamiltonian given by Eqs. 2 and 5 can be also used to describe gapless bosonic and spin $-\frac{1}{2}$ systems away from particle hole symmetric ground states. We present main results on singularities of their dynamic response functions in SOM (11).

We have constructed universal low-energy theory of a wide class of interacting 1D quantum liquids without resorting to the simplifications of the Tomonaga-Luttinger model accepted in the phenomenological LL description. Unlike the latter, we keep the nonlinear dispersion relation of the fermions intact. The replacement of the dispersion relation by a linear one, $\omega = vp$, results in an artificial introduction of Lorentz invariance into the system. Although not affecting the low-energy behavior of local properties (such as the local tunneling density of states), the introduced

symmetry alters qualitatively the predictions for the momentum-resolved quantities, such as the spectral function. Keeping the nonlinearity allows us to find the generic low-energy behavior of the dynamic response functions of a system of interacting fermions, bosons, and spins. Possible extensions of our theory should be able to describe the effects of finite temperature, spin systems at particle-hole symmetric points, systems with long-range interactions, and fermions with spin.

References and Notes

1. F. D. M. Haldane, *Phys. Rev. Lett.* **47**, 1840 (1981).
2. F. D. M. Haldane, *J. Phys. C* **14**, 2585 (1981).
3. T. Giamarchi, *Quantum Physics in One Dimension* (Oxford Univ. Press, New York, 2004).
4. M. Pustilnik, E. G. Mishchenko, L. I. Glazman, A. V. Andreev, *Phys. Rev. Lett.* **91**, 126805 (2003).
5. O. M. Auslaender et al., *Science* **295**, 825 (2002).
6. S. Tomonaga, *Prog. Theor. Phys.* **5**, 544 (1950).
7. J. M. Luttinger, *J. Math. Phys.* **4**, 1154 (1963).
8. D. C. Mattis, E. H. Lieb, *J. Math. Phys.* **6**, 304 (1965).
9. I. E. Dzyaloshinskii, A. I. Larkin, *Sov. Phys. JETP* **38**, 202 (1974).
10. A. Luther, I. Peschel, *Phys. Rev. B* **9**, 2911 (1974).
11. Materials and methods are available as supporting material on Science Online.
12. E. Bettelheim, A. G. Abanov, P. Wiegmann, *Phys. Rev. Lett.* **97**, 246402 (2006).
13. E. Bettelheim, A. G. Abanov, P. Wiegmann, *J. Phys. A* **41**, 392003 (2008).
14. D. A. Abanin, L. S. Levitov, *Phys. Rev. Lett.* **93**, 126802 (2004).

15. D. A. Abanin, L. S. Levitov, *Phys. Rev. Lett.* **94**, 186803 (2005).
16. L.-M. Duan, *Phys. Rev. Lett.* **96**, 103201 (2006).
17. T.-L. Dao, A. Georges, J. Dalibard, C. Salomon, I. Carusotto, *Phys. Rev. Lett.* **98**, 240402 (2007).
18. S. R. White, *Phys. Rev. Lett.* **69**, 2863 (1992).
19. U. Schollwöck, *Rev. Mod. Phys.* **77**, 259 (2005).
20. R. G. Pereira et al., *Phys. Rev. Lett.* **96**, 257202 (2006).
21. K. Samokhin, *J. Phys.* **10**, L533 (1998).
22. M. Pustilnik, M. Khodas, A. Kamenev, L. I. Glazman, *Phys. Rev. Lett.* **96**, 196405 (2006).
23. M. Khodas, M. Pustilnik, A. Kamenev, L. I. Glazman, *Phys. Rev. B* **76**, 155402 (2007).
24. R. G. Pereira, S. R. White, I. Affleck, *Phys. Rev. Lett.* **100**, 027206 (2008).
25. V. V. Cheianov, M. Pustilnik, *Phys. Rev. Lett.* **100**, 126403 (2008).
26. A. Imambekov, L. I. Glazman, *Phys. Rev. Lett.* **100**, 206805 (2008).
27. A. V. Rozhkov, *Eur. Phys. J. B* **47**, 193 (2005).
28. A. V. Rozhkov, *Phys. Rev. B* **74**, 245123 (2006).
29. A. V. Rozhkov, *Phys. Rev. B* **77**, 125109 (2008).
30. We thank A. Kamenev and D. Abanin for useful discussions. This work was supported by U.S. Department of Energy grant no. DE-FG02-08ER46482.

Supporting Online Material

www.sciencemag.org/cgi/content/full/1165403/DC1

Materials and Methods

Fig. S1

Table S1

References

3 September 2008; accepted 10 November 2008

Published online 27 November 2008;

10.1126/science.1165403

Include this information when citing this paper.

Direct Measurement of Molecular Mobility in Actively Deformed Polymer Glasses

Hau-Nan Lee, Keewook Paeng, Stephen F. Swallen, M. D. Ediger

When sufficient force is applied to a glassy polymer, it begins to deform through movement of the polymer chains. We used an optical photobleaching technique to quantitatively measure changes in molecular mobility during the active deformation of a polymer glass [poly(methyl methacrylate)]. Segmental mobility increases by up to a factor of 1000 during uniaxial tensile creep. Although the Eyring model can describe the increase in mobility at low stress, it fails to describe mobility after flow onset. In this regime, mobility is strongly accelerated and the distribution of relaxation times narrows substantially, indicating a more homogeneous ensemble of local environments. At even larger stresses, in the strain-hardening regime, mobility decreases with increasing stress. Consistent with the view that stress-induced mobility allows plastic flow in polymer glasses, we observed a strong correlation between strain rate and segmental mobility during creep.

Glasses form when molecular motion becomes slow, and thus liquidlike flow in a glass would seem impossible by definition. Nevertheless, polymer glasses under stress can yield and undergo plastic flow (1). In this process, the glass dissipates enormous amounts of energy without breaking. This toughness is

the critical design requirement in many applications, and efforts to understand it go back more than 70 years. In 1936, Eyring (2) proposed a model in which external loading lowers the energy barriers for molecular motion and thus effectively transforms a glass into a viscous liquid. Other workers (1, 3–7) have modified Eyring's approach in important ways while maintaining the central idea that stress can induce molecular mobility.

Department of Chemistry, University of Wisconsin–Madison, Madison, WI 53706, USA.

Recent work on “jamming” systems (amorphous systems that develop a yield stress) suggests the generality of this idea; as in the case of sand piles or colloids, one can unjam polymer glasses by applying stress (8). Mechanical measurements have been used to infer huge increases in molecular mobility in polymer glasses due to stress (9–11), but this interpretation is controversial (12). Nuclear magnetic resonance (13), an optical technique (14), and several simulations (15–18) have directly demonstrated that molecular mobility in polymer glasses is accelerated during deformation. Nevertheless, the absence of quantitative molecular mobility measurements on polymer glasses during deformation limits the development of predictive models of polymer deformation. In the absence of such information, the Eyring model or a related approach is assumed to be valid (1, 4–6).

Here we report optical measurements of stress-induced molecular mobility in a lightly cross-linked poly(methyl methacrylate) (PMMA) glass with a glass transition temperature $T_g = 395$ K (19). We quantitatively measured changes in polymer segmental mobility with external loading and compared these data to the Eyring model (2). In the low-stress regime, the Eyring model correctly describes changes in the segmental mobility. However, as deformation continues into the flow regime, mobility speeds up by more than a factor of 1000, and the Eyring model fails to capture this behavior. We show that spatially heterogeneous dynamics (20) have a substantial influence on the deformation of polymer glasses in this regime. In addition, we observed a strong correlation between strain rate and mobility, supporting the view that stress-induced mobility allows polymer glasses to flow.

We used a confocal fluorescence microscope system to measure molecular mobility during deformation, as described previously (14). We deformed the PMMA glass uniaxially in tension with a constant external load. During this creep experiment, we used an optical photobleaching technique to measure the reorientation of a dilute molecular probe (N,N' -dipentyl-3,4,9,10-perylenedicarboximide). The reorientation of this probe is an excellent reporter of the segmental dynamics of PMMA (21) (fig S2). We optically measured strain and mobility in the same small region (~200 by 250 μm) of the sample.

Mobility changes during one creep experiment on PMMA glass at 375.7 K ($T_g - 19$ K) are shown in Fig. 1. The strain change during creep with engineering stress equal to 16.0 MPa followed by recovery at 0.7 MPa are shown in Fig. 1A. Strain (ϵ) is defined as $\epsilon(t) = [L(t) - L_0]/L_0$, where L_0 is the initial distance (~200 μm) between two lines photobleached in the sample and $L(t)$ is the distance at time t . We observed homogeneous deformation up to $\epsilon = 0.15$, after which necking occurred. Initially, the strain rate continuously increased as the sample flowed. After 5000 s, the strain rate decreased, which indicated that strain-hardening was occurring

(22, 23). Creep experiments at lower stresses additionally exhibited an initial regime in which the strain rate decreased before increasing; we define flow onset as this minimum in the local strain rate.

During creep and recovery, we performed ~35 photobleaching experiments to determine

the mobility of PMMA. The anisotropy decay function $r(t)$, measured with a polarized photobleaching technique, describes probe reorientation with time. Some anisotropy decays are shown in Fig. 1B. As the strain and strain rates increased, we observed faster $r(t)$ decays (curve a to curve e), indicating higher mobility. In the

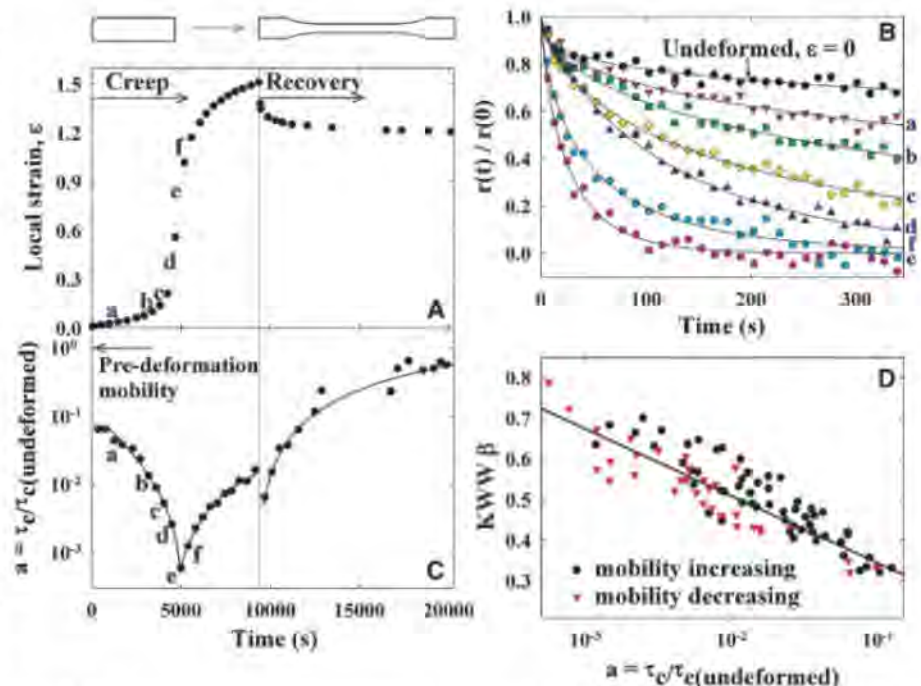


Fig. 1. Simultaneous local measurements of strain and mobility in PMMA glass. (A) Strain during creep experiments at 375.7 K with an engineering stress of 16.0 MPa, followed by recovery. The initial and final shapes of the sample are shown. (B) Normalized anisotropy decays obtained during the creep experiment at times indicated by letters a to f. As the strain rate increased, higher mobility (faster anisotropy decay) was observed. The solid lines are KWW fits to the data. (C) Mobility shift factor during creep and recovery. Mobility increased by up to a factor of 1000. The solid lines are guides to the eye. (D) Correlation between the KWW β parameter and mobility for three different trials with stresses in the range of 15.5 to 16.0 MPa. Data were acquired as the mobility was both increasing (●) and decreasing (▼). The solid line is a fit to the data.

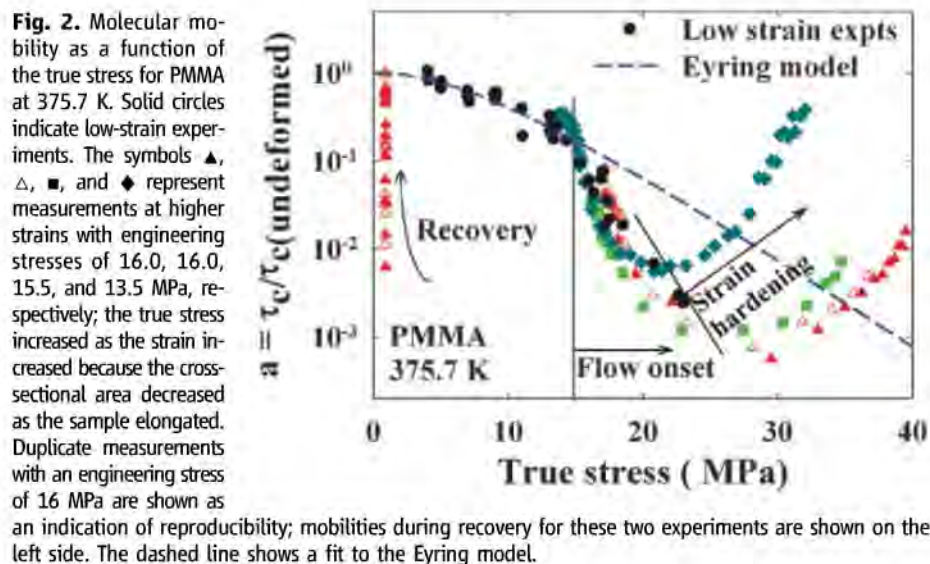


Fig. 2. Molecular mobility as a function of the true stress for PMMA at 375.7 K. Solid circles indicate low-strain experiments. The symbols Δ , \square , and \diamond represent measurements at higher strains with engineering stresses of 16.0, 16.0, 15.5, and 13.5 MPa, respectively; the true stress increased as the strain increased because the cross-sectional area decreased as the sample elongated. Duplicate measurements with an engineering stress of 16 MPa are shown as an indication of reproducibility; mobilities during recovery for these two experiments are shown on the left side. The dashed line shows a fit to the Eyring model.

strain-hardening regime, the strain rate decreases, and $r(t)$ decays more slowly (curve e to curve f).

To quantitatively analyze mobility changes during creep and recovery, we fit the anisotropy decay to the Kohlrausch-Williams-Watts (KWW) equation $r(t) = r(0)\exp[-(t/\tau)^\beta]$, where β determines the nonexponentiality of the decay and τ is the rotational relaxation time. The integral of $r(t)/r(0)$ provides the rotational correlation time τ_c , and we define the mobility shift factor $a = \tau_{c,\text{deformed}}/\tau_{c,\text{undeformed}}$.

The changes in mobility during creep and recovery are shown in Fig. 1C. Immediately after the stress was applied, the mobility increased by a factor of 10 and then further increased until dynamics were accelerated 1000-fold relative to the undeformed glass. In the strain-hardening regime, the mobility decreased as the strain rate decreased, even though the strain and true stress increased. After the stress was removed, the mobility first increased and then decreased toward the mobility of the undeformed PMMA.

To compare our results with theoretical models, we plot the segmental mobility as a function of true stress in Fig. 2; two different types of experiments are shown. For low-strain experiments, we performed a single mobility measurement immediately after applying the stress. In these experiments, the deformations are homogenous, and the strains are generally very small ($\epsilon \ll 0.1$). Results are also presented for experiments such as the one illustrated in Fig. 1; here, multiple mobility measurements were performed during one creep experiment, and the overall strain was large ($\epsilon \sim 1.4$).

Three different regimes are illustrated in Fig. 2. In the low-stress regime (<15 MPa), the Eyring model can describe the data. The Eyring model predicts that the response of the segmental relaxation time τ of a polymer glass to an applied stress σ is $\tau \propto \sigma / \sinh(\frac{\sigma}{2} \frac{V}{k_B T})$, where k_B is the Boltzmann constant, T is the temperature, and V is the activation volume. Fitting the low-stress data to the Eyring model yields $V = 2.7 \text{ nm}^3$,

which can be interpreted as indicating the cooperative movement of two to three statistical (or Kuhn) segments. This activation volume is qualitatively consistent with the size of shear transformation zones (24) for colloidal glasses as determined by visualizing microscopic strain during shear; the reported activation volume is about four particle volumes (25). The data in the low-stress regime are also consistent with the predictions of Chen and Schweizer (7), who incorporate ideas from Eyring's treatment into a microscopic model of cage escape.

Figure 2 shows a very large mobility enhancement with the onset of flow ($\sigma > 15$ MPa), and the Eyring model fails to capture this behavior. In this regime, in addition to lowering the barriers for molecular motion, deformation apparently modifies spatially heterogeneous dynamics in the glass. Molecular motions in supercooled liquids and glasses are spatially heterogeneous (20, 26), and the KWW β parameter provides an indication of the distribution of relaxation times (20). In the low-stress regime, β was unaltered from that of the undeformed sample ($\beta = 0.32$). As mobility increased in the flow regime, the anisotropy decay function became more exponential ($\beta \rightarrow 1$) (Fig. 1D). This result indicates a narrowing of the distribution of relaxation times that reflects the dynamics in slow regions accelerating more than in mobile regions. We speculate that stress is concentrated in slow regions during flow.

At the largest stresses shown in Fig. 2, the mobility decreased with increasing stress in a manner that depended upon the deformation history of particular samples. All of the samples shown were in the strain-hardening regime with strains greater than ~ 0.7 . Such large strains orient the polymer chains (27), and the resulting structure effectively resists deformation (23). The Eyring model does not incorporate polymer structure and qualitatively predicts the wrong trend in this regime.

Consistent with earlier experiments (13) and simulations (15, 17, 18), we emphasize that mo-

lecular mobility in polymer glasses depends on more than the instantaneous true stress. In contrast to Eyring's prediction, the recovery data in Figs. 1 and 2 show a wide range of mobilities even though the stress is constant at a very low value. Although true stress is an important parameter for determining the mobility of polymer glasses, variables such as strain and strain rate can also play an important role.

The connection between molecular motion and macroscopic mechanical properties is illustrated in Fig. 3, in which we plot the dimensionless strain rate as a function of instantaneous molecular mobility. An excellent master curve is obtained for experiments at three temperatures. Also shown in Fig. 3 are predictions from a microscopic theory of mobility in PMMA (28) and the result of computer simulations of a coarse-

Fig. 3. Dimensionless strain rate as a function of molecular mobility, illustrating that stress-induced mobility allows polymer flow. The solid line is a fit to the data. The long-dashed line is the model prediction from (28) and the short-dashed line is the molecular dynamics simulation from (18).

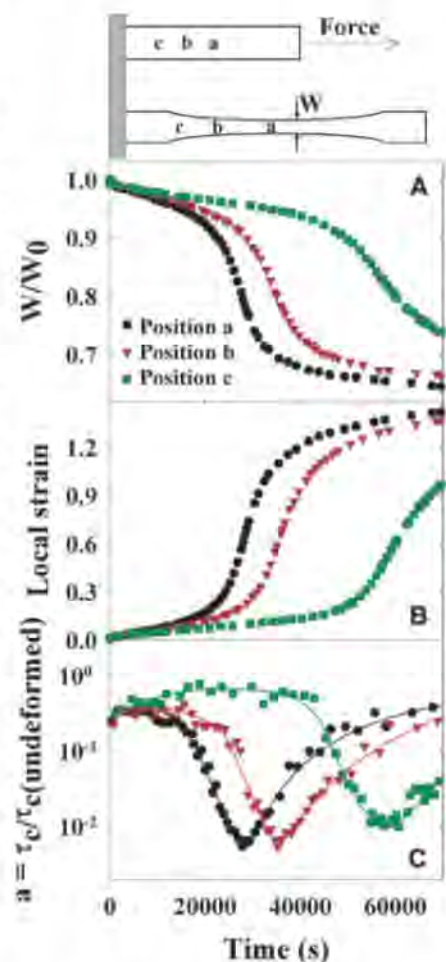
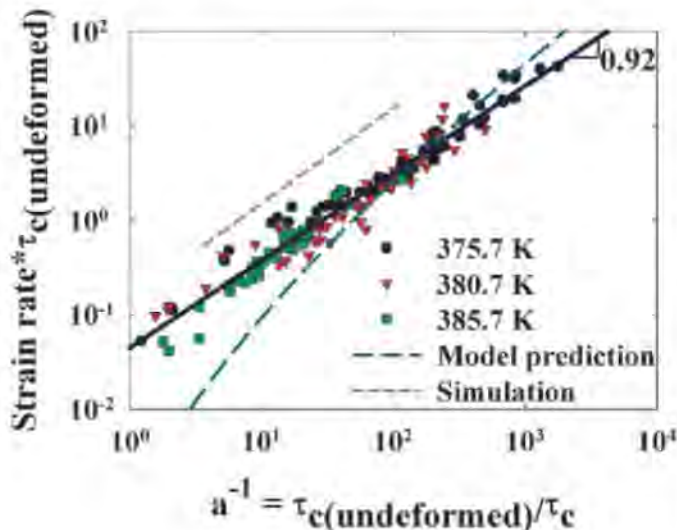


Fig. 4. Simultaneous strain and mobility measurements in three different positions of an inhomogeneously deformed PMMA glass at 375.7 K. Panels show the time evolution of the sample width (A), the local strain (B), and the mobility (C). The engineering stress is 13.5 MPa, the initial width (W_0) is 2.3 mm (W , final width). The picture on the top illustrates positions a, b, and c before and after the deformation. Before the deformation, positions b and c were 1.5 and 2.7 mm away from position a, respectively. The solid lines are guides to the eye.

grained polymer glass (18). Our results confirm that stress-induced mobility allows polymer glasses to flow; a 1000-fold increase in mobility very nearly resulted in a 1000-fold increase in the flow rate. These results also strongly support the reliability of probe reorientation as an indicator of polymer mobility during deformation. Figure 3 only includes data from single-step creep experiments; data from recovery and multistep creep experiments do not fall on the same curve. This finding suggests that no mechanical variable universally exhibits a simple relation with molecular mobility.

Because we measured the strain and segmental mobility locally, we were able to perform simultaneous measurements in different parts of an inhomogeneously deformed sample. Mobility changes in three different positions of a sample that necked during deformation are shown in Fig. 4. Plots of sample width and local strain versus time are shown in Fig. 4, A and B, and illustrate necking that begins at position a and then propagates toward positions b and c. Changes in mobility at positions a, b, and c are shown in Fig. 4C. At each position, mobility accelerates as the local strain rate increases; data from all three positions are quantitatively consistent with the master curve in Fig. 3. In a necked sample, molecular mobility is fastest in the shoulder, rather than the neck, even though the true stress in the neck is greater than any other region in the sample.

Polymer glasses are nonequilibrium thermodynamic systems, and we briefly discuss how this influences the interpretation of our measurements. Physical aging describes the change in mechanical properties that occurs over time because of the very slow molecular rearrangements in a glass (11); molecular motions have been shown to slow during physical aging (29). Mechanical experiments on polymer glasses have sometimes been interpreted as a reversal of physical aging, or "rejuvenation" (1, 9–12). We attribute the changes in mobility in our experiment to the combination of deformation-induced mobility and physical aging/rejuvenation. It appears that deformation-induced mobility is the much greater effect in these experiments. For example, the green curve in Fig. 4C shows a small mobility decrease in the first 30,000 s, which we attribute to physical aging. This mobility decrease is similar in magnitude to the decrease caused by physical aging in the undeformed sample during the same time period.

Concepts from the jamming field might be useful for describing the behavior of polymer glasses under stress (8). According to this view, one can unjam glasses either by raising the temperature or applying stress (8, 18, 30). In our experiments, temperature and stress had a qualitatively different effect on molecular mobility. A 1000-fold increase in mobility by deformation at constant temperature changed the KWW β to about 0.8 (Fig. 1D). In the absence of deformation, a 1000-fold increase in mobility occurred

when the temperature was increased by 18 K, but at this temperature β was unchanged at 0.32. Thus, stress not only increased mobility but also, in contrast to temperature, sharpened the distribution of relaxation times. In the low-stress regime in Fig. 2, temperature and stress both increased mobility without narrowing the distribution of relaxation times.

Our results quantify mobility changes in an actively deformed polymer glass and establish a quantitative connection between molecular mobility and macroscopic deformation. We find that mobility is not a function of instantaneous stress alone but can also depend on strain and the deformation history. Plastic flow appears to modify spatially heterogeneous dynamics in the glass, which suggests that there is a complex interplay between microscopic motions and flow. We anticipate that quantitative measurements of molecular mobility during deformation, coupled with appropriate microscopic theory, will lead to substantially improved predictions of the nonlinear deformation behavior of polymer glasses.

References and Notes

- H. E. Meijer, L. E. Govaert, *Prog. Polym. Sci.* **30**, 915 (2005).
- H. Eyring, *J. Chem. Phys.* **4**, 283 (1936).
- R. E. Robertson, *J. Chem. Phys.* **44**, 3950 (1966).
- M. C. Boyce, D. M. Parks, A. S. Argon, *Mech. Mater.* **7**, 15 (1988).
- C. P. Buckley, D. C. Jones, *Polymer* **36**, 3301 (1995).
- J. M. Caruthers, D. B. Adolf, R. S. Chambers, P. Shrikhande, *Polymer* **45**, 4577 (2004).
- K. Chen, K. S. Schweizer, *Europhys. Lett.* **79**, 26006 (2007).
- A. J. Liu, S. R. Nagel, *Nature* **396**, 21 (1998).
- A. F. Yee, R. J. Bankert, K. L. Ngai, R. W. Rendell, *J. Polym. Sci. Part Polym. Phys.* **26**, 2463 (1988).
- J. J. Martinez-Vega, H. Trumel, J. L. Gacougnolle, *Polymer* **43**, 4979 (2002).
- L. C. E. Struik, *Physical Aging in Amorphous Polymers and Other Materials* (Elsevier, New York, 1978).
- G. B. McKenna, *J. Phys. Condens. Matter* **15**, 5737 (2003).
- L. S. Loo, R. E. Cohen, K. K. Gleason, *Science* **288**, 116 (2000).
- H.-N. Lee, K. Paeng, S. F. Swallen, M. D. Ediger, *J. Chem. Phys.* **128**, 134902 (2008).
- F. M. Capaldi, M. C. Boyce, G. C. Rutledge, *Phys. Rev. Lett.* **89**, 175505 (2002).
- A. V. Lyulin, B. Vorselaars, M. A. Mazo, N. K. Balabaev, M. A. J. Michels, *Europhys. Lett.* **71**, 618 (2005).
- R. A. Riggelman, H.-N. Lee, M. D. Ediger, J. J. de Pablo, *Phys. Rev. Lett.* **99**, 215501 (2007).
- R. A. Riggelman, K. S. Schweizer, J. J. de Pablo, *Macromolecules* **41**, 4969 (2008).
- Materials and methods are available as supporting material on Science Online.
- M. D. Ediger, *Annu. Rev. Phys. Chem.* **51**, 99 (2000).
- R. Bergman, F. Alvarez, A. Alegria, J. Colmenero, *J. Non-Cryst. Solids* **235**, 580 (1998).
- H. G. H. van Melick, L. E. Govaert, H. E. H. Meijer, *Polymer* **44**, 2493 (2003).
- E. J. Kramer, *J. Polym. Sci. Part B Polym. Phys.* **43**, 3369 (2005).
- M. L. Falk, J. S. Langer, *Phys. Rev. E* **57**, 7192 (1998).
- P. Schall, D. A. Weitz, F. Spaepen, *Science* **318**, 1895 (2007).
- E. R. Weeks, J. C. Crocker, A. C. Levitt, A. Schofield, D. A. Weitz, *Science* **287**, 627 (2000).
- F. Casas, C. Alba-Simionesco, H. Montes, F. Lequeux, *Macromolecules* **41**, 860 (2008).
- K. Chen, K. S. Schweizer, *Macromolecules* **41**, 5908 (2008).
- C. T. Thurnau, M. D. Ediger, *J. Chem. Phys.* **116**, 9089 (2002).
- T. K. Haxton, A. J. Liu, *Phys. Rev. Lett.* **99**, 195701 (2007).
- This work was supported by NSF through grant NIRT-0506840. We thank K. Schweizer, J. Caruthers, G. Medvedev, J. de Pablo, and R. Riggelman for helpful discussions.

Supporting Online Material

www.sciencemag.org/cgi/content/full/1165995/DC1
Materials and Methods
Figs. S1 to S3
References

16 September 2008; accepted 18 November 2008
10.1126/science.1165995

Suppression of Metallic Conductivity of Single-Walled Carbon Nanotubes by Cycloaddition Reactions

Mandakini Kanungo,¹ Helen Lu,² George G. Malliaras,¹ Graciela B. Blanchet^{2*}

The high carrier mobility of films of semiconducting single-walled carbon nanotubes (SWNTs) is attractive for electronics applications, but the presence of metallic SWNTs leads to high off-currents in transistor applications. The method presented here, cycloaddition of fluorinated olefins, represents an effective approach toward converting the "as grown" commercial SWNT mats into high-mobility semiconducting tubes with high yield and without further need for carbon nanotube separation. Thin-film transistors, fabricated from percolating arrays of functionalized carbon nanotubes, exhibit mobilities >100 square centimeters per volt-second and on-off ratios of 100,000. This method should allow for the use of semiconducting carbon nanotubes in commercial electronic devices and provide a low-cost route to the fabrication of electronic inks.

Single-walled carbon nanotubes (SWNTs) are potential candidates for application in electronic devices (1–4). The most severe drawback in this effort has been that the as-synthesized SWNTs are a mixture of semi-

conducting (SC) and metallic (M) tubes, hindering their application in thin-film transistors (TFTs), where high mobility and on/off ratios are essential. The nascent SWNTs also form as bundles that need to be further dispersed. Numer-

ous approaches have been taken for the separation of M and SC tubes. Post treatments (5, 6) lead to a high degree of separation, but the extremely low concentration of tubes in the dispersing solvent hinders the formation of percolating SC-SWNT arrays. Burning off metallic tubes after fabrication with high currents leads to high-mobility devices but is neither controllable nor scalable (7).

An alternative approach is to manipulate the electronic properties of SWNT through covalent chemical functionalization (8); that is, disrupt the π bonding system (sp^2) by converting some sites into sp^3 carbon atoms (9, 10). Using such an approach, one should, in principle, be able to lower the conductivity of the M nanotubes significantly and achieve low off-currents while maintaining a mobility sufficiently high for good device performance. We show here that both these parameters can be simultaneously controlled by the degree of functionalization. Several methods that allow either anchoring atoms or molecules (reactants) to the carbon nanotube framework or selectively aligning nanotubes of specific types or chirality onto treated surfaces (11, 12) have been explored. When functionalization of the nanotube walls is achieved through the presence of a strong oxidizer or highly reactive radical species, electronic properties are significantly degraded (13). Finding an effective, low-cost method to eliminate or convert M-SWNT is essential to reduce off-currents. Snow's early work on TFTs using random percolating arrays of SWNT (2, 14) showed carrier mobilities of $150 \text{ cm}^2/\text{Vsec}$ but on/off ratios far too low for

device applications. In an attempt to increase the on/off ratio, Bo *et al.* (15) constructed near-percolating SWNT arrays connected by organic semiconducting links. Although this method largely increased the on/off ratio (10^5), it greatly reduced the device's mobility.

Recent theoretical (9, 10, 16–21) and experimental (22–24) studies point to sizeable differences in the electronic properties of SWNTs modified by monovalent relative to divalent (cycloaddition) chemical functionalization. The early work on monovalent functionalization (25, 26), shows that fluorine functionalization leads to highly resistive material with fluorination-induced strains and fractures in the tube walls (27). In more recent work, a preferential etching of M-SWNT was achieved using a mild fluorine gas-phase reaction (28) and sidewall functionalization of carbon nanotubes with diazonium salts (29, 30). Reports on divalent functionalization have focused on optical studies (22–24).

In this work, we show that high mobility and high on/off ratios can concurrently be achieved in a random array of percolating high-pressure CO (HiPco) tubes functionalized through a controlled cycloaddition reaction with fluorinated polyolefins. The "as grown" commercial nanotube mats are functionalized into a network of tubes that can then be dispersed in an organic solvent. The resulting "denser" semiconducting inks (denser by a factor of about 30), when coated as a percolating array, lead to high-mobility devices without requiring further nanotube separation.

We performed two separate [2+2] cycloaddition reactions of SWNTs; the first with perfluoro-2(2-fluorosulfonylethoxy) propyl vinyl ether (PSEPVE) and the second with perfluoro (5-methyl-3,6-dioxanon-1-ene) (PMDE) (31). The corresponding functionalized SWNTs are

referred as FSWNT-PSEPVE and FSWNT-PMDE. The results from TFTs fabricated with percolating arrays of functionalized tubes, which were spin-coated onto substrates, show mobilities of $10 \text{ cm}^2/\text{Vsec}$ for FSWNT-PSEPVE and $110 \text{ cm}^2/\text{Vsec}$ for FSWNT-PMDE, both with on/off ratios of 10^5 .

The effect of a systematic [2+2] cycloaddition reaction on the mobility and off-current (I_{off}) of a percolating array of FSWNT is illustrated for FSWNT-PSEPVE in Fig. 1. The dramatic reduction of the I_{off} with increasing reactant concentration (c , the ratio of the moles of reactant that successfully reacted to the moles of SWNT) is key to this work. Devices fabricated from a percolating array of pristine HiPco tubes have high mobilities but also high I_{off} , which indicates that conduction pathways are dominated by metallic tubes (30, 32). Increasing PSEPVE functionalization led to a dramatic decrease in I_{off} , caused by a reduction in the number of metallic percolating pathways. For $c < 0.01$, high mobility is preserved, but I_{off} was reduced by almost 5 orders of magnitude as compared with pristine SWNTs. For $0.01 < c < 0.02$, I_{off} decreased further, but the carrier mobility decreased as well. At higher reactant concentrations, the mobility dropped precipitously, which suggests that the electronic properties of the M and SC-SWNTs have changed considerably. The dependence of the on- and off-currents on channel length is shown in the inset to Fig. 1. The low I_{off} maintained at very small channel lengths further confirms the disappearance of conducting pathways between source and drain at a 0.018 degree of fluorination. Gate sweeps for FSWNT-PSEPVE and FSWNT-PMDE under optimum functionalization conditions at reactant/CNT concentration are shown in Fig. 2A for $c = 0.012$ and Fig. 2B for $c = 0.019$. The field-effect mobilities deduced

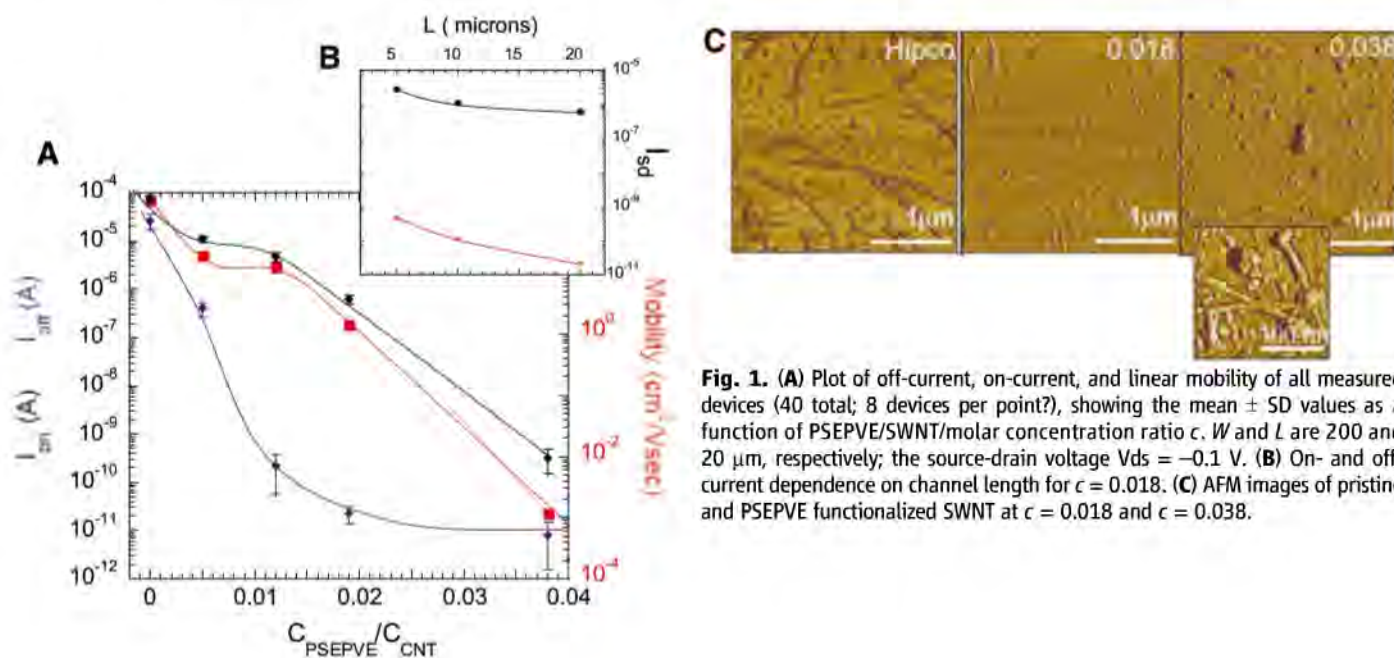


Fig. 1. (A) Plot of off-current, on-current, and linear mobility of all measured devices (40 total; 8 devices per point?), showing the mean \pm SD values as a function of PSEPVE/SWNT molar concentration ratio c . W and L are 200 and 20 μm , respectively; the source-drain voltage $V_{\text{ds}} = -0.1 \text{ V}$. (B) On- and off-current dependence on channel length for $c = 0.018$. (C) AFM images of pristine and PSEPVE functionalized SWNT at $c = 0.018$ and $c = 0.038$.

¹Cornell University, Department of Material Sciences, Ithaca, NY 14850, USA. ²DuPont, Material Science and Engineering, Wilmington, DE 19880, USA.

*To whom correspondence should be addressed. E-mail: graciela.b.blanchet@usa.dupont.com

from the linear regime are $10 \text{ cm}^2/\text{Vsec}$ and $110 \text{ cm}^2/\text{Vsec}$ with on/off ratios in excess of 10^5 .

To further understand the relative metallic content of the various fluorination levels, we studied the effect of the SWNT density on the electrical properties of the FSWNT arrays at the various functionalization levels (31). The network density, maintained above percolation, was varied from 8 to $40 \text{ SWNT}/\mu^2$. The effect of FSWNT density (ρ) on electrical properties for $c = 0.012$ is striking. At $\rho = 35 \text{ tubes}/\mu^2$, I_{on} values comparable to those of bare HiPco reflect the formation of a percolating network of M tubes. At lower densities ($\rho = 8.5$ and $17.7 \text{ tubes}/\mu^2$), I_{on} drops by more than 4 orders of magnitude to 10^{-10} A , which reflects a sub-percolating concentration of M tubes. At slightly higher fluorination ($c = 0.018$), the remaining M tubes appear to be fully removed. Low off-currents (10^{-10} A) can be maintained for both high-density arrays and low-channel-length transistors.

Atomic force microscopy (AFM) images of the pristine and functionalized arrays (Fig. 1B) show pristine HiPco (left) as well as lower and higher degrees of functionalization, $c = 0.18$ (center) and $c = 0.038$ (right). The HiPco ropes have largely exfoliated by $c = 0.018$, whereas at $c = 0.038$ the tubes coalesce into nearly spherical particles, which consist of smaller particles $\sim 20 \text{ nm}$ in diameter, as seen in the magnified inset.

To elucidate the origin of this SWNT transformation, we performed several analyses. Optical spectra (ultraviolet-visible-near-infrared, Fig. 3A) on mats treated with four different concentrations, c , display the transitions between the Van Hove singularities in the density of states that are characteristics of one-dimensional (1D) systems (33, 34). The broad features at 0.9 to 1.6 eV, associated with the E_{11}^S and E_{22}^S semiconducting transitions, remain practically unchanged for $c < 0.02$, where high mobility is also retained. In contrast, both E_{11}^S and E_{22}^S transitions disappear at higher levels of functionalization, indicating a deleterious effect of further functionalization on the SC tubes.

The Raman spectra in Fig. 3B show the disorder D and tangential G bands (12, 13, 35) in the 1200 to 1700 cm^{-1} region upon excitation at 514 nm for pristine and FSWNT-PSEPVE at $c = 0.012$ and $c = 0.019$. The G band of semiconducting tubes consists of two peaks at 1568 cm^{-1} (radial) and at 1591 cm^{-1} (longitudinal). The G band spectrum of the metallic tubes also shows two bands at 1589 cm^{-1} (radial) and at 1544 cm^{-1} (longitudinal), the latter broadened into a Breit-Wigner Fano line shape caused by a strong coupling in the density of states. The spectra of Fig. 2B show that only the metallic band at 1544 cm^{-1} band is affected by functionalization, essentially disappearing for $c \sim 0.02$. Thus, the disappearance of the metallic band, concurrently with the decrease in I_{on} shown in Fig. 1, sug-

gests that cycloaddition in the low reactant regime primarily affects the M tubes. The intensity of the disorder D ($\sim 1325 \text{ cm}^{-1}$) band also remains essentially unchanged in the low c regime.

In the present functionalization scheme, the presence of fluorine in the reactants helps in carrying out a divalent, 2-2 cycloaddition functionalization of the side wall. Having studied two reactants, PSEPVE and PMDE, gives us a means to understand whether the electrical changes are solely controlled by cycloaddition reaction or whether the side chain has an effect as well. The two side chains are nearly identical except that the PSEPVE side chain, $\text{OCF}_2\text{CF}(\text{CF}_3)\text{OCF}_2\text{CF}_2\text{SO}_2\text{F}$, has a sulfonic group whereas the PMDE side chain, $\text{OCF}_2\text{CF}(\text{CF}_3)\text{OCF}_2\text{CF}_2\text{CF}_3$, does not. The mobility of FSWNT-PMDE is ~ 10 times as high as that of FSWNT-PSEPVE, which suggests that SO_2F leads to acid formation and doping.

A 60 to 70 Å square between cyclobutyl rings along the side walls is independent of the reactant concentration in the low-concentration regime (31). These data suggest that initially, the reactant anchors onto the walls of the ropes overcoming the Van der Waals interaction between tubes, inducing de-rope. We suggest that as the ropes exfoliate into smaller-diameter ropes, new sites become available and functionalization progresses, leading to further exfoliation until the status of single tubes is reached, with properties initially beneficial for electron transport. On the other hand, the high-resolution AFM for $c = 0.038$ suggests that for high concentrations, single functionalized tubes have transitioned from an extended into a coiled conformation in a manner analogous to a rod-to-coil phase transition observed in many polymer systems. Indeed, the smaller spherical entities of $\sim 20 \text{ nm}$ in diameter are similar in volume to that of a single tube of 10 Å diameter and $0.6 \mu\text{m}$ in length.

From the electrical and optical data, we deduce that cycloaddition proceeds differently on M and SC SWNTs. In the low reactant regime (< 0.02)—of interest for devices—the optical and electrical data suggest that the M-SWNTs have been reduced, whereas the SC-SWNTs remain largely unaffected. This preferential modification of M tubes is probably caused by their much larger electron density near the Fermi level (22). Thus, cycloaddition of PSEPVE, in the low-concentration regime, either renders M-SWNTs inert or converts them into SC-SWNTs. The latter hypothesis is supported by the theoretical investigations of the effect of cycloaddition on the conductance of a metal carbon nanotube (10, 16, 18, 19) and by the work of Kamaras *et al.* (22).

We have developed a simple, high-yield method for the divalent functionalization of as-grown HiPco mats into preferentially semiconducting tubes with properties that are suitable for device applications. This work represents the first time that “bulk” quantities of commercial HiPco mats have been functionalized, dispersed into a high solid-content ink, and used to fab-

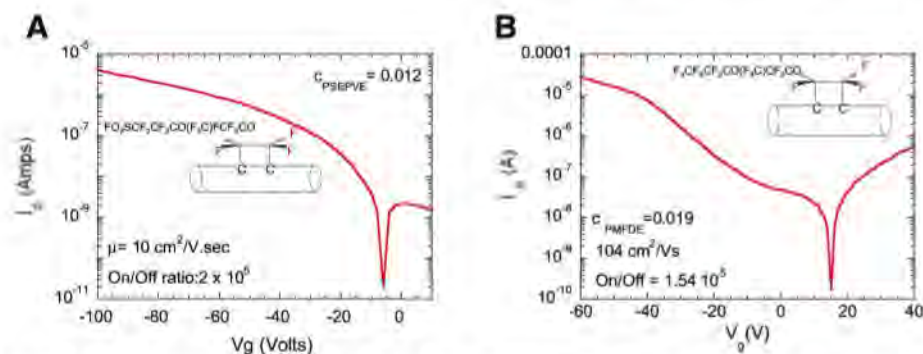


Fig. 2. Plot of source-drain current versus gate voltage for (A) FSWNT-PSEPVE and (B) FSWNT-PMDE TFTs at $c = 0.018$ and $V_{\text{ds}} = -0.1 \text{ V}$ and -0.01 V , respectively.

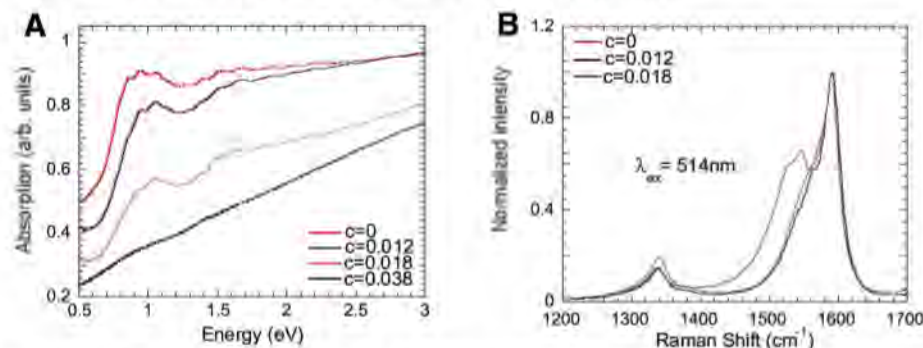


Fig. 3. (A) Optical spectra (of pristine HiPco tubes and the functionalized tubes). (B) Raman spectra of tangential and disorder mode region at 514-nm excitation wavelength. Spectra are normalized to the 1591 cm^{-1} band.

ricate percolating semiconducting arrays. We propose that, in the low concentration regime ($c < 0.02$), cycloaddition provides an effective method to anchor molecules to the carbon nanotube framework and to either eliminate or transform metallic tubes. The data presented here suggest that $c \sim 0.018$ fluorination level is sufficient to achieve the complete conversion of the metallic tubes without degrading the semiconducting tubes. The latter is a necessary step for the production of semiconducting inks suitable for printable electronics. While the cycloaddition reaction provides the anchoring sites, the long, highly fluorinated side chains are quite effective in exfoliating the ropes, thus enabling the effective conversion of M-SWNT even deep inside the ropes, as is necessary for achieving high-performance devices. We demonstrated the utility of the method by fabricating TFTs using percolating arrays of functionalized carbon nanotubes as the semiconducting layer with mobilities of $100 \text{ cm}^2/\text{Vsec}$ and on/off ratios of 10^5 .

References and Notes

1. P. Avouris, Z. Chen, V. Perebeinos, *Nat. Nanotechnol.* **2**, 605 (2007).
2. E. S. Snow, P. M. Campbell, M. G. Ancona, *Appl. Phys. Lett.* **86**, 033105 (2005).
3. E. S. Snow *et al.*, *J. Vac. Sci. Technol. B* **22**, 1990 (2004).
4. E. Artukovic, M. Kaempgen, D. S. Hecht, S. Roth, G. Gruner, *Nano Lett.* **5**, 757 (2005).
5. H. Peng, N. T. Alvarez, C. Kittrell, R. H. Hauge, H. K. Schimdt, *J. Am. Chem. Soc.* **128**, 8396 (2006).
6. M. S. Arnold, A. A. Gree, J. F. Hulvat, S. I. Stupp, M. C. Hersam, *Nat. Mater.* **1**, 60 (2006).
7. P. G. Collins, M. S. Arnold, P. Avoris, *Science* **292**, 706 (2001).
8. M. S. Strano *et al.*, *Science* **301**, 1519 (2003).
9. J. Zhao, H. Park, J. Han, J. P. Lu, *J. Phys. Chem. B* **108**, 4227 (2004).
10. H. Park, J. Zhao, J. P. Lu, *Nano Lett.* **6**, 916 (2006).
11. R. Mclean, W. Huang, C. Khripin, A. Jogota, M. Zheng, *Nano Lett.* **6**, 55 (2006).
12. C. LeMieux *et al.*, *Science* **321**, 101 (2008).
13. Z. Chen, K. J. Ziegler, J. Shaver, R. H. Hauge, R. E. Smalley, *J. Phys. Chem. B* **110**, 11624 (2006).
14. E. S. Snow, J. P. Novak, P. M. Campbell, D. Park, *Appl. Phys. Lett.* **82**, 2145 (2003).
15. X.-Z. Bo *et al.*, *Appl. Phys. Lett.* **87**, 203510 (2005).
16. J. Zhao, Z. Chen, Z. Zhou, H. Park, P. R. Schyler, J. P. Lu, *Chem. Phys. Chem.* **6**, 598 (2005).
17. M. V. Veloso, A. G. Souza Filho, J. Mendes Filho, S. B. Fagan, R. Mota, *Chem. Phys. Lett.* **430**, 71 (2006).
18. Y.-S. Lee, N. Marzari, *J. Phys. Chem. C* **112**, 4480 (2008).
19. Y.-S. Lee, N. Marzari, *Phys. Rev. Lett.* **97**, 116801 (2006).
20. K. A. Park, Y. S. Choi, C. Kim, Y. H. Lee, *Phys. Rev. B* **68**, 045429 (2003).
21. J. Lu *et al.*, *J. Phys. Chem. B* **110**, 5655 (2006).
22. K. Kamaras, M. E. Itkis, H. Hu, B. Zhao, R. C. Haddon, *Science* **301**, 1501 (2003).
23. H. Hu *et al.*, *J. Am. Chem. Soc.* **125**, 14893 (2003).
24. C. Menard-Moyon, N. Izard, E. Doris, C. Mioskowski, *J. Am. Chem. Soc.* **128**, 6552 (2006).
25. K. S. Kim *et al.*, *Adv. Mater.* **14**, 1818 (2002).
26. K. H. An *et al.*, *Appl. Phys. Lett.* **80**, 4235 (2002).
27. H. F. Bettinger, K. N. Kudin, G. E. Scuseria, *J. Am. Chem. Soc.* **123**, 12849 (2001).
28. C.-M. Yang *et al.*, *Phys. Rev. B* **73**, 075419 (2006).
29. N. Nair, W.-J. Kim, M. L. Usrey, M. S. Strano, *J. Am. Chem. Soc.* **129**, 3946 (2007).
30. C. Wang *et al.*, *J. Am. Chem. Soc.* **127**, 11460 (2005).
31. Materials and methods are available as supporting material on Science Online.
32. J. Vavro, J. M. Kikkawa, J. E. Fischer, *Phys. Rev. B Condens. Matter* **71**, 155410 (2005).
33. A. Hagen, G. Moos, V. Talalaev, T. Hertel, *Appl. Phys. A* **78**, 1137 (2004).
34. J. Chen *et al.*, *Science* **282**, 95 (1998).
35. M. S. Dresselhaus, G. Dresselhaus, R. Saito, *Phys. Rep.* **409**, 47 (2005).
36. Supported by Air Force grant FA9550-071-0411. We thank H. L. Stormer and G. D. Jaycox for careful reading of the manuscript; R. Wheland for many interesting discussions; and D. Walls, J. Wyre, and N. G. Tassi for Raman, x-ray photoelectron spectroscopy, and high-resolution AFM inset at $c = 0.038$, respectively.

Supporting Online Material

www.sciencemag.org/cgi/content/full/323/5911/234/DC1
Materials and Methods
Figs. S1 to S5

18 September 2008; accepted 19 November 2008
10.1126/science.1166087

Self-Organization of a Mesoscale Bristle into Ordered, Hierarchical Helical Assemblies

Boaz Pokroy, Sung H. Kang, L. Mahadevan, Joanna Aizenberg*

Mesoscale hierarchical helical structures with diverse functions are abundant in nature. Here we show how spontaneous helicity can be induced in a synthetic polymeric nanobristle assembling in an evaporating liquid. We use a simple theoretical model to characterize the geometry, stiffness, and surface properties of the pillars that favor the adhesive self-organization of bundles with pillars wound around each other. The process can be controlled to yield highly ordered helical clusters with a unique structural hierarchy that arises from the sequential assembly of self-similar coiled building blocks over multiple length scales. We demonstrate their function in the context of self-assembly into previously unseen structures with uniform, periodic patterns and controlled handedness and as an efficient particle-trapping and adhesive system.

Non-centrosymmetric chiral, coiled, and spiral configurations are ubiquitous in nature, spanning from amino acids to mollusk shells to galaxies (1). On a mesoscopic scale, such structures are abundant in biology, and these are usually composed of helical fibers that are often further assembled into higher-order hierarchical materials. Natural examples include DNA helices, amyloid fibers (2), cellulose fibrils in wood (3), hierarchy in bone (4, 5), and chirally

spinning nodal cilia (6), to name a few, with implications on a variety of functions from information transfer to mechanical integrity and control of the body symmetry in morphogenesis. Man-made coiled and spiral materials and designs on a macroscopic scale are widely used in our everyday life—from ropes and bolts to helicopter rotors. On the molecular scale, chirality plays a critical role in asymmetric chemical synthesis and catalysis (7), liquid crystals (8), supramolecular chemistry (9, 10), and organic and inorganic crystal engineering (11). Artificial coiled structures at the mesoscale are rare, and these usually have simple geometries of one-dimensional helical fibers and ribbons (1, 8–10, 12). At any length scale, twist and handedness in superstructures gener-

ally originate from either the assembly of non-centrosymmetric building blocks or the application of a chiral field or template (1–5, 8–13). Here we report on the induction of capillarity-driven self-organization of a nanobristle into helical clusters and demonstrate the fabrication of non-trivial, hierarchically assembled, coiled meso-structures over large areas, in which neither the assembling elements nor the environment are chiral, guided by and consistent with simple theoretical considerations.

Our approach is presented in Fig. 1A. We consider a periodic array of nanopillars, each of which is anchored at one end on a substrate and free at the other. A locally stable configuration of the bristles is just a uniform array of non-interacting straight pillars (first-order structures). However, this is not necessarily a globally stable state: When the array is immersed in a liquid that is then evaporated, capillary forces associated with the liquid/vapor menisci between the free ends of the geometrically soft bristles may cause them to deform laterally and adhere to each other. The effect of elastocapillary coalescence (14) has been described for a well-known phenomenon of clumping in wet hair (15) or paintbrush immersed in paint (16). Similar clustering behavior is observed in nature in the examples of the tarsi of beetles (17) and spiders (18). The morphology and dynamics of the ensuing structures are a result of the competition between intrapillar elasticity and inter-pillar adhesion (14–16). Individual pillars that are long enough can bend easily to accommodate the capillary forces associated with the menisci between adjacent pillars.

School of Engineering and Applied Sciences, Wyss Institute for Biologically Inspired Engineering, Harvard University, Cambridge, MA 02138, USA.

*To whom correspondence should be addressed. E-mail: jaiz@seas.harvard.edu

A simple scaling analysis allows us to construct a set of rough criteria for the existence of these structures, in terms of the properties of the elastic circular nanopillars of radius r , length L , interpillar distance d , Young's modulus E , bending stiffness $B \sim Er^4$, and adhesive energy per unit area J (19) as well as the properties of the evaporating liquid of interfacial tension γ , in which they are immersed. Assuming that the pillars do not break through the meniscus, the longitudinal forces due to the pinned contact line cause the pillars to buckle (14); however, because the pillars have a circular cross section, there is no preferred plane of buckling. In addition, the multiple pinned menisci attract each other via a weak capillary interaction mediated by the interface (20). For the pillars to come together, the force $F_B \sim Bd/L^3$ to bend two adjacent pillars until they are just in contact at their tips must be comparable to the capillary force $F_C \sim \gamma r$ due to the menisci connecting the hemispherical ends. This yields a critical pillar length $L_c \sim (Bd/\gamma r)^{1/3} \sim (Ed/\gamma)^{1/3} r$, below which capillary forces will be unable to maintain a bent configuration and the bent pillars return to their upright state once the liquid has evaporated

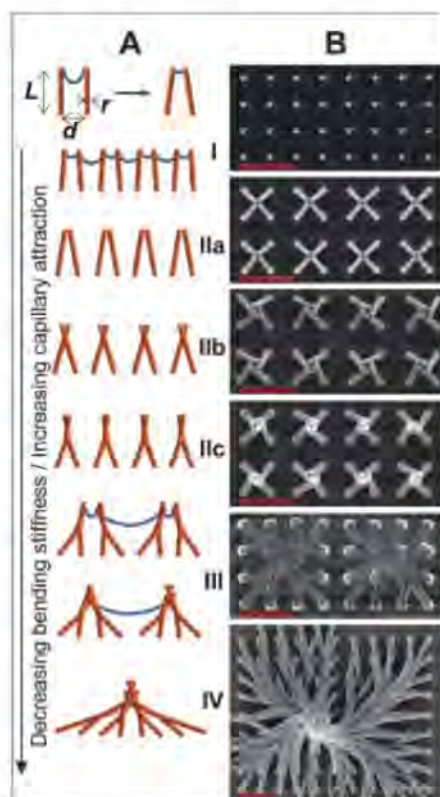


Fig. 1. (A) Schematic diagrams and (B) corresponding scanning electron microscopy (SEM) images showing the morphogenesis of helical patterns, from the first-order unclustered nanobristle to the fourth-order coiled bundle. Scale bars, 4 μm . Note the hierarchical nature of the assembly reflected in the presence of the lower-order braids in the large clusters braided in a unique structure reminiscent of modern dreadlocks or mythical Medusa.

(regime I). When $L > L_c$, two neighboring pillars can retain contact as long as they are held together by either capillary forces or short-range van der Waals forces (after drying). A different characteristic length scale, $L_a \sim (Ed/J)^{1/3} r$, based on interpillar adhesion dictates whether the pillars will stay in their adhered state once capillary forces bring them together; for instance, if $L_a > L_c$ and $L_a > L > L_c$, the pillars will come together during the drying process but then separate eventually, corresponding to regime I. (These length scales may be modified by the wettability of the pillars, a detail that we will not discuss further here). When $L > L_c$ and $L \geq L_a$, we expect the pillars to form second-order stable clusters that usually reflect the symmetry of the underlying lattice (regime IIa). When $L \gg L_a$, the filaments can cluster to increase their adhesive contact via a chiral rearrangement of the pillars (regime IIb) and eventually twist around each other (regime IIc).

To understand this in a minimal model, we consider the adhesion of two initially straight free pillars (21) wound around each other along uniform helices of pitch p and radius R (19). Adhesive contact can now occur over a patch of approximately constant width a that winds around each filament and is determined by the solution of a JKR-like problem (22), yielding $a \sim (J/E)^{1/3} r^{2/3}$ [up to logarithmic factors of the form $\ln(L/r)$]. Then the total energy of two pillars of length L is the sum of the adhesive energy and the elastic energy (assumed to be caused by bending alone) and can be written as $U \sim -JaL(1 + 1/P^2)^{1/2} + BL/R^2(1 + P^2)^2$, where $P = p/2\pi R$. Here, the first

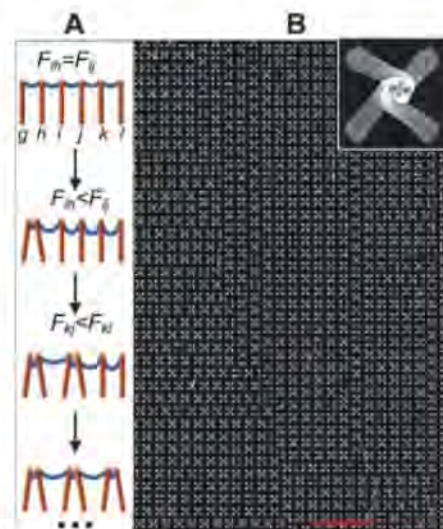


Fig. 2. Large-area self-organization of the bristle. (A) Schematic diagram showing the mechanism of the formation of the long-range order in the assembled bristle. See text for further details. (B) SEM image showing the assembly into uniform, periodic fourfold clusters of nanopillars over the submillimeter area. Note the different coherent domains that arise from the multiple nucleation sites. Scale bar, 20 μm .

term corresponds to the energy of adhesion between two helices, whereas the second term corresponds to the elastic energy required to deform a naturally straight filament into a helix (23). For relatively stiff pillars, when $B/JaR^2 > 1$, it is evident that the minimum energy solution favors $P \rightarrow \infty$ (i.e., straight pillars); whereas for soft pillars, when $B/JaR^2 \leq 1$, minimizing U requires that the dimensionless pitch be as small as possible, which may be achieved by having $R \sim r$, $P \sim O(1)$ [i.e., a tightly wound helical configuration maximizing the length of contact between the filaments and corresponding to a second-order cluster (regime IIc)]. For pillars that have rotationally symmetric circular cross sections and are driven by a homogeneously drying front, the chirality of an individual cluster should be random. However, any asymmetry in the pillar cross section, pillar orientation, or the direction of the drying front can clearly lead to a specific handedness in the pattern. In any event, these helical clusters will then interact via the meniscus-driven capillary field to form higher-order coiled assemblies (III, IV, ...) until the growing assembly is eventually halted by the elastic field that penalizes large deformations (15).

To test these ideas, we studied the evaporation-induced self-assembly in a square array of epoxy nanopillars fabricated as described previously (24). Droplets of wetting liquids (including anhydrous ethanol, isopropyl alcohol, anhydrous toluene, acetone, and mixtures of ethanol and water at different ratios) were placed on horizontally oriented substrates ($d = 2 \mu\text{m}$, $r = 150 \text{ nm}$, $L = 4$ to $9 \mu\text{m}$, $E = 0.1$ to 2 GPa , and controlled wall roughness) and were allowed to evaporate at ambient conditions. The evaporation-induced interactions and self-organization of the bristle were studied with the use of optical microscopy (Leica DMRX connected to a QImaging Evolution VF cooled color CCD camera) and a field emission scanning electron microscope (Zeiss Ultra 55).

The resulting structures were in substantial agreement with the simple theory sketched above, and all of the predicted structures—from the first-order unclustered nanobristle to the fourth-order helical bundles—were observed (Fig. 1B). By using a periodic square array of nanopillars, we achieved a long-range order in the assembled bristle, such that large-area (up to millimeters), uniform domains of highly periodic bundles were generated from the nanometer-sized building blocks. Figure 2A and movie S1 illustrate the mechanism for the propagation of order in the array of the assembling pillars. When the liquid evaporates to the level of the free tips, a meniscus connecting the neighboring pillars is formed. In an equally spaced array, the lateral capillary forces acting on each pillar are fully balanced, and no lateral movement occurs. However, imperfections and instabilities, which include local differences in the evaporation rate, pinning of the contact line, and variations in the interpillar

lattice spacing, will nucleate the first pillar cluster at a particular location rather than randomly (for example, between pillars h and g). As a

result, the next pillar i will sense an anisotropic force field where $F_{ih} < F_{ij}$ and will bend in the direction of the pillar j . This process will prop-

agate through the bristle and generate long-range ordered domains (Fig. 2A). For example, to bias the system to form periodic second-order bundles over a large area, we chose conditions that would lead solely to the formation of clusters of four bristles whose stiffness would not allow their further assembly into higher-order structures. Epoxy bristles with $E = 1$ GPa, $r = 150$ nm, $L = 5$ μ m, and $d = 2$ μ m immersed in ethanol as a wetting liquid satisfied this condition. Figure 2B shows a fragment of the corresponding assembled structure with the marked long-range order.

A detailed microscopy study shows that the cluster twisting is a dynamic, multistep process with distinctive kinetics and a growth mechanism that involves the sequential coalescence of self-similar coiled blocks to yield organized helical patterns on very large scales (Fig. 3 and movie S2). To achieve the formation of higher-order structures III to V, the nanopillars were specifically designed to have rough, banded walls. In addition to increasing flexibility, this segmented, "wormlike" geometry (Fig. 3A, inset) provides the pinning of the receding contact line by re-entrant curvature (25, 26) and, thus, an increase in the capillary attraction necessary to bring the larger clusters together. The history of the hierarchical assembly process is imprinted in the makeup of the final helical structures: The lower-order braids and bundles can be clearly identified in the larger coiled clusters (Figs. 1B, bottom, and 3). The kinetics of this multistep process are depicted in Fig. 3B.

Because the instabilities leading to the chiral rearrangement of the clustered pillars are random, a mixture of bundles with the right- and left-handed twist was observed. To optimize our system to achieve the uniform handedness of the clusters, we used two approaches to the bristle design. The pillars were either (i) rendered elliptical in cross section or (ii) an array of tilted pillars was used (24). The ellipses' axes or the tilt direction of the pillars were chosen to make a small angle with the principal unit cell directions in the underlying square lattice (Fig. 4A). Such a design induces an anisotropy in the stiffness of the bristle that results in a directional, off-axis bending of the pillars under the influence of the capillary forces and allows us to form an ordered array of helices with uniform controlled right- or left-handedness (Fig. 4A). This is similar in concept to the use of a pre-tilt layer in liquid crystal displays to bias otherwise vertically aligned nematic crystals and prevent the formation of defects during switching (27). Alternatively, the pattern and orientation of the assembled coiled bundles could also be orchestrated by changing the direction of the evaporation front. Figure 4B provides an example of the latter approach—a woven carpet composed of braids of nanopillars uniformly plaited parallel to the surface—that results from the evaporation front moving parallel to the substrate.

Recent studies show that the adhesive properties in a variety of biological systems arise

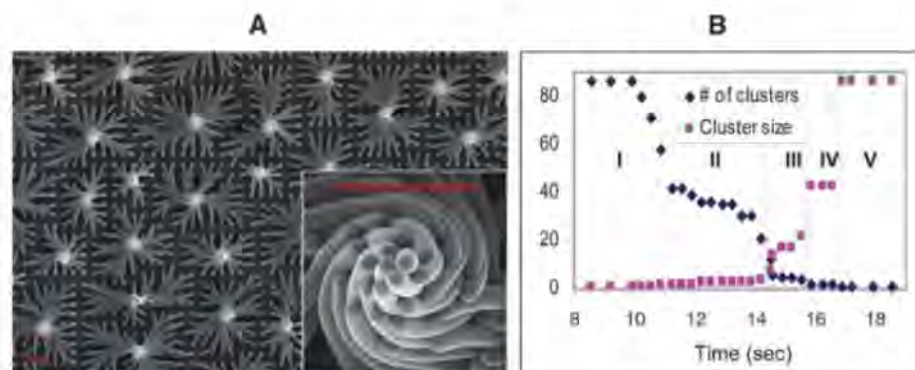


Fig. 3. Hierarchical assembly into large coiled clusters. (A) SEM showing an array of pillars ($L = 8$ μ m) self-organized from the ethanol solution into the level IV and V helical assemblies. (Inset) Magnified view of the coiled core. Scale bars, 3 μ m. (B) Kinetics of the hierarchical assembly. The growth of one representative cluster is shown. The number of clusters was monitored by analyzing the consecutive images from movie S2. The cluster size is defined as the number of pillars in the bundle. The multistep, sequential coalescence of the small blocks into higher-order structures is apparent. The y axis denotes the number or size of clusters.

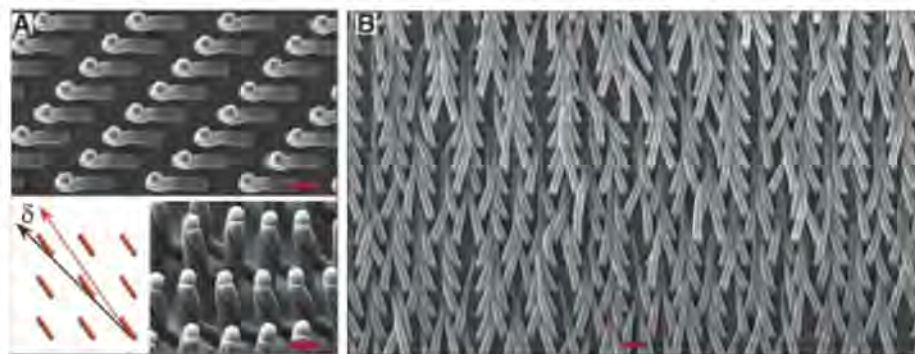
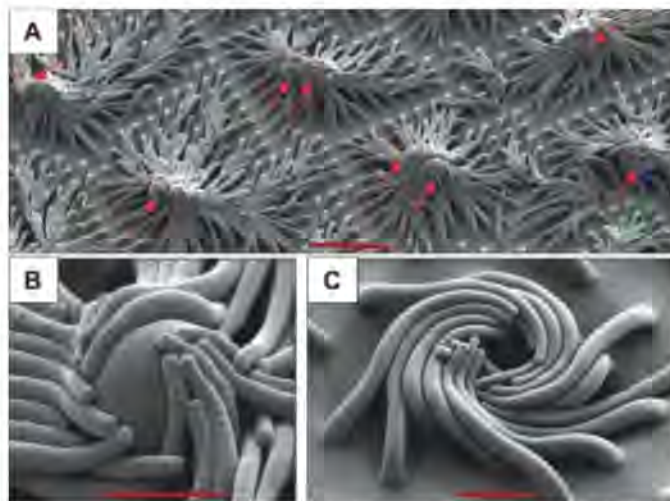


Fig. 4. Controlling handedness and pattern of assembled structures. (A) Top and angled SEM views showing an array of ordered helical pairs with uniform handedness. (Inset) Schematic diagram that illustrates the substrate design. The bristles were first tilted in the direction that forms a small angle δ with the principal diagonal direction of the underlying square lattice (shown by the red and black lines, respectively) and then allowed to assemble. (B) Evaporation along the surface results in the woven braids assembled parallel to the substrate. Scale bars, 2 μ m.

Fig. 5. Illustration of the adhesive and particle-trapping potential of the helically assembling bristle. (A) Low-magnification SEM showing the capture of the 2.5- μ m polystyrene spheres (indicated by arrows). Scale bar, 10 μ m. (B) Magnified view depicting a single sphere trapped through the conformal wrapping of the nanobristle. Scale bar, 2 μ m. (C) Coiled whirlpools remain after the removal of the spheres. Scale bar, 2 μ m.



from the conformational attachment of microscopic fibers to surfaces and objects and their subsequent entanglement (17, 28). The observed mechanical interlocking in our artificial, spirally assembling bristle can be used in a similar manner and may lead to an effective adhesive and particle-trapping system. Figure 5 shows microspheres that are captured through conformational wrapping and twisting of the nanobristle. The adhesion is extremely stable, and the particles remain attached even after rigorous sonication. The process is equally applicable for attaching to objects with arbitrary shapes and surfaces with various topographies.

Though lateral adhesion is known to occur in high-aspect ratio structures such as photoresists and soft lithographic stamps (29, 30), arrays of carbon and ZnO nanotubes (31, 32), and biomimetic setal adhesives (33), this process has been generally described as an unwanted outcome that leads to the uncontrolled collapse of the structures. The clustered features were usually irregular in size, and no order over the large area was observed unless templating was used (34). Here we have demonstrated that the process can, in fact, be finely tuned to yield organized nontrivial, helical assemblies with controlled size, pattern, hierarchy, and handedness over large areas. These mesoscale coiled structures may be useful in a number of applications: They have the ability to store elastic energy and information embodied in the adhesive patterns that can be created at will. Additionally, they may be used as an efficient adhesive or capture-and-release system, provide the foundation for hierarchically assembled structural materials, and be used to induce chiral flow patterns in the ambient flow and thus be applied for enhanced mixing and directed transport at the micron and submicron scale. These structures may serve as the seed for the spontaneous breaking of symmetry on large scales, just as

chirally spinning cilia ultimately control the left-right asymmetry in vertebrate morphogenesis (6).

References and Notes

- M. M. Green, R. J. M. Nolte, E. W. Meijer, *Materials-Chirality*, vol. 24 of *Topics in Stereochemistry*, S. E. Denmark, J. Siegel, Eds. (Wiley, Hoboken, NJ, 2003).
- N. Rubin, E. Perugia, M. Goldschmidt, M. Fridkin, L. Addadi, *J. Am. Chem. Soc.* **130**, 4602 (2008).
- H. Lichtenegger, M. Muller, O. Paris, C. Riekel, P. Fratzl, *J. Appl. Crystallogr.* **32**, 1127 (1999).
- W. Wagermaier et al., *Biointerphases* **1**, 1 (2006).
- S. Weiner, H. D. Wagner, *Annu. Rev. Mater. Sci.* **28**, 271 (1998).
- J. J. Essner et al., *Nature* **418**, 37 (2002).
- H. C. Kolb, M. S. Vannieuwenhze, K. B. Sharpless, *Chem. Rev.* **94**, 2483 (1994).
- J. W. Goodby, *J. Mater. Chem.* **1**, 307 (1991).
- E. D. Sone, E. R. Zubarev, S. I. Stupp, *Angew. Chem. Int. Ed.* **41**, 1705 (2002).
- J. S. Moore, S. I. Stupp, *J. Am. Chem. Soc.* **114**, 3429 (1992).
- T. E. Gier, X. H. Bu, P. Y. Feng, G. D. Stucky, *Nature* **395**, 154 (1998).
- J. Zhu et al., *Nat. Nanotechnol.* **3**, 477 (2008).
- C. A. Orme et al., *Nature* **411**, 775 (2001).
- A. E. Cohen, L. Mahadevan, *Proc. Natl. Acad. Sci. U.S.A.* **100**, 12141 (2003).
- J. Bico, B. Roman, L. Moulin, A. Boudaoud, *Nature* **432**, 690 (2004).
- H. Y. Kim, L. Mahadevan, *J. Fluid Mech.* **548**, 141 (2006).
- T. Eisner, D. J. Aneshansley, *Proc. Natl. Acad. Sci. U.S.A.* **97**, 6568 (2000).
- O. Betz, G. Kolsch, *Arthropod Struct. Dev.* **33**, 3 (2004).
- S. Neukirch, G. van der Heijden, *J. Elast.* **69**, 41 (2002).
- M. M. Nicolson, *Proc. Cambridge Philos. Soc.* **45**, 288 (1949).
- This is a simplification of the actual geometry of the pillars that are attached to a substrate at one end and free at the other. Yet, the case of free pillars that can bend, twist, and adhere is sufficient to understand the conditions when helical structures can arise. In the experimental setup, however, it is this broken symmetry induced by the attachment that leads to the observed complex braided structures of generalized helices of variable pitch and radius.
- K. L. Johnson, *Contact Mechanics* (Cambridge Univ. Press, Cambridge, 1985).
- For a pillar with a circular cross section, the twist of the cross section is a constant. Although adhesion can lead to twisting, because there is a lubricating layer of fluid between the pillars, we will assume that the pillars can bend without twisting as they wind around each other. The bending energy of a filament of length L is $U_b \sim B\kappa^2 L$. Therefore, for a helix of radius R and pitch p ($p = p/2\pi R$) that has curvature $\kappa = 1/R(1 + p^2)$, $U_b \sim BL/R^2(1 + p^2)^2$. For helically entwined pillars that are relatively straight (i.e., have a large pitch), the contact zone is straight and thus smaller than the pillar length (a consequence of the relative inextensibility of the pillars) and confers no energetic advantage. However, when the pitch of the tightly entwined pillars falls below a threshold, contact itself occurs over a helical patch (19) with a length that scales as $(L(1 + 1/p^2))^{1/2}$, so that the adhesion energy $U_a \sim -\gamma aL(1 + 1/p^2)^{1/2}$ increases as the pitch decreases further.
- B. Pokroy, A. Epstein, M. C. M. Persson Gulda, J. Aizenberg, *Adv. Mater.*, published online 18 November 2008; 10.1002/adma.200801432.
- A. Ahuja et al., *Langmuir* **24**, 9 (2008).
- A. Tuteja et al., *Science* **318**, 1618 (2007).
- P. J. Collings, M. Hird, *Introduction to Liquid Crystals* (Taylor and Francis, Bristol, UK, 1997).
- K. Autumn et al., *Nature* **405**, 681 (2000).
- C. Y. Hui, A. Jagota, Y. Y. Lin, E. J. Kramer, *Langmuir* **18**, 1394 (2002).
- Y. G. Y. Huang et al., *Langmuir* **21**, 8058 (2005).
- A. Dev, S. Chaudhuri, *Nanotechnology* **18**, 175607 (2007).
- H. Liu, J. Zhai, L. Jiang, *Soft Matter* **2**, 811 (2006).
- A. K. Geim et al., *Nat. Mater.* **2**, 461 (2003).
- A. Sidorenko, T. Krupenkin, A. Taylor, P. Fratzl, J. Aizenberg, *Science* **315**, 487 (2007).
- This work was partially supported by the Materials Research Science and Engineering Center under NSF award no. DMR-0213805. We acknowledge the use of the facilities at the Harvard Center for Nanoscale Systems supported by NSF award no. ECS-0335765. B.P. is grateful to the Fulbright Visiting Scholar Program for financial support.

Supporting Online Material

www.sciencemag.org/cgi/content/full/323/5911/237/DC1
Movies S1 and S2

8 September 2008; accepted 21 November 2008
10.1126/science.1165607

Historical Warnings of Future Food Insecurity with Unprecedented Seasonal Heat

David. S. Battisti¹ and Rosamond L. Naylor²

Higher growing season temperatures can have dramatic impacts on agricultural productivity, farm incomes, and food security. We used observational data and output from 23 global climate models to show a high probability (>90%) that growing season temperatures in the tropics and subtropics by the end of the 21st century will exceed the most extreme seasonal temperatures recorded from 1900 to 2006. In temperate regions, the hottest seasons on record will represent the future norm in many locations. We used historical examples to illustrate the magnitude of damage to food systems caused by extreme seasonal heat and show that these short-run events could become long-term trends without sufficient investments in adaptation.

The food crisis of 2006–2008 demonstrates the fragile nature of feeding the world's human population. Rapid growth in demand for food, animal feed, and biofuels, cou-

pled with disruptions in agricultural supplies caused by poor weather, crop disease, and export restrictions in key countries like India and Argentina, have created chaos in international mar-

kets (1). Coping with the short-run challenge of food price volatility is daunting. But the longer-term challenge of avoiding a perpetual food crisis under conditions of global warming is far more serious. History shows that extreme seasonal heat can be detrimental to regional agricultural productivity and human welfare and to international agricultural markets when policy-makers intervene to secure domestic food needs.

We calculated the difference between projected and historical seasonally averaged temperatures (2) throughout the world by using output from the 23 global climate models contributing to the Intergovernmental Panel on Climate Change's (IPCC) 2007 scientific synthesis (3). Our results show that it is highly likely (greater than 90%

¹Department of Atmospheric Sciences, University of Washington, Seattle, WA 98195–1640, USA. E-mail: battisti@u.washington.edu ²Program on Food Security and the Environment, Stanford University, Stanford, CA 94305–6055, USA. E-mail: roz@stanford.edu

chance) that growing season temperatures by the end of the 21st century will exceed even the most extreme seasonal temperatures recorded from 1900 to 2006 for most of the tropics and subtropics. Presently there are more than 3 billion people living in the tropics and subtropics, many of whom live on under \$2 per day and depend primarily on agriculture for their livelihoods (4). With growing season temperatures rising beyond historical bounds, the inevitable question arises: Will people in these regions have sufficient access to food to meet population- and income-

driven growth in demand in the future, and thus to achieve food security?

The IPCC concluded that elevated greenhouse gas concentrations are likely to lead to a general drying of the subtropics by the end of this century, creating widespread stress on agriculture (3, 5). Although much attention is focused on threats of increased droughts in subtropical agriculture, the potential impacts of seasonal average temperature changes in both the tropics and subtropics, which are expected to be large relative to the historical range of variation, are often over-

looked (6). Experimental and crop-based models for major grains in these regions show direct yield losses in the range of 2.5 to 16% for every 1°C increase in seasonal temperature (7, 8) [supporting online material (SOM)]. Large additional losses are expected from sea level rise and decreased soil moisture caused by higher average temperatures (3, 5, 9). Despite the general perception that agriculture in temperate latitudes will benefit from increased seasonal heat and supply food to deficit areas, even mid-latitude crops will likely suffer at very high temperatures in the absence of adaptation (10). Global climate change thus presents widespread risks of food insecurity.

It is conceivable that the warmest summers during the past century will represent the norm by the end of this century (Fig. 1A). But what if the average future seasonal temperature were to exceed the hottest seasons on record (Fig. 1B)? Entering a whole new realm of high seasonally averaged temperatures, not just multiday heat waves, will surely challenge the global population's ability to produce adequate food in the future or even to cope physically with chronic heat stress, unless major adaptations are made.

To put Fig. 1A in perspective, recall the record hot summer in Western Europe in 2003

Fig. 1. Hypothetical distributions of summer season temperatures from 1900–2000 and 2080–2100. *x* axis indicates seasonal temperature; *y* axis, probability of occurrence (number of years in the century).

(A) The highest growing-season temperature of the 20th century represents the median seasonal temperature by the end of the 21st century. (B) Future temperatures are out-of-bounds hot: that is, it is certain that the growing season temperature at the end of the 21st century will exceed the hottest growing season ever observed.

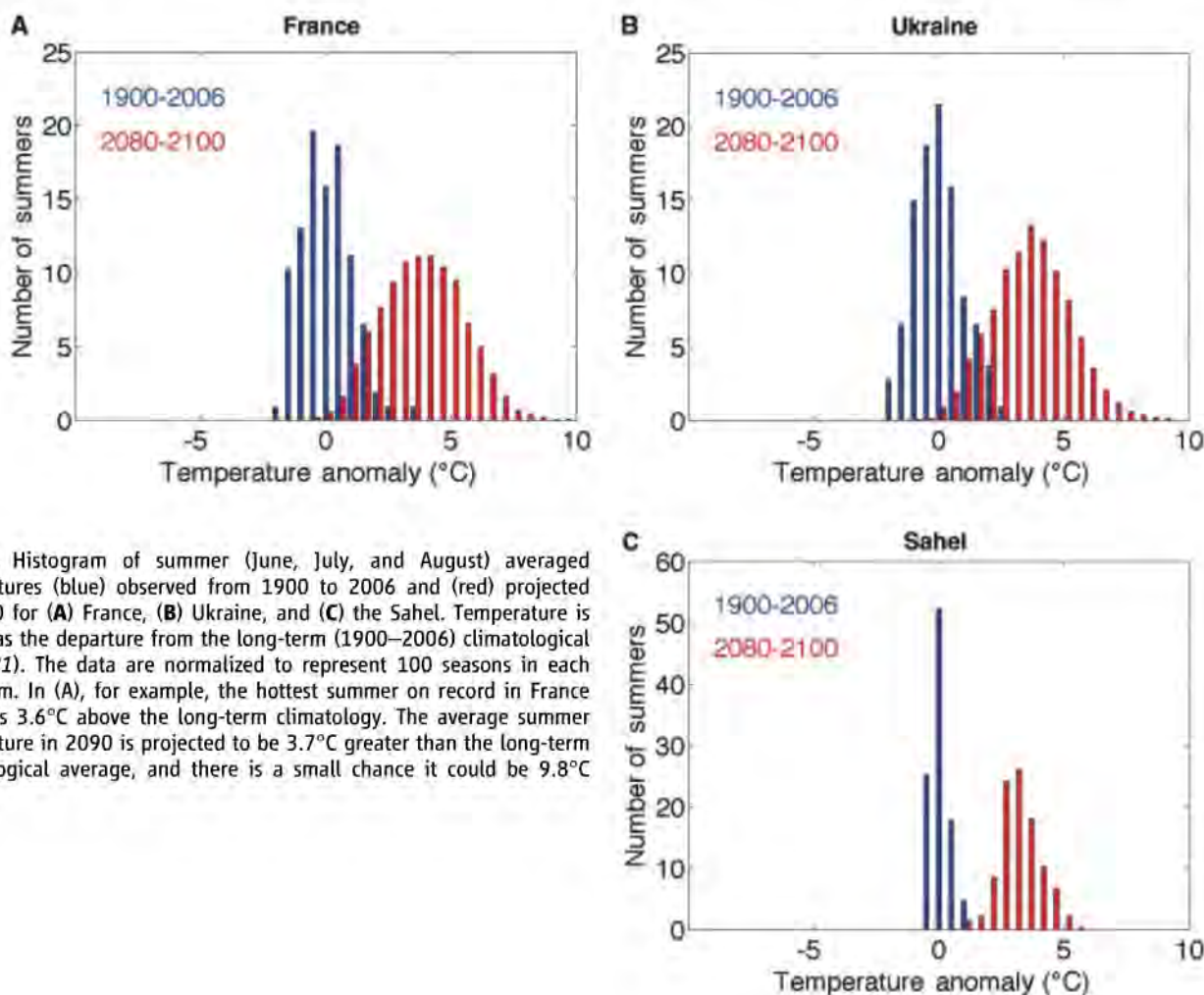
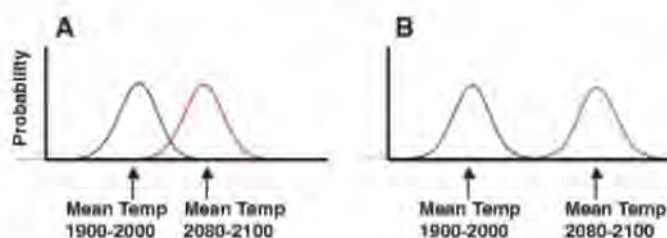


Fig. 2. Histogram of summer (June, July, and August) averaged temperatures (blue) observed from 1900 to 2006 and (red) projected for 2090 for (A) France, (B) Ukraine, and (C) the Sahel. Temperature is plotted as the departure from the long-term (1900–2006) climatological mean (21). The data are normalized to represent 100 seasons in each histogram. In (A), for example, the hottest summer on record in France (2003) is 3.6°C above the long-term climatology. The average summer temperature in 2090 is projected to be 3.7°C greater than the long-term climatological average, and there is a small chance it could be 9.8°C higher.

when an estimated 52,000 people died between June and August from heat stress, making it one of the deadliest climate-related disasters in Western history (11). The most intense seasonal temperature and the majority of fatalities were

centered in France and northern Italy, where over 30,000 people perished from heat-related causes (11, 12). In France, the mean summer temperature (June to August) was 3.6°C (3.5 standard deviations) above the long-term mean. Unfor-

tunately, by the end of the century, summer heat like that of 2003 is likely to be the norm for the country (Fig. 2A).

Severe heat in the summer of 2003 affected food production as well as human lives in Eu-

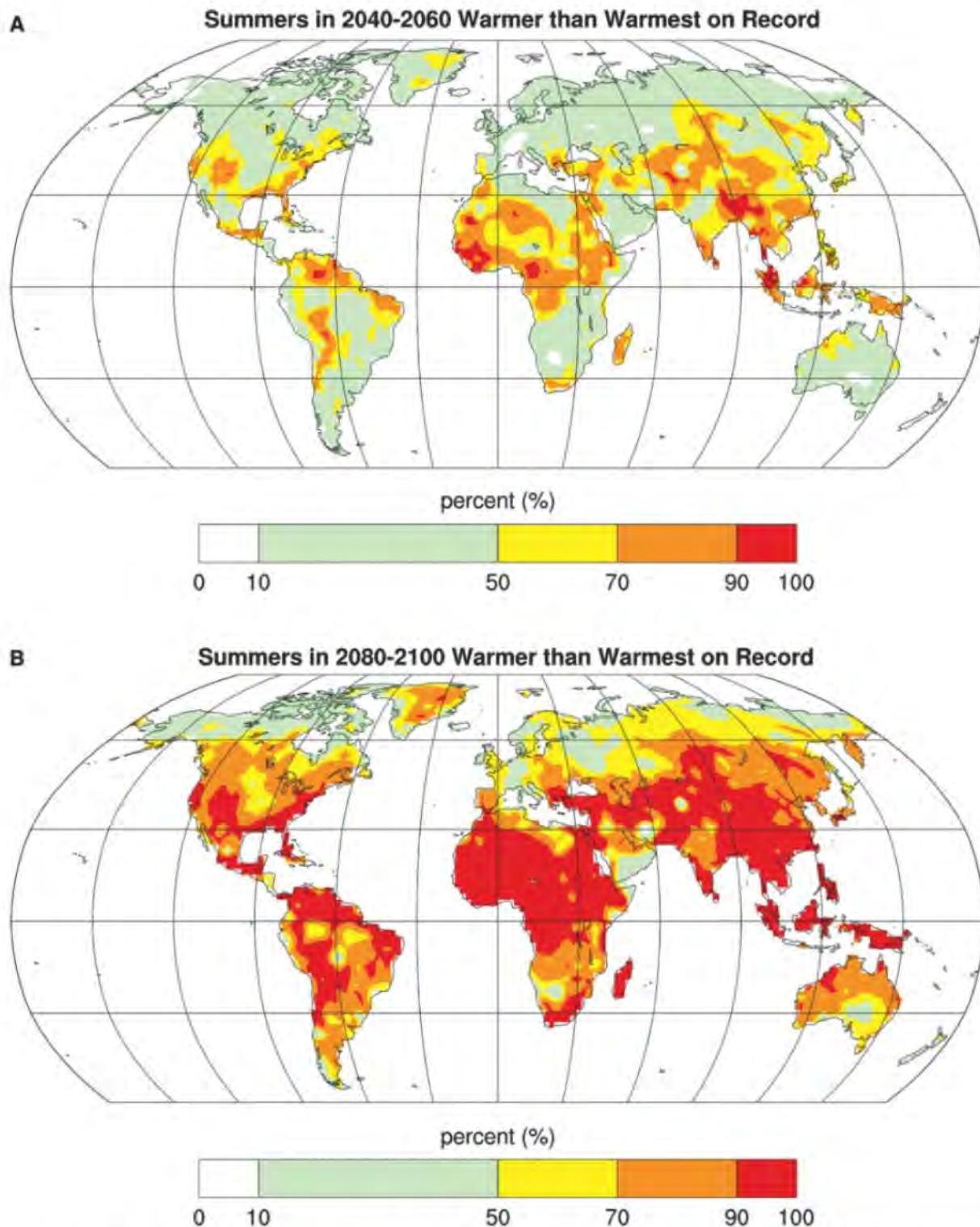


Fig. 3. Likelihood (in percent) that future summer average temperatures will exceed the highest summer temperature observed on record (**A**) for 2050 and (**B**) for 2090. For example, for places shown in red

there is greater than a 90% chance that the summer-averaged temperature will exceed the highest temperature on record (1900–2006) (22).

rope. Record high daytime and nighttime temperatures over most of the summer growing season reduced leaf and grain-filling development of key crops such as maize, fruit trees, and vineyards; accelerated crop ripening and maturity by 10 to 20 days; caused livestock to be stressed; and resulted in reduced soil moisture and increased water consumption in agriculture (5, 13) (SOM). Italy experienced a record drop in maize yields of 36% from a year earlier, whereas in France maize and fodder production fell by 30%, fruit harvests declined by 25%, and wheat harvests (which had nearly reached maturity by the time the heat set in) declined by 21% (5). These production shortfalls hurt the region's farmers economically, although global food trade, subsidies, and insurance compensation helped to avert serious price hikes or reductions in regional or global food security.

By comparison, extremely high summer-averaged temperature in the former Soviet Union (USSR) in 1972 contributed to disruptions in world cereal markets and food security that remain a legacy in the minds of food policy analysts to this day. What sticks in most people's minds is the towering price spike between 1972 and 1974 that occurred within a long-term trend decline in grain prices during a 50-year period after World War II. Nominal prices for wheat—the crop most affected by the USSR weather shock—rose from \$60 to \$208 per metric ton in international markets between the first quarters of 1972 and 1974, and real prices more than tripled (14). Although extreme summer averaged temperature in the USSR was among several factors contributing to the international price spike, this climate event was largely responsible for setting the dynamics in motion (15).

The prolonged hot period in the summer of 1972 in southeast Ukraine and southwest Russia—major breadbaskets in the former USSR—ranks in the top 10% of temperature anomalies over the observational period 1900–2006. Summer temperatures in this region ranged from 2° to 4°C above the long-term mean. The vast majority of news reports at the time focused on drought as opposed to extreme heat, although fully one-third of summers in this area over the past 100 years were drier than in 1972 (only 0.5 standard deviations below the long-term mean). A peak of high temperatures exceeding 30°C set in during July and August during key crop development stages for wheat and coarse grains, causing a 13% decline in grain production from a year earlier for the USSR as a whole (16) (SOM). Such high summer temperatures in the region will likely be the norm in 2050 and well below the median of projected summer temperature by the end of the century (Fig. 2B).

The USSR had long been known for its variable climate and crop yields. What changed in 1972 was the Soviets' unexpected intervention in international markets to compensate for anticipated crop shortfalls—a marked shift from their earlier policy of internal adjustments through the culling of livestock herds (16). The USSR en-

tered the world grain market at a time when import demand was rising rapidly in Asia because of expanding populations, low-yield growth, and (in the same year) weak monsoon rains (15). Governments in several developing countries, particularly in Asia, feared political instability with rising grain prices and implemented food self-sufficiency (minimum trade) policies that remained in effect for decades.

A major lesson from this case and the recent food crisis is that regional disruptions can easily become global in character. Countries often respond to production and price volatility by restricting trade or pursuing large grain purchases in international markets—both of which can have destabilizing effects on world prices and global food security. In the future, heat stress on crops and livestock will occur in an environment of steadily rising demand for food and animal feed worldwide, making markets more vulnerable to sharp price swings. High and variable prices are most damaging to poor households that spend the majority of their incomes on staple foods.

Another region at risk from higher temperatures is the Sahel, where crop and livestock production play an essential role in the region's economy, employing roughly 60% of the active population and contributing 40% to gross national product (17). The Sahel suffered a prolonged drought from the late 1960s to the early 1990s that caused crop and livestock productivity to plummet, and which contributed to countless hunger-related deaths and unprecedented rates of migration from north to south, from rural to urban areas, and from landlocked to coastal countries (18). Although the Sahel's climate disaster was largely one of extended drought, the specter of high and rising temperature lurks in the background. Year-to-year temperature variability in the Sahel has been low during the past century (particularly in comparison with temperate countries like France and Ukraine), but the growing season temperature has been very high, with long-term daily averaged summer temperature ranging from 25°C in the south to 35°C in the north. Moreover, temperatures have trended upward since 1980. Despite rains returning to some locations of the Sahel during the past 15 years, the growing season for staple crops has been reduced, maize yields have remained far below varietal potential, and millet and sorghum yields continue to stagnate (18). Hundreds of thousands of children and infants in the region still die each year from hunger-related causes, and malnutrition contributes to long-term mental and physical disabilities. Over recent decades most of the region's poorest households have lost their livestock or other assets; they remain net consumers of food and struggle to purchase staples even when they are available in the market. These households farm at an extreme disadvantage irrespective of climate change, with limited access to improved crop varieties, seed supplies, fertilizers, credit, and irrigation and transportation infrastructure (19).

Most worrisome for the Sahel is that average growing season temperatures by the end of this century, and even earlier for some parts of the region, are expected to exceed the hottest seasons recorded during the past century (Fig. 2C). Such heat will compound food insecurity caused by variable rainfall in the region, and it will increase the incidence of agricultural droughts (as opposed to meteorological droughts) defined by elevated evapotranspiration, low soil moisture, and high rates of water runoff from hard pan soils when it rains. Even today, temperatures in the Sahel can be so high that the rain evaporates before it hits the ground (18). New bounds of heat stress will make the region's population far more vulnerable to poverty and hunger-related deaths and will likely drive many people out of agriculture altogether, thus expanding migrant and refugee populations.

These historical examples illustrate the profound damage that can be caused (or in the near future may be caused) by high seasonal heat, but they also represent short-run impacts. We chose France (2003) and Ukraine (1972) as examples specifically because temperature deviations were large in comparison to precipitation deviations relative to the observational record. In the Sahel case, drought and heat stress are tightly coupled, with heat stress becoming increasingly important during the past decade. The threats to food security and human lives caused by unusually high seasonal temperature in France, Ukraine, and the Sahel in the 20th century were ameliorated when the extreme temperatures subsided, when markets balanced acute regional food deficits with food surpluses from other locations, and when farmers autonomously adapted their practices or migrated. The future, however, could be entirely different. If growing season temperatures by the end of the 21st century remain chronically high and greatly exceed the hottest temperature on record throughout the much of the world, not just for these three examples, then global food security will be severely jeopardized unless large adaptation investments are made.

Climate model projections from the IPCC 2007 assessment suggest that this outcome is indeed very likely (Fig. 3). Figure 3A shows that, as early as 2050, the median projected summer temperature is expected to be higher than any year on record in most tropical areas. By the end of the century, it is very likely (greater than 90% chance) that a large proportion of tropical and subtropical Asia and Africa will experience unprecedented seasonal average temperature, as will parts of South, Central, and North America and the Middle East (Fig. 3B). High seasonal temperatures beyond what has been experienced during the past century will thus become widespread.

Three important conclusions can be drawn from these projections. First, tropical countries experience less year-to-year temperature extremes than do temperate countries and therefore will be the first to experience unprecedented heat

stress because of global climate change. By the end of the century, however, the seasonal growing temperature is likely to exceed the hottest season on record in temperate countries (e.g., equivalent to what France experienced in 2003), and the future for agriculture in these regions will become equally daunting.

Second, the projected seasonal average temperature represents the median, not the tail, of the climate distribution and should therefore be considered the norm for the future. Indeed, the probability exceeds 90% that by the end of the century, the summer average temperature will exceed the hottest summer on record throughout the tropics and subtropics (Fig. 3B). Because these regions are home to about half the world's population, the human consequences of global climate change could be enormous.

Lastly, with growing season temperatures in excess of the hottest years on record for many countries, the stress on crops and livestock will become global in character. It will be extremely difficult to balance food deficits in one part of the world with food surpluses in another, unless major adaptation investments are made soon to develop crop varieties that are tolerant to heat and heat-induced water stress and irrigation systems suitable for diverse agroecosystems. The genetics, genomics, breeding, management, and engineering capacity for such adaptation can be developed globally but will be costly and will require political prioritization (5, 8, 9, 20). National and international agricultural investments have been waning in recent decades and remain insufficient to meet near-term food needs in the world's poorest countries, to say nothing of

longer-term needs in the face of climate change (1). History provides some guide to the magnitude and effects of high seasonal averaged temperature projected for the future. Ignoring climate projections at this stage will only result in the worst form of triage.

References and Notes

1. R. Naylor, W. Falcon, *Boston Rev.* **33**, 13 (2008).
2. We approximated the main growing season to be summer in the extratropics. Hence north of the equator we used the three-month average temperature June through August (and for south of the equator we used December through February), periods that broadly capture growing season conditions for many crops.
3. IPCC, *Fourth Assessment Report: Synthesis*, published online 17 November 2007, www.ipcc.ch/ipccreports/ar4-syr.htm.
4. World Bank, *World Development Report 2008: Agriculture for Development* (World Bank, Washington, DC, 2007).
5. W. Easterling et al., in *Climate Change 2007: Impacts, Adaptation, and Vulnerability*, M. Parry et al., Eds. (Cambridge Univ. Press, New York, 2007), p. 976.
6. D. Lobell, M. Burke, *Environ. Res. Lett.* **3**, 034007 (2008).
7. S. Peng et al., *Proc. Natl. Acad. Sci. U.S.A.* **101**, 9971 (2004).
8. D. B. Lobell et al., *Science* **319**, 607 (2008).
9. B. Barnabas et al., *Plant Cell Environ.* **31**, 11 (2008).
10. W. Schlenker, M. J. Roberts, *Rev. Agric. Econ.* **28**, 391 (2006).
11. J. Larsen, *Earth Policy Institute*, published online 28 July 2006 (www.earth-policy.org/Updates/2006/Update56.htm).
12. P. Pirard et al., *Eurosurveillance* **10**, 554 (2005).
13. A. De Bono et al., "Environmental alert bulletin: Impacts of summer 2003 heat wave in Europe" (United Nations Environmental Programme, Nairobi, Kenya, 2004).
14. International Financial Statistics Database, "United States Gulf ports wheat prices," published online July 2008, www.imfstatistics.org.
15. D. Hathaway et al., *Brookings Pap. Econ. Act.* **1**, 63 (1974).

16. N. Dronin, E. Bellinger, *Climate Dependence and Food Problems in Russia 1900-1990* (Central European Univ. Press, New York, 2005).
17. World Bank, *Africa Development Indicators 2007* (World Bank, Washington, DC, 2007).
18. S. Kandji, L. Verchot, J. Mackensen, *Climate Change and Variability in the Sahel Region: Impacts and Adaptation Strategies in the Agricultural Sector* (United Nations Environmental Programme and World Agroforestry Center, Nairobi, Kenya, 2006).
19. T. Jayne, in *The Transformation of Agri-Food Systems: Globalization, Supply Chains, and Smallholder Farmers*, E. B. McCullough et al., Eds. (Earthscan, London, 2008).
20. S. Takeda, M. Matsuoka, *Nat. Rev. Genet.* **9**, 444 (2008).
21. To calculate the projected climate for 2090, we first added the observed temperature departures (in blue) to the change in the summer temperature, taken to be the mean summer temperature for 2080–2100 minus that for 1980–2000, simulated by each of the 23 climate models from the IPCC AR4 forced by the "middle of the road" emission scenario, A1B. We then combined the 23×107 projections to create the probability distribution function for summer temperature in 2090 (see SOM).
22. The probability distribution of future summer temperature is calculated as described in (21). Here, summer is defined north of the equator as the average temperature from June through August and south of the equator as December through February. In the immediate vicinity of the equator, values in Fig. 3 are qualitatively insensitive to the choice of months that define the season.
23. This work was made possible by grants from the NSF (grant SES 0433679) and the Tamaki Foundation. We thank M. Baker, M. Burke, W. Falcon, D. Kennedy, S.-H. Kim, D. Lobell, R. Nicholas, K. Niemi Johnson, K. Rennert, and D. Vimont for comments and/or assistance on the draft.

Supporting Online Material

www.sciencemag.org/cgi/content/full/323/5911/240/DC1
Materials and Methods
SOM Text
References and Notes

7 August 2008; accepted 2 December 2008
10.1126/science.1164363

Foraminiferal Isotope Evidence of Reduced Nitrogen Fixation in the Ice Age Atlantic Ocean

H. Ren,^{1*} D. M. Sigman,¹ A. N. Meckler,² B. Plessen,³ R. S. Robinson,⁴ Y. Rosenthal,⁵ G. H. Haug^{6,7}

Fixed nitrogen (N) is a limiting nutrient for algae in the low-latitude ocean, and its oceanic inventory may have been higher during ice ages, thus helping to lower atmospheric CO₂ during those intervals. In organic matter within planktonic foraminifera shells in Caribbean Sea sediments, we found that the ¹⁵N/¹⁴N ratio from the last ice age is higher than that from the current interglacial, indicating a higher nitrate ¹⁵N/¹⁴N ratio in the Caribbean thermocline. This change and other species-specific differences are best explained by less N fixation in the Atlantic during the last ice age. The fixation decrease was most likely a response to a known ice age reduction in ocean N loss, and it would have worked to balance the ocean N budget and to curb ice age–interglacial change in the N inventory.

The sources of fixed N to the ocean are terrestrial runoff, atmospheric deposition, and, most important, marine N fixation. The main sinks are sedimentary denitrification, mostly in continental shelf sediments, and water column denitrification in the eastern tropical Pacific and the Arabian Sea. Sediment records

from modern denitrification zones show clear N isotopic evidence of reduced water column denitrification during the Last Glacial Maximum (LGM) relative to the current interglacial (Holocene) (1, 2). The history of other processes, especially N fixation, has proven more difficult to reconstruct. Decreased denitrification and/or

increased N fixation would have raised the N inventory of the ocean during the LGM, thereby strengthening the ocean's biological pump and contributing to the observed reduction in atmospheric CO₂ during the ice age (1–5).

N fixation produces oceanic fixed N with $\delta^{15}\text{N}$ values between –2 and 0 per mil (‰), close to that of atmospheric N₂ (6, 7). Sedimentary denitrification removes nitrate (NO₃[–]) from the ocean with minimal isotope discrimination (8). In contrast, water column denitrification leaves residual nitrate enriched in ¹⁵N that raises the $\delta^{15}\text{N}$ of mean ocean nitrate above that of newly

¹Department of Geosciences, Guyot Hall, Princeton University, Princeton, NJ 08544, USA. ²Geological and Planetary Sciences Division, California Institute of Technology, Pasadena, CA 91125, USA. ³Helmholtz-Zentrum Potsdam, Deutsches GeoForschungsZentrum (GFZ), Potsdam 14473, Germany. ⁴Graduate School of Oceanography, University of Rhode Island, Narragansett, RI 02882, USA. ⁵Institute of Marine and Coastal Sciences and Department of Geological Sciences, Rutgers University, New Brunswick, NJ 08901, USA. ⁶Geological Institute, Department of Earth Sciences, ETH Zürich, Zürich 8092, Switzerland. ⁷DFG Leibniz Center for Earth Surface Process and Climate Studies, Institute for Geosciences, Potsdam University, Potsdam D-14476, Germany.

*To whom correspondence should be addressed. E-mail: hren@princeton.edu

fixed N (9). In the context of mean ocean nitrate with a $\delta^{15}\text{N}$ of $\sim 5\text{‰}$, N fixation causes a regional decrease in the $\delta^{15}\text{N}$ of thermocline nitrate, which is observed throughout the western subtropical and tropical North Atlantic (10–12).

Thus, the $\delta^{15}\text{N}$ of organic N sinking out of the surface ocean, if preserved in the sediments, should record N fixation by two related mechanisms. First, most newly fixed N is remineralized in the thermocline, producing low- $\delta^{15}\text{N}$ nitrate,

which is then provided repeatedly to the euphotic zone. Second, N fixation can contribute low- $\delta^{15}\text{N}$ N directly to the plankton in the surface ocean and the sinking flux that they produce. However, in the low-productivity, low-latitude

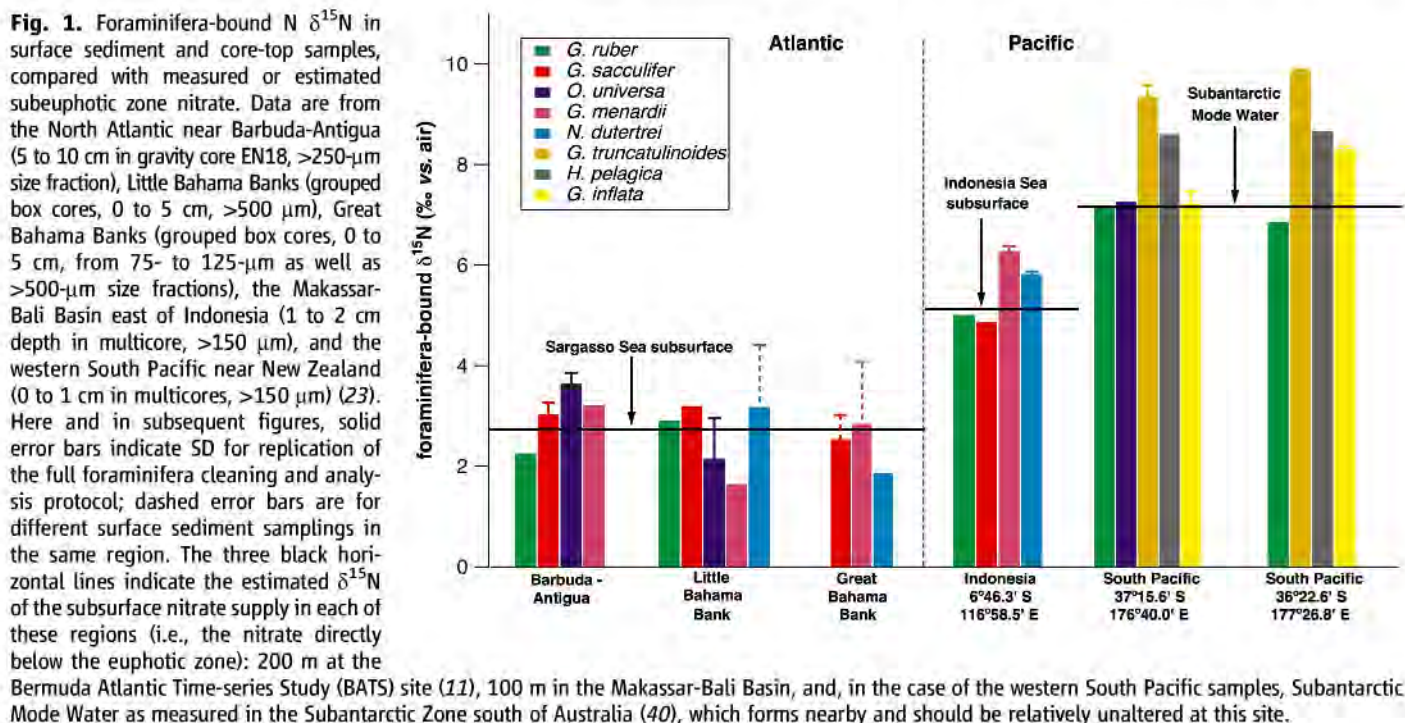
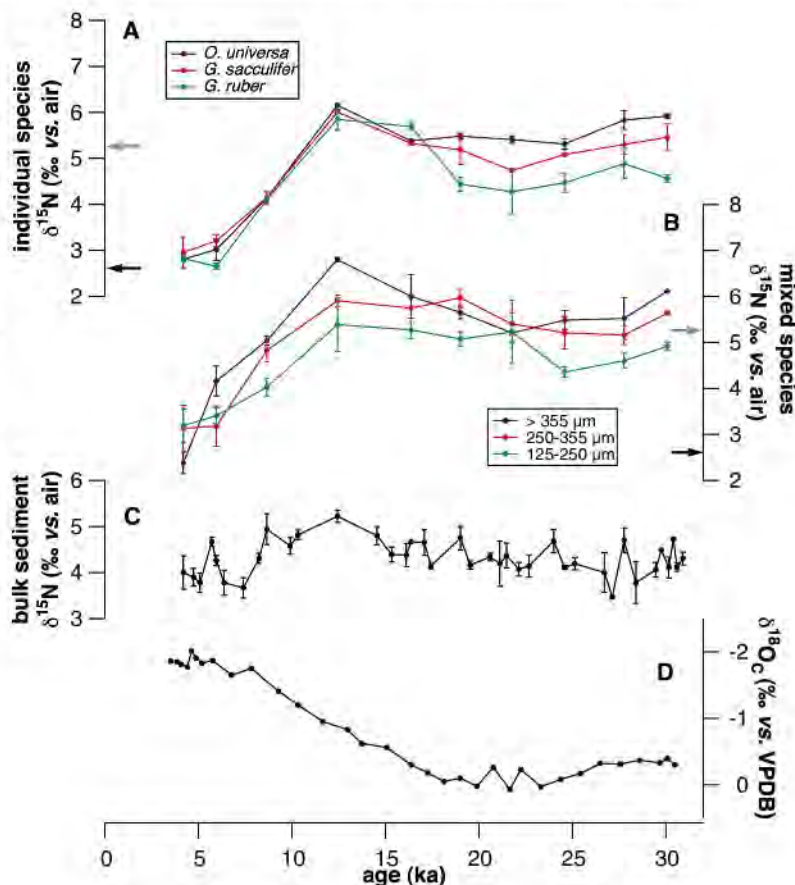


Fig. 2. Foraminifera-bound and bulk sedimentary $\delta^{15}\text{N}$ in the Caribbean Sea from ODP 999A ($12^{\circ}45'\text{N}$, $78^{\circ}44'\text{W}$; 2827 m; sedimentation rate $\sim 4\text{ cm per } 1000\text{ years}$) during the past 30,000 years (ka, thousands of years ago). (A) Planktonic foraminifera-bound $\delta^{15}\text{N}$ of individual species. Blue, *O. universa*; red, *G. sacculifer*; green, *G. ruber*. *O. universa* and *G. sacculifer* were picked from the $>355\text{-}\mu\text{m}$ size fraction; *G. ruber* was picked from the $>250\text{-}\mu\text{m}$ size fraction. (B) Planktonic foraminifera-bound $\delta^{15}\text{N}$ of different foraminifera size fractions. Blue, $>355\text{-}\mu\text{m}$; red, 250 to 355 μm ; green, 125 to 250 μm . *Neogloboquadrina dutertrei*, *O. universa*, *G. sacculifer*, and *G. ruber* are abundant in the $>355\text{-}\mu\text{m}$ size fraction. *O. universa*, *G. sacculifer*, and *G. ruber* are abundant in the 250- to 355- μm size fraction. *G. ruber* and *G. bulloides* are abundant in the 125- to 250- μm size fraction. Black and gray arrows indicate present-day subeuphotic zone and subthermocline nitrate $\delta^{15}\text{N}$ in the western North Atlantic, respectively (12). (C) Bulk sedimentary $\delta^{15}\text{N}$, with error bars indicating SD calculated from replicates. (D) $\delta^{18}\text{O}$ of *G. ruber* (pink) calcite [‰ versus Vienna Pee Dee belemnite (VPDB) standard] from (41). The age model is from (41), based on ^{14}C dating and $\delta^{18}\text{O}$ correlation.



open ocean where N fixation is thought to be focused, seafloor processing increases the $\delta^{15}\text{N}$ of bulk sedimentary N from that of sinking N (13), reducing confidence in sedimentary N as a recorder of sinking-flux $\delta^{15}\text{N}$. In these environments, where little marine organic N is preserved and buried, foreign (e.g., terrestrial) N can also contaminate the regional ocean signal.

In the subtropical and tropical ocean, planktonic foraminifera are an important component of the sinking flux to the sediments. The organic matrix laid down in foraminiferal tests is physically protected by the test during sedimentary diagenesis (14, 15). Thus, foraminifera-bound N is a promising paleoceanographic archive in sites where sedimentary processes may complicate bulk sediment N isotope records (16, 17). Planktonic foraminifera are heterotrophic zooplankton, and many species also have dinoflagellate symbionts. They obtain N mostly from particulate organic matter (POM), including phyto- and zooplankton (18). The $\delta^{15}\text{N}$ of zooplankton, including foraminifera, tends to be $\sim 3\text{‰}$ higher than that of their food source because of preferential excretion of ^{14}N -rich ammonia (19, 20). The ammonia excretion, in turn, lowers the $\delta^{15}\text{N}$ of POM relative to the N supply to the euphotic zone (21). In the modern Sargasso Sea, the $\delta^{15}\text{N}$ of subsurface nitrate supplied to the euphotic zone is 2 to 3‰ (11), the $\delta^{15}\text{N}$ of suspended POM is closer to 0‰ (21, 22), and the $\delta^{15}\text{N}$ of zooplankton appears to center around 2 to 3‰ (21), similar to the $\delta^{15}\text{N}$ of nitrate supply and the N export (22). Thus, we expect the $\delta^{15}\text{N}$ of foraminifera to be similar to and correlated with the integrated $\delta^{15}\text{N}$ of the new N supply to the euphotic zone, including nitrate from below and N fixation.

We measured the foraminifera-bound $\delta^{15}\text{N}$ in surface sediments from several regions (23) (fig. S3) and compared them with the $\delta^{15}\text{N}$ of subsurface nitrate. The foraminifera-bound $\delta^{15}\text{N}$ of most species from these locations is close to (rarely more than 1‰ different from) the $\delta^{15}\text{N}$ of the shallow thermocline nitrate available for upward transport into the euphotic zone (Fig. 1). At some sites, deeper-dwelling species (in particular, *Globorotalia truncatulinoides* in the southwest Pacific samples) have a higher $\delta^{15}\text{N}$ than other species, which is best explained by the broadly observed increase in POM $\delta^{15}\text{N}$ with depth below the euphotic zone (24). One weakness of the comparison in Fig. 1 is that it does not take into account N fixation as a low- $\delta^{15}\text{N}$ N source within the euphotic zone that augments the nitrate supply, but this simplification appears reasonable (23).

Foraminifera-bound $\delta^{15}\text{N}$ and bulk sedimentary $\delta^{15}\text{N}$ were measured in sediments representing the past 30,000 years at Ocean Drilling Program (ODP) Site 999A in the Colombian Basin of the Caribbean Sea. In individual foraminifera species (Fig. 2A) as well as in mixed foraminifera samples of varying sizes (Fig. 2B), the LGM $\delta^{15}\text{N}$ is higher than the interglacial values.

Focusing on the picked species data, the interglacial $\delta^{15}\text{N}$ is 2.7 to 3.2‰, similar to the thermocline nitrate $\delta^{15}\text{N}$ observed today in the tropical and subtropical western North Atlantic (11, 12). The glacial $\delta^{15}\text{N}$ is 4.3 to 5.9‰, varying with species. This is generally close to the $\delta^{15}\text{N}$ of modern deep Atlantic nitrate measured just below the thermocline, 5.0 to 5.5‰ (11, 12). The higher foraminifera-bound $\delta^{15}\text{N}$ in the LGM could be due to higher mean ocean nitrate $\delta^{15}\text{N}$ at that time. However, in relevant (i.e., non-polar) open-ocean records, which derive from various oceanographic environments, there is as yet no evidence for a 2‰ decrease in mean ocean nitrate $\delta^{15}\text{N}$ upon deglaciation (25).

The low $\delta^{15}\text{N}$ of Holocene and surface sediment foraminifera from the North Atlantic tracks the low $\delta^{15}\text{N}$ of thermocline nitrate in the region, which in turn derives from the remineralization of newly fixed N. Thus, we interpret the high LGM foraminiferal $\delta^{15}\text{N}$ to reflect a weakening in the $\delta^{15}\text{N}$ decrease that occurs upward through the thermocline in the modern North Atlantic, such that the euphotic zone was supplied with

nitrate with a $\delta^{15}\text{N}$ much more similar to the nitrate currently found at the base of the thermocline (Fig. 3). This most likely requires that N fixation was much reduced in the ice age Atlantic; a simple estimation, assuming no glacial-to-interglacial changes in thermocline circulation, suggests that it was $\sim 20\%$ of the Holocene rate (23) (fig. S5).

In addition to the clear glacial-to-interglacial change, there is a small (0.5 to 1.5‰) deglacial maximum in $\delta^{15}\text{N}$ apparent in each of the individual species records and in at least the $>355\text{-}\mu\text{m}$ size fraction record. This feature, which is common in the deglacial section of sediment records from all basins (25), most likely reflects a peak in the $\delta^{15}\text{N}$ of mean ocean nitrate. It may result from a transient deglacial peak in water column denitrification relative to sediment denitrification and/or from a transient N loss from the ocean (16), the former process better matching the available data (26). Our record at Site 999 suggests that the deglacial $\delta^{15}\text{N}$ maximum is relatively weak in comparison to observations from denitrification-influenced records, but we

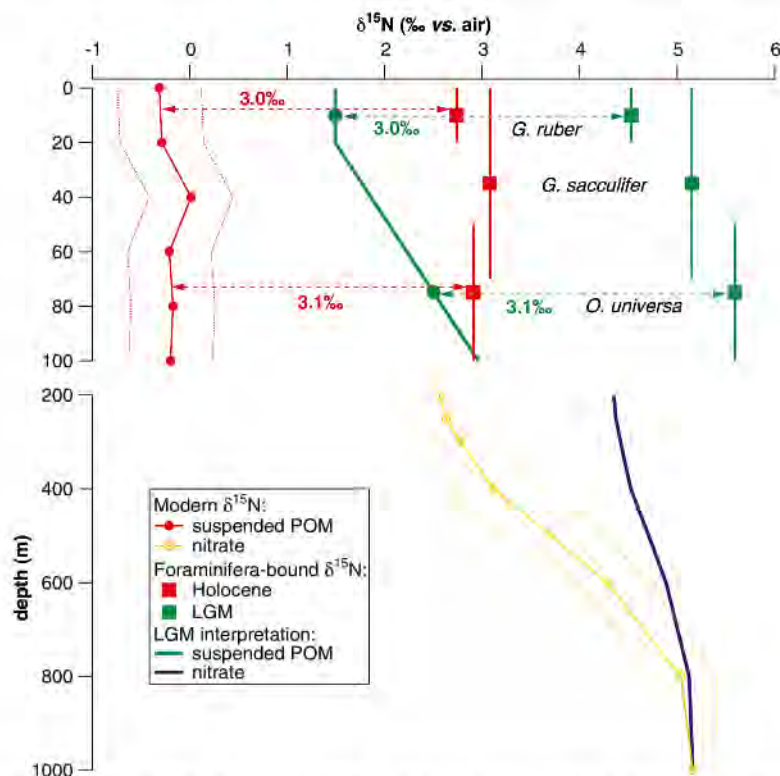


Fig. 3. Depth profile of $\delta^{15}\text{N}$ of suspended POM and nitrate in western North Atlantic during the present interglacial and the last ice age. Solid red circles denote the $\delta^{15}\text{N}$ of suspended particles in the surface 100 m near the Bermuda Atlantic Time-series Site (BATS) averaged over 1985 to 1988 [data from (31)]; dotted lines indicate 1 SD. Note that the suspended POM $\delta^{15}\text{N}$ increase accompanying the decreasing POM concentration below the euphotic zone (24), mentioned in the text, occurs below the depth range shown here. Orange circles denote average $\delta^{15}\text{N}$ of nitrate in the upper 200 to 1000 m at BATS (11); dotted lines indicate the measured range. Solid red and green squares denote foraminifera-bound $\delta^{15}\text{N}$ during the Holocene and the LGM, respectively. Foraminiferal depth maxima are taken from (30). Green and blue lines are proposed LGM depth profiles of the $\delta^{15}\text{N}$ of suspended POM in the photic zone and of nitrate in the thermocline (POM calculated from LGM-to-Holocene changes, using the depth ranges indicated for *G. ruber* and *O. universa* and assuming a constant foraminifera-POM $\delta^{15}\text{N}$ relationship for each of these two species; nitrate calculated from the *G. ruber* change).

suspect that it was overprinted by an increase in Atlantic N fixation at that time (Fig. 4, dashed interval).

The Caribbean foraminiferal $\delta^{15}\text{N}$ record is similar to the bulk sediment $\delta^{15}\text{N}$ record from Cariaco Basin (27, 28) (Fig. 4). The Cariaco Basin record is from anoxic waters, and seafloor isotopic alteration and allochthonous N are demonstrably unimportant there today (29). However, the basin's barriers to circulation have complicated the interpretation of its $\delta^{15}\text{N}$ record, potentially affecting its changes. Nonetheless, the published interpretation of the deglacial $\delta^{15}\text{N}$ decrease in the Cariaco record—enhanced Atlantic N fixation upon deglaciation (27, 28)—is supported by our open Caribbean foraminiferal data.

The foraminiferal species *Orbulina universa*, *Globigerinoides sacculifer*, and *Globigerinoides ruber* have similar $\delta^{15}\text{N}$ during the deglaciation and interglacial; however, they are coherently different during the LGM, with *O. universa* the highest and *G. ruber* the lowest (Fig. 2A). In the modern ocean, *G. ruber* is most abundant in

the mixed layer, roughly the upper 30 m in this region. *G. sacculifer* inhabits a broader depth interval down to the deep chlorophyll maximum (DCM), at ~80 m in this region, and *O. universa* tends to have its abundance maximum near the DCM (30) (Fig. 3). Thus, the order of decreasing $\delta^{15}\text{N}$ during the last ice age coincides with habitats of progressively shallower depth.

In the modern tropical and subtropical western Atlantic, across the ~100-m-deep euphotic zone, suspended POM $\delta^{15}\text{N}$ is uniformly low relative to the thermocline nitrate supply, as a result of some combination of N fixation and N recycling (Fig. 3) (21, 22). This rough uniformity is consistent with the similarity in $\delta^{15}\text{N}$ of *O. universa*, *G. sacculifer*, and *G. ruber*. The $\delta^{15}\text{N}$ divergence of these species during the last ice age probably arose from an increase with depth in euphotic zone suspended POM $\delta^{15}\text{N}$. This might have been the result of a larger $\delta^{15}\text{N}$ difference between N fixation and the subsurface nitrate supply, which, according to our data, had a higher $\delta^{15}\text{N}$ during the LGM. However, the species converge in $\delta^{15}\text{N}$ during the deglaciation, before the $\delta^{15}\text{N}$ of the nitrate

supply had decreased, which suggests that this is not the sole explanation for the interspecific differences during the LGM.

In the modern Sargasso Sea, preferential ^{14}N recycling should work to lower the $\delta^{15}\text{N}$ of the mixed layer relative to the deeper euphotic zone (31), but this gradient is apparently diluted by N inputs to the entire euphotic zone, including N fixation. With less N fixation during the LGM, the recycling-driven $\delta^{15}\text{N}$ gradient may have been unobscured and thus stronger, leading to the clear $\delta^{15}\text{N}$ differences among species. It is also possible that, with less N fixation, the remaining fixation and its isotopic signal [as well as that of atmospheric deposition (32)] was focused in the warm, nutrient-poor surface mixed layer, isolated from the nitrate supply from below. In this scenario, the species' convergence in $\delta^{15}\text{N}$ at the $\delta^{15}\text{N}$ maximum marks the deglacial acceleration in Atlantic N fixation (Fig. 4).

Our bulk sediment $\delta^{15}\text{N}$ record from ODP Site 999 has limited correspondence to our foraminiferal records, possibly showing a deglacial maximum but only a weak (<0.5‰) glacial-to-interglacial decrease that is insignificant in a Student *t* test (Fig. 2C). We suspect that changing inputs of shelf material to Site 999 have altered the relationship of sinking to sedimentary N across the deglaciation. At Site 999, Holocene sediment has ~35% terrigenous material by weight, with ~60% during the LGM (33). Associated with this change, the $\delta^{13}\text{C}$ of organic matter is ~1‰ lower during the LGM (fig. S6), whereas marine POM $\delta^{13}\text{C}$ should have been higher (34). This is consistent with a greater proportion of terrestrial organic matter during the LGM. The sediment organic carbon–total nitrogen ratio is lower in the LGM interval (fig. S6), and distinct trends in this ratio during the LGM and Holocene intervals imply a greater contribution of clay-bound N during the LGM (fig. S7). Both terrestrial organic matter and clay-bound N tend to be low in $\delta^{15}\text{N}$ (35) and would have worked to lower bulk sediment $\delta^{15}\text{N}$ during the last ice age, and thus would have destructively interfered with the oceanic change apparent in the foraminiferal $\delta^{15}\text{N}$ data.

The Site 999 data indicate that N fixation in the Atlantic was low during the LGM, when water column denitrification in the eastern Pacific and Arabian Sea was reduced (Fig. 4) and when sedimentary denitrification was probably also much lower (36). In this context, the LGM-to-Holocene increase in N fixation is consistent with a proposed negative feedback on ocean N content, due to N fixation: Denitrification-driven deficits in N relative to phosphorus (P) stimulate N fixation because N fixers are favored in N-depleted, P-bearing surface waters (37), causing N fixers to restore the ocean N:P ratio toward the ~16:1 "Redfield" ratio of plankton (38, 39).

It has been argued that the micronutrient iron controls or modulates N fixation rate (3, 4). The higher dust flux during the last ice age has been proposed to have caused higher N fixation at that time (3, 4), a hypothesis apparently disproved by

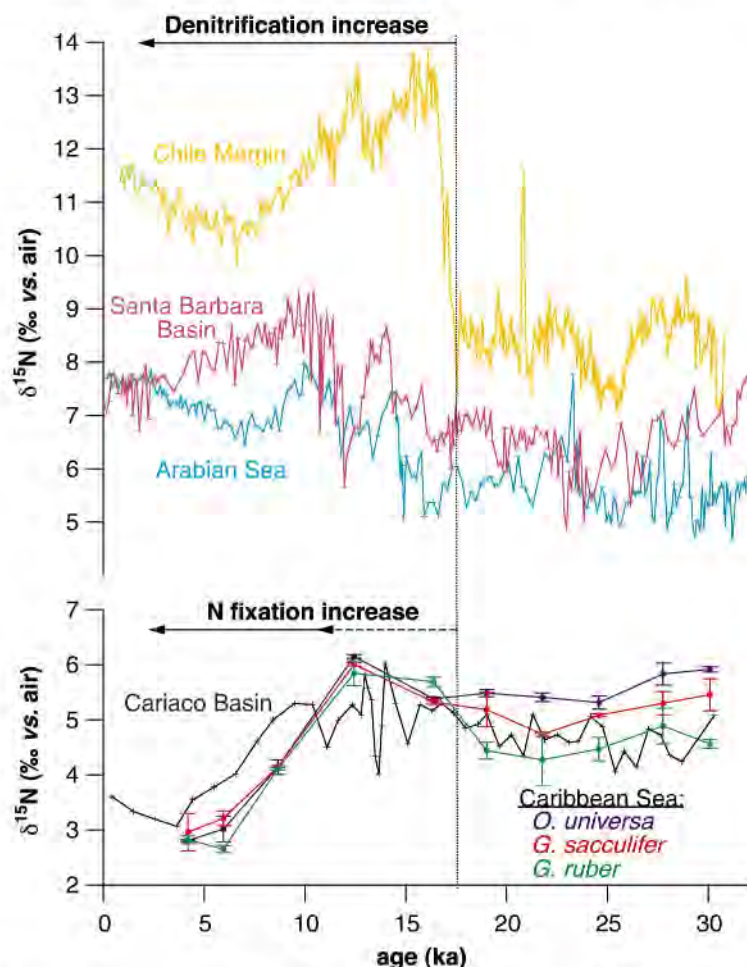


Fig. 4. Comparison of the ODP 999 species-specific foraminifera-bound $\delta^{15}\text{N}$ records for the past 30,000 years with bulk sediment $\delta^{15}\text{N}$ records from each of the major water column denitrification zones and from the nearby Cariaco Basin (27). Denitrification zone records are from the eastern Pacific off Chile (42), the eastern Pacific off California (Santa Barbara Basin) (43), and the Arabian Sea off Oman (44) (fig. S3).

our data for the Atlantic. However, we have not constrained the history of N fixation in the Indo-Pacific, where iron is typically more scarce. Moreover, although our results demonstrate a response from N fixation that works to stabilize the N budget, they do not preclude a glacial-to-interglacial decrease in the N inventory. Reconstruction of N fixation in the other basins and better information about the timing of changes should help to quantify the strength of the N fixation feedback and the limits that it places on the ocean N inventory. Foraminifera-bound N will facilitate this effort.

References and Notes

1. M. A. Altabet, R. Francois, D. W. Murray, W. L. Prell, *Nature* **373**, 506 (1995).
2. R. S. Ganeshram, T. F. Pedersen, S. E. Calvert, D. W. Murray, *Nature* **376**, 755 (1995).
3. P. G. Falkowski, *Nature* **387**, 272 (1997).
4. W. S. Broecker, G. M. Henderson, *Paleoceanography* **13**, 352 (1998).
5. M. B. McElroy, *Nature* **302**, 328 (1983).
6. E. Wada, A. Hattori, *Geochim. Cosmochim. Acta* **40**, 249 (1976).
7. $\delta^{15}\text{N} = \{[(^{15}\text{N}/^{14}\text{N})_{\text{sample}}]/(^{15}\text{N}/^{14}\text{N})_{\text{reference}}\} - 1\} \times 1000\text{‰}$, where the reference is N_2 in air.
8. J. A. Brandes, A. H. Devol, *Geochim. Cosmochim. Acta* **61**, 1793 (1997).
9. C. C. Barford, J. P. Montoya, M. A. Altabet, R. Mitchell, *Appl. Environ. Microbiol.* **65**, 989 (1999).
10. D. Karl et al., *Biogeochemistry* **57–58**, 47 (2002).
11. A. N. Knapp, D. M. Sigman, F. Lipschultz, *Global Biogeochem. Cycles* **19**, GB1018 (2005).
12. A. N. Knapp, P. J. DiFiore, C. Deutsch, D. M. Sigman, F. Lipschultz, *Global Biogeochem. Cycles* **22**, GB3014 (2008).
13. M. A. Altabet, R. Francois, *Global Biogeochem. Cycles* **8**, 103 (1994).
14. K. King Jr., P. E. Hare, *Micropaleontology* **18**, 285 (1972).
15. L. L. Robbins, K. Brew, *Geochim. Cosmochim. Acta* **54**, 2285 (1990).
16. M. A. Altabet, W. B. Curry, *Global Biogeochem. Cycles* **3**, 107 (1989).
17. T. Nakatsuka et al., *Geophys. Res. Lett.* **22**, 2525 (1995).
18. M. E. Uhle et al., *Limnol. Oceanogr.* **44**, 1968 (1990).
19. D. M. Checkley Jr., C. A. Miller, *Deep Sea Res. I* **36**, 1449 (1989).
20. M. E. Uhle, S. A. Macko, H. J. Spero, M. H. Engel, D. W. Lea, *Org. Geochem.* **27**, 103 (1997).
21. J. P. Montoya, E. J. Carpenter, D. G. Capone, *Limnol. Oceanogr.* **47**, 1617 (2002).
22. M. A. Altabet, *Deep Sea Res.* **35**, 535 (1988).
23. See supporting material on Science Online.
24. K. Mintenbeck, U. Jacob, R. Knust, W. E. Arntz, T. Brey, *Deep Sea Res. I* **54**, 1015 (2007).
25. S. J. Kao, K. K. Liu, S. C. Hsu, Y. P. Chang, M. H. Dai, *Atmos. Chem. Phys. Discuss.* **5**, 1017 (2008) and references therein.
26. C. Deutsch, D. M. Sigman, R. C. Thunell, A. N. Meckler, G. H. Haug, *Global Biogeochem. Cycles* **18**, GB4012 (2004).
27. G. H. Haug et al., *Paleoceanography* **13**, 427 (1998).
28. A. N. Meckler et al., *Global Biogeochem. Cycles* **21**, GB4019 (2007).
29. R. C. Thunell, D. M. Sigman, F. Muller-Karger, Y. Astor, R. Varela, *Global Biogeochem. Cycles* **18**, GB3001 (2004).
30. A. C. Ravelo, R. G. Fairbanks, *Paleoceanography* **7**, 815 (1992).
31. M. A. Altabet, *Limnol. Oceanogr.* **34**, 1185 (1989).
32. M. G. Hastings, D. M. Sigman, F. Lipschultz, *J. Geophys. Res.* **108**, 4790 (2003).
33. G. Mora, J. I. Martinez, *Paleoceanography* **20**, PA4013 (2005).
34. J. P. Jasper, J. M. Hayes, *Nature* **347**, 462 (1990).
35. R. E. Sweeney, I. R. Kaplan, *Mar. Chem.* **9**, 145 (1980).
36. J. P. Christensen, *Cont. Shelf Res.* **14**, 547 (1994).
37. D. W. Schindler, *Science* **195**, 260 (1977).
38. A. C. Redfield, *Am. Sci.* **46**, 205 (1958).
39. W. S. Broecker, *Prog. Oceanogr.* **11**, 151 (1982).
40. P. J. DiFiore et al., *J. Geophys. Res.* **111**, C08016 (2006).
41. M. W. Schmidt, H. J. Spero, D. W. Lea, *Nature* **428**, 160 (2004).
42. R. De Pol-Holz et al., *Geophys. Res. Lett.* **33**, L04704 (2006).
43. E. Emmer, R. C. Thunell, *Paleoceanography* **15**, 377 (2000).
44. M. A. Altabet, M. J. Higginson, D. W. Murray, *Nature* **415**, 159 (2002).
45. We thank J. Bernhard and D. McCorkle for supplying surface sediment samples; Y. Wang, M. Coray, and S. Bishop for technical assistance; B. Brunelle for advice; and two anonymous reviewers for comments. Supported by NSF grants ANT-0453680, OCE-9981479, and OCE-0447570 (D.M.S.), OCE-0220776, OCE-0341412, and OCE-0502504 (Y.R.), and OCE-0437366 and OCE-0350794 (J. Bernhard), a Schlanger Ocean Drilling Fellowship (H.R.), BP through the Princeton Carbon Mitigation Initiative, and Deutsche Forschungsgemeinschaft grants (G.H.H.). This research used samples provided by the ODP, which is sponsored by NSF and participating countries under the management of Joint Oceanographic Institutions.

Supporting Online Material

www.sciencemag.org/cgi/content/full/1165787/DC1

Materials and Methods

SOM Text

Figs. S1 to S7

Table S1

References

10 September 2008; accepted 25 November 2008

Published online 18 December 2008;

10.1126/science.1165787

Include this information when citing this paper.

Drosophila Stem Cells Share a Common Requirement for the Histone H2B Ubiquitin Protease Scrawny

Michael Buszczak,* Shelley Paterno, Allan C. Spradling†

Stem cells within diverse tissues share the need for a chromatin configuration that promotes self-renewal, yet few chromatin proteins are known to regulate multiple types of stem cells. We describe a *Drosophila* gene, *scrawny* (*scny*), encoding a ubiquitin-specific protease, which is required in germline, epithelial, and intestinal stem cells. Like its yeast relative UBP10, Scrawny deubiquitylates histone H2B and functions in gene silencing. Consistent with previous studies of this conserved pathway of chromatin regulation, *scny* mutant cells have elevated levels of ubiquitylated H2B and trimethylated H3K4. Our findings suggest that inhibiting H2B ubiquitylation through *scny* represents a common mechanism within stem cells that is used to repress the premature expression of key differentiation genes, including Notch target genes.

Stem cells are maintained in an undifferentiated state by signals that they receive within the niche and are subsequently guided toward particular fates upon niche exit (1). Within embryonic stem (ES) cells and during differentiation, cell state changes are controlled at the level of chromatin by alterations involving higher-order nucleosome packaging and histone tail modifications (2). Polycomb group (PcG)

and Trithorax group (trxG) genes influence key histone methylation events at the promoters of target genes, including H3K27 and H3K4 modifications associated with gene repression and activation, respectively, but few other genes with a specific role in stem cells are known.

Histone H2A and H2B monoubiquitylation play fundamental roles in chromatin regulation, and H2A ubiquitylation has been linked to PcG-

mediated gene repression and stem cell maintenance. The mammalian Polycomb repressive complex 1 (PRC1) component RING1B is an H2A ubiquitin ligase that is required to block the elongation of poised RNA polymerase II on bivalent genes in ES cells (3). Mutations in the PRC1 component BMI-1, which complexes with RING1B, cause multiple types of adult stem cells to be prematurely lost (4). The role of H2B ubiquitylation in stem cells is unclear, however. In yeast, ubiquitylation of histone H2B by the RAD6 and BRE1 ligases controls H3K4 methylation (H3K4me3) (5, 6), a process that requires the polymerase accessory factor PAF1 (7, 8). Conversely, H2B deubiquitylation by the ubiquitin-specific protease (USP) family member UBP10 is required for silencing telomeres, ribosomal DNA, and other loci (9). The *Drosophila* homolog of BRE1, dBRE1, also is needed for H3K4 methylation, which suggests that this

Howard Hughes Medical Institute Research Laboratories, Department of Embryology, Carnegie Institution, Baltimore, MD 21218, USA.

*Present address: University of Texas Southwestern Medical Center, Department of Molecular Biology, Dallas, TX 75390, USA.

†To whom correspondence should be addressed. E-mail: spradling@ciwemb.edu

pathway is conserved (10). Furthermore, the *Drosophila* ubiquitin-specific protease USP7 is part of a complex that selectively deubiquitylates H2B and genetically interacts with PcG mutations (11). Mutations in another USP family member, Nonstop, increase H2B ubiquitylation and cause axon targeting defects in the eye (12).

To gain further insight into the role of H2B ubiquitylation in stem cells, we characterized a *Drosophila* gene, *scrawny* (*scny*) (CG5505), whose encoded USP family protein shares homology with human USP36 and among yeast USPs closely matches UBP10 within the core protease domain (13) (Fig. 1A). Strains bearing *scny* insertions (Fig. 1B), except for a viable green fluorescent protein (GFP) protein trap (CA06690), were female sterile or lethal and proved to be allelic (13) (table S1). Transposon excision or expression of a *scny*-RB cDNA reverts the phenotype of tested alleles. An antibody to SCNY raised against a domain common to all SCNY isoforms recognizes wild type and SCNY-GFP on a Western blot (Fig. 1C). SCNY protein levels in homozygous third-instar larvae are greatly reduced in lethal mutants (Fig. 1C), and SCNY expression is also lower in stem cell-enriched ovarian tissue from adults homozygous for the sterile d06513 allele (Fig. 1D). Consistent with a role in gene silencing, several *scny* mutations act as dominant suppressors of position effect variegation (Fig. 1E and fig. S1).

Further studies strongly suggested that SCNY functions in vivo as an H2B-ubiquitin protease. Recombinant full-length SCNY protein, but not a version bearing a point mutation in the protease domain, efficiently deubiquitylates histone H2B in vitro (Fig. 2A). *scny*^{f01742} homozygous tissue contains levels of Ub-H2B that are elevated at least twofold compared with wild type (Fig. 2B and fig. S2). As expected if Ub-H2B is required for H3K4 methylation, clones of homozygous *scny*^{e00340} mutant cells stain more strongly for H3K4me3 than heterozygous cells (Fig. 2, C and C'). Consistent with a direct rather than an indirect action on Ub-H2B levels, antibodies to SCNY, but not preimmune serum, coimmunoprecipitated H2B from *Drosophila* embryonic nuclear extracts (Fig. 2D). Moreover, epitope-tagged SCNY coimmunoprecipitated *Drosophila* PAF1, but not Cyclin T (or several other tested chromatin proteins), when coexpressed in S2 tissue culture cells (Fig. 2E). Together, these data support the view that SCNY participates in a conserved pathway of chromatin regulation linking H2B ubiquitylation with H3K4me3 methylation. Because the effects of *scny* mutation on Ub-H2B and H3K4me3 are opposite to those of *dbpA* mutation (10), SCNY likely opposes *dbpA* action on H2B, just as UBP10 opposes BRE1 action on H2B in yeast.

Drosophila male and female gonads contain well-characterized germline stem cells (GSCs) that allow the effects of genes on stem cell maintenance to be quantitatively analyzed (14). High levels of *scny* expression were observed in fe-

male and male GSCs using SCNY-GFP (Fig. 3, A and B), and identical staining was observed using anti-SCNY immunofluorescence (fig. S3). SCNY protein resides in cell nuclei and is enriched in nucleoli (fig. S3). In sterile or semi-sterile *scny* mutant adults, the numbers of germline stem cells surrounding the testis hub (Fig. 3C and fig. S4) and within germaria (fig. S5) were clearly reduced. The half-lives of female GSCs bearing clones of three different *scny* alleles were all sharply reduced (Fig. 3D). Later follicular development was also abnormal, which suggests that *scny* continues to function after the stem cell stage. However, previous studies indicate that accelerated GSC loss is a specific phenotype, and hence that *scny* has a preferential requirement in GSCs (1, 15).

A known mechanism of increased GSC loss is the premature activation of differentiation genes. Staining germaria with an antibody specific for multiple sites of histone H3 acetylation (H3-Ac) suggested that *scny* mutation affects the global chromatin organization of GSCs (Fig. 3, E and F). Wild-type GSCs (arrow) contain lower levels of H3-Ac than slightly older germ cells within cysts (Fig. 3E, arrowhead). Presumptive GSCs

located in the GSC niche in *scny* mutants frequently stained more strongly (Fig. 3F), which suggests that they have begun to up-regulate general transcription. Some *scny* GSC-like cells also expressed *bag-of-marbles* (*bam*) (fig. S6), a key cystoblast differentiation gene (1), and GSC-like cells in *scny*^{d06513}; *bam*^{Δ86} mutant females persist in the germarium (fig. S7). However, we could not completely rule out that the observed increases in H3-Ac levels and *bam* expression were a result rather than a cause of the premature differentiation and loss of *scny* GSCs.

To determine whether *scny* is also required in a very different type of stem cell, the epithelial follicle cell stem cell (FSC) (16), we quantitatively analyzed the persistence of individual *scny* mutant FSCs. The half-life of FSCs mutant for *scny*^{l(3)02331} was reduced by a factor of more than 10, while the *scny*^{f01742} mutation also caused a sharp decline (Fig. 4A). However, mutant follicle cells continued to develop normally at later stages (fig. S8). Thus, *scny* is preferentially required to maintain FSCs as well as GSCs.

The largest population of *Drosophila* stem cells are the hundreds of multipotent intestinal stem cells (ISCs) that maintain the adult posterior

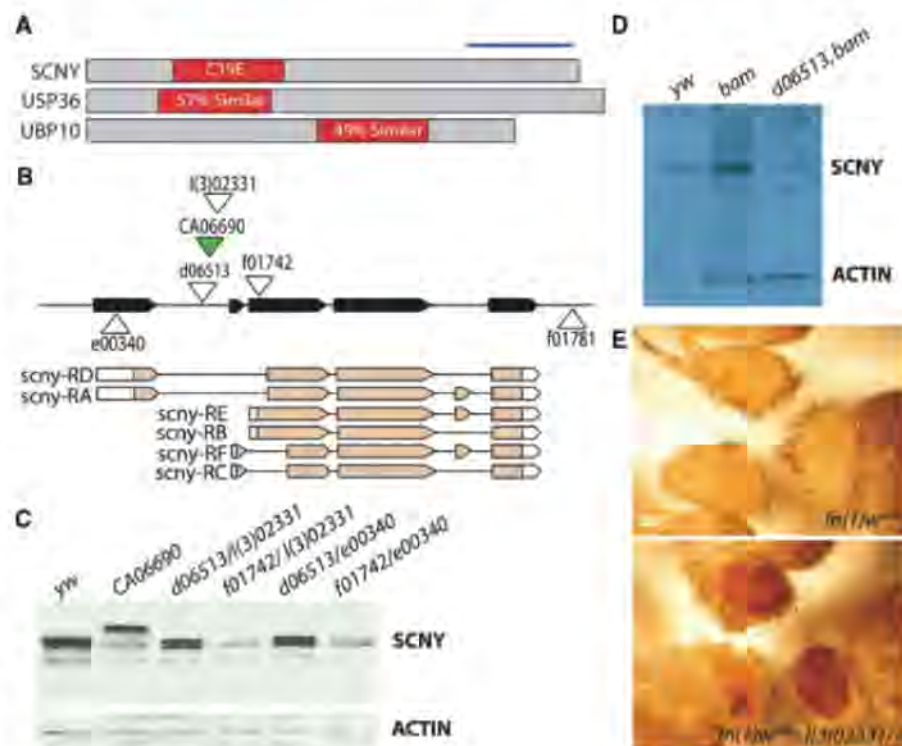


Fig. 1. *scny* encodes a ubiquitin-specific protease family member and functions in gene silencing. (A) Schematic of SCNY protein shows similarity to human USP36 and yeast UBP10 in the conserved protease (C19E) domain (red boxes). Blue bar indicates region used for antibody production. (B) *scny* locus structure showing transposon insertion sites (triangles), including the GFP protein trap CA06690 (green). *scny* transcripts identified by cDNA sequencing are shown below. (C and D) Western blot showing predicted size increase of SCNY in CA06690 and reduced SCNY levels in extracts from third-instar larvae bearing lethal alleles: l(3)02331, e00340, and f01742 (C) and in ovarian tissue from d06513 homozygous adults that were also mutant for *bam* to enrich for germline stem cells (D). (E) *scny*^{l(3)02331} dominantly suppresses *In(1)w^{l(4)h}*-induced position-effect variegation in eye pigmentation (see also fig. S1).

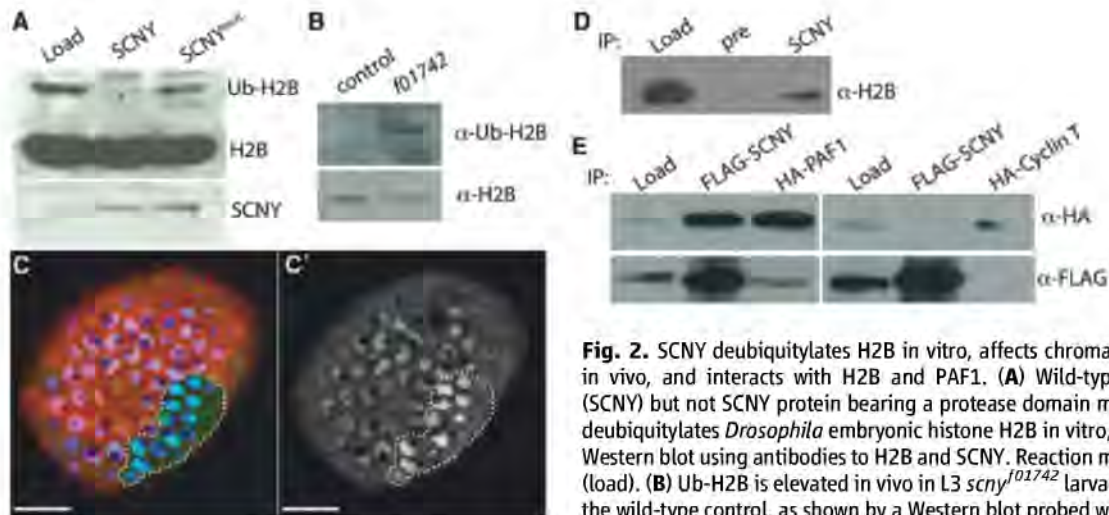


Fig. 2. SCNY deubiquitylates H2B in vitro, affects chromatin modification in vivo, and interacts with H2B and PAF1. **(A)** Wild-type SCNY protein (SCNY) but not SCNY protein bearing a protease domain mutant (SCNY^{mut}) deubiquitylates *Drosophila* embryonic histone H2B in vitro, as visualized by Western blot using antibodies to H2B and SCNY. Reaction mix without SCNY (load). **(B)** Ub-H2B is elevated in vivo in L3 *scny*^{f01742} larvae compared with the wild-type control, as shown by a Western blot probed with antibodies to Ub-H2B (upper panel) normalized by using antibody to H2B (lower panel). **(C)** H3K4me3 (green) is elevated in follicle cell clone mutant for *scny*^{f00340} (dotted line) marked by the absence of LacZ (red). DNA (blue). **(C')** H3mK4 channel alone. Scale bar, 10 μ m. **(D)** Coimmunoprecipitation of histone H2B from nuclear extracts of *Drosophila* embryos (load) with antibody to SCNY (SCNY) but not pre-immune serum (pre). **(E)** Coimmunoprecipitation with SCNY of PAF1, but not of the Cyclin T control, and coimmunoprecipitation with PAF1 of SCNY but not of the Cyclin T control from S2 cell extracts overexpressing these proteins. Starting extract: Load.

midgut (17, 18). ISC's signal to their daughters by Delta-Notch signaling to specify enterocyte versus enteroendocrine cell fate, but the pathway must remain inactive in the ISCs themselves to avoid differentiation (19). Most ISCs (those about to produce enterocytes) express high levels of the Notch ligand Delta, allowing them to be specifically distinguished from other diploid gut cells (19). We found that SCNY-GFP is expressed in ISCs (Fig. 4B, arrow), which suggests that SCNY plays a role in these stem cells as well. Whereas 7-day-old normal adult midguts contain a high density of ISCs, as revealed by Delta staining (Fig. 4C), we found that corresponding tissue from 7-day-old *scny*^{f01742} (fig. S9) or *scny*^{f01742/scny}^{f(3)02331} (Fig. 4D) escaper adults possess very few Delta-positive cells. ISCs are present in near normal numbers at eclosion but are rapidly lost in the mutant adults, which indicates that *scny* is required for ISC maintenance (Fig. 4F).

We suspected that inappropriate Notch pathway activation was responsible for the premature ISC loss in *scny* mutants. *dBre1* mutations strongly reduce Notch signaling, which suggests that Notch target genes are particularly dependent on H2B monoubiquitylation and H3K4 methylation (10). Consequently, *scny* mutations, which have the opposite effects on Ub-H2B and H3K4me3 levels, might up-regulate Notch target genes, stimulating ISCs to differentiate prematurely. We tested this idea by supplementing the food of newly eclosed *scny*^{f01742}/*scny*^{f(3)02331} adults with 8 mM DAPT, a gamma-secretase inhibitor that blocks Notch signaling and phenocopies *Notch* mutation when fed to wild-type animals (17). *scny*^{f01742/scny}^{f(3)02331} DAPT-treated adults remained healthy and the guts of 7-day-old animals still contained many ISCs (Fig. 4E), although not as many as wild type

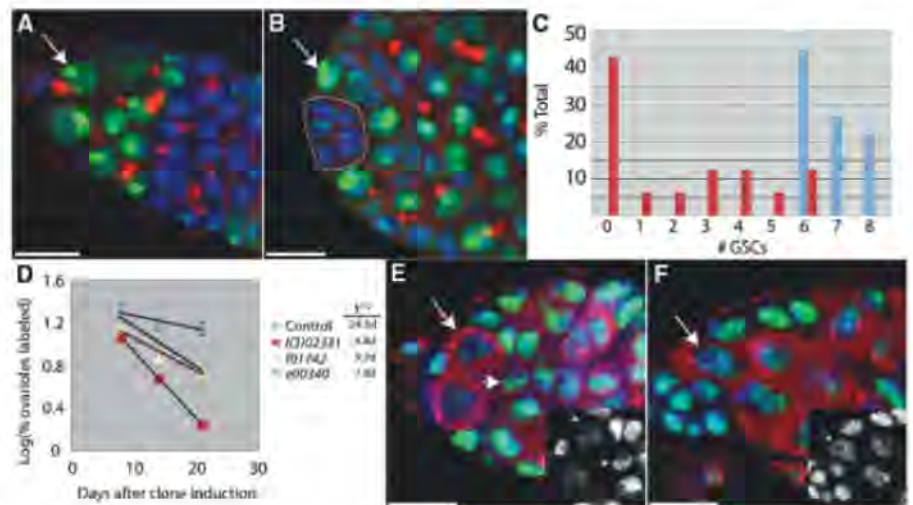


Fig. 3. SCNY maintains germline stem cells. Wide expression of *scny*-GFP (green) during early oogenesis **(A)** and spermatogenesis **(B)**, including GSCs (arrows). SCNY protein localizes to the nucleus and is highly enriched in the nucleolus. HTS (red). Hub (dashed line). **(C)** Reduced GSC number in 1- to 2-day-old adult *scny*^{d06513} testes (red bars) compared with wild type (blue bars). **(D)** Reduced half-life (*t*^{1/2}) of female GSCs for *scny*. **(E)** GSCs (arrow) have lower global levels of acetylated histone H3 (green) than cyst cells (arrowhead). Vasa (red). Inset: Ac-H3 channel. **(F)** GSC-like anterior germ cells in *scny*^{d06513} germaria have global Ac-H3 (green) levels more comparable to cyst cells. VASA (red). Inset: Ac-H3 channel. Scale bars, 10 μ m.

(Fig. 4F). Tumors like those produced in wild-type animals fed DAPT (17, 18) were not observed. Thus, in these animals, endogenous stem cell loss can be slowed by drug treatment.

Our experiments provide strong evidence that a pathway involving the ubiquitin protease Scrawny and the ubiquitin ligase dBRE1 controls the levels of Ub-H2B and H3K4me3 at multiple target sites in the *Drosophila* genome. Although, other ubiquitin proteases also act on Ub-H2B in *Drosophila* (11, 12), the direct interaction be-

tween SCNY and H2B and the strong effects of *scny* mutations argue that it plays an essential, direct role in silencing genomic regions critical for cellular differentiation, including Notch target genes. SCNY interacts with the RNA polymerase accessory factor complex component, PAF1. Up-regulation of H2B ubiquitylation and H3 methylation in yeast is mediated by the PAF1 complex and is associated with elongating RNA Pol II (7, 8, 20). *Drosophila* PAF1 is required for normal levels of H3K4me3 at the *hsp70* gene (21),

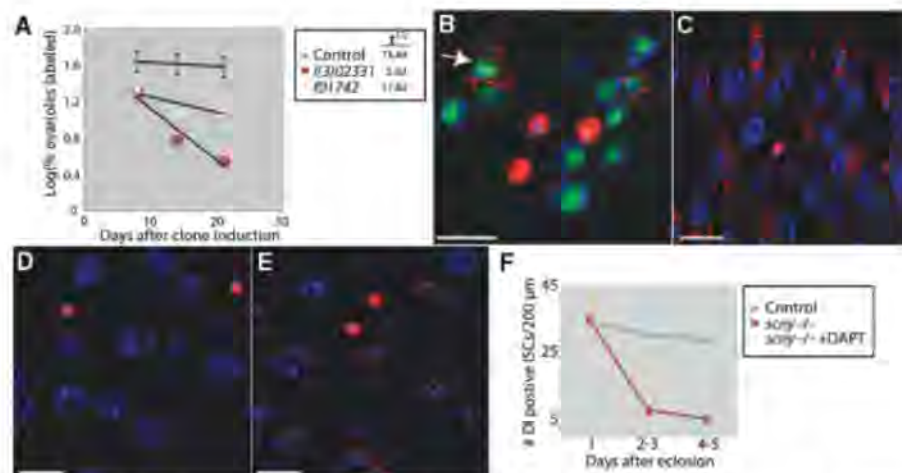


Fig. 4. SCNY maintains FSCs and ISCs. (A) Reduced half-life ($t^{1/2}$) of FSCs mutant for *scny*. (B) SCNY-GFP (green) is highly expressed in nuclei and nucleoli of ISCs (arrow, contains cytoplasmic Delta) and in developing enterocytes (lacks Delta), but is low in enteroendocrine cells (contain nuclear Prospero). (C to F) ISCs (red, cytoplasmic) in 7-day-old wild-type adult midguts (C) are lost prematurely in *scny*^{f01742}/*scny*^{l3/02331} flies (D) but not in *scny*^{f01742}/*scny*^{l3/02331} adults whose food was supplemented with the Notch inhibitor DAPT (8 mM) (E). (F) Quantitation of the midgut ISC density as a function of time in wild type (blue), *scny*^{f01742}/*scny*^{l3/02331} (red), and *scny*^{f01742}/*scny*^{l3/02331} + 8 mM DAPT (yellow). In (B) to (E), Prospero (red, nuclear) marks enteroendocrine cells, and Delta (red, cytoplasmic) mark ISCs. DNA (blue). Scale bars, 10 µm.

and another PAF1 complex member, RTF1, is needed for H3K4 methylation and Notch target gene expression (22). Indeed, the pathway connecting Ub-H2B, H3K4me3, and gene silencing appears to be conserved in organisms as distant as *Arabidopsis* (23). A human protein closely related to SCNY, USP36, is overexpressed in ovarian cancer cells (24), and our results suggest that it may act as an oncogene by suppressing differentiation.

Above all, our experiments indicate that SCNY-mediated H2B deubiquitylation is required to maintain multiple *Drosophila* stem cells, including progenitors of germline, epithelial, and endodermal lineages. In ES cells, and presumably in adult stem cells, many differentiation genes contain promoter-bound, arrested RNA Pol II and are associated with Polycomb group proteins (2, 3). We envision that, in the niche environment, SCNY activity overrides that of dBRE1, keeping levels of Ub-H2B (and hence H3K4me3) low at key differentiation genes (fig. S10). Upon exit from the niche, the balance of signals shifts to favor H2B ubiquitylation, H3K4 trimethylation, and target gene activation. Thus, the control of H2B ubiquitylation, like H2A ubiquitylation, plays a fundamental interactive role in maintaining the chromatin environment of the stem cell state.

References and Notes

1. S. J. Morrison, A. C. Spradling, *Cell* **132**, 598 (2008).
2. M. Spivakov, A. G. Fisher, *Nat. Rev. Genet.* **8**, 263 (2007).
3. J. K. Stock et al., *Nat. Cell Biol.* **9**, 1428 (2007).
4. M. E. Valk-Lingbeek, S. W. Bruggeman, M. van Lohuizen, *Cell* **118**, 409 (2004).
5. Z. W. Sun, C. D. Allis, *Nature* **418**, 104 (2002).

6. J. Dover et al., *J. Biol. Chem.* **277**, 28368 (2002).
7. A. Wood, J. Schneider, J. Dover, M. Johnston, A. Shilatifard, *J. Biol. Chem.* **278**, 34739 (2003).
8. H. H. Ng, S. Dole, K. Struhl, *J. Biol. Chem.* **278**, 33625 (2003).

9. R. G. Gardner, Z. W. Nelson, D. E. Gottschling, *Mol. Cell. Biol.* **25**, 6123 (2005).
10. S. Bray, H. Musisi, M. Bienz, *Dev. Cell* **8**, 279 (2005).
11. J. A. van der Knaap et al., *Mol. Cell* **17**, 695 (2005).
12. V. M. Weake et al., *EMBO J.* **27**, 394 (2008).
13. Materials and methods are available as supporting material on Science Online.
14. T. Xie, A. C. Spradling, *Cell* **94**, 251 (1998).
15. H. Lin, A. C. Spradling, *Development* **124**, 2463 (1997).
16. T. G. Nystul, A. C. Spradling, *Cell Stem Cell* **1**, 277 (2007).
17. B. Ohlstein, A. C. Spradling, *Nature* **439**, 470 (2006).
18. C. A. Micchelli, N. Perrimon, *Nature* **439**, 475 (2006).
19. B. Ohlstein, A. C. Spradling, *Science* **315**, 988 (2007).
20. T. Xiao et al., *Mol. Cell. Biol.* **25**, 637 (2005).
21. K. Adelman et al., *Mol. Cell. Biol.* **26**, 250 (2006).
22. K. Tenney et al., *Proc. Natl. Acad. Sci. U.S.A.* **103**, 11970 (2006).
23. H. Wang et al., *Nature* **431**, 873 (2004).
24. J. Li et al., *Int. J. Med. Sci.* **5**, 133 (2008).
25. This work was supported by the Howard Hughes Medical Institute. M.B. was supported in part by American Cancer Society Fellowship PF-04-022-01-CSM. We thank D. McKearin, M. Oren, and the Bloomington Stock Center for reagents; B. Ohlstein for helpful advice and for assisting with the initial characterization of the *scny* midgut phenotype; and T. Nystul for critical reading of the manuscript.

Supporting Online Material

www.sciencemag.org/cgi/content/full/1165678/DC1
Materials and Methods
Figs. S1 to S10
Table S1
References

9 September 2008; accepted 10 November 2008
Published online 27 November 2008;
10.1126/science.1165678
Include this information when citing this paper.

The Aryl Hydrocarbon Nuclear Translocator Alters CD30-Mediated NF-κB-Dependent Transcription

Casey W. Wright^{1*} and Colin S. Duckett^{1,2†}

Expression and signaling of CD30, a tumor necrosis factor receptor family member, is up-regulated in numerous lymphoid-derived neoplasias, most notably anaplastic large-cell lymphoma (ALCL) and Hodgkin's lymphoma. To gain insight into the mechanism of CD30 signaling, we used an affinity purification strategy that led to the identification of the aryl hydrocarbon receptor nuclear translocator (ARNT) as a CD30-interacting protein that modulated the activity of the RelB subunit of the transcription factor nuclear factor κB (NF-κB). ALCL cells that were deficient in ARNT exhibited defects in RelB recruitment to NF-κB-responsive promoters, whereas RelA recruitment to the same sites was potentiated, resulting in the augmented expression of these NF-κB-responsive genes. These findings indicate that ARNT functions in concert with RelB in a CD30-induced negative feedback mechanism.

The activation of the transcription factor nuclear factor κB (NF-κB) as a consequence of signaling from the tumor necrosis factor receptor (TNFR) family member CD30 accounts for many of the physiological phenomena regulated by CD30 (1, 2). For example, CD30 signaling contributes to the tumorigenesis of Hodgkin's lymphoma (HL) cells by increasing NF-κB ac-

tivity (3, 4). TNFR-associated factor (TRAF) proteins are important for CD30-mediated NF-κB activation (5–8), but other proteins may also participate in the regulation of CD30 signaling. Furthermore, aspects of NF-κB regulation remain enigmatic, especially regarding the mechanisms that control NF-κB transactivation at the chromatin level (9). Therefore, in an attempt to

identify signaling intermediates between CD30 and NF- κ B activity, we conducted a biochemical affinity screen (10, 11) in Karpas 299, a cell line exhibiting inducible CD30 signaling that was derived from a patient with anaplastic large-cell lymphoma (12). Analysis of the biochemically purified products revealed the aryl hydrocarbon receptor nuclear translocator (ARNT; also known as hypoxia-inducible factor 1- β) as a CD30-interacting protein (Fig. 1 and fig. S1). ARNT is a transcription factor that is integral to the regulation of xenobiotic and hypoxic responses (13–15).

We cloned the coding sequence of ARNT from Karpas 299 cells and used it to derive nested deletions of ARNT (fig. S1C) (16). We tested three major regions of ARNT, the basic helix-

loop-helix (bHLH) domain, the period-ARNT-single-minded (PAS) domain (a protein-protein interface), and the transactivation domain, for their ability to bind the cytoplasmic region of CD30. Precipitation analysis of the different ARNT constructs with a tagged form of CD30, in which the cytoplasmic domain of CD30 was fused downstream of glutathione-S-transferase (GST), confirmed that ARNT interacted with CD30 through the PAS and transactivation domains (Fig. 1A). Thus, at least two regions of ARNT are responsible for its binding to the cytoplasmic tail of CD30, and other regions of ARNT appear to negatively regulate this binding (Fig. 1A).

To explore the spatial and temporal colocalization of CD30 and ARNT, we surface-labeled Karpas 299 cells, expressing either green fluorescent protein (GFP) or ARNT-GFP, with a CD30 antibody conjugated to phycoerythrin (anti-CD30-PE). Confocal microscopy showed that CD30 was predominantly localized to the plasma membrane 3 hours after stimulation with anti-CD30-PE (Fig. 1B and fig. S2), whereas ARNT was localized to the nucleus, as expected, and no colocalization was detected with CD30 at the

plasma membrane. In contrast, 24 hours after stimulation, all of the originally surface-labeled CD30 was found in the cytoplasm, which was consistent with a previous report (17). ARNT-GFP was also detected in the cytoplasm at this later time point, in which it colocalized with internalized CD30. A panel of classical NF- κ B-responsive genes showed increased transcription when CD30 was labeled with anti-CD30-PE to a level comparable with that in cells stimulated for 10 min with the CD30 ligand (CD30L) (Figs. 1C and 2A), ensuring that anti-CD30-PE induces CD30 signaling. Thus, the association of ARNT with CD30 appears to occur in the cytoplasm late in CD30 signaling.

The interaction of ARNT with CD30 was greatly impaired if the last 36 amino acids of CD30 were deleted (Fig. 1C). The sequences for TRAF binding are within these 36 amino acids of CD30, and the ability to recruit the TRAF proteins is required for full NF- κ B activation (8), which suggests that ARNT might influence CD30-mediated NF- κ B activity. We investigated this possibility with two small interfering RNA (siRNA) oligonucleotides that

¹Department of Pathology, University of Michigan Medical School, Ann Arbor, MI 48109, USA. ²Department of Internal Medicine, University of Michigan Medical School, Ann Arbor, MI 48109, USA.

*Present address: College of Pharmacy, University of Texas at Austin, 1 University Station A1915, Austin, TX 78712, USA. †To whom correspondence should be addressed. E-mail: colind@umich.edu

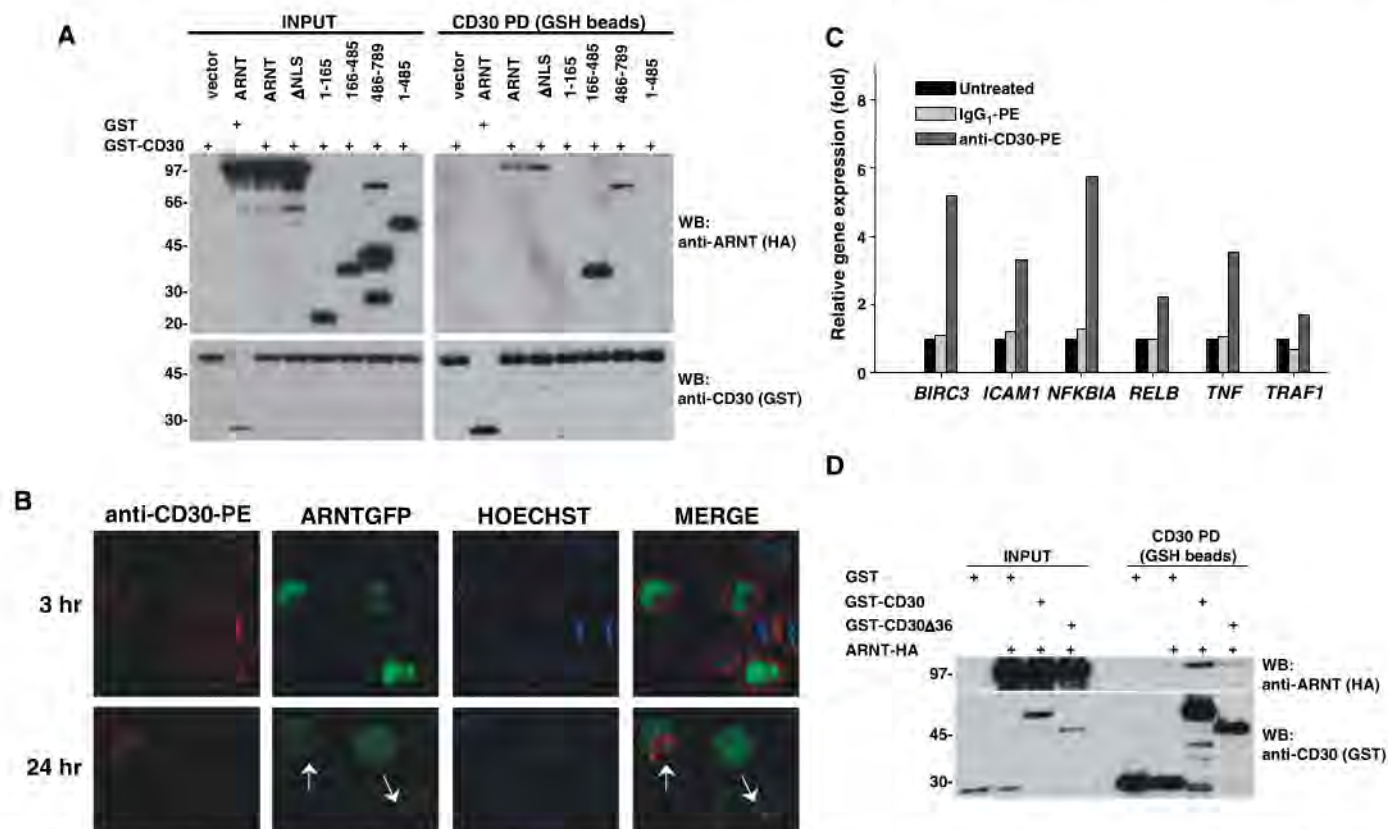


Fig. 1. Association of ARNT with CD30. **(A)** Two regions of ARNT mediate the interaction with CD30. HEK293 cells were transfected with plasmids for the expression of combinations of GST-CD30 and HA-tagged versions of the mutants depicted in fig. S1C. CD30 pull-downs (PD) were performed with GSH-sepharose, and the eluates were probed for ARNT (HA) and CD30 (GST). **(B)** Localization of CD30 with ARNT in the cytoplasm late in CD30 signaling. Karpas 299 cells expressing ARNT-GFP were labeled with anti-CD30-PE and analyzed by use of confocal microscopy at 3 and 24 hours. **(C)** Anti-CD30-PE is an agonistic antibody that stimulates CD30-mediated NF- κ B activation.

Karpas 299 cells were treated as indicated for 3 hours. Total RNA was isolated and subjected to reverse transcription followed by analysis with real-time PCR. All samples were normalized to control unstimulated cells. **(D)** CD30 associates with ARNT through the cytoplasmic TRAF-binding domain. HEK293 cells were transfected with plasmids for the expression of ARNT-HA and either GST, GST-CD30, or GST-CD30 Δ 36. Lysates were precipitated with GSH-sepharose and the eluates were probed for ARNT (HA) and CD30 (GST). **(A)**, **(B)**, and **(D)** are representative of one individual experiment that was repeated three times. **(C)** represents two independent experiments performed in triplicate.

suppress ARNT expression in Karpas 299 cells. After ARNT suppression, Karpas 299 cells were exposed to either a 10-min CD30 stimulation by the physiological CD30 ligand (Fig. 2A) or a continuous suboptimal dose of agonistic antibody to the type 2 TNFR (TNFR2) (Fig. 2B), a TNFR family member closely related to CD30. Real-time polymerase chain reaction (PCR) analysis was used to measure receptor-dependent transcriptional activity from the endogenous NF- κ B-responsive genes *intercellular adhesion molecule-1* (*ICAM1*), *RelB* (*RELB*), and *NF- κ B inhibitor alpha* (*I κ B α* ; *NFKBIA*) (Fig. 2). In cells in which ARNT was suppressed, the CD30-induced increase in mRNA abundance from NF- κ B-responsive genes was two- to threefold greater than that in control cells (Fig. 2A). A similar trend was observed for a TNFR2 signal in the absence of ARNT. Although basal levels of NF- κ B activity were increased before a TNFR2 signal in cells where ARNT was suppressed, there was a substantial augmentation in NF- κ B activation in ARNT-suppressed cells after a TNFR2 signal; however, we cannot rule out the possibility of a TNFR2-

independent role for ARNT in NF- κ B regulation (Fig. 2B). The TNFR2-dependent activation of NF- κ B exhibited a characteristic biphasic activation, as previously described (18, 19).

Stimulation of CD30 had a minimal effect on basal transcription from genes regulated by ARNT, including cytochrome P450 (*CYP1A1*) and the facilitated glucose transporter (*SLC2A1*) (Fig. 2), which suggests that the observed increases in NF- κ B-induced transcription appear to result from the loss of ARNT and not a change in ARNT-responsive gene transcription. Furthermore, for genes considered ARNT-responsive, the loss of ARNT resulted in decreased expression, even under normoxic conditions, which indicates that the observed augmentation in NF- κ B transactivation was not the result of a general increase in transcription.

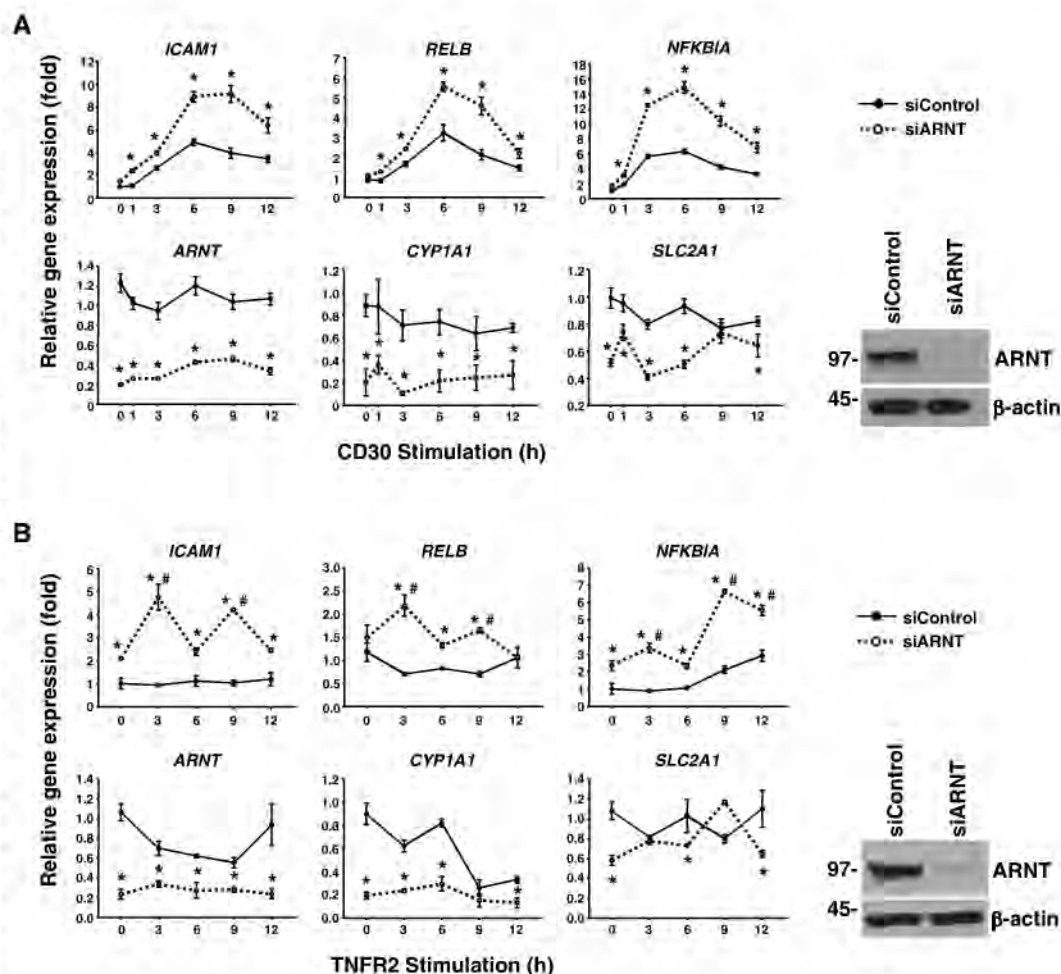
To uncover the regulatory control point of ARNT in the NF- κ B pathway, nuclear extracts from control-suppressed and ARNT-suppressed Karpas 299 cells were analyzed by use of an electrophoretic mobility shift assay (EMSA). Suppression of ARNT resulted in an altered migration

pattern of the NF- κ B-DNA probe complex after CD30 stimulation (Fig. 3A), which suggests that ARNT is a component of the NF- κ B complex or directs the binding of one or more NF- κ B subunits, or both. To address this, each NF- κ B subunit was fused with GST, individually coexpressed with hemagglutinin (HA)-tagged ARNT in human embryonic kidney (HEK)-293 cells and precipitated with (reduced form) glutathione (GSH)-sepharose. ARNT did not interact with GST-RelA or GST-p50 but was precipitated with GST-RelB and to a lesser extent associated with GST-c-Rel and GST-p52 (Fig. 3B). The interaction of RelB with ARNT was confirmed by coimmunoprecipitation of the endogenous proteins from Karpas 299 nuclear extracts after a 10-min treatment with CD30L. The association of RelB with ARNT in the nucleus correlated with CD30 stimulation (Fig. 3C). We propose that ARNT may bind to RelB and direct the DNA binding of RelB-containing complexes during a CD30 signal.

The role of the RelB-ARNT interaction was further examined through studies in HEK293 cells by expressing different combinations of ARNT,

Fig. 2. Augmented CD30-mediated

activation of NF- κ B after the suppression of ARNT. siControl or siARNT oligonucleotides were introduced into Karpas 299 cells, followed by a (A) 10-min exposure to CD30L or (B) continuous exposure to a suboptimal concentration of agonistic antibody to TNFR2. Cells were collected at the times indicated; total RNA was isolated and subjected to reverse transcription followed by quantitative real-time PCR analysis for the indicated genes. All samples were normalized to control unstimulated cells. The results represent the mean \pm SD of three independent experiments performed in triplicate. Statistical analyses were performed with a two-way analysis of variance followed by Student-Newman-Keuls post hoc analysis. (A) The expression of the NF- κ B-responsive genes *ICAM1*, *RELB*, and *NFKBIA* (*I κ B α*) was increased in ARNT-suppressed cells as compared with that in siControl cells at each time point after CD30 stimulation (* P < 0.01). (B) ARNT suppression increased basal and TNFR-induced expression of *ICAM1* and *NFKBIA* at each time point (* P < 0.01). Basal expression of *RELB* was not increased, but expression was increased at 3 to 9 hours after TNFR2 stimulation in cells in which ARNT was depleted (* P < 0.01). In ARNT-depleted cells, expression of *ICAM1* and *RELB* was increased at 3 and 9 hours after TNFR2 stimulation as compared with that in ARNT-suppressed cells at time zero (#, P < 0.01). Similarly, expression of *NFKBIA* in ARNT-suppressed cells was increased at 3, 9, and 12 hours after TNFR2 stimulation as compared with that in ARNT-suppressed cells at time 0 (#, P < 0.01). In (A) and



(B), the basal expression of the ARNT-responsive genes *CYP1A1* and *SLC2A1* was significantly reduced in the absence of ARNT (* P < 0.01). To confirm the suppression of ARNT, cDNA was analyzed (ARNT graph; * P < 0.01), and lysates from unstimulated samples were probed for ARNT and β -actin.

Fig. 3. ARNT as a NF- κ B-associated coregulator. (A) ARNT modulates NF- κ B DNA binding potential. Karpas 299 cells were transfected with either siControl or siARNT. Nuclear extracts were probed for ARNT to ensure suppression and analyzed by means of EMSA. The asterisk denotes the altered migration of the NF- κ B-DNA complex. (B and C) Binding of ARNT to the NF- κ B subunit RelB. (B) Lysates from HEK293 cells transfected with the indicated expression plasmids were precipitated with GSH-sepharose. Inputs were probed for ARNT (HA) or the NF- κ B subunits (GST), and the elutions were probed for ARNT. (C) Nuclear extracts from Karpas 299 cells were prepared at the indicated times, after a 10-min CD30L exposure. Immunoprecipitations were performed with a RelB or control antibody and eluates were probed for ARNT. (D) Effect of ARNT on NF- κ B subunit binding to DNA. Nuclear extracts prepared from HEK293 cells transfected with the indicated plasmids were analyzed by means of EMSA. The binding of RelA-p50 complexes was 1.07 times greater in the presence of ARNT, whereas the binding of RelB-p50 complexes was 1.3 times greater in the presence of ARNT as determined by densitometry analysis. (E) Effect of ARNT on RelB-p50 binding to DNA. RelB and p50 were expressed with a control vector or 0.5 or 1 μ g of vector encoding ARNT in HEK293 cells. Nuclear extracts were prepared and analyzed by use of EMSA. The expression of ARNT increased the binding of RelB-p50 complexes by 1.5-fold (0.5 μ g of ARNT) and 2-fold (1 μ g of ARNT), as determined by densitometry analysis. All experiments were performed at least three times, and representative data are shown.

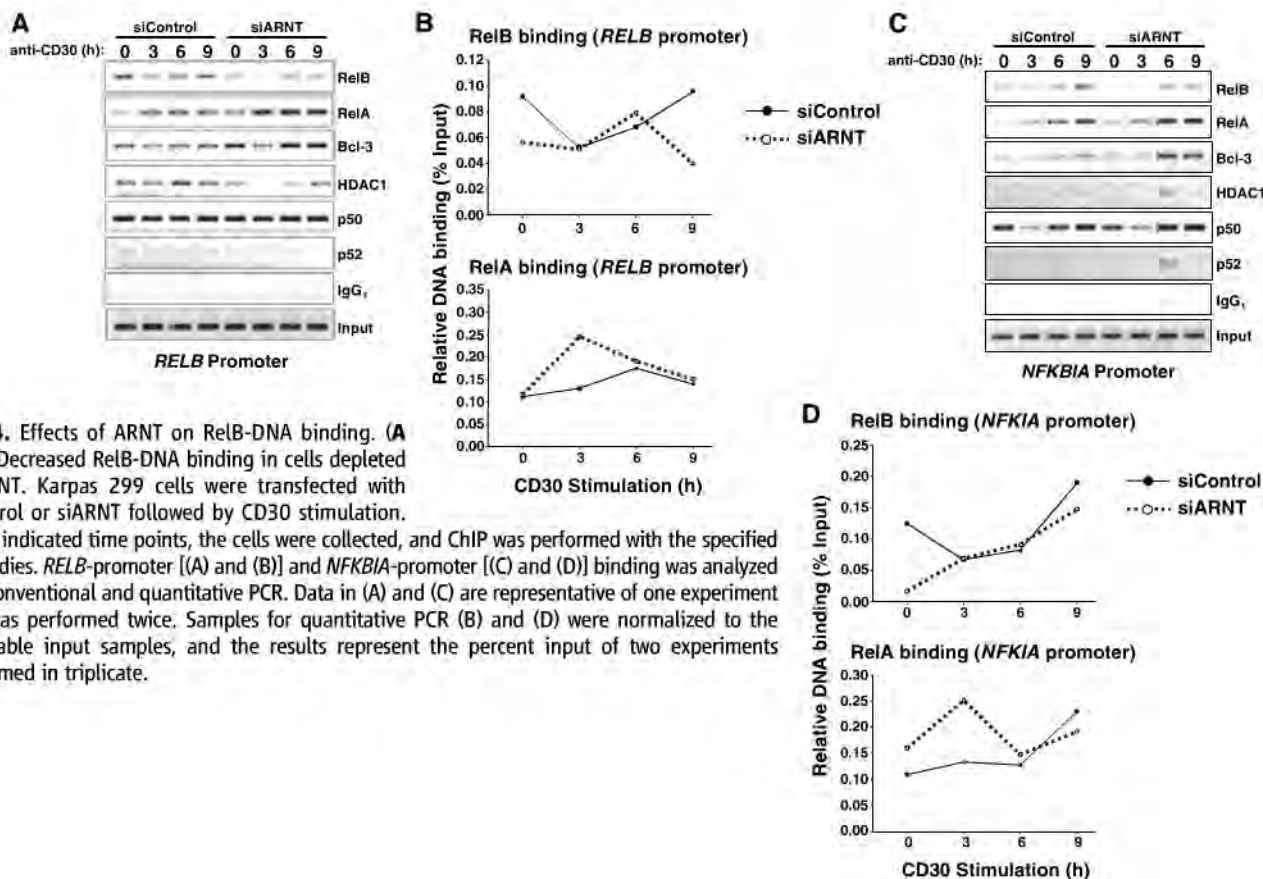
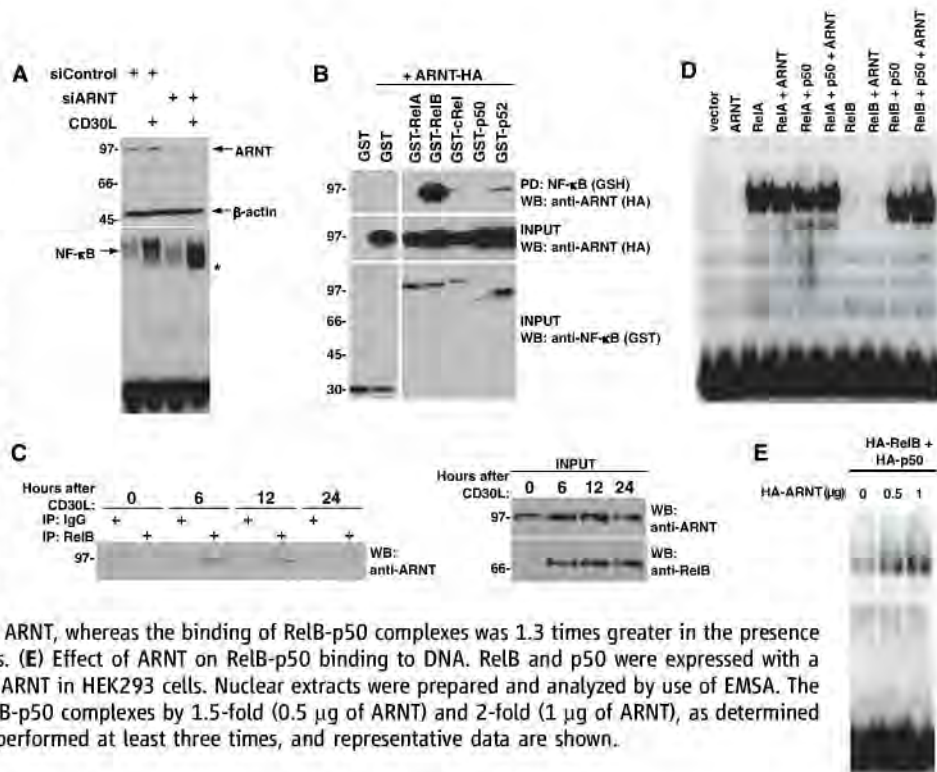


Fig. 4. Effects of ARNT on RelB-DNA binding. (A to D) Decreased RelB-DNA binding in cells depleted of ARNT. Karpas 299 cells were transfected with siControl or siARNT followed by CD30 stimulation. At the indicated time points, the cells were collected, and ChIP was performed with the specified antibodies. *RELB*-promoter [(A) and (B)] and *NFKBIA*-promoter [(C) and (D)] binding was analyzed with conventional and quantitative PCR. Data in (A) and (C) are representative of one experiment that was performed twice. Samples for quantitative PCR (B) and (D) were normalized to the applicable input samples, and the results represent the percent input of two experiments performed in triplicate.

RelA, RelB, and p50. Nuclear extracts isolated from these cells and analyzed with EMSA showed that the binding of ectopically expressed ARNT to a NF- κ B-specific probe was not detected, and ARNT had little effect on the binding of RelA homodimers or RelA-p50 heterodimers (Fig. 3D). RelB did not bind to the NF- κ B probe when expressed alone, as expected, and the addition of ARNT did not change the amount of RelB homodimer binding. The expression of ARNT with RelB-p50 heterodimers did result in a slight enhancement of binding (Fig. 3D), and coexpressing ARNT with RelB-p50 at two different concentrations revealed a dose-dependent enhancement of RelB-p50 DNA binding (Fig. 3E). These data raise the possibility that the presence of ARNT facilitated the binding of RelB-containing complexes to DNA.

RelB has both transcriptional promoting and repressing activity, depending on the signaling context or cell type (20–23). Our observations (Figs. 2 and 3) suggest that RelB is a repressor of CD30-mediated canonical NF- κ B-responsive genes. We thus examined the binding pattern of endogenous NF- κ B subunits to the promoters of the *RELB* and *NFKB1A* genes by use of chromatin immunoprecipitation (ChIP). RelB was present on the promoters before a CD30 signal was initiated and was subsequently replaced by RelA 3 hours after CD30 stimulation [Fig. 4, A

to D, control siRNA (siControl)]. Histone deacetylase 1 (HDAC1), a corepressor, bound to the *RELB* promoter in a pattern similar to that of the RelB subunit, which suggests that RelB might recruit HDAC1 to effectively repress RelA-p50 activity (Fig. 4A and fig. S4A). To test whether the augmentation of NF- κ B transcription observed in the absence of ARNT (Fig. 2) was a direct result of a decreased RelB binding to NF- κ B-responsive promoters, promoter binding was analyzed in ARNT-suppressed Karpas 299 cells. When ARNT was depleted, the amount of RelB bound to promoters before CD30 stimulation was decreased. Furthermore, the binding of RelB to the indicated promoters was diminished at later time points [Fig. 4, A and C, ARNT siRNA (siARNT)] when, in control cells, CD30-dependent transcription would normally begin to decline (Fig. 2). The decrease in RelB-promoter binding, in cells in which ARNT was suppressed, was not a function of destabilized RelB protein or defective RelB translocation to the nucleus (fig. S3). Although RelB-promoter binding was decreased in ARNT-suppressed cells, RelA appeared at the promoters sooner and in higher amounts. This was concomitant with the enhanced recruitment of the coactivator Bcl-3 (Fig. 4, A and C, and fig. S4, A and B), whereas in the case of the *RELB* promoter, the recruitment of HDAC1 was diminished (Fig. 4A and fig. S4A). These data support

the observed increase in transcription of NF- κ B-responsive genes in CD30-stimulated cells lacking ARNT (Fig. 2) and reveal the role of ARNT as a possible cofactor of RelB-repressive function.

How NF- κ B selectively binds and is regulated at κ B sites in target promoters is an area of intense interest but remains incompletely understood (24–28). We observed a repressive function for RelB in a TNFR pathway and provided evidence for a role of ARNT in regulation of DNA binding by RelB-containing complexes (Fig. 5). These findings provide a possible mechanistic basis for how ARNT might be redirected from TNFR superfamily signaling by a xenobiotic or hypoxic insult toward a transcriptional role, thus resulting in altered NF- κ B activity.

References and Notes

1. A. Younes, B. B. Aggarwall, *Cancer* **98**, 458 (2003).
2. R. Chiarle *et al.*, *Clin. Immunol.* **90**, 157 (1999).
3. R. Horie *et al.*, *Oncogene* **21**, 2493 (2002).
4. R. Horie *et al.*, *Cancer Cell* **5**, 353 (2004).
5. S. Y. Lee *et al.*, *Proc. Natl. Acad. Sci. U.S.A.* **93**, 9699 (1996).
6. S. Aizawa *et al.*, *J. Biol. Chem.* **272**, 2042 (1997).
7. L. M. Boucher, L. E. M. Marengere, Y. Lu, S. Thukral, T. W. Mak, *Biochem. Biophys. Res. Commun.* **233**, 592 (1997).
8. C. S. Duckett, R. W. Gedrich, M. C. Gilfillan, C. B. Thompson, *Mol. Cell. Biol.* **17**, 1535 (1997).
9. M. S. Hayden, S. Ghosh, *Cell* **132**, 344 (2008).
10. G. Rigaut *et al.*, *Nat. Biotechnol.* **17**, 1030 (1999).
11. E. Burstein *et al.*, *J. Biol. Chem.* **280**, 22222 (2005).
12. C. Wolke *et al.*, *Int. J. Mol. Med.* **17**, 275 (2006).
13. R. J. Kewley, M. L. Whitelaw, A. Chapman-Smith, *Int. J. Biochem. Cell Biol.* **36**, 189 (2004).
14. E. Matthei, J. V. Schmidt, D. Baunoch, C. A. Bradfield, M. C. Simon, *Nature* **386**, 403 (1997).
15. N. S. Chandel, M. C. Simon, *Cell Death Differ.* **15**, 619 (2008).
16. Materials and methods are available as supporting material on Science Online.
17. M. S. Sutherland *et al.*, *J. Biol. Chem.* **281**, 10540 (2006).
18. D. E. Nelson *et al.*, *Science* **306**, 704 (2004).
19. J. E. Thompson, R. J. Phillips, H. Erdjument-Bromage, P. Tempst, S. Ghosh, *Cell* **80**, 573 (1995).
20. D. S. Weih, Z. B. Yilmaz, F. Weih, *J. Immunol.* **167**, 1909 (2001).
21. F. Weih *et al.*, *Cell* **80**, 331 (1995).
22. Y. Xia *et al.*, *Mol. Cell. Biol.* **19**, 7688 (1999).
23. B. K. Yoza, J. Y. Hu, S. L. Cousart, L. M. Forrest, C. E. McCall, *J. Immunol.* **177**, 4080 (2006).
24. J. Wang, H. An, M. W. Mayo, A. S. Baldwin, W. G. Yarbrough, *Cancer Cell* **12**, 239 (2007).
25. F. Wan *et al.*, *Cell* **131**, 927 (2007).
26. N. D. Perkins, *Nat. Rev. Mol. Cell Biol.* **8**, 49 (2007).
27. L. F. Chen, W. C. Greene, *Nat. Rev. Mol. Cell Biol.* **5**, 392 (2004).
28. G. N. Maine, X. Mao, C. M. Komarck, E. Burstein, *EMBO J.* **26**, 436 (2007).
29. We thank E. Burstein and members of the Duckett laboratory for helpful discussions, C. Duvauchelle for assistance with statistical analyses, and A. Savory for assistance with the manuscript. This work was supported by NIH grant R01 GM067827 and an award from the Cancer Research Fund of the University of Michigan Comprehensive Cancer Center to C.S.D.

Supporting Online Material

www.sciencemag.org/cgi/content/full/323/5911/251/DC1
Materials and Methods
Figs. S1 to S4
References

7 July 2008; accepted 14 November 2008
10.1126/science.1162818

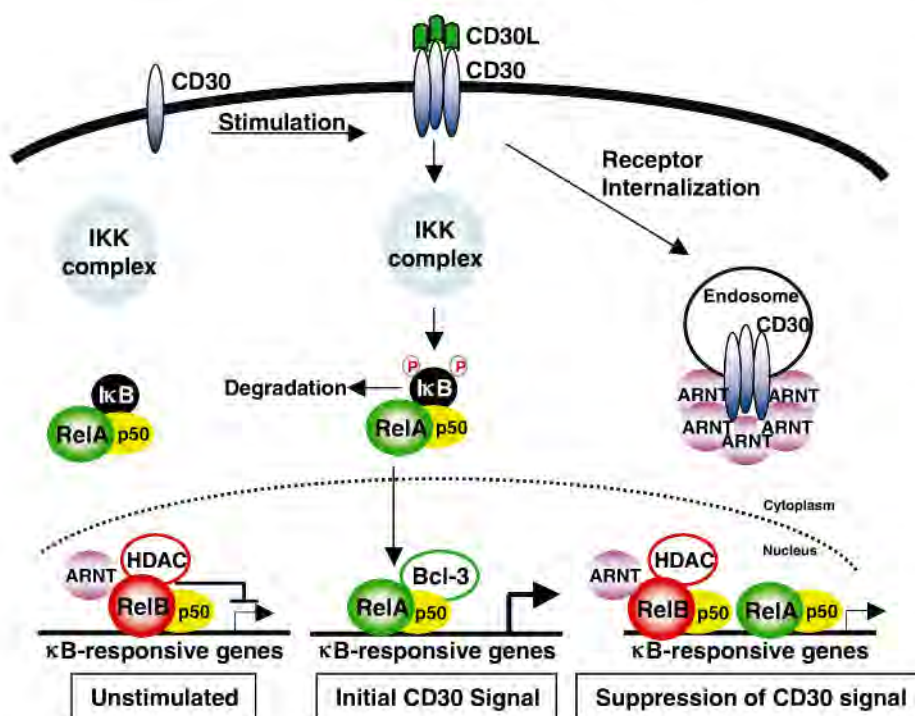


Fig. 5. Proposed model of ARNT regulation of CD30-mediated NF- κ B activity. Before CD30 stimulation, RelB is present at classical RelA-p50-regulated target promoters. An initial CD30 signal results in RelA-p50 translocation to the nucleus, which replaces the RelB complex, and transcription ensues. As the CD30 signal progresses, RelB translocates to the nucleus, where it associates with ARNT, enhancing the binding of RelB to DNA and negatively regulating RelA-p50 complexes. Furthermore, ARNT associates with the TRAF-binding region of internalized CD30, which may assist in the negative feedback loop of CD30 signaling by blocking TRAF binding.

HDAC4 Regulates Neuronal Survival in Normal and Diseased Retinas

Bo Chen and Constance L. Cepko

Histone deacetylase 4 (HDAC4) shuttles between the nucleus and cytoplasm and serves as a nuclear co-repressor that regulates bone and muscle development. We report that HDAC4 regulates the survival of retinal neurons in the mouse in normal and pathological conditions. Reduction in HDAC4 expression during normal retinal development led to apoptosis of rod photoreceptors and bipolar (BP) interneurons, whereas overexpression reduced naturally occurring cell death of the BP cells. HDAC4 overexpression in a mouse model of retinal degeneration prolonged photoreceptor survival. The survival effect was due to the activity of HDAC4 in the cytoplasm and relied at least partly on the activity of hypoxia-inducible factor 1 α (HIF1 α). These data provide evidence that HDAC4 plays an important role in promoting the survival of retinal neurons.

Blindness often results from the death of rod and cone photoreceptor cells, which respond directly to light and thus mediate the first step in vision. Histone deacetylases (HDACs) regulate the structure of chromatin through deacetylation of histones, though they also have other targets (1). HDAC4 is expressed in the nervous system and is predominantly cytoplasmic in neurons (2). The neurodegenerative disease protein ataxin-1 antagonizes the neuronal survival function of the transcription factor myocyte enhancer factor 2 (MEF2), which forms a complex with HDAC4, suggesting a role of HDAC4 in supporting neuronal survival (3). HDAC4 shuttles between the nucleus and cytoplasm (4, 5). In muscle and bone, it interacts with MEF2 to inhibit differentiation as a transcription repressor in the nucleus (6–9).

We examined HDAC4 expression by immunohistochemistry, in the postnatal day 1 (P1) murine retina (Fig. 1A), where it was seen in the inner neuroblastic layer (INBL). It was mostly excluded from the nuclei of developing amacrine cells (ACs) and ganglion cells in the INBL (fig. S1). It also was seen in the cytoplasm of cells in the outer neuroblastic layer (ONBL), which contains mitotic progenitor cells and newborn photoreceptor cells. HDAC4 immunoreactivity was lower in the mature retina (Fig. 1B), in the inner segment (IS) of photoreceptor cells, but not in the outer segments (OS) or in cell bodies located in the outer nuclear layer (ONL). In the inner nuclear layer (INL), faint immunoreactivity was detected in the cytoplasm of bipolar (BP) cells and ACs. Nuclear staining was seen in the ganglion cell layer (GCL) and in the two plexiform layers, the outer plexiform layer (OPL) and the inner plexiform layer (IPL), where processes are located. HDAC4 immunoreactivity was abolished by preincubation of the antibody with the cognate blocking peptide (Fig. 1, C and D).

To investigate the function of HDAC4 in vivo, we transfected a plasmid with a short hair-

pin RNA (shRNA) directed to HDAC4 (fig. S2), or a control shRNA against glyceraldehyde-3-phosphate dehydrogenase (GAPDH), into the P0 mouse retina by in vivo electroporation (10). To label transfected cells, we also electroporated a plasmid (pCAG-GFP) encoding green fluorescent protein (GFP) driven by a broadly active promoter, CAG. Retinas electroporated with the GAPDH shRNA showed that most transfected cells were rod photoreceptors, and a minority were BP cells, ACs, and Müller glial cells, located in the INL (10) (Fig. 2A). When HDAC4 was targeted, the number of cells expressing GFP declined rapidly (fig. S3H), and very few were seen at P6 (Fig. 2B). Thus, HDAC4 appeared to be required for survival. The RNA interference (RNAi) phenotype observed was not due to an off-target effect because transfection of a pCAG vector expressing an allele of HDAC4 that is resistant to HDAC4 shRNA rescued the cells (Fig. 2C). A terminal deoxynucleotidyl transferase-

mediated deoxyuridine triphosphate nick-end labeling (TUNEL) assay showed that cells receiving HDAC4 shRNA died from apoptosis (fig. S3, A to C), as did an assay for caspase activation in P5 retinal sections (fig. S3, D to G).

We overexpressed HDAC4 in the P0 mouse retinas. Electroporated retinas were collected at P14, when retinal neurogenesis is complete (11). HDAC4 overexpression led to more GFP-expressing BP cells in the upper INL than were observed in retinas electroporated by pCAG-GFP (fig. S4). During retinal development, BP cells are overproduced, and many are eliminated by P14 (12). The higher number of BP cells after HDAC4 electroporation suggested that HDAC4 might protect BP cells from naturally occurring cell death. Previous lineage analyses showed that a P0 retinal progenitor can give rise to a rod photoreceptor and a BP cell, as well as many clones with only a single rod (13). Because many BP cells die naturally, it is likely that some rod-only clones result from loss of a BP cell from clones that initially have both a rod and a BP cell. We therefore did clonal analysis with a replication-incompetent retrovirus, LIA, expressing human placental alkaline phosphatase to mark infected cells, and HDAC4, or without HDAC4 (Fig. 2, D to F). There was a statistically significant increase in the number of clones containing one rod and one BP cell or two rods and one BP cell after LIA-HDAC4 infection. The percentage of BP cell-containing clones increased from 9.1% for LIA infection to 20.6% for LIA-HDAC4 infection. These results are consistent with increased survival of BP cells and complement the findings from the HDAC4 RNAi treatment.

There is little naturally occurring rod death in normal development (14). Therefore, we assayed

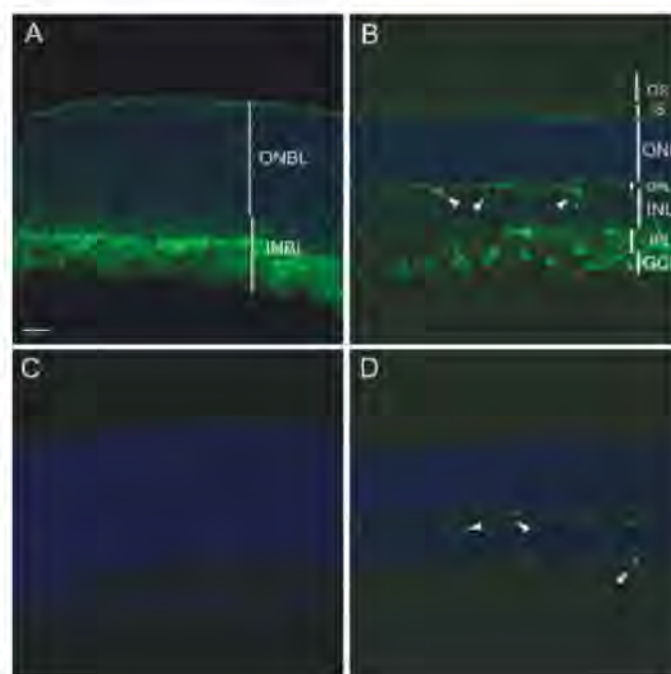


Fig. 1. (A and B) HDAC4 immunohistochemistry on mouse retinal sections at P1 and P21, respectively. (C and D) Preincubation of anti-HDAC4 with blocking peptide led to a lack of staining at P1 and P21. Arrowheads (B and D), blood vessels labeled by the mouse antibody.

Departments of Genetics and Ophthalmology and Howard Hughes Medical Institute, Harvard Medical School, 77 Avenue Louis Pasteur, Boston, MA 02115, USA. E-mail: bochen@genetics.med.harvard.edu; cepko@genetics.med.harvard.edu

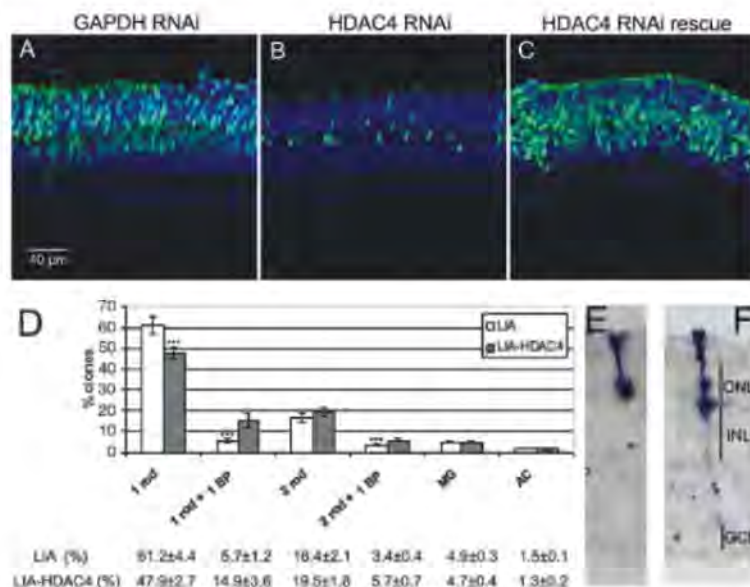


Fig. 2. HDAC4 is required for retinal cell survival and rescues BP cells from naturally occurring cell death. RNAi vectors targeting GAPDH or HDAC4 were electroporated into the wild-type mouse retina at P0, with assay at P6 (**A** to **C**). (**A**) Cryosections from retinas with GAPDH RNAi, (**B**) HDAC4 RNAi, and (**C**) HDAC4 shRNA and an RNAi resistant HDAC4-expressing construct. (**D**) Clonal analysis at P21 with replication-incompetent retrovirus LIA, or LIA-HDAC4, injected at P0. LIA-HDAC4 clones exhibited an increased percentage of BP cell-containing clones and a reduced percentage of single-rod clone. Eight hundred to 1000 clones were analyzed on each of three retinas infected by LIA or LIA-HDAC4. *** $P < 0.05$ by Student's t test. (**E**) Retinal section showing a typical single-rod clone, which constitutes most of the clone types. (**F**) Retinal section showing a typical single-rod plus single-BP cell clone, the clone type labeled by LIA-HDAC4 that was most increased in number.

rod survival after introduction of HDAC4 in a mouse model of retinal degeneration. The *rd1* mutation is in the rod-specific gene PDE6 β (phosphodiesterase 6 β subunit), which encodes a key enzyme in the phototransduction cascade. This mutation causes photoreceptor degeneration (15, 16). In *rd1* mice, nearly all rod photoreceptors die by P21, and cone death follows over the next few months (17). By P35, ~20% of cone photoreceptors remain (18). Electroporation at P0 results in transfection of many rods, but few cones (10). We electroporated pCAG-HDAC4 or pCAG-HDAC6 into P0 *rd1* mice. HDAC6 was included for a test of specificity, and because it rescues retinal degeneration in *Drosophila* (19). Retinas were analyzed at P50 with an antibody to rhodopsin (anti-rhodopsin), a rod-specific marker. In the transfected areas labeled by co-electroporated pCAG-GFP, many rods were present in retinas overexpressing HDAC4, but not in retinas overexpressing HDAC6 (fig. S5) or HDAC5 (fig. S6). We also assayed the activity of the rhodopsin promoter with a reporter plasmid for rhodopsin, Rho-DsRed (10), in which a 2.2-kb rhodopsin promoter drives the expression of DsRed, a red fluorescent protein. Rho-DsRed was electroporated with pCAG-HDAC4 into the P0 *rd1* retina. Tissues harvested at P70 showed that rods, marked by anti-rhodopsin immunohistochemistry (Fig. 3E), expressed DsRed (Fig. 3F) in the GFP-labeled electroporated area

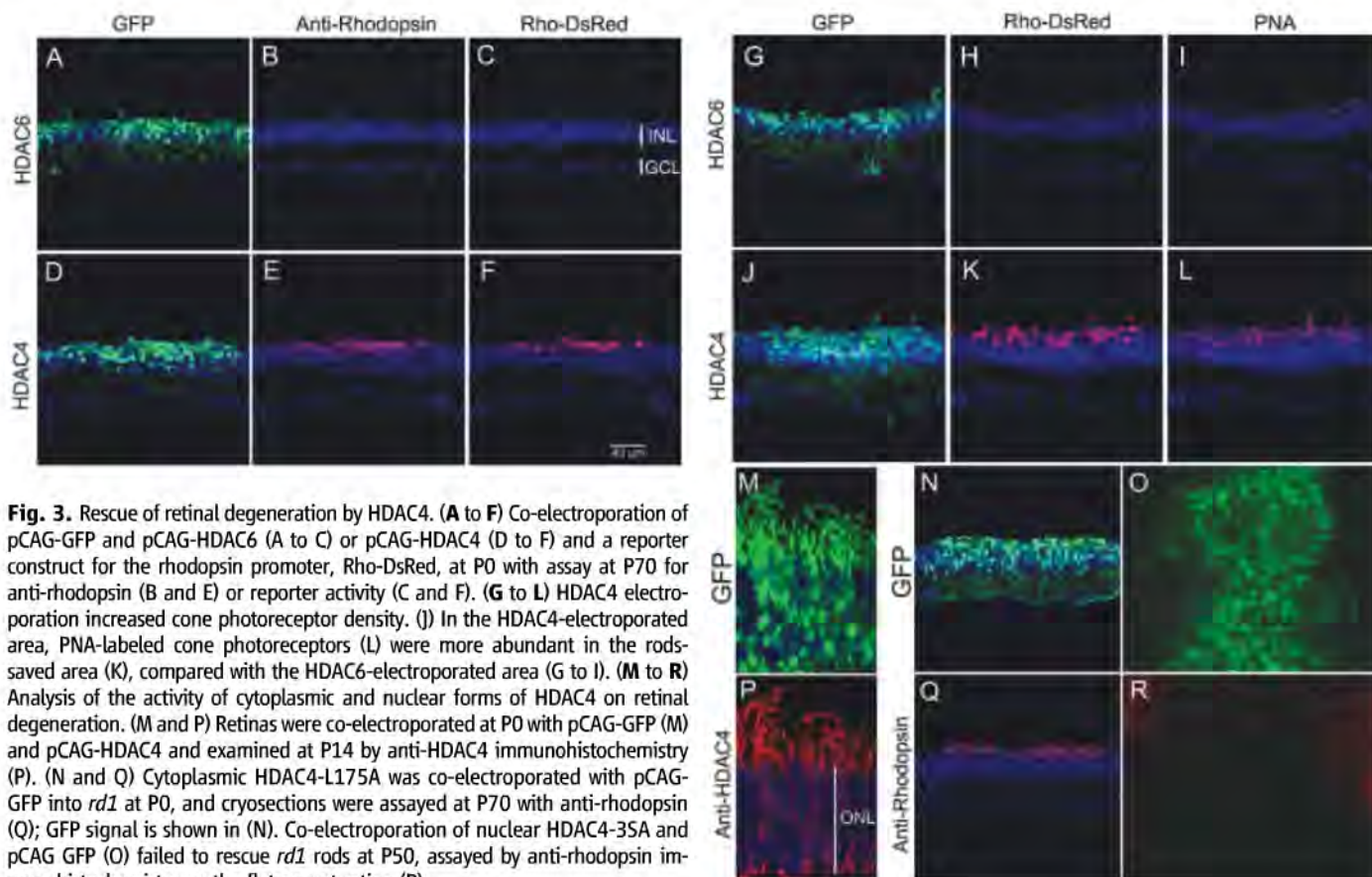


Fig. 3. Rescue of retinal degeneration by HDAC4. (**A** to **F**) Co-electroporation of pCAG-GFP and pCAG-HDAC6 (**A** to **C**) or pCAG-HDAC4 (**D** to **F**) and a reporter construct for the rhodopsin promoter, Rho-DsRed, at P0 with assay at P70 for anti-rhodopsin (**B** and **E**) or reporter activity (**C** and **F**). (**G** to **L**) HDAC4 electroporation increased cone photoreceptor density. (**I**) In the HDAC4-electroporated area, PNA-labeled cone photoreceptors (**L**) were more abundant in the rods-saved area (**K**), compared with the HDAC6-electroporated area (**G** to **I**). (**M** to **R**) Analysis of the activity of cytoplasmic and nuclear forms of HDAC4 on retinal degeneration. (**M** and **P**) Retinas were co-electroporated at P0 with pCAG-GFP (**M**) and pCAG-HDAC4 and examined at P14 by anti-HDAC4 immunohistochemistry (**P**). (**N** and **Q**) Cytoplasmic HDAC4-L175A was co-electroporated with pCAG-GFP into *rd1* at P0, and cryosections were assayed at P70 with anti-rhodopsin (**Q**); GFP signal is shown in (**N**). Co-electroporation of nuclear HDAC4-35A and pCAG GFP (**O**) failed to rescue *rd1* rods at P50, assayed by anti-rhodopsin immunohistochemistry on the flat-mount retina (**R**).

(Fig. 3D). The HDAC6-electroporated retina did not exhibit rhodopsin-immunoreactive cells or rhodopsin promoter activity (Fig. 3, A to C). We scored 24.3 ± 7.2 rhodopsin-positive cells per 100- μm section for HDAC4-treated retinas and 0 rhodopsin-positive cells in the HDAC6-electroporated retinas ($n = 3$). However, HDAC6 seemed to be as effective as HDAC4 in protecting BP cells from naturally occurring cell death in the *rd1* retina (Fig. 3, A and G), as well as in the wild-type retina (fig. S7).

Because the survival of cone photoreceptors depends on the survival of rod photoreceptors,

HDAC4-treated retinas were collected at P70 and stained with peanut agglutinin (PNA), which labels cones. HDAC4 overexpression (Fig. 3J) led to increased cone density (Fig. 3L) in the area with rescued rods (Fig. 3K), compared with retinas overexpressing HDAC6 (Fig. 3, G to I).

HDAC4 shuttles between the nucleus and cytoplasm. Retention of HDAC4 in the nucleus requires its interaction with MEF2 transcription factors (4). Phosphorylated HDAC4 moves into the cytoplasm, terminating its nuclear function (5). In wild-type photoreceptors, endogenous (Fig. 1B) or overexpressed HDAC4 (fig. S8) was pre-

dominantly located in the cytoplasm, including the photoreceptor IS and OS, as well as in axonal endings (Fig. 3, M and P). Thus, HDAC4-mediated photoreceptor survival in *rd1* mice might result from its cytoplasmic function. To investigate whether cytoplasmic or nuclear HDAC4 mediated the photoreceptor survival effect, we tested HDAC alleles modified to be targeted primarily to the cytoplasm or nucleus. The cytoplasmic HDAC4-L175A mutant, in which Lys¹⁷⁵ is mutated to Ala, does not interact with MEF2 transcription factors and thus stays primarily in the cytoplasm (4) (fig. S9). The HDAC4-3SA mu-

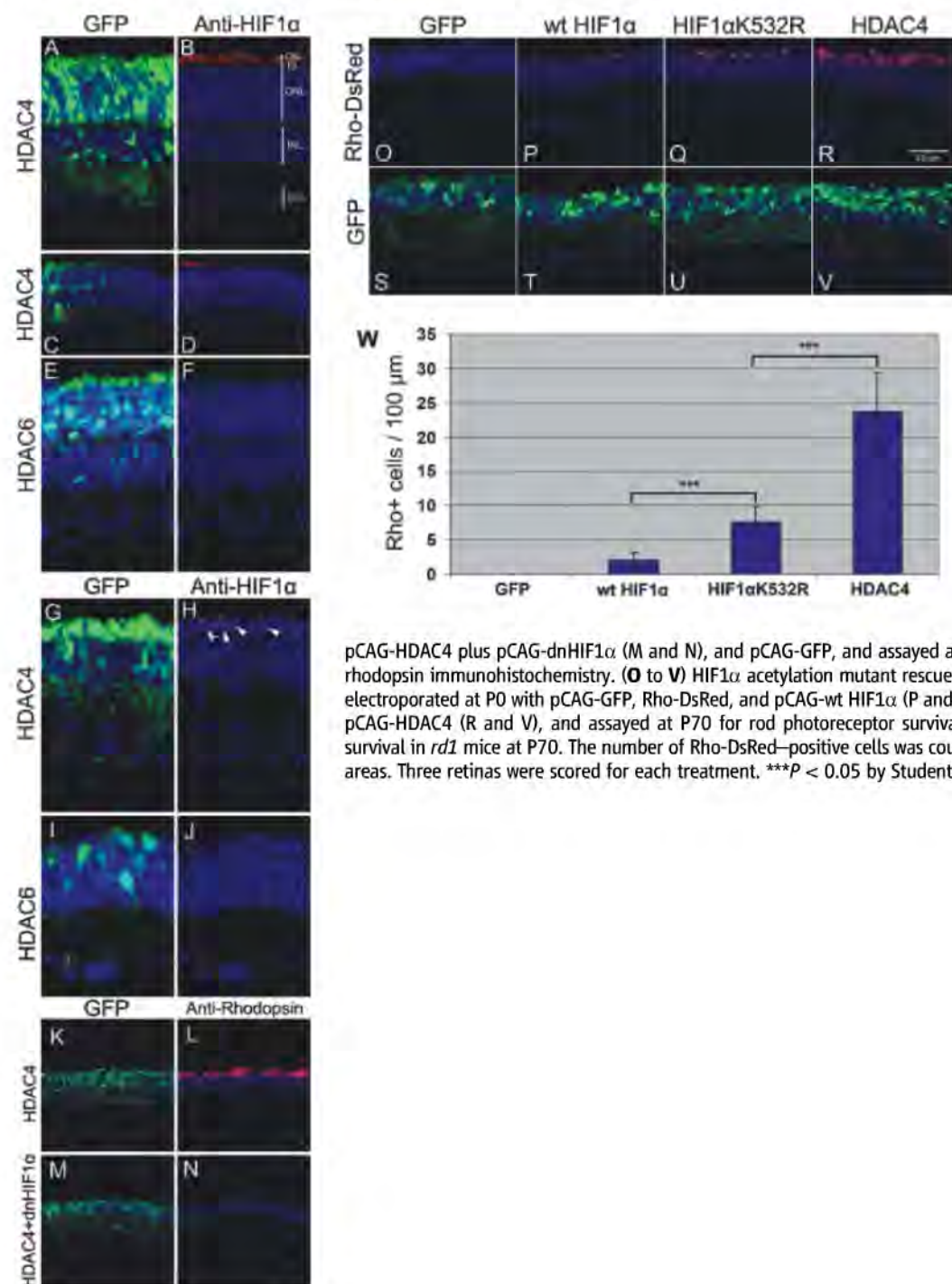


Fig. 4. Role of HIF1 α in HDAC4 survival activity. (A to F) Wild-type retinas electroporated at P0 with pCAG-HDAC4 and pCAG-GFP, or pCAG-HDAC6 and pCAG-GFP, and assayed at P14 by anti-HIF1 α immunohistochemistry on retinal sections. (A) HIF1 α protein in the photoreceptor OS by anti-HIF1 α in HDAC4-electroporated retina (B), only in the HDAC4-electroporated area (C and D). (E) In the HDAC6-electroporated area, no HIF1 α immunoreactivity (F) was detected. (G to J) HIF1 α in the *rd1* retina. *rd1* retinas were co-electroporated at P0 with pCAG-HDAC4 and pCAG-GFP (G and H) or pCAG-HDAC6 and pCAG-GFP (I and J), and assayed at P22 by anti-HIF1 α immunohistochemistry. Arrowheads (H), HIF1 α nuclear immunoreactivity. (K to N) HIF1 α protein is required for rescue of photoreceptors by HDAC4. *rd1* retinas were co-electroporated at P0 with pCAG-HDAC4 (K and L) or pCAG-HDAC4 plus pCAG-dnHIF1 α (M and N), and pCAG-GFP, and assayed at P70 for rod photoreceptor survival by rhodopsin immunohistochemistry. (O to V) HIF1 α acetylation mutant rescues retinal degeneration. *rd1* retinas were electroporated at P0 with pCAG-GFP, Rho-DsRed, and pCAG-wt HIF1 α (P and T), or pCAG-HIF1 α K532R (Q and U), or pCAG-HDAC4 (R and V), and assayed at P70 for rod photoreceptor survival. (W) Quantification of photoreceptor survival in *rd1* mice at P70. The number of Rho-DsRed-positive cells was counted per 100- μm section in transfected areas. Three retinas were scored for each treatment. *** $P < 0.05$ by Student's t test.

tant, which has its three serine phosphorylation sites mutated to alanine, stays primarily in the nucleus (5, 7) (fig. S9). The transfected cytoplasmic HDAC4-L175A mutant preserved *rdl* rods until at least P70 (Fig. 3, N and Q), whereas the nuclear HDAC4-3SA mutant failed to rescue *rdl* rods even at P50 (Fig. 3, O and R).

HIF1 α plays a central role in the regulation of oxygen homeostasis (20). HIF1 α protein is not detectable in the mature mouse retina (21). Exposure of retinas to hypoxia stabilizes HIF1 α and protects photoreceptors from light-induced retinal degeneration (21). HIF1 α protein stability is decreased by lysine acetylation. Acetylation of HIF1 α by the acetyltransferase ARD1 enhances its degradation (22). HIF1 α stabilization thus might provide a mechanism for HDAC4-induced photoreceptor protection in *rdl* mice. HIF1 α protein was detected by immunohistochemistry in the OS of wild-type photoreceptors after HDAC4 electroporation (Fig. 4, A to D). No HIF1 α immunoreactivity was detected after overexpression of HDAC6 (Fig. 4, E and F). Likewise, expression of HDAC4, but not that of HDAC6 (Fig. 4, I and J), led to the detection of HIF1 α that appeared nuclear or perinuclear in the photoreceptors of the *rdl* retina (Fig. 4, G and H). Expression of a dominant negative HIF1 α (dnHIF1 α) construct (23) with pCAG-HDAC4 in the *rdl* retina negated the photoreceptor survival effect of HDAC4 (Fig. 4, K to N). A plasmid with an shRNA directed to HIF1 α also blocked HDAC4-mediated photoreceptor survival (fig. S10). Thus, HIF1 α appears to be required for the HDAC4 survival effect.

To determine whether acetylation of HIF1 α might influence rod death in the *rdl* retina, we expressed HIF1 α K532R, an acetylation mutant of HIF1 α that is more stable than its wild-type form (22), and the wild-type HIF1 α in the *rdl* retina. Wild-type HIF1 α preserved a few rods (Fig. 4, P and T) and HIF1 α K532R preserved more (Fig. 4, Q and U). HDAC4 was the most effective in saving rod photoreceptors (Fig. 4, R, V, and W). No additive effects were seen when HDAC4 was coexpressed with HIF1 α K532R (fig. S11). The greater efficacy of HDAC4 relative to HIF1 α K532R might result from HDAC4 having target(s) in addition to HIF1 α , or HIF1 α K532R could be less effective than deacetylated wild-type HIF1 α .

In the mouse retina, HDAC4 has an essential role in neuronal survival. From a therapeutic perspective, HDAC4 prolonged photoreceptor survival in mice undergoing retinal degeneration. HDAC6 did not lead to increased abundance of HIF1 α protein or promote rod survival in mice, although it rescued degeneration in *Drosophila* (19). Therefore, more than one pathway for neuronal survival may be regulated by HDACs.

References and Notes

1. X. J. Yang, E. Seto, *Oncogene* **26**, 5310 (2007).
2. T. A. Bolger, T. P. Yao, *J. Neurosci.* **25**, 9544 (2005).
3. T. A. Bolger, X. Zhao, T. J. Cohen, C. C. Tsai, T. P. Yao, *J. Biol. Chem.* **282**, 29186 (2007).
4. A. H. Wang, X. J. Yang, *Mol. Cell. Biol.* **21**, 5992 (2001).
5. X. Zhao et al., *J. Biol. Chem.* **276**, 35042 (2001).
6. E. A. Miska et al., *EMBO J.* **18**, 5099 (1999).
7. R. B. Vega et al., *Cell* **119**, 555 (2004).
8. J. Lu, T. A. McKinsey, C. L. Zhang, E. N. Olson, *Mol. Cell* **6**, 233 (2000).

9. M. A. Arnold et al., *Dev. Cell* **12**, 377 (2007).
10. T. Matsuda, C. L. Cepko, *Proc. Natl. Acad. Sci. U.S.A.* **101**, 16 (2004).
11. R. W. Young, *Anat. Rec.* **212**, 199 (1985).
12. J. T. Voyvodic, J. F. Burne, M. C. Raff, *Eur. J. Neurosci.* **7**, 2469 (1995).
13. D. L. Turner, C. L. Cepko, *Nature* **328**, 131 (1987).
14. R. W. Young, *J. Comp. Neurol.* **229**, 362 (1984).
15. C. Bowes et al., *Nature* **347**, 677 (1990).
16. M. E. McLaughlin, M. A. Sandberg, E. L. Berson, T. P. Dryja, *Nat. Genet.* **4**, 130 (1993).
17. L. D. Carter-Dawson, M. M. LaVail, R. L. Sidman, *Invest. Ophthalmol. Vis. Sci.* **17**, 489 (1978).
18. K. Komeima, B. S. Rogers, L. Lu, P. A. Campochiaro, *Proc. Natl. Acad. Sci. U.S.A.* **103**, 11300 (2006).
19. U. B. Pandey et al., *Nature* **447**, 859 (2007).
20. G. L. Semenza, *J. Appl. Physiol.* **88**, 1474 (2000).
21. C. Grimm et al., *Nat. Med.* **8**, 718 (2002).
22. J. W. Jeong et al., *Cell* **111**, 709 (2002).
23. B. H. Jiang, E. Rue, G. L. Wang, R. Roe, G. L. Semenza, *J. Biol. Chem.* **271**, 17771 (1996).
24. We thank J. R. Lu for providing HDAC4, HDAC5, and HDAC6 expression constructs; T. P. Yao for providing HDAC4-3SA mutant; X. J. Yang for providing HDAC4-L175A mutant; G. L. Semenza for providing dnHIF1 α constructs and K. W. Kim for providing HIF1 α and HIF1 α K532R constructs; and T. Matsuda for assistance with various techniques. Supported by NIH grant EYO 14466, the Foundation for Retinal Research, a gift from Merck, and the Howard Hughes Medical Institute (HHMI). C.L.C. is an Investigator of HHMI and B.C. is a postdoctoral fellow of HHMI. C.L.C. and B.C. have filed a U.S. patent application, 61/088,455, based on the work in this paper.

Supporting Online Material

www.sciencemag.org/cgi/content/full/323/5911/256/DC1

Materials and Methods

Figs. S1 to S11

References

22 September 2008; accepted 10 November 2008
10.1126/science.1166226

Genetic Code Supports Targeted Insertion of Two Amino Acids by One Codon

Anton A. Turanov,^{1*} Alexey V. Lobanov,^{1*} Dmitri E. Fomenko,¹ Hilary G. Morrison,² Mitchell L. Sogin,² Lawrence A. Klobutcher,³ Dolph L. Hatfield,⁴ Vadim N. Gladyshev^{1†}

Strict one-to-one correspondence between codons and amino acids is thought to be an essential feature of the genetic code. However, we report that one codon can code for two different amino acids with the choice of the inserted amino acid determined by a specific 3' untranslated region structure and location of the dual-function codon within the messenger RNA (mRNA). We found that the codon UGA specifies insertion of selenocysteine and cysteine in the ciliate *Euplotes crassus*, that the dual use of this codon can occur even within the same gene, and that the structural arrangements of *Euplotes* mRNA preserve location-dependent dual function of UGA when expressed in mammalian cells. Thus, the genetic code supports the use of one codon to code for multiple amino acids.

Although codons can be recoded to specify other amino acids or to have ambiguous meanings (1, 2), and stop codons can be suppressed to insert amino acids (3), insertion of different amino acids into separate positions within nascent polypeptides by the same codeword is believed to be inconsistent with

ribosome-based protein synthesis. In ciliated protozoa from the *Euplotes* genus, cysteine (Cys) is encoded by three codons, UGA, UGU, and UGC (4, 5). UGA is a stop signal in the universal genetic code, and this codon can also code for the 21st amino acid, selenocysteine (Sec) (6).

Metabolic labeling with ⁷⁵Se showed that *E. crassus* contains multiple selenoproteins (fig. S1). To identify the codon used for Sec, we sequenced 15,000 *E. crassus* expressed sequence tags (ESTs) (fig. S2) and the full-length eGPx1 cDNA sequence. The eGPx1 cDNA encodes a 22-kD protein with a single in-frame UGA codon (Fig. 1A) and a Sec insertion sequence (SECIS) element (7) in its 3' untranslated region (3'UTR) (Fig. 1B), which suggests that this UGA encodes Sec. Therefore, UGA may be used for both Cys and Sec insertion in *Euplotes*. Expression of eGPx1 as a fusion protein with green fluorescent protein (GFP) in human embryonic kidney (HEK) 293 cells revealed specific ⁷⁵Se incorporation (Fig. 1C). The corresponding full-size protein was also detected by Western blotting (Fig. 1D).

¹Department of Biochemistry and Redox Biology Center, University of Nebraska, Lincoln, NE 68588, USA. ²Josephine Bay Paul Center, Marine Biological Laboratory, Woods Hole, MA 02543, USA. ³Department of Molecular, Microbial and Structural Biology, University of Connecticut Health Center, Farmington, CT 06032, USA. ⁴Molecular Biology of Selenium Section, Laboratory of Cancer Prevention, Center for Cancer Research, National Cancer Institute, National Institutes of Health, Bethesda, MD 20892, USA.

*These authors contributed equally to this work.

†To whom correspondence should be addressed. E-mail: vgladyshev1@unl.edu

Mutation of the core region of the eGPx1 SECIS element prevented ^{75}Se incorporation and protein synthesis (Fig. 1, C and D), indicating that SECIS was required for Sec insertion in response to UGA.

E. crassus genome sequencing and analysis revealed eight selenoprotein genes (figs. S3 to S16) and three tRNAs that recognize UGA codons, including Sec tRNA, mitochondrial Trp tRNA, and a novel Cys tRNA (Fig. 2A and fig. S17). A Cys tRNA recognizing UGU and

UGC codons was also detected. Four of the eight selenoprotein genes contained multiple UGA codons (fig. S4). Comparison with known selenoproteins suggested the use of one codon for Sec and an additional UGA codon (or codons) within the same gene for Cys insertion. *E. crassus* thioredoxin reductases 1 (eTR1) and 2 (eTR2) had seven in-frame UGA codons, with the first six predicted to code for Cys and the last one to code for Sec (figs. S5, S6, and S18). To

examine coding functions of UGA codons, we cloned a novel selenoprotein ep22, selenoprotein W2 (eSelW2), and eTR1 (figs. S5, S8, S10, and S19) and expressed them in the form of GFP-fusion proteins in HEK 293 cells. Specific ^{75}Se incorporation was observed into GFP-ep22 (Fig. 1, E and F) and GFP-eSelW2 (Fig. 1G), which had single UGA codons.

In the case of GFP-eTR1, we initially did not observe ^{75}Se incorporation (Fig. 2B, lane 2),



Fig. 1. *E. crassus* selenoproteins encode Sec with UGA codon as directed by SECIS element. (A) Schematic representation of eGPx1 mRNA. The positions of the start (AUG), Sec (UGA), and stop (UAA) codons and the SECIS element in the 3'UTR are shown. (B) eGPx1 SECIS element. "Core" highlights the mutations made in the SECIS core. (C) Expression of GFP-eGPx1 fusion in HEK 293 cells. Cells were transfected with the pEGFP-C3 vector, pEGFP-eGPx1 construct, or construct with mutations in the SECIS core (pEGFP-eGPx1core) [see (B)], labeled with ^{75}Se and analyzed as given in (11). Selenoprotein patterns were visualized with a PhosphorImager on SDS–polyacrylamide gel electrophoresis (SDS–PAGE) gels. (D) Western blot analysis of samples shown in (C) with antibody to GFP. Arrows show the positions of GFP and GFP-eGPx1. (E) Expression of GFP-ep22 fusion protein in HEK 293 cells. Cells were transfected with the pEGFP-C3 vector or pEGFP-ep22 construct, labeled with ^{75}Se , and analyzed as in (C). (F) Western blot analysis of samples shown in (E) with antibodies to GFP. Arrows show the positions of GFP and GFP-ep22. (G) Expression of GFP-eSelW2 fusion protein in HEK 293 cells. Arrow shows the position of the GFP-eSelW2 fusion selenoprotein. Molecular masses of protein standards (in kD) are shown on the left.

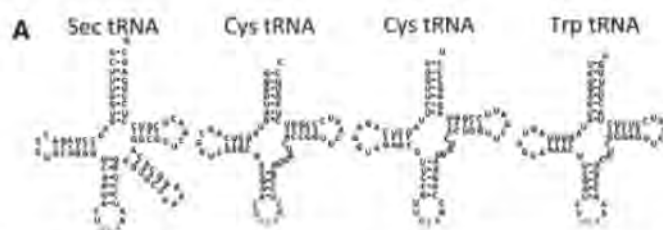
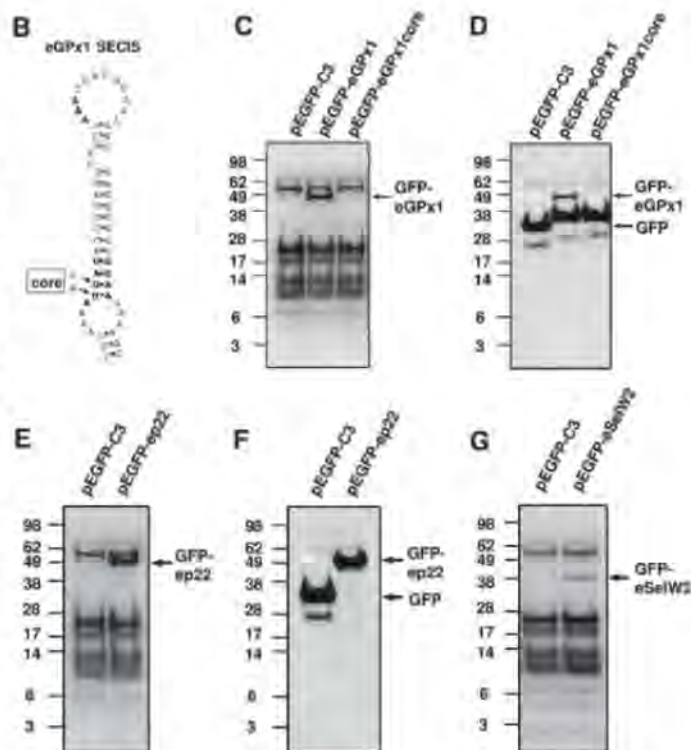
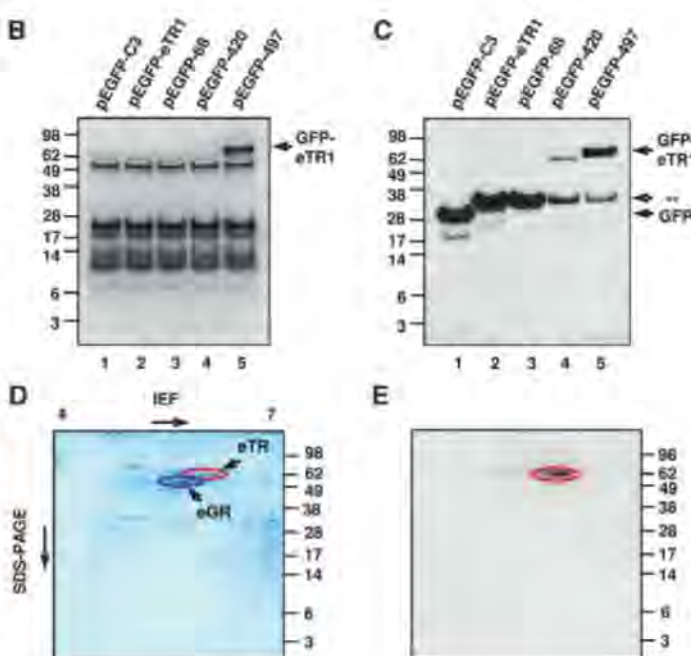


Fig. 2. Sec and Cys insertion in eTR1. (A) Structures of *E. crassus* tRNAs. Sec tRNA, Cys tRNAs with UCA and GCA anticodons, and a mitochondrial Trp tRNA are shown. Anticodons are highlighted in red (UCA) or blue (GCA). (B) Expression of GFP-eTR1 in HEK 293 cells. Cells were transfected with pEGFP-C3 vector (lane 1), pEGFP-eTR1 (lane 2), or constructs with multiple UGA to UGC mutations in which the number indicates the amino acid residue for which the UGA codon is retained: pEGFP-68 (lane 3), pEGFP-420 (lane 4), and pEGFP-497 (lane 5). Cells were analyzed as described in Fig. 1C. Arrow shows the position of the GFP-eTR1 fusion selenoprotein. (C) Western blot analysis of samples shown in (B) with antibodies to GFP. Arrows show the positions of GFP and truncated and full-size GFP-eTR1. Asterisks show the position of truncated GFP-eTR1 fusions in lanes 2 and 3. (D) Partially purified eTR sample analyzed by two-dimensional PAGE and stained with Coomassie Blue. (E) Visualization of the ^{75}Se -labeled sample shown in (D) with a PhosphorImager. The spots of eGR are indicated by a blue oval (D) and of eTR by red ovals (D and E).



This was likely due to termination at UGAs coding for Cys in *Euplotes*, which were recognized as stop signals in mammalian cells. We therefore prepared mutant forms of GFP-eTR1, in which six of the seven UGA codons were replaced with UGC, leaving single UGA at positions 68, 420, or 497. Of these, amino acids 68 and 420 corresponded to Cys, and 497 corresponded to Sec in other TRs. We found that ^{75}Se (and, therefore, Sec) could be inserted only at position 497 (Fig. 2B, lane 5). Western blotting confirmed the synthesis of truncated proteins when UGA was at positions 68 and 420, and of the full-size protein at position 497 (Fig. 2C). Thus, Sec was only inserted into the classical Sec site in eTR1, whereas other UGA positions were not served by SECIS for Sec insertion and instead supported termination of translation in mammalian cells (in *Euplotes*, Cys would be inserted).

To confirm Cys insertion at UGA codons other than codon 497 in eTR1, we purified the ^{75}Se -labeled 55-kD selenoprotein band from *E. crassus* after a series of chromatographic steps

(Fig. 2, D and E). Liquid chromatography–tandem mass spectrometry sequencing revealed peptides corresponding to eTR1 and a more abundant glutathione reductase (eGR) (figs. S20 to S22). This analysis identified eTR1 peptides containing Cys in positions 63, 68, 208, and 270, which are encoded by UGA codons (figs. S5 and S18), whereas peptides containing Sec at these positions were not detected. Thus, UGA differentially codes for Cys and Sec in different positions within the *E. crassus* eTR1 gene.

To determine whether Cys and/or Sec insertion is associated with UGA position within the gene, we prepared GFP-eTR1 mutants containing single UGA codons in unnatural codon positions: 246, 441, 467, 478, 489, 494, or 496. ^{75}Se -labeling and Western blotting revealed that UGA terminated translation in positions 246, 441, and 467 but inserted Sec in positions 489 and 494 (Fig. 3, A to E). Sec was also inserted at position 496 (fig. S23), whereas position 478 was intermediate, supporting a low level of Sec insertion (Fig. 3, C and D). Thus, Sec insertion was restricted to approximately the last 20 codons,

whereas the region upstream supported termination by UGA in mammalian cells (and, therefore, Cys insertion in *E. crassus*).

We replaced a segment corresponding to part of the eTR1 3'UTR, including the entire SECIS element, with the 3'UTR region of *Toxoplasma* selenoprotein T (SelT), which also has a SECIS element (8). In this mutant, Sec insertion was detected at position 420, that is, upstream of codon 478 (Fig. 3F), indicating that replacement of the functional 3'UTR region changed the coding function of UGA. Similarly, Sec could be inserted in the N-terminal region of ep22, in addition to its natural C-terminal penultimate position (Fig. 3G), which suggests a model wherein Sec insertion is dependent on an RNA structure (fig. S24).

We have demonstrated that UGA can designate different amino acids within the same gene, with the choice of the amino acid inserted determined by availability of the functional element within the 3'UTR and the location of UGA within the gene. Although dual functions of stop codons have previously been described, they support the insertion of single amino acids (e.g., Sec or pyrrolysine) in competition with termination (9) or ambiguous codon function due to dual specificity of a particular tRNA (10). Here, we show that one codon supports specific insertion of multiple amino acids, indicating that evolutionary expansion of the genetic code is possible.

References and Notes

1. O. Namy, J. P. Rousset, S. Naphine, I. Brierley, *Mol. Cell* **13**, 157 (2004).
2. J. F. Atkins, P. V. Baranov, *Nature* **448**, 1004 (2007).
3. J. C. Anderson et al., *Proc. Natl. Acad. Sci. U.S.A.* **101**, 7566 (2004).
4. S. Osawa, T. H. Jukes, K. Watanabe, A. Muto, *Microbiol. Rev.* **56**, 229 (1992).
5. F. Meyer et al., *Proc. Natl. Acad. Sci. U.S.A.* **88**, 3758 (1991).
6. D. L. Hatfield, V. N. Gladyshev, *Mol. Cell. Biol.* **22**, 3565 (2002).
7. M. J. Berry et al., *Methods Enzymol.* **347**, 17 (2002).
8. S. V. Novoselov et al., *Proc. Natl. Acad. Sci. U.S.A.* **104**, 7857 (2007).
9. G. Srinivasan, C. M. James, J. A. Krzycki, *Science* **296**, 1459 (2002).
10. T. Suzuki, T. Ueda, K. Watanabe, *EMBO J.* **16**, 1122 (1997).
11. Materials and methods are available as supporting material on Science Online.
12. We thank K. Hammar for constructing the EST library and I. Sorokina (Midwest Bio Services) for protein sequencing. This work was supported by NIH GM061603 and GM065204 to V.N.G., AI058054 to M.L.S., NSF 0343813 to L.A.K., and the Intramural Research Program, National Cancer Institute, NIH, to D.L.H. Sequences for tRNA and selenoprotein genes have been deposited in the GenBank database under accession numbers FJ440148 to FJ440159.

Supporting Online Material

www.sciencemag.org/cgi/content/full/323/5911/259/DC1
Materials and Methods
Figs. S1 to S24
References

18 August 2008; accepted 11 November 2008
10.1126/science.1164748

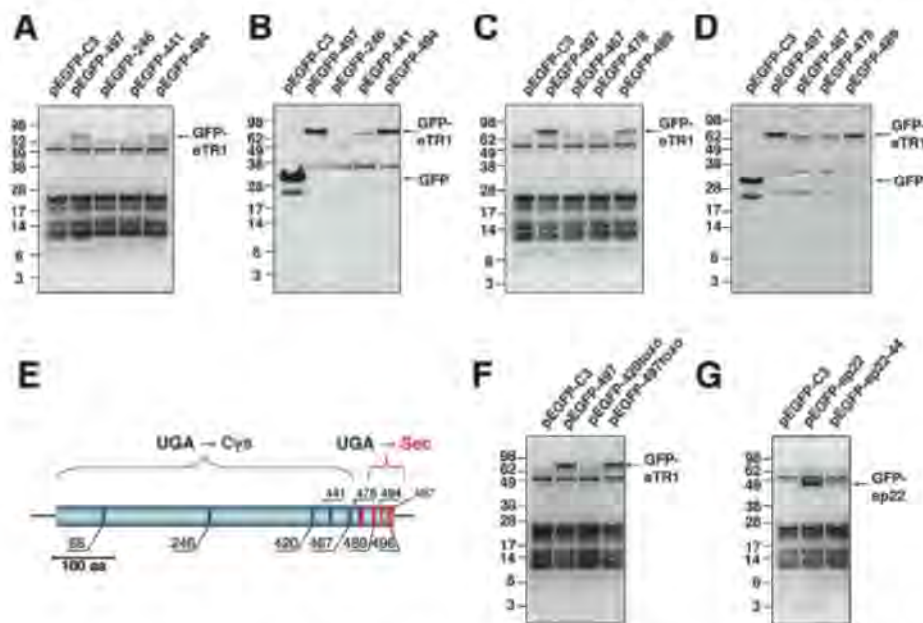


Fig. 3. Position-dependent Sec insertion in eTR1. (A) Expression of GFP-eTR1 in HEK 293 cells. Cells were transfected with pEGFP-C3 vector, a GFP-eTR1 construct containing a single UGA codon at the natural Sec position 497 (pEGFP-497), or constructs that had UGA at unnatural positions 246 (pEGFP-246), 441 (pEGFP-441), or 494 (pEGFP-494). Cells were analyzed as described in Fig. 1C. (B) Western blot analysis of samples shown in (A) with antibodies to GFP. (C) Cells were transfected with pEGFP-C3 vector, a GFP-eTR1 construct containing a single UGA codon at the natural Sec position 497 (pEGFP-497), or constructs that had UGA at unnatural positions 467 (pEGFP-467), 478 (pEGFP-478), or 489 (pEGFP-489). (D) Western blot analysis of samples shown in (C) with antibodies to GFP. (E) Summary of experimental evidence for Sec and Cys insertion in eTR1. The positions of Cys insertion (corresponding to termination in mammalian cells) are shown by blue lines, and Sec insertion by red lines. Position 478 supported low-level Sec insertion. (F) Cells were transfected with pEGFP-C3 vector, a GFP-eTR1 construct containing a single UGA codon at the natural Sec position 497 (pEGFP-497), or constructs containing a 3'UTR segment of *Toxoplasma* SelT and UGA at position 420 (pEGFP-420tox) or 497 (pEGFP-497tox). (G) Cells were transfected with pEGFP-C3 vector or with ep22 constructs in which UGA corresponded to positions 190 (pEGFP-ep22) or 44 (pEGFP-ep22-44). Arrows show the positions of GFP and full-size GFP-eTR1 or GFP-ep22.

tasselseed1 Is a Lipxygenase Affecting Jasmonic Acid Signaling in Sex Determination of Maize

Iván F. Acosta,^{1*} Hélène Laparra,¹ Sandra P. Romero,¹ Eric Schmelz,² Mats Hamberg,³ John P. Mottinger,⁴ Maria A. Moreno,¹ Stephen L. Dellaporta^{1†}

Sex determination in maize is controlled by a developmental cascade leading to the formation of unisexual florets derived from an initially bisexual floral meristem. Abortion of pistil primordia in staminate florets is controlled by a *tasselseed*-mediated cell death process. We positionally cloned and characterized the function of the sex determination gene *tasselseed1* (*ts1*). The TS1 protein encodes a plastid-targeted lipxygenase with predicted 13-lipxygenase specificity, which suggests that TS1 may be involved in the biosynthesis of the plant hormone jasmonic acid. In the absence of a functional *ts1* gene, lipxygenase activity was missing and endogenous jasmonic acid concentrations were reduced in developing inflorescences. Application of jasmonic acid to developing inflorescences rescued stamen development in mutant *ts1* and *ts2* inflorescences, revealing a role for jasmonic acid in male flower development in maize.

Most flowering plants produce perfect flowers containing both the male organs (stamens) and female organs (pistils). In maize, which has physically separated male and female inflorescences, floral meristems become unisexual through sex determination [reviewed in (1, 2)]. The basic unit of the maize inflorescence, called a spikelet, contains one upper and one lower flower (known as florets in grasses). Each floret initiates a series of floral organs including three stamen primordia and a central pistil primordium (3, 4). These initially bisexual florets become exclusively staminate in the tassel (by abortion of pistil primordia) and exclusively pistillate in the ear (by arrest of developing stamens) (3, 5). Each ear spikelet produces a solitary functional pistil in the upper floret due to abortion of the pistil in the lower floret (3–5).

Mutations altering the sexual fate of florets in maize indicate that sex determination is under genetic control. The nonhomeotic *tasselseed* (*ts*) mutations *ts1* and *ts2* result in the conversion of the tassel inflorescence from staminate to pistillate (6, 7). Both *ts1* and *ts2* are required to eliminate pistil primordia through cell death (8, 9). The *ts2* gene encodes a short-chain dehydrogenase/reductase (10) with broad activity, which has complicated the discovery

of its natural substrate (11). It is unknown how *ts* genes mediate pistil cell death, although it has been suggested that the dehydrogenase/reductase activity of *ts2* may produce a proapoptotic signal or metabolize a substrate required for cell viability (8, 11). Even less is known about the *ts1* gene. *TS2* transcripts are low or undetectable in *ts1* mutant tassels, which suggests that *ts1* may act upstream of *ts2* by regulating *ts2* RNA levels and possibly other sex determination genes (8).

We positionally cloned and mapped *ts1* (12) (fig. S1), which is located in a region with extensive synteny with rice (13). The *ts1* syntenic interval within the sequenced genome of rice contains nine genes (12). We found no maize orthologs for four of these genes, and another three mapped to locations unlinked to the *ts1* locus in maize. Maize homologs of the remaining two rice genes, one encoding a putative glutamate decarboxylase and the other encoding a putative lipxygenase, were confirmed to be contained within the *ts1* physical interval (fig. S1).

Sequencing showed that the gene encoding glutamate decarboxylase was monomorphic, whereas the gene encoding lipxygenase in the *ts1-ref* line showed an 864-base pair (bp) insertion in the predicted first exon with complete linkage with the *ts1* phenotype in mapping populations. To confirm that the lipxygenase corresponded to the *ts1* gene, we analyzed eight *ts1* mutant alleles. Each contained an independent mutation in the gene encoding lipxygenase (Fig. 1A and table S1). Complementary DNA sequence analysis showed that the *ts1* gene contains seven exons with a coding sequence of 2757 bp (Fig. 1A). A closely related gene was also identified in the database of the TIGR AZM 4.0 assembly and by Southern blot analysis (fig. S2). This gene, named *ts1b*, has an identical exon-intron structure to that of *ts1* and shares 93% nucleotide similarity. The

ts1b gene is located on maize chromosome 10S, a segmental duplication of chromosome 2S (14). The TS1 protein displays 38 to 60% similarity to plant lipxygenases and contains two conserved domains characteristic of this family: a beta-barrel (cd01751) and a catalytic helical bundle (pfam00305) (15) (Fig. 1B and fig. S3).

Lipxygenases are nonheme iron-containing fatty acid dioxygenases that catalyze the peroxidation of polyunsaturated fatty acids such as linoleic acid, α -linolenic acid, and arachidonic acid. They are classified according to the positional specificity of linoleic acid oxygenation, which occurs at carbon 9 of the hydrocarbon backbone for the 9-LOX types and at carbon 13 for the 13-LOX types; a further subdivision (classes 1 and 2) has been recognized for 13-lipxygenases without or with a putative chloroplast transit peptide (cTP), respectively (16). According to ChloroP, a neural network-based method for predicting cTPs, the N-terminal 48 amino acids of the TS1 protein contain a cTP (17) (Fig. 1B and fig. S3). Additionally, TS1 contains a conserved phenylalanine (Phe⁶³⁶) previously identified as a determinant of 13-LOX regiospecificity (18, 19). Therefore, the primary structure of TS1 suggests that it is a member of the class 2 plastid-localized 13-lipxygenases. This prediction was supported by Bayesian and maximum parsimony phylogenetic analyses of plant lipxygenases, which placed TS1 and TS1b in a clade including characterized and predicted class 2 13-lipxygenase (Fig. 1C and fig. S4).

The tissue-specific expression of both *ts1* and *ts1b* was established by quantitative reverse transcription polymerase chain reaction (RT-PCR) analysis of root, stem, leaf, tassel, and ear transcripts. The *ts1* RNA was detected in all maize tissues examined, whereas *ts1b* RNA was detected at very low levels (less than that of *ts1* by a factor of 90 to 500) (Fig. 2A). The low expression of *ts1b* may explain why it does not also appear to be a component of sex determination in *ts1* mutant plants. The broad expression of *ts1* was unexpected because its mutant phenotype suggests a sex-specific function. Although no alterations in other tissues have been reported, it is possible that additional phenotypes for the *ts1* mutation may be uncovered by more careful analyses. The *ts2* gene was expressed almost as broadly as *ts1*, except in stem tissue, where expression was less than that of *ts1* by a factor of ~35.

In situ hybridization showed that TS1 transcripts form stripes following the borders of the central inflorescence axis and projecting toward the spikelet attachment points (Fig. 2, B and D). In spikelet adaxial views, TS1 expression domains surround the spikelets, delineating their base (Fig. 2C). None of these expression patterns were observed in a homozygous *ts1-Mu01* deletion mutant line containing a functional *ts1b* gene (Fig. 2E). These

¹Department of Molecular, Cellular and Developmental Biology, Yale University, New Haven, CT 06511, USA. ²Center for Medical, Agricultural and Veterinary Entomology, U.S. Department of Agriculture–Agricultural Research Service, Gainesville, FL 32608, USA. ³Division of Physiological Chemistry II, Department of Medical Biochemistry and Biophysics, Karolinska Institutet, S-17177 Stockholm, Sweden. ⁴Department of Cell and Molecular Biology, University of Rhode Island, Kingston, RI 02881, USA.

*Present address: IFA, Département de Biologie Moléculaire Végétale, Université de Lausanne, CH-1015 Lausanne, Switzerland.

†To whom correspondence should be addressed. E-mail: stephen.dellaporta@yale.edu

Fig. 1. (A) Structure of the *ts1* gene and the *ts1* mutant alleles. Hollow boxes at left and right are 5' and 3' untranslated regions (UTRs), respectively; black boxes are exons and angled lines are introns. Mutations in eight *ts1* mutant alleles are positioned above the corresponding exons. Insertions are represented by inverted triangles and a single deletion by a triangle. **(B)** TS1 protein features include a predicted chloroplast transit peptide (cTP, green), the PLAT/LH2 beta-barrel (pink), and the lipoxigenase domain (blue) as well as five conserved residues (H, His; I, Ile; N, Asn) necessary for iron binding (red) and the phenylalanine (F) residue predicting 13-LOX regio-specificity (black). **(C)** Bayesian and maximum parsimony consensus tree of predicted type 2 13-lipoxigenases in angiosperms. The red arrowhead indicates the position of the maize *ts1*-encoded lipoxigenase. Posterior probabilities from Bayesian inference and bootstrap support from maximum parsimony analysis less than 100% are displayed below internal nodes to the left and right of a slash, respectively. This subclade is part of a more extensive phylogenetic analysis shown in fig. S4.

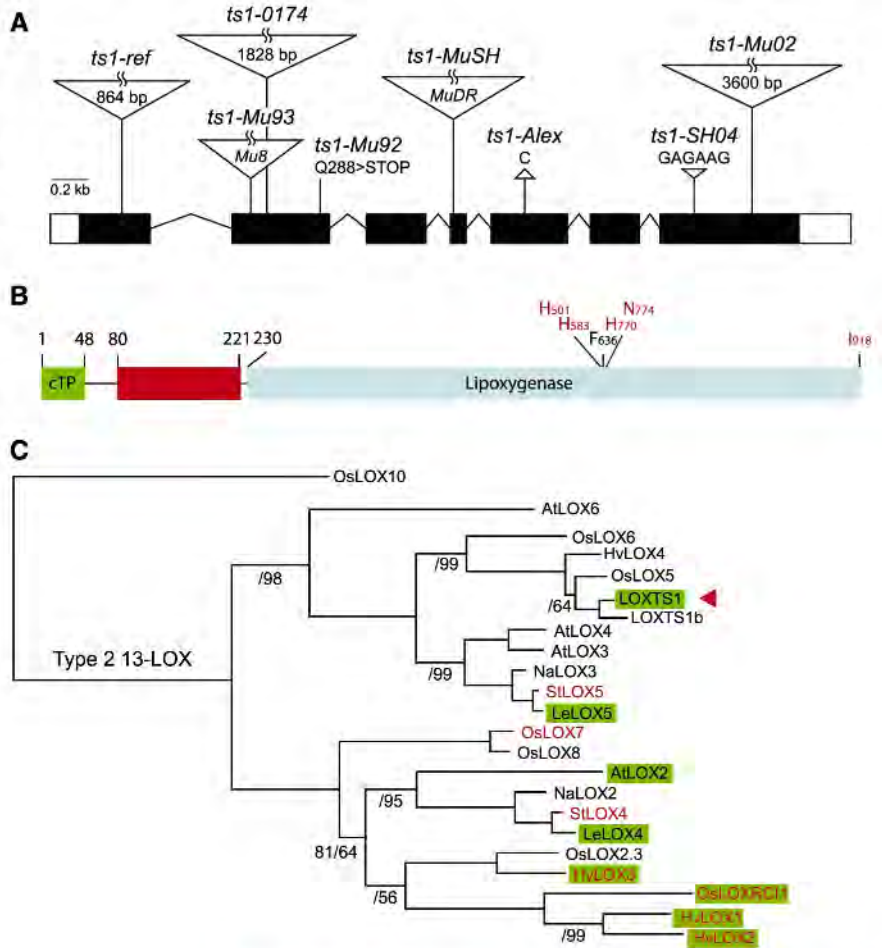
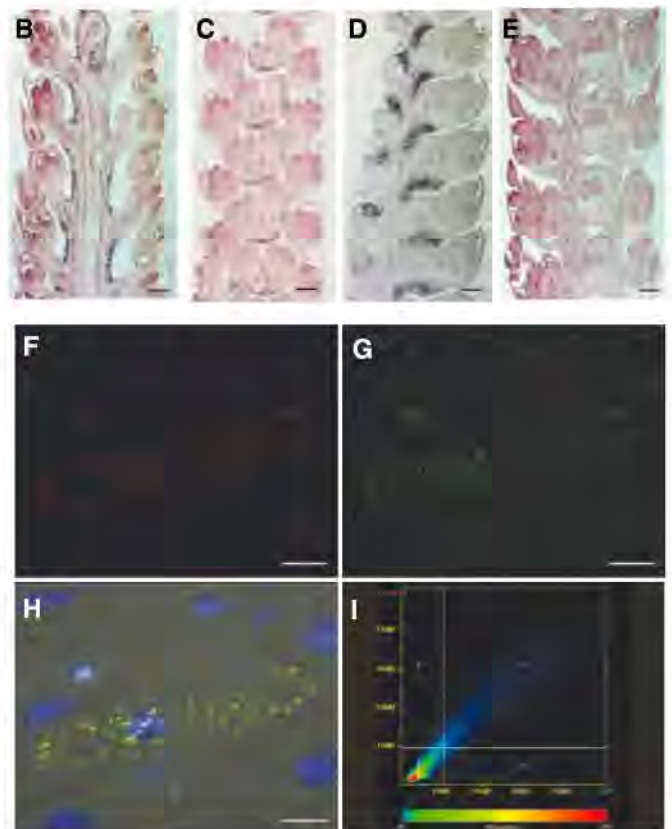
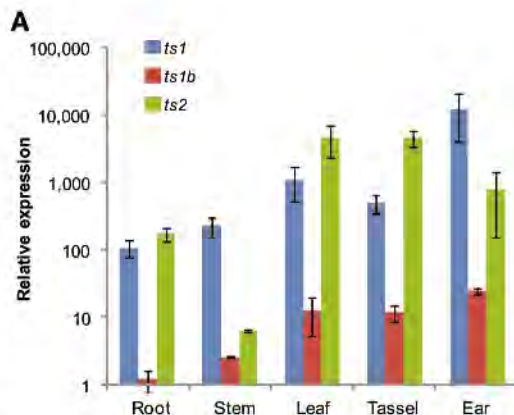


Fig. 2. (A) Expression profile of *ts1*, *ts1b*, and *ts2* in different maize tissues by quantitative RT-PCR on three biological replicates for each tissue. Results are plotted as the ratio to the lowest detected level (*ts1b* in root) \pm SE. Note that the y axis is in logarithmic scale. **(B to E)** RNA in situ hybridization targeting the 3'UTR of *ts1* (dark purple) in developing inflorescences. Scale bars, 200 μ m. **(B)** and **(C)** Wild-type heterozygote male inflorescences (tassels) of 1.6 and 1.5 cm, respectively. **(D)** Wild-type female inflorescence (ear) of 1.5 cm. **(E)** Homozygous *ts1-Mu01* deletion mutant tassel showing no hybridization signal. **(F to I)** Colocalization of TS1:mCherry and RbcSnt:GFP fusion proteins in plastids of transfected onion epidermal cells. Scale bars, 50 μ m. **(F)** TS1:mCherry red fluorescence. **(G)** RbcSnt:GFP green fluorescence. **(H)** Merge of TS1:mCherry and RbcSnt:GFP plus two additional channels: 4',6'-diamidino-2-phenylindole (blue fluorescence) for distinguishing nuclei, and differential interference contrast (DIC) for displaying cellular morphology. **(I)** Scatterplot of pixel gray value frequencies for RbcSnt:GFP (x axis) and TS1:mCherry (y axis) channels. Frequencies are displayed using a rainbow lookup table (bottom, units between 0 and 255). Region 3 (upper right) contains pixels with signal above background in both channels, and a linear correlation in this region is a qualitative indicator of colocalization (12).



observations indicate that *TS1* transcripts subtend maize spikelets at their junction with the central inflorescence axis (rachis). This expression domain suggests a function for *TS1*, as

metabolites synthesized through the lipoxygenase encoded by *ts1* could act as diffusible signals affecting floral development in a non-cell-autonomous fashion.

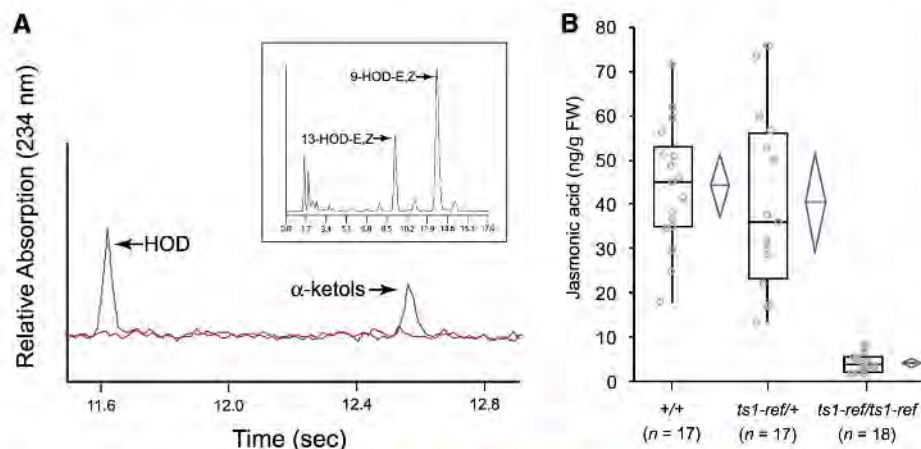


Fig. 3. (A) Partial gas chromatography–MS chromatograms displaying linoleic acid oxidation products generated by crude extracts of wild-type W22 tassels (blue line) but not *ts1-ref* tassels (red line). HPLC analysis of oxidation products (inset) indicated that the lipid hydroperoxide (HOD) peak was a mixture of 9-hydroxy-10,12-octadecadienoic acid (9-HOD) and 13-hydroxy-9,11-octadecadienoic acid (13-HOD). (B) Box plots summarizing the distribution of jasmonic acid in three tassel sets. Gray circles represent individual measurements. Blue diamonds show the 95% confidence interval of the mean (horizontal blue line). *+/+* corresponds to inbred line W22. (C) Blank-treated mutant *ts1* tassel. (D) JA-treated *ts1* tassel. (E) JA-treated *ts2* tassel.

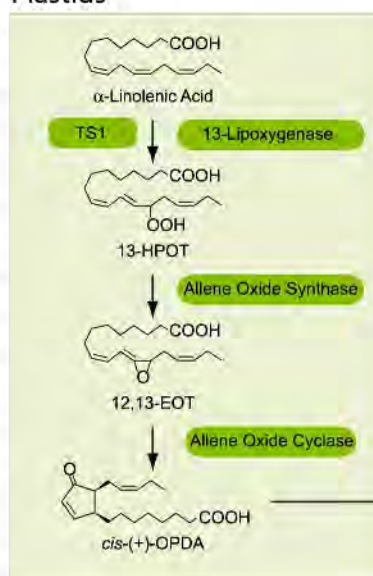


The ChloroP-based prediction that *TS1* localizes in plastids was confirmed with a fluorescent-tagged *TS1* protein (*TS1:mCherry*) and a plastid-localized *RbcSnt:GFP* protein (20). Both fluorescent fusion proteins colocalized in a punctuated pattern throughout the cytoplasm of transfected cells (Fig. 2, F to I), indicating that *TS1:mCherry* protein is targeted to the same subcellular compartment as *RbcSnt:GFP*. Therefore, we conclude that *TS1* is targeted to plant plastids. Biochemical analysis of protein extracts from developing tassels for activity on the lipoxygenase substrate linoleic acid suggests that *TS1* is capable of lipid peroxidation. Protein extracts from wild-type tassels catalyzed hydroperoxidation of linoleic acid, whereas no such activity was detected in mutant *ts1-ref/ts1-ref* developing tassels (Fig. 3A). Mass spectrometry (MS) and high-performance liquid chromatography (HPLC) analyses showed that the products of this lipoxygenase activity are a mixture of 9- and 13-hydroperoxides in a 50:50 ratio (Fig. 3A), a somewhat unexpected result given that *TS1* was predicted to be a lipoxygenase with 13-regiospecificity. Therefore, it is possible that *TS1* possesses dual 9- and 13-regiospecificity—which has not previously been described for a plastid-localized lipoxygenase—or that *TS1* function promotes the action of a separate 9-lipoxygenase.

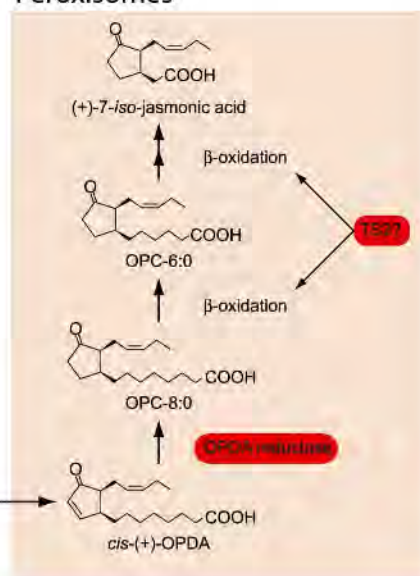
Class 2 13-lipoxygenases participate in the biosynthesis of the plant hormone jasmonic acid (JA) (21) (Fig. 4). We tested whether *TS1* is involved in JA biosynthesis by measuring endogenous JA levels in developing wild-type and *ts1-ref/ts1-ref* mutant tassels. The average concentration of JA in wild-type and *ts1-ref/+* heterozygotes was 44.2 ± 13.9 ng per gram of fresh weight (ng/g FW) and 40.3 ± 20.2 ng/g

Fig. 4. Biosynthesis of jasmonic acid through the octadecanoid pathway [adapted from (21)]. The first dedicated step in jasmonate biosynthesis is the peroxidation of α -linolenic acid (18:3) by 13-lipoxygenase to form (13S)-hydroperoxyoctadecatrienoic acid (13-HPOT). This is the putative function of *TS1*. 13-HPOT is transformed into the specific stereoisomer *cis*-(+)-12-oxophytodienoic acid (OPDA) through the sequential action of allene oxide synthase [yielding (13S)-12,13-epoxy-octadecatrienoic acid (12,13-EOT)] and allene oxide cyclase. These steps in JA biosynthesis occur in plant plastids (green box), where the corresponding enzymes are localized. Subsequent reactions occur in the peroxisomes (red box). First, the cyclopentenone ring of OPDA is reduced to 12-oxophytoic acid (OPC-8) by OPDA reductase. Next, three β -oxidation cycles are proposed to shorten the carboxylic side chain of OPC-8 to produce the 12-carbon JA (21, 24). A β -oxidation cycle is a set of four enzymatic reactions: oxidation, hydration, oxidation, and thiolysis. Not all enzymes acting on β -oxidation during JA biosynthesis have been identified. Because the oxidation in the third step is normally performed by a dehydrogenase activity, it is possible that *TS2* may participate in this step of JA biosynthesis.

Plastids



Peroxisomes



FW, respectively (Fig. 3B). Homozygous *ts1-ref/ts1-ref* tassels showed an average JA concentration of 4.3 ± 2.1 ng/g FW (Fig. 3B), significantly below that of the wild type in a Kruskal-Wallis test and pairwise comparisons with a Bonferroni correction ($P < 0.0001$). Therefore, we estimate that the *ts1* mutation reduces JA levels by a factor of ~ 10 , indicating a role for the hormone in the pistil cell death process. Note that JA levels of wild-type and mutant *ts1* tassels are similar to those of wounded and nonwounded maize seedlings, respectively (22), which supports the notion that JA is actively synthesized during normal tassel development.

The developmental timing of the pistil abortion process occurs in tassel inflorescences when they are 1.0 to 3.0 cm in length (23), which was also the stage at which *ts1* expression occurred in the subtending glumes (Fig. 2, B to D). We applied 0.005% ethanol with or without 1 mM JA to tassels of ~ 1 cm in wild-type (*ts1-ref/+*) or *ts1* mutant (*ts1-ref/ts1-ref*) sibling plants (12). In *ts1* mutant plants, JA application reversed feminization, as evidenced by the presence of staminate spikelets mostly in the mid- to apical regions (Fig. 3D). Wild-type rescue in *ts1* mutants was observed in the appearance of subtending floral bracts (glumes) about 3 to 4 weeks after treatment. JA-treated glumes in *ts1* mutants were elongated, were covered with numerous trichomes, and had a ring of anthocyanin deposited at the base (Fig. 3D), all three characteristics of wild-type staminate spikelets. Later in floral development, stamens emerged from JA-treated *ts1* mutant spikelets (fig. S5B).

Staminate florets from rescued JA-treated *ts1/ts1* plants produced viable pollen, which was used for both self-pollination and test crosses to untreated *ts1/ts1* mutant sibs. All test cross progeny ($n > 100$) were homozygous for the *ts1-ref* allele and displayed a complete *ts1* mutant phenotype. The JA-rescued phenotype of the tassel inflorescence was incomplete in that some spikelets were bisexual (fig. S5A), containing both pistils and stamens, and others (mainly those located at the base of the inflorescence) were pistillate. These effects, however, may have been due to the timing of JA treatments, because the stage of floral maturation differs in a positionally dependent fashion throughout the inflorescence. Rescued staminate spikelets were never observed in blank-treated *ts1-ref/ts1-ref* plants (Fig. 3C, fig. S5D, and table S2), nor did JA treatment affect heterozygous *ts1-ref/+* sibs (table S2). The similar phenotype of *ts1* and *ts2* mutations indicates that both genes may act in the same metabolic pathway. Therefore, we also applied JA to mutant *ts2-ref/ts2-ref* and *ts2-ref/+* plants, which responded in the same manner as the JA-treated *ts1* mutants (Fig. 3E, fig. S5C, and table S2). These results indicate that JA can restore the wild-type phenotype in both *ts1* and *ts2* mutant

plants. Moreover, this suggests an unexpected role for TS2 in JA biosynthesis, perhaps as one of the yet-unidentified enzymes catalyzing a series of β -oxidations in this metabolic pathway (Fig. 4) (24).

Genes regulating meristem determinacy early in maize inflorescence development are expressed at the boundary of the meristem and the inflorescence axis rather than within the meristem itself. These genes, such as *ramosa1*, *ramosa3*, and *barren stalk1* (25–27), probably act non-cell-autonomously by producing a diffusible signal at the base of the meristem (27). Analogously, *ts1* expression at the boundary of developing spikelet initials and inflorescence axis produce the hormone JA, which may diffuse within the spikelet to regulate sexual development. This situation parallels JA-mediated anther dehiscence in *Arabidopsis*, where JA biosynthetic genes are highly expressed in the anther filament where it signals development both in the filament and within the anther (28, 29). We previously reported that the expression of *ts2* is reduced in *ts1* mutants (8). The finding that *ts2* may be involved in the same biosynthetic pathway as *ts1* is not necessarily at odds with our previous observation, as most genes encoding enzymes of the JA biosynthetic pathway are transcriptionally up-regulated by JA in a characteristic positive feedback loop (21).

JA signals plant responses to biotic and abiotic stresses (21) and regulates plant developmental processes such as root growth (30) and mechanotransduction (31). In *Arabidopsis*, JA is required for male fertility because pollen maturation and anther dehiscence are blocked in mutations that impair JA biosynthesis (28, 29). JA may promote anther dehiscence by signaling degeneration of the stomium, a group of specialized cells that run along the length of the anther and are necessary for dehiscence (32, 33).

The plant hormone ethylene has been observed to promote feminization in cucumber [reviewed in (34)]. Recent genetic and biochemical evidence has confirmed the role of ethylene in sex determination of melon, a related species (35). Conversely, gibberellin has masculinizing effects in cucumber but promotes feminization in maize (36), and auxin also has opposing effects in cucumber and *Mercurialis annua* (34). The present results imply a role for JA in maize sex determination, wherein JA is necessary for signaling the *tasselseed*-mediated pistil abortion and the acquisition of the male characteristics of staminate spikelets. The diverse mechanisms of hormonal control in plant sex determination support the notion that the systems have evolved independently multiple times (37).

References and Notes

1. S. L. Dellaporta, A. Calderon-Urrea, *Science* **266**, 1501 (1994).

2. E. Irish, *Bioessays* **18**, 363 (1996).
3. O. T. Bonnet, *J. Agric. Res.* **60**, 25 (1940).
4. T. Kiesselbach, *The Structure and Reproduction of Corn* (Univ. of Nebraska Press, Lincoln, NE, 1949).
5. P. C. Cheng, R. I. Gryson, D. B. Walden, *Am. J. Bot.* **70**, 450 (1983).
6. R. A. Emerson, *J. Hered.* **11**, 65 (1920).
7. N. H. Nickerson, E. E. Dale, *Ann. Mo. Bot. Gard.* **42**, 195 (1955).
8. A. Calderon-Urrea, S. L. Dellaporta, *Development* **126**, 435 (1999).
9. J. C. Kim *et al.*, *Genetics* **177**, 2547 (2007).
10. A. DeLong, A. Calderon-Urrea, S. L. Dellaporta, *Cell* **74**, 757 (1993).
11. X. Wu *et al.*, *FEBS J.* **274**, 1172 (2007).
12. See supporting material on Science Online.
13. J. Salse, B. Piegu, R. Cooke, M. Delseny, *Plant J.* **38**, 396 (2004).
14. B. S. Gaut, *Genome Res.* **11**, 55 (2001).
15. D. Shibata, B. Axelrod, *J. Lipid Mediat. Cell Signal.* **12**, 213 (1995).
16. I. Feussner, C. Wasternack, *Annu. Rev. Plant Biol.* **53**, 275 (2002).
17. O. Emanuelsson, H. Nielsen, G. von Heijne, *Protein Sci.* **8**, 978 (1999).
18. E. Hornung, M. Walther, H. Kuhn, I. Feussner, *Proc. Natl. Acad. Sci. U.S.A.* **96**, 4192 (1999).
19. A. Liavonchanka, I. Feussner, *J. Plant Physiol.* **163**, 348 (2006).
20. K. H. Lee, D. H. Kim, S. W. Lee, Z. H. Kim, I. Hwang, *Mol. Cells* **14**, 388 (2002).
21. C. Wasternack, *Ann. Bot.* **100**, 681 (2007).
22. J. Engelberth, I. Seidl-Adams, J. C. Schultz, J. H. Tumlinson, *Mol. Plant Microbe Interact.* **20**, 707 (2007).
23. E. E. Irish, T. M. Nelson, *Am. J. Bot.* **80**, 292 (1993).
24. S. Goepfert, Y. Poirier, *Curr. Opin. Plant Biol.* **10**, 245 (2007).
25. A. Gallavotti *et al.*, *Nature* **432**, 630 (2004).
26. N. Satoh-Nagasawa, N. Nagasawa, S. Malcomber, H. Sakai, D. Jackson, *Nature* **441**, 227 (2006).
27. E. Vollbrecht, P. S. Springer, L. Goh, E. S. Buckler IV, R. Martienssen, *Nature* **436**, 1119 (2005).
28. S. Ishiguro, A. Kawai-Oda, J. Ueda, I. Nishida, K. Okada, *Plant Cell* **13**, 2191 (2001).
29. P. M. Sanders *et al.*, *Plant Cell* **12**, 1041 (2000).
30. P. E. Staswick, W. Su, S. H. Howell, *Proc. Natl. Acad. Sci. U.S.A.* **89**, 6837 (1992).
31. E. W. Weiler *et al.*, *Phytochemistry* **32**, 591 (1993).
32. P. M. Sanders *et al.*, *Sex. Plant Reprod.* **11**, 297 (1999).
33. P. M. Sanders, A. Q. Bui, B. H. Le, R. B. Goldberg, *Sex. Plant Reprod.* **17**, 219 (2005).
34. S. Yamasaki, N. Fujii, H. Takahashi, *Vitam. Horm.* **72**, 79 (2005).
35. A. Boualem *et al.*, *Science* **321**, 836 (2008).
36. R. Bensen *et al.*, *Plant Cell* **7**, 75 (1995).
37. C. Ainsworth, J. Parker, V. Buchanan-Wollaston, *Curr. Top. Dev. Biol.* **38**, 167 (1998).
38. We thank S. Hake, P. Chomet, and B. Lowe for providing *ts2* mutant alleles; A. Signorovitch and R. Rosengarten for help with phylogenetic analyses; E. Bortiri, C. Whipple, P. Bommert, and D. Jackson for advice on *in situ* hybridizations; I. Hwang for the pRbcSnt:GFP construct; and R. Tsien for the *mCherry* gene. Supported by NIH grant R01 GM38148 (S.L.D.) and USDA grant 99-35301-8048 (J.P.M.). Sequences obtained in this study were deposited in GenBank (accession numbers FJ360855 and FJ360856).

Supporting Online Material

www.sciencemag.org/cgi/content/full/323/5911/262/DC1
Materials and Methods

SOM Text

Figs. S1 to S5

Tables S1 to S5

References

14 August 2008; accepted 10 November 2008
10.1126/science.1164645

Structure of a Type IV Secretion System Core Complex

Rémi Fronzes,¹ Eva Schäfer,^{1*} Luchun Wang,^{1*} Helen R. Saibil,¹ Elena V. Orlova,¹ Gabriel Waksman^{1,2†}

Type IV secretion systems (T4SSs) are important virulence factors used by Gram-negative bacterial pathogens to inject effectors into host cells or to spread plasmids harboring antibiotic resistance genes. We report the 15 angstrom resolution cryo-electron microscopy structure of the core complex of a T4SS. The core complex is composed of three proteins, each present in 14 copies and forming a ~1.1-megadalton two-chambered, double membrane-spanning channel. The structure is double-walled, with each component apparently spanning a large part of the channel. The complex is open on the cytoplasmic side and constricted on the extracellular side. Overall, the T4SS core complex structure is different in both architecture and composition from the other known double membrane-spanning secretion system that has been structurally characterized.

Type IV secretion systems (T4SSs) are macromolecular nanomachines utilized for the transport of proteins or DNA across the bacterial cell envelope of Gram-negative bacteria (1, 2). The archetypal *Agrobacterium tumefaciens* T4SS comprises 12 proteins named VirB1 through VirB11 and VirD4. T4SSs in other bacteria can display additional components or have homologs for only a subset of those proteins (1). T4SSs likely span the periplasm and both bacterial membranes. An extracellular pilus is associated with some T4SSs and is composed of a major (VirB2) and a minor (VirB5) subunit. Three adenosine triphosphatases (ATPases), VirB4, VirB11, and VirD4, are involved in substrate secretion and in system assembly. VirB6, VirB8, and VirB10 may form an inner membrane channel (3, 4). At the outer membrane, the composition of the pore is unknown. The periplasmic protein VirB9 in complex with the short lipoprotein VirB7 could be part of this structure (5, 6). However, no transmembrane region could be found or predicted in either protein.

Moreover, VirB9 proteins share no sequence similarities with outer membrane secretins. Protein-protein interaction studies have identified a core T4SS complex consisting of four proteins, VirB7, 8, 9, and 10 (1, 7). Together with VirB4, this T4SS core complex is the minimal functional entity (8, 9). Here, we provide structural and functional insights on the equivalent core T4SS complex encoded by the plasmid pKM101.

The *virB7-10* gene cluster of the pKM101 plasmid was cloned and expressed (10). In this cluster, these genes are named *traN*, *traE*, *traO*, and *traF*, respectively. For clarity, each gene and protein will be named hereafter using both the Tra and VirB nomenclatures. Cloning of the *traN/virB7-traF/virB10* cluster introduced a Strep-tag at the C terminus (C-ST) of TraF/VirB10 (TraF/VirB10_{C-ST}) (fig. S1, A and B). Induction of gene expression, preparation of the membrane fraction followed by solubilization of membrane proteins, and a two-step purification procedure resulted in the purification of a complex containing TraN/VirB7, TraO/VirB9, and TraF/VirB10_{C-ST} [the “wild-type core” complex (Fig. 1A) (10)]. TraE/VirB8 (although strongly expressed) was not present in the purified complex. The stoichiometry of the different components of the core complex was shown to be 1:1:1 (fig. S1C) (10). The core TraN/VirB7-TraO/VirB9-TraF/VirB10

complex purified as a ~1100-kD complex (Fig. 1B) (10). Wild-type core complexes were then visualized by negative-stain electron microscopy (EM) (10). We observed ringlike and multilayered particles, corresponding to end and side views of the complex, respectively (fig. S2A). Rotational symmetry analysis of end-view class averages revealed a clear 14-fold symmetry (fig. S2) (10). Thus, the T4SS core complex is formed of 14 copies each of three proteins.

The importance and role of TraN/VirB7 lip- idation on core complex formation and local- ization were examined. TraN/VirB7 becomes acylated on Cys¹⁵ (11). This residue was mu- tated to Ser (TraN_{Cys15Ser}) (fig. S3A), and the resulting *traN/virB7_{Cys15Ser}-traF/virB10_{C-ST}* cluster was expressed (10). A complex (ΔL1) similar in size to the wild-type core complex was pu- rified (fig. S3A). Thus, lipidation of TraN/VirB7 is not required for core complex formation. We next examined the membrane localization of the ΔL1 core complex and established that both the wild-type and ΔL1 core complexes reside in the inner membrane; however, only the wild- type core complex is found in the outer membrane (fig. S3A) (10). Thus, lipidation of TraN/VirB7 is required for targeting of the core complex to the outer membrane. This interpretation was con- firmed by accessibility studies on whole cells (fig. S3B) (10). Finally, we investigated the role of each of the genes in the *traN/virB7-traF/virB10* cluster by deleting them one at a time and dem- onstrated that TraE/VirB8 is not involved in the assembly of the core complex but that TraN/VirB7, TraO/VirB9, and TraF/VirB10 are essential for the formation of the 14-oligomer ring complex (fig. S3) (10).

To obtain a detailed view of the three- dimensional (3D) structure of the TraN-TraO- TraF_{C-ST} complex, a cryo-electron microscopy (cryo-EM) data set was collected and used to reconstruct a 15 Å resolution 3D map of the complex with 14-fold symmetry (fig. S4) (10). The final structure is shown in Fig. 2. The T4SS core complex has an overall dimension of 185 Å in both height and diameter (Fig. 2). It is made of two main layers, labeled inner (I) and outer (O) with reference to the orientation, which will be

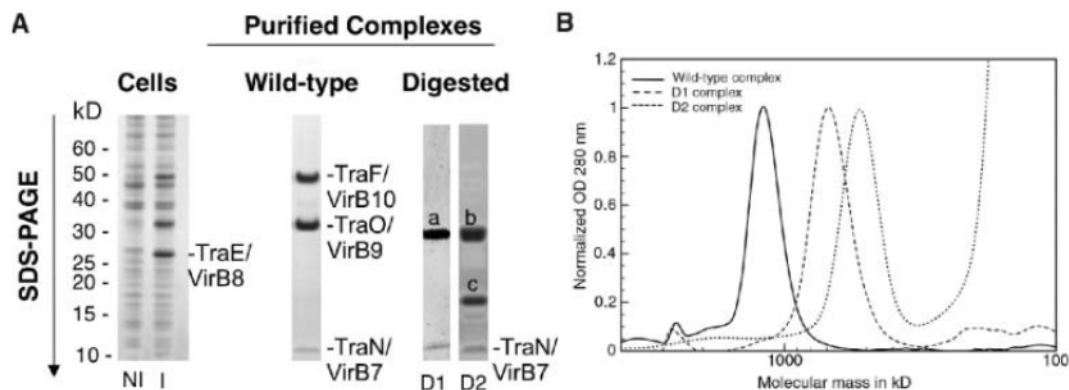
¹Institute of Structural and Molecular Biology, School of Crystallography, Birkbeck College, Malet Street, London, WC1E 7HX, UK. ²Division of Biosciences, University College London, Gower Street, London, WC1E 6BT, UK.

*These authors contributed equally to this work.

†To whom correspondence should be addressed. E-mail: g.waksman@ucl.ac.uk, g.waksman@mail.cryst.bbk.ac.uk

Fig. 1. Purification of the pKM101-encoded T4SS complex core. (A) SDS-polyacrylamide electrophoresis analysis of the noninduced (NI) and induced (I) cells (left), the pure wild-type core complex (middle), and digested D1 and D2 complexes (right). (Right) The top left band, a, contains a C-terminal fragment of TraF/VirB10 and full-length TraO/VirB9; the top right band, b, contains a C-terminal fragment of TraF/VirB10, and the middle band, c, which contains a C-terminal fragment of TraO/VirB9.

The content of the a, b, and c bands was assessed by mass spectrometry and N-terminal sequencing. (B) Gel filtration of the wild-type, D1, and D2 complexes.



discussed later (Fig. 2A). Both layers are either in part (the I layer) or entirely (the O layer) composed of two walls (Fig. 2B).

The O layer consists of two regions: the cap, which is 110 Å in diameter and 40 Å high, and the main body, which is 185 Å in diameter

and 60 Å high (Fig. 2A). In the cap, the internal wall forms a 20 Å hole that tapers off to a 10 Å diameter constriction at the main body (Fig. 2B). In the main body, the internal wall forms a chamber (Fig. 2B) that is 110 Å wide and 30 Å high. Internal protuberances are clearly visible at

the bottom of the chamber; these leave a large opening of 55 Å.

The I layer resembles a cup. It is linked to the O layer by thin stretches of density. The two walls of the cup merge into a single wall near the base. The internal wall defines a chamber that is as wide as the chamber in the O layer, but double the height at 60 Å. This chamber tapers off at the bottom to a diameter of 55 Å, where it reaches the 30 Å high base from which 14 fingers of density extend downwards.

To locate specific proteins in the core complex, we used limited proteolysis followed by imaging of the resulting complexes by either negative-stain or cryo-EM (10). A limited proteolysis performed at low trypsin concentration (2 µg/ml) generated a first subcomplex (D1) of ~700 kD, where the residues 1 to 129 of TraF/VirB10 were removed from the core complex (Fig. 1). More extensive digestion with 2 mg/ml trypsin produced a second subcomplex of ~500 kD (D2) in which residues 1 to 155 of TraF/VirB10 and residues 1 to 149 of the mature TraO/VirB9 were removed (Fig. 1).

Both the D1 and D2 complexes were visualized using negative-stain, and a cryo-EM structure was determined for D2 (figs. S2 and S4). Particles in the D1 negative-stain and D2 negative-stain EM data sets exhibited clear 14-fold symmetry (fig. S2E). The only difference between the negative-stained wild-type and D1 complex structures is the disappearance of the base in the I layer, indicating that the base is made of the N terminus of TraF/VirB10 (Fig. 3, A and B). As this part of TraF/VirB10 is known to insert in the inner membrane, this observation was used to orient the complex and positioned the I layer toward the inner membrane and the O layer toward the outer membrane.

Comparison of the cryo-EM structures of the wild-type and D2 complexes (Fig. 3, C and D) demonstrates that the structure of the O layer in the wild-type core complex is similar to that of the D2 complex. Thus, given that the composition of the D2 complex is known (Fig. 1), we can conclude that the O layer is mainly composed of the C-terminal domain of TraF/VirB10 (TraF/VirB10_{Cterm} residues 156 to 386), the C terminus of TraO/VirB9 (TraO/VirB9_{Cterm} residues 150 to 271 of the mature protein), and TraN/VirB7 (Figs. 1 and 3E). Fourteen of each of these would give a mass of 602 kD, consistent with the complex mass calculated from the cryo-EM map (647 kD when the volume is calculated on the basis of a mass of 1050 kD for the whole structure). This implies that the I layer is composed of the N-terminal regions of TraF/VirB10 and TraO/VirB9, a conclusion also supported by the small difference between the wild-type and D1 negative-stain structures in the base region of the I layer.

To confirm the placement of the N terminus of TraF/VirB10 at or near the base of the I layer, a sequence encoding a His₆-tag was introduced at the 5' end of the *traF/virB10* gene (resulting

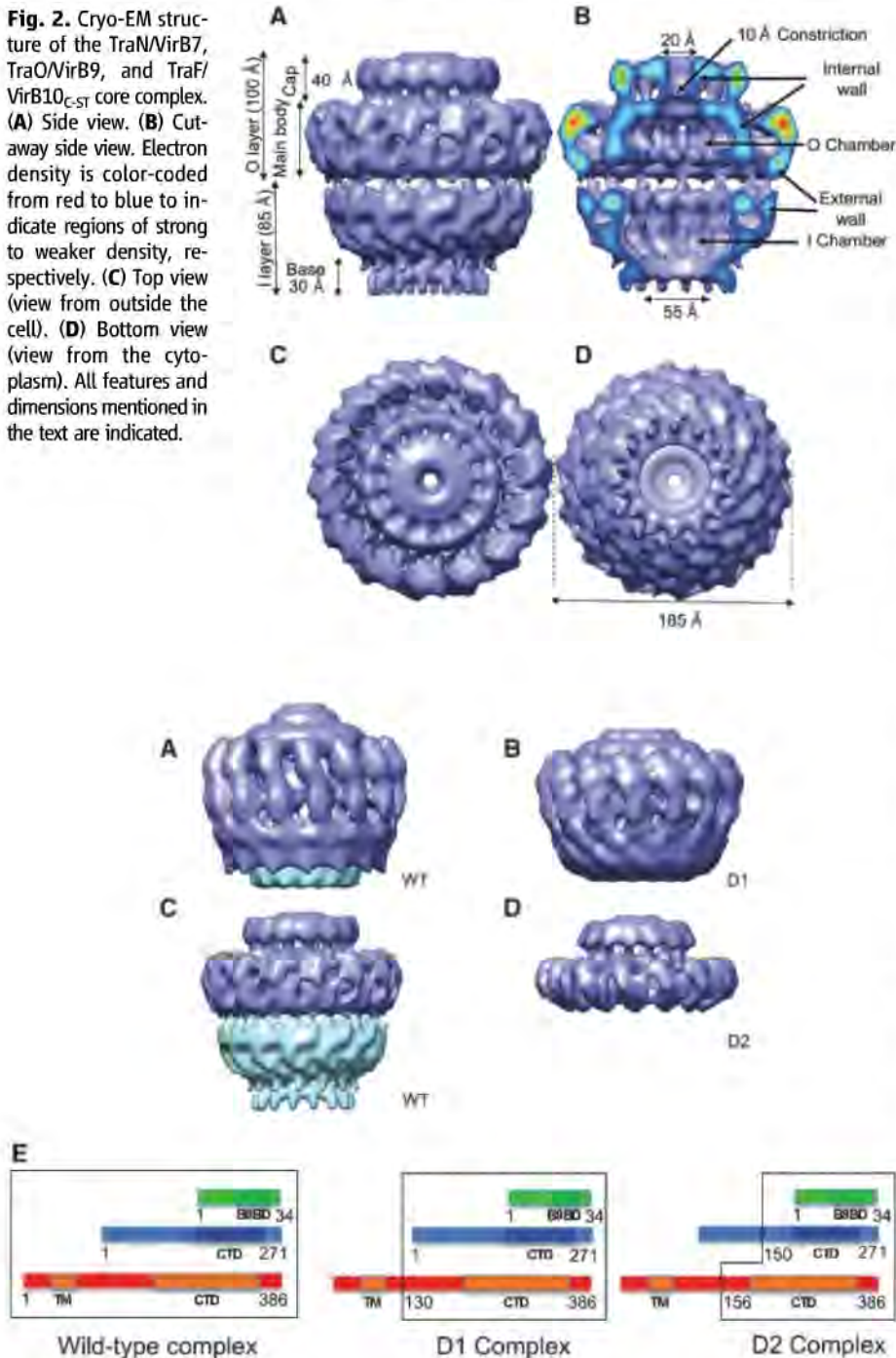


Fig. 3. Comparison of the structures of the wild-type complex, (A) and (C); D1, (B); and D2, (D); as revealed by negative-stain EM (A) and (B) and cryo-EM (C) and (D). Parts removed by proteolysis are shown in cyan. (E) Schematic diagrams of the composition of each of the complexes. TraN, TraO, and TraF are in the same representation and color-coding as in fig. S1A. Numbering for TraN and TraO are for the mature proteins (signal sequence excluded). A black outline encloses the parts of the proteins included in the various complexes.

in the *traN*-*N418*/*traF*-*C57* cluster) (10). The resulting core complex is similar to the wild-type complex. When incubated with His₆-specific antibodies and imaged using negative-stain EM (10), this complex shows clear additional electron density in the vicinity of the base of the I layer in both the raw data and class averages (Fig. 4A).

From the known data, the most likely region of the O layer to insert in the outer membrane is the C-terminal domain of TraO/VirB9 (12). The structure of this domain bound to TraN/VirB7 (12) shows a three-stranded β appendage in TraO, which loosely associates with the TraO β barrel. This β appendage was hypothesized to undergo a large conformational change to protrude out of the cell (12). It is likely that the structure adopted by this region of the TraO/VirB9 C-terminal domain forms one of the two walls in the cap region of the O layer, which suggests that the cap is inserted in the outer membrane. Thus, the O and I chambers likely form a periplasmic channel, which extends over a distance of 105 Å, a distance comparable to that observed in the WzA/WzC complex, where the two transmembrane regions are 100 Å apart (13) (fig. S5B).

The known structure of the C-terminal domain of the ComB10 protein (a structural prototype for C-terminal domains of VirB10 homologs) was fitted into the electron density of the external wall of the O layer's main body, with its N terminus directed toward the I layer (fig. S5D)

(10, 14). The rationale for locating the structure in that region is threefold: (i) in terms of shape complementarity, this is the only part of the O-layer electron density where the structure can fit; (ii) the goodness-of-fit parameter is high [0.48 as determined by SITUS (15)]; (iii) this external wall of the O layer is not accessible to the substrate, and it has been shown that, in *A. tumefaciens*, the substrate does not contact VirB10 directly during transfer (16). In the proposed location, VirB10 would be in an ideal position to play its role of energy transducer that has been characterized in the *A. tumefaciens* T4SS. In *A. tumefaciens*, VirB10 undergoes a conformational change induced by the inner membrane ATPases and the presence of adenosine triphosphate, a conformational change that is required to bring VirB9 and VirB10 together and to activate the T4SS (17). Clearly, in the pKM101 T4SS, the ATPases are not required to bring the two proteins together because the core complex forms spontaneously in the presence of the three core proteins TraN/VirB7, TraO/VirB9, and TraF/VirB10; however, they may be necessary for activation of the machinery. We suggest that ATPase function (perhaps together with VirB6 and VirB8) at the inner membrane induces conformational changes in the C-terminal domain of VirB10 that results in the opening of the constriction in the cap, which is required to allow passage of nucleoprotein complexes.

Our interpretation of the data presented here can be summarized in a model in which TraF/VirB10 forms the major part of the outer surface of the core complex (except the cap), whereas TraO/VirB9 together with TraN/VirB7 form the internal walls of the core complex. In that configuration, TraF/VirB10 would not directly take part in substrate transfer, but would play a role in reshaping the inner TraO surface to allow passage of the substrate through the O-layer cap (Fig. 4B).

The structure of the core T4SS machinery presented here is different from that of the type III secretion system (T3SS) (18) (fig. S5C). Indeed, the components of the two systems share no sequence similarity, and the envisaged multimerization order of each component is different. T4SSs have likely evolved the architecture revealed here in order to secrete a wide variety of substrates including large DNA-protein complexes.

References and Notes

1. P. J. Christie, K. Atmakuri, V. Krishnamoorthy, S. Jakubowski, E. Cascales, *Annu. Rev. Microbiol.* **59**, 451 (2005).
2. G. Schröder, E. Lanka, *Plasmid* **54**, 1 (2005).
3. L. Krall et al., *Proc. Natl. Acad. Sci. U.S.A.* **99**, 11405 (2002).
4. D. V. Ward, O. Draper, J. R. Zupan, P. C. Zambryski, *Proc. Natl. Acad. Sci. U.S.A.* **99**, 11493 (2002).
5. S. J. Jakubowski, E. Cascales, V. Krishnamoorthy, P. J. Christie, *J. Bacteriol.* **187**, 3486 (2005).
6. C. Baron, Y. R. Thorstenson, P. C. Zambryski, *J. Bacteriol.* **179**, 1211 (1997).
7. A. Das, Y. H. Xie, *J. Bacteriol.* **182**, 758 (2000).
8. Z. Liu, A. N. Binns, *J. Bacteriol.* **185**, 3259 (2003).
9. R. L. Harris, V. Homb, P. M. Silverman, *Mol. Microbiol.* **42**, 757 (2001).
10. Materials and methods, supporting text, and figures are available as supporting materials on Science Online.
11. D. Fernandez et al., *J. Bacteriol.* **178**, 3156 (1996).
12. R. Bayliss et al., *Proc. Natl. Acad. Sci. U.S.A.* **104**, 1673 (2007).
13. R. F. Collins et al., *Proc. Natl. Acad. Sci. U.S.A.* **104**, 2390 (2007).
14. L. Terradot et al., *Proc. Natl. Acad. Sci. U.S.A.* **102**, 4596 (2005).
15. W. Wriggers, R. A. Milligan, J. A. McCammon, *J. Struct. Biol.* **125**, 185 (1999).
16. E. Cascales, P. J. Christie, *Science* **304**, 1170 (2004).
17. E. Cascales, P. J. Christie, *Proc. Natl. Acad. Sci. U.S.A.* **101**, 17228 (2004).
18. T. C. Marlovits et al., *Science* **306**, 1040 (2004).
19. This work was funded by research grants from the Wellcome Trust to G.W. and UK Biotechnology and Biological Sciences Research Council to H.R.S. and by an equipment grant from the Wellcome Trust to H.R.S. and E.V.O. Also, H.R.S. and E.V.O. thank the European Union Network of Excellence in Three-Dimensional Electron Microscopy (3DEM) for support. EM maps have been deposited to the EM data bank under the entry codes EMD-5031 to EMD-5035 for cryo-EM wild-type, negative-stain EM wild-type, negative-stain EM D1, cryo-EM D2, and negative-stain Δ L2 complexes, respectively.

Supporting Online Material

www.sciencemag.org/cgi/content/full/323/5911/266/DC1
Materials and Methods

Figs. S1 to S6

Table S1

References

18 September 2008; accepted 14 November 2008

10.1126/science.1166101

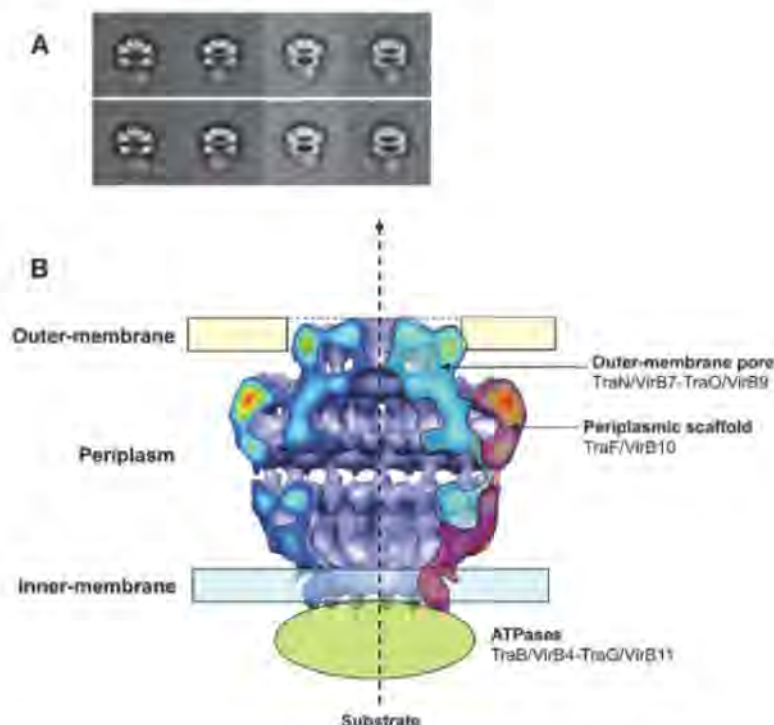


Fig. 4. Localization of core complex macromolecular components to the various regions of the cryo-EM structure. (A) Immunolocalization of the N terminus of TraF/VirB10 by negative-stain EM. Representative class averages are shown, with (bottom) additional density due to His₆-specific antibodies colored in red. (B) Localization of TraO/VirB9 (blue) and TraF/VirB10 (red) within the cryo-EM structure of the wild-type core complex.

AMPylation of Rho GTPases by *Vibrio* VopS Disrupts Effector Binding and Downstream Signaling

Melanie L. Yarbrough,¹ Yan Li,^{2,3} Lisa N. Kinch,⁴ Nick V. Grishin,⁴ Haydn L. Ball,^{2,3} Kim Orth^{1*}

The *Vibrio parahaemolyticus* type III effector VopS is implicated in cell rounding and the collapse of the actin cytoskeleton by inhibiting Rho guanine triphosphatases (GTPases). We found that VopS could act to covalently modify a conserved threonine residue on Rho, Rac, and Cdc42 with adenosine 5'-monophosphate (AMP). The resulting AMPylation prevented the interaction of Rho GTPases with downstream effectors, thereby inhibiting actin assembly in the infected cell. Eukaryotic proteins were also directly modified with AMP, potentially expanding the repertoire of posttranslational modifications for molecular signaling.

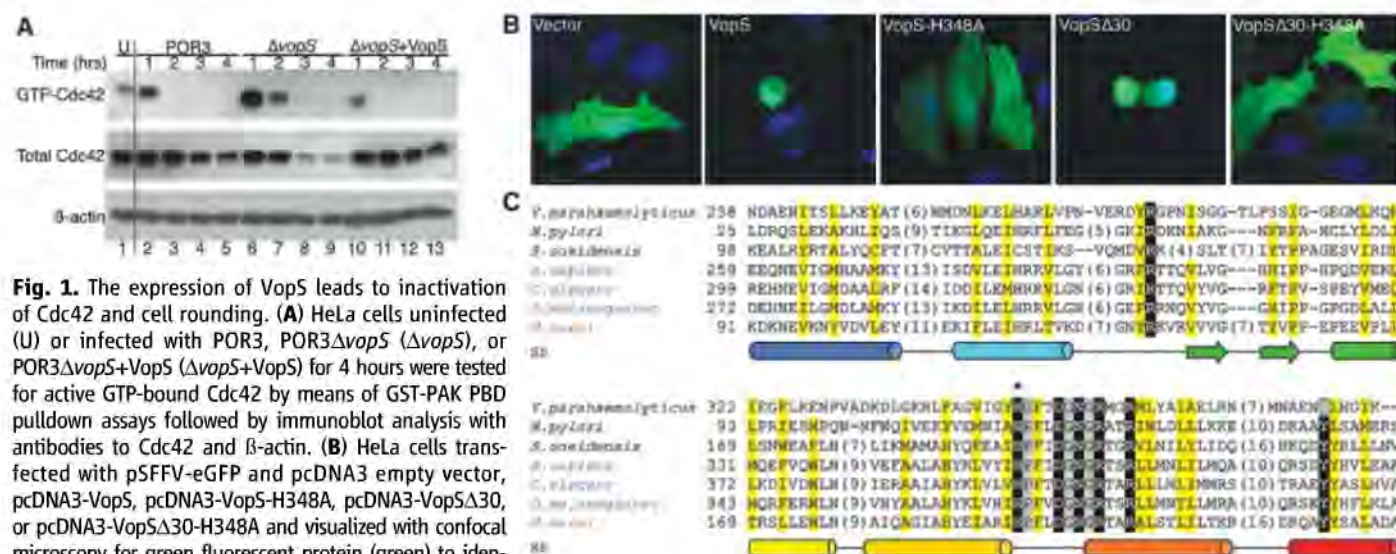
Vibrio parahaemolyticus is a Gram-negative halophilic bacterium that causes foodborne illness worldwide, and infections with it lead to acute gastroenteritis (1). Sequencing of a pathogenic strain of *V. parahaemolyticus* revealed the presence of a previously well-characterized virulence factor called the thermostable direct hemolysin (TDH) and two type III secretion systems (T3SSs) (2, 3). These bacterial T3SSs deliver proteins, called

effectors, into the cytosol of host cells during infection (4). The first system on chromosome one, T3SS1, uses a multifaceted mechanism to cause the cytotoxicity of host cells, involving the induction of autophagy, cell rounding, and cell lysis (5). These events occur in parallel, using multiple effectors to induce cytotoxicity.

The T3SS1 effector VopS (VP1686) was implicated in cell rounding by its inactivation of Rho family guanine triphosphatases (GTPases), including Rac, Rho, and Cdc42 (6). After 1 hour of infection of HeLa cells with the *V. parahaemolyticus* POR3 strain, which contains a functional T3SS1 and inactivating mutations for both TDHs and T3SS2 (7), we observed the presence of active GTP-bound Cdc42, as measured by the ability of Cdc42 to interact with a glutathione *S*-transferase (GST) fusion of its downstream effector, the p21-activated kinase 3 Cdc42-protein binding

domain (GST-PAK PBD) (Fig. 1A). Beyond 1 hour after infection, the presence of VopS in the POR3 strain was consistent with the inactivation of Cdc42, because the population of active GTP-bound Cdc42 was no longer observed (Fig. 1A). In cells infected with a VopS deletion strain (POR3ΔvopS), levels of Cdc42 in the active GTP-bound state persisted, but all Cdc42 was eventually inactivated by 4 hours, suggesting the presence of another factor contributing to the destabilization of Rho family GTPases (Fig. 1A). Reconstitution of the POR3ΔvopS strain with wild-type VopS caused a loss of active Cdc42 1 hour after infection, similar to that seen in the POR3 strain (Fig. 1A). During infection with all three strains, the total level of Cdc42 was reduced at the later time points of infection. However, cell rounding was delayed in the POR3ΔvopS strain occurring at 2 hours after infection (Fig. 1A and fig. S1A).

The expression of full-length VopS induced a severely rounded phenotype in transfected HeLa cells, probably due to a VopS-dependent disruption of Rho GTPase signaling (Fig. 1B). VopS includes a C-terminal domain of unknown function called Fic (filamentation induced by cAMP). Fic domains are found in a variety of species and contain an invariant histidine (H) within a conserved motif [HPFX(D/E)GNR] (8, 9) (Fig. 1C). Mutation of the Fic domain at this conserved histidine (VopS-H348A) abrogated the VopS-mediated cell rounding (Fig. 1B). Because VopS is an effector secreted by T3SS1 during infection, we determined whether the secretion signal sequence was required for cell-rounding activity. We observed that transfection of VopSΔ30, a mutant in which the putative signal sequence was



consistent in all Fic domain structures are indicated below the alignment (cylinder for helix and arrow for strand) and are colored from N to C terminus in rainbow succession. An asterisk above the alignment marks the VopS H348 mutation. Alignments refer to the following proteins in the order listed: VopS, GenInfo Identifier 88192876 (gil88192876), gil151567990, gil42794620, gil17544594, gil24582217, and gil21228708.

Fig. 2. VopS inhibits in vitro binding of the Rho GTPase Rac to its downstream effector PAK. (A) GST pull-down of in vitro translated ^{35}S -Rac and GTP- γ -S-loaded ^{35}S -Rac with GST (G), GST-PAK PBD (P), GST-VopS Δ 30 (S), or GST-VopS Δ 30-H348A (H/A). (B) ^{35}S -DA-Rac was pre-incubated with VopS Δ 30 or VopS Δ 30-H348A, followed by a GST pull-down with GST-PAK PBD. (C) ^{35}S -DA-Rac was pre-incubated with decreasing concentrations of VopS Δ 30 or VopS Δ 30-H348A (125 to 0.125 pmol) or left untreated (U), followed by a GST pull-down with GST-PAK PBD or GST alone (G). (D) ^{35}S -DA-Rac was pre-incubated over time with 0.25 pmol of VopS Δ 30 or VopS Δ 30-H348A, followed by a pull-down assay with GST-PAK PBD. Samples were separated by SDS-polyacrylamide gel electrophoresis (SDS-PAGE) and analyzed by autoradiography. Inputs (I) correspond to 5% of material in pull-down.

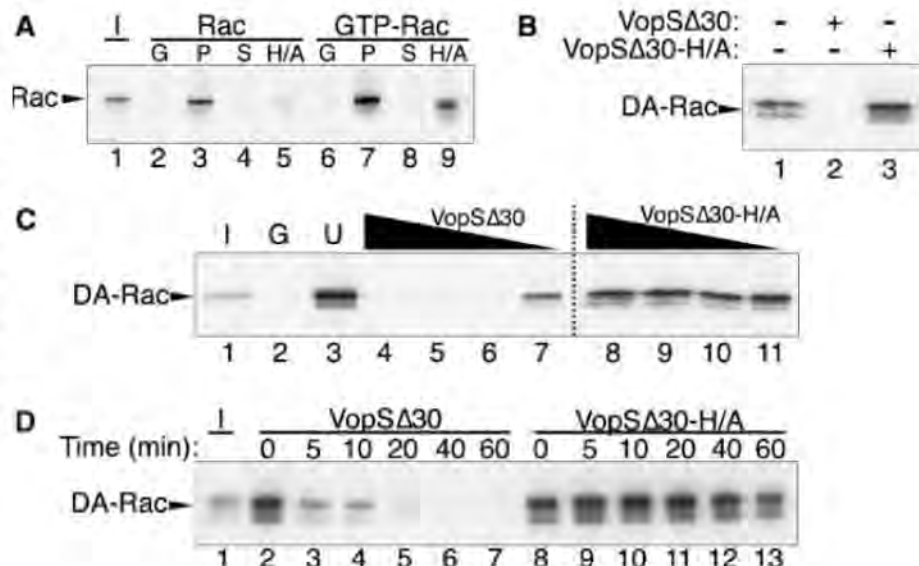
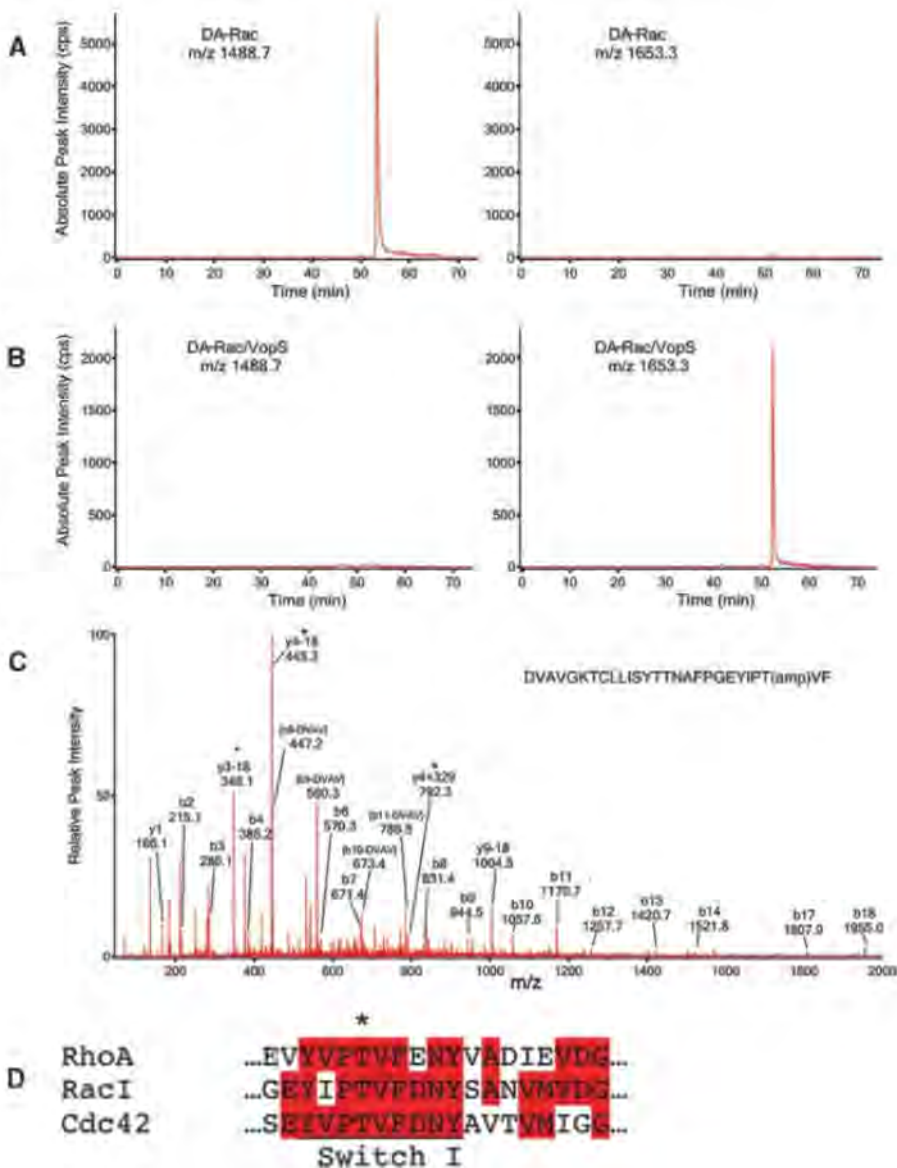


Fig. 3. DA-Rac-VopS is AMPylated on Thr 35 in the switch I region. (A and B) Extracted ion chromatogram (XIC) of the wild-type peptide A ($m/z = 1488.7$) and the modified peptide A ($m/z = 1653.3$) for DA-Rac (A) and DA-Rac/VopS (B). The XIC indicates the intensity of the ion as a function of time during the LC-MS/MS process. (C) Electrospray ionization MS/MS spectra of modified peptide A. The b and y ions are marked on the MS/MS spectra. Ions corresponding to products of internal fragmentation are marked in brackets. Compared to the MS/MS of the wild-type peptide A (see supporting online material), two forms of mass shift were detected, either with a mass decrease of 18 daltons or with a mass increase of 329 daltons. Ions with a mass shift are marked with an asterisk. The mass shift started with y3, indicating that the modification site is Thr 35 . A further cut of peptide A with AspN resulted in an ion corresponding to peptide B (amino acids 32 to 37) with a mass increase of 329 daltons, and the MS/MS spectrum of modified peptide B further confirmed that Thr 35 is the modification site. (D) Alignment of the effector loop region corresponding to residues 32 to 50 of RhoA and 30 to 48 of Rac1 and Cdc42. Conserved residues are shown in red and the switch I region is underlined. The asterisk denotes the AMPylated Thr residue.



deleted, caused rounding of HeLa cells similar to that produced by wild-type VopS (Fig. 1B). As expected, VopSΔ30-H348A did not cause any obvious changes in the actin cytoskeleton of transfected cells (Fig. 1B). Thus, VopS cell-rounding activity is independent of its signal sequence but requires a wild-type Fic domain.

To elucidate the biochemical mechanism used by VopS to inhibit Rho family GTPases, we produced soluble recombinant GST-VopSΔ30 and GST-VopSΔ30-H348A that lacks the largely hydrophobic 30-amino acid signal sequence. Although ³⁵S-radiolabeled Rac (³⁵S-Rac) did not interact with GST-VopSΔ30, it did interact with GST-VopSΔ30-H348A (Fig. 2A). In addition, GTP loading of the ³⁵S-Rac increased the amount of ³⁵S-Rac that interacted with recombinant VopSΔ30-H348A (Fig. 2A), reminiscent of the conformation-dependent interaction of GTP-bound Rac with its downstream effector PAK (10). When we loaded ³⁵S-Rac with GTP, more ³⁵S-Rac interacted with GST-PAK PBD (Fig. 2A). Many type III effectors use a catalytic mechanism to alter eukaryotic signaling pathways, and in some cases the catalytically inactive form of the effector can act as a substrate trap (11). The VopSΔ30-H348A mutant might act as a trap by binding its substrate, the active GTP-bound Rac, but failing to release a product.

To further analyze the possibility that GTP-bound Rho family GTPases might be substrates for VopS, we produced the ³⁵S-radiolabeled constitutively active form of Rac (³⁵S-DA-Rac). We pre-incubated ³⁵S-DA-Rac with 25 pmol of purified recombinant VopSΔ30 or VopSΔ30-H348A

and then tested whether the ³⁵S-DA-Rac was able to interact with its downstream effector GST-PAK PBD. Although ³⁵S-DA-Rac pre-incubated with the mutant VopSΔ30-H348A interacted with GST-PAK PBD, ³⁵S-Rac pre-incubated with VopSΔ30 was unable to interact with GST-PAK PBD (Fig. 2B). We then pre-incubated ³⁵S-DA-Rac with serial 10-fold dilutions of purified recombinant VopSΔ30 (125 to 0.125 pmol) for 15 min and tested whether the ³⁵S-DA-Rac could bind to GST-PAK PBD (Fig. 2C). Incubation of ³⁵S-DA-Rac with as little as 1.25 pmol of VopSΔ30 prevented the binding of ³⁵S-DA-Rac to GST-PAK PBD (Fig. 2C). As expected, the incubation of DA-Rac with decreasing amounts of VopSΔ30-H348A had no effect on the ability of DA-Rac to bind to GST-PAK PBD (Fig. 2C). Next, we incubated ³⁵S-DA-Rac with a limiting amount of VopSΔ30 (0.25 pmol) over 1 hour. By 40 min, no ³⁵S-DA-Rac interacted with GST-PAK PBD (Fig. 2D). Thus, VopS uses an enzymatic activity to inhibit the interaction of Rho family GTPases with their respective downstream effectors.

To determine the activity that VopS exerts on the Rho family GTPases, we expressed histidine-tagged DA-Rac either alone (DA-Rac) or with active GST-tagged VopSΔ30 (DA-Rac/VopS). Both forms of recombinant DA-Rac could be loaded with ³⁵S-radiolabeled GTP-γ-S, a non-hydrolyzable form of GTP, eliminating the possibility that VopS inhibited the Rho family of proteins by preventing GTP binding (fig. S2A). To determine whether DA-Rac was altered by coexpression with VopS, we measured the mass

of recombinant DA-Rac by mass spectrometry. Although DA-Rac had the expected molecular weight, DA-Rac/VopS had an increase in molecular weight of 329 daltons (fig. S2, B and C). As expected, DA-Rac coexpressed with the mutant VopS did not show an increase in molecular weight. The increase of 329 daltons is consistent with the mass of adenosine 5'-monophosphate (AMP). To identify where this putative covalent modification occurred on Rac, we analyzed tryptic and AspN peptides using liquid chromatography followed by tandem mass spectrometry (LC-MS/MS). When the samples were digested with AspN, peptide A [amino acids 11 to 37, mass-to-charge ratio (*m/z*) = 1488.7 when *z* = 2] was observed for DA-Rac (Fig. 3A). For DA-Rac/VopS, only the modified form of peptide A was observed [amino acids 11 to 37, with a mass increase of 329.1 daltons, *m/z* = 1653.3 when *z* = 2] (Fig. 3B). Peptide A contained a covalent modification of 329 daltons on Thr³⁵ (Fig. 3C), a conserved residue located in the effector loop of the switch I region of Rho family GTPases that plays a role in GTP, Mg²⁺, and effector binding (Fig. 3D) (10, 12). Thus, VopS modifies the Rho family GTPases with AMP, which prevents Rho GTPases from binding to downstream effectors by steric hindrance.

To test directly whether VopS functions as an enzyme to modify Rho family GTPases with AMP, we performed an in vitro labeling assay with ³²P-α-labeled adenosine triphosphate (ATP). Incubation of purified recombinant VopSΔ30 with recombinant DA-Rac and ³²P-α-labeled ATP resulted in VopS-dependent modification of DA-Rac

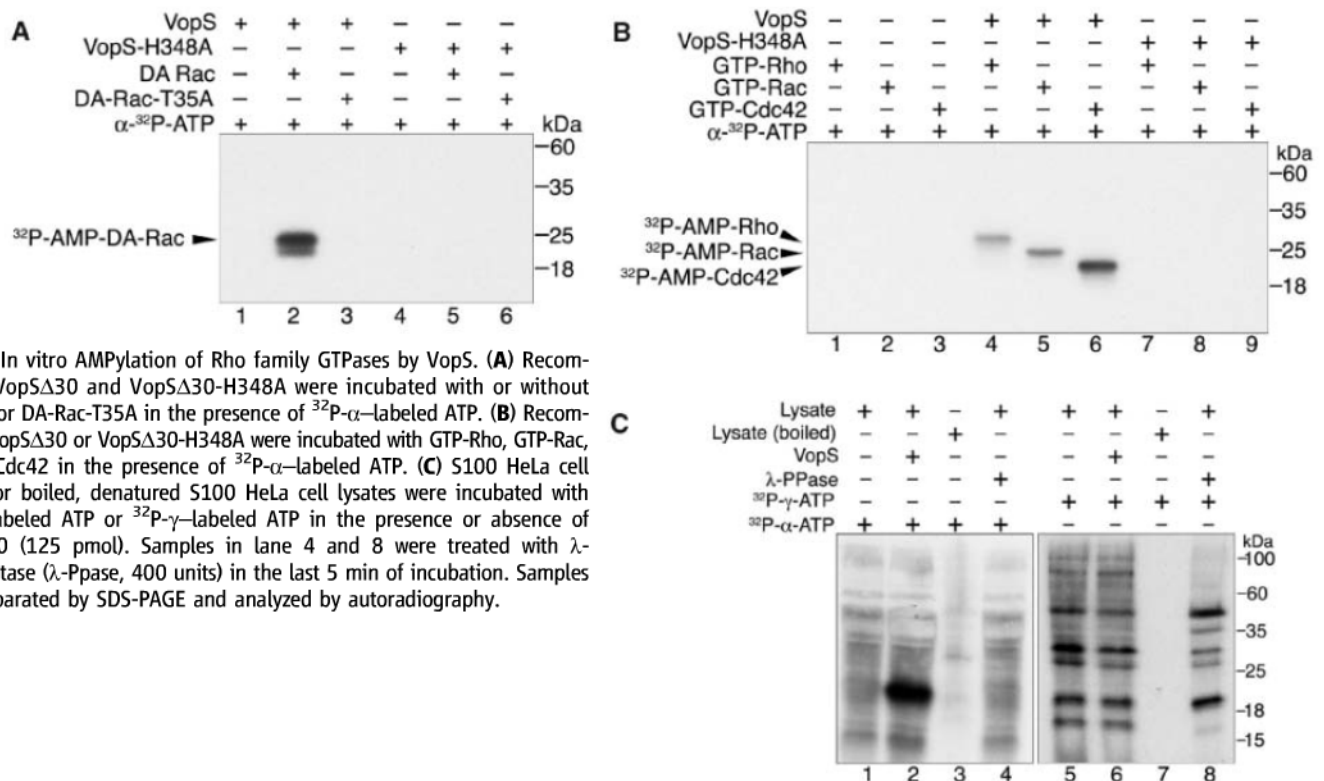


Fig. 4. In vitro AMPylation of Rho family GTPases by VopS. **(A)** Recombinant VopSΔ30 and VopSΔ30-H348A were incubated with or without DA-Rac or DA-Rac-T35A in the presence of ³²P-α-labeled ATP. **(B)** Recombinant VopSΔ30 or VopSΔ30-H348A were incubated with GTP-Rho, GTP-Rac, or GTP-Cdc42 in the presence of ³²P-α-labeled ATP. **(C)** S100 HeLa cell lysates or boiled, denatured S100 HeLa cell lysates were incubated with ³²P-α-labeled ATP or ³²P-γ-labeled ATP in the presence or absence of VopSΔ30 (125 pmol). Samples in lane 4 and 8 were treated with λ-phosphatase (λ-Pase, 400 units) in the last 5 min of incubation. Samples were separated by SDS-PAGE and analyzed by autoradiography.

(Fig. 4A). VopSΔ30 did not modify DA-Rac-T35A, confirming that the AMP modification is specific for Thr³⁵ (Fig. 4A). As expected, DA-Rac incubated with VopS-H348A was not modified (Fig. 4A). To confirm that VopS modifies other members of the Rho family GTPases, we repeated the *in vitro* labeling assay using Rho, Rac, and Cdc42. In the presence of VopS, all of the GTPases were modified with AMP, whereas they were not modified in the presence of ³²P-α-labeled ATP alone or by VopS-H348A (Fig. 4B). Thus, VopS modifies Rho GTPases with AMP. We now refer to this activity as AMPylation and the enzyme as an AMPylator. VopS uses this posttranslational modification of AMPylation to hinder signaling between Rho GTPases and their downstream effectors by blocking the effector binding site on the switch I region of the GTPase with AMP.

Both VopS and protein kinases use ATP to modify substrates, but the phosphate attached to the substrate is distinct. Kinases use the γ phosphate of ATP to modify their substrates on tyrosine, threonine, and serine residues, whereas VopS uses the α phosphate linked to adenosine to modify its substrate on a threonine residue. This type of posttranslational modification on eukaryotic proteins has not previously been observed. However, it has been observed for bacterial glutamine synthetase, albeit autocatalytically on a tyrosine residue, resulting in the sensitization of end-product inhibition (13, 14). Because bacterial type III secreted effectors often mimic eukaryotic mechanisms, the observation of AMPylation by a bacterial effector prompted us to investigate whether eukaryotes use this posttranslational modification. Incubation of S100 HeLa cell lysates with ³²P-γ-labeled ATP predictably revealed many phosphorylated protein substrates (Fig. 4C). This modification, phosphorylation, was labile in the presence of a phosphatase (Fig. 4C). To test whether the same type of experiment would reveal AMPylated protein substrates, we incubated S100 lysate with ³²P-α-labeled ATP. A number of radiolabeled proteins were observed but were insensitive to phosphatase treatment (Fig. 4C). The addition of purified recombinant VopSΔ30 to the reaction using ³²P-α-labeled ATP, but not ³²P-γ-labeled ATP, specifically increased labeling at the predicted size of the Rho GTPases (Fig. 4C). Thus, VopS is not a promiscuous AMPylator but rather targets the Rho family of GTPases. Consistent with this observation, phosphorylation and AMPylation did not occur in the presence of denatured protein (Fig. 4C). Thus, eukaryotic proteins can use ATP to modify proteins by AMPylation.

VopS contains a C-terminal Fic domain, and mutation of an invariant histidine residue within this domain led to the discovery of the catalytic activity of modifying proteins with AMP. The conserved histidine is critical for the AMPylation activity. The limited eukaryotic distribution of Fic resembles that of other components of signal transduction machinery and might support a role for AMPylation by eukaryotic Fic domains in signaling. Structures of Fic domains place the con-

served polar residues of this motif within a cleft that could represent an active site, with conserved side chains (from E and N) forming polar contacts with a phosphate in one structure (fig. S3A) (15). A β hairpin located near the motif binds peptide in another structure, placing a side chain of the peptide within van der Waals contact of the motif histidine (fig. S3B). Although enzymes, such as an activated E1, form AMP-bound covalent enzyme intermediates to drive chemical ligation reactions (16), AMP has not previously been shown to be used as a stable posttranslational modification for a protein. This activity represents an ideal posttranslational modification because it (i) uses a highly abundant high-energy substrate, ATP; (ii) results in the formation of a reversible phosphodiester bond; (iii) is bulky enough to bind to an adaptor protein and be used in dynamic multidomain signaling complexes; and (iv) alters the activity of the protein it modifies. It is intriguing that we observed this modification on threonine because this residue is used in many other modifications that might compete with AMPylation. The identification of the substrates and enzymes involved in eukaryotic AMPylation will undoubtedly add a new layer to the expanding complexity of our information about cellular signal transduction.

References and Notes

1. N. A. Daniels *et al.*, *J. Infect. Dis.* **181**, 1661 (2000).
2. K. Makino *et al.*, *Lancet* **361**, 743 (2003).
3. K. S. Park *et al.*, *Microbiol. Immunol.* **48**, 313 (2004).
4. P. Ghosh, *Microbiol. Mol. Biol. Rev.* **68**, 771 (2004).
5. D. L. Burdette, M. L. Yarbrough, A. Orvedahl, C. J. Gilpin, K. Orth, *Proc. Natl. Acad. Sci. U.S.A.* **105**, 12497 (2008).
6. T. Casselli, T. Lynch, C. M. Southward, B. W. Jones, R. DeVinney, *Infect. Immun.* **76**, 2202 (2008).

7. K. S. Park *et al.*, *Infect. Immun.* **72**, 6659 (2004).
8. Single-letter abbreviations for the amino acid residues are as follows: A, Ala; C, Cys; D, Asp; E, Glu; F, Phe; G, Gly; H, His; I, Ile; K, Lys; L, Leu; M, Met; N, Asn; P, Pro; Q, Gln; R, Arg; S, Ser; T, Thr; V, Val; W, Trp; X, any amino acid; and Y, Tyr.
9. R. Utsumi, Y. Nakamoto, M. Kawamukai, M. Himeno, T. Komano, *J. Bacteriol.* **151**, 807 (1982).
10. T. Hakoshima, T. Shimizu, R. Maesaki, *J. Biochem.* **134**, 327 (2003).
11. J. B. Bliska, K. L. Guan, J. E. Dixon, S. Falkow, *Proc. Natl. Acad. Sci. U.S.A.* **88**, 1187 (1991).
12. N. Abdul-Manan *et al.*, *Nature* **399**, 379 (1999).
13. P. B. Chock, S. G. Rhee, E. R. Stadtman, *Annu. Rev. Biochem.* **49**, 813 (1980).
14. M. S. Brown, A. Segal, E. R. Stadtman, *Proc. Natl. Acad. Sci. U.S.A.* **68**, 2949 (1971).
15. M. E. Cuff *et al.*, Midwest Center for Structural Genomics; structure has been deposited in the Protein Data Bank (www.rcsb.org) with the identification number 2F65.
16. A. L. Haas, J. V. Warms, I. A. Rose, *Biochemistry* **22**, 4388 (1983).
17. We thank N. Alto, R. Taussig, P. Sternweis, S. Mukherjee, M. Rosen, E. Olson, J. Goldstein, M. Brown, T. Iida, T. Honda, L. McCarter, and the Orth lab for insightful discussions, critical reading, and/or generous supply of reagents. K.O. and M.L.Y. are supported by grants from NIH—Allergy and Infectious Disease (R01-AI056404) and the Welch Foundation (I-1561). L.N.K. and N.G. are supported by the Welch Foundation (I-1505) and Howard Hughes Medical Institute. K.O. is a Beckman Young Investigator, Burroughs Wellcome Investigator, and W. W. Caruth Biomedical Scholar.

Supporting Online Material

www.sciencemag.org/cgi/content/full/1166382/DC1
Materials and Methods
Figs. S1 to S3
References

25 September 2008; accepted 14 November 2008
Published online 27 November 2008;
10.1126/science.1166382
Include this information when citing this paper.

Simpson's Paradox in a Synthetic Microbial System

John S. Chuang,* Olivier Rivoire, Stanislas Leibler

The maintenance of "public" or "common good" producers is a major question in the evolution of cooperation. Because nonproducers benefit from the shared resource without bearing its cost of production, they may proliferate faster than producers. We established a synthetic microbial system consisting of two *Escherichia coli* strains of common-good producers and nonproducers. Depending on the population structure, which was varied by forming groups with different initial compositions, an apparently paradoxical situation could be attained in which nonproducers grew faster within each group, yet producers increased overall. We show that a simple way to generate the variance required for this effect is through stochastic fluctuations via population bottlenecks. The synthetic approach described here thus provides a way to study generic mechanisms of natural selection.

A simple general principle has emerged from theoretical and experimental studies of common-good producer–nonproducer interactions: For producers to be selected and maintained, they have to be the privileged recipients of the common good (1–18). Producers may become privileged recipients by virtue of kinship or spatial proximity or discrimination through reciprocity or some distinctive feature (1–5, 9, 10, 14).

In this work, we considered the scenario in which producers and nonproducers are distributed heterogeneously into subpopulations of varying composition, some starting with higher

Center for Studies in Physics and Biology and Laboratory of Living Matter, The Rockefeller University, 1230 York Avenue, New York, NY 10065, USA.

*To whom correspondence should be addressed. E-mail: chuangj@rockefeller.edu

and some with lower fractions of producers. As each of these subpopulations grows, its fraction of producers falls. Yet, it is possible for the overall fraction of producers to rise. This phenomenon, usually analyzed in terms of kin selection or group selection (3), can be distilled into an elementary mathematical feature known as Simpson's paradox (5, 19, 20) (Fig. 1). Because the global producer proportion is a weighted sum of the subpopulation proportions, when there is sufficient covariance between growth rate of a subpopulation and its fraction of producers, a counter-intuitive behavior of the whole population can be observed: Producers increase overall.

A similar situation may arise in natural microbial systems (7, 8, 13), but the effects associated with population heterogeneities are difficult there to assess quantitatively. In addition, in natural systems, evolutionary pressures may have selected for genetic backgrounds that limit the spread of nonproducer mutants and ensure that producers have the growth advantage (11). We have taken a synthetic approach (21–25), which circumvents the difficulties of quantifying the interactions in natural populations. Having no evolutionary history, a synthetic system can furthermore be engi-

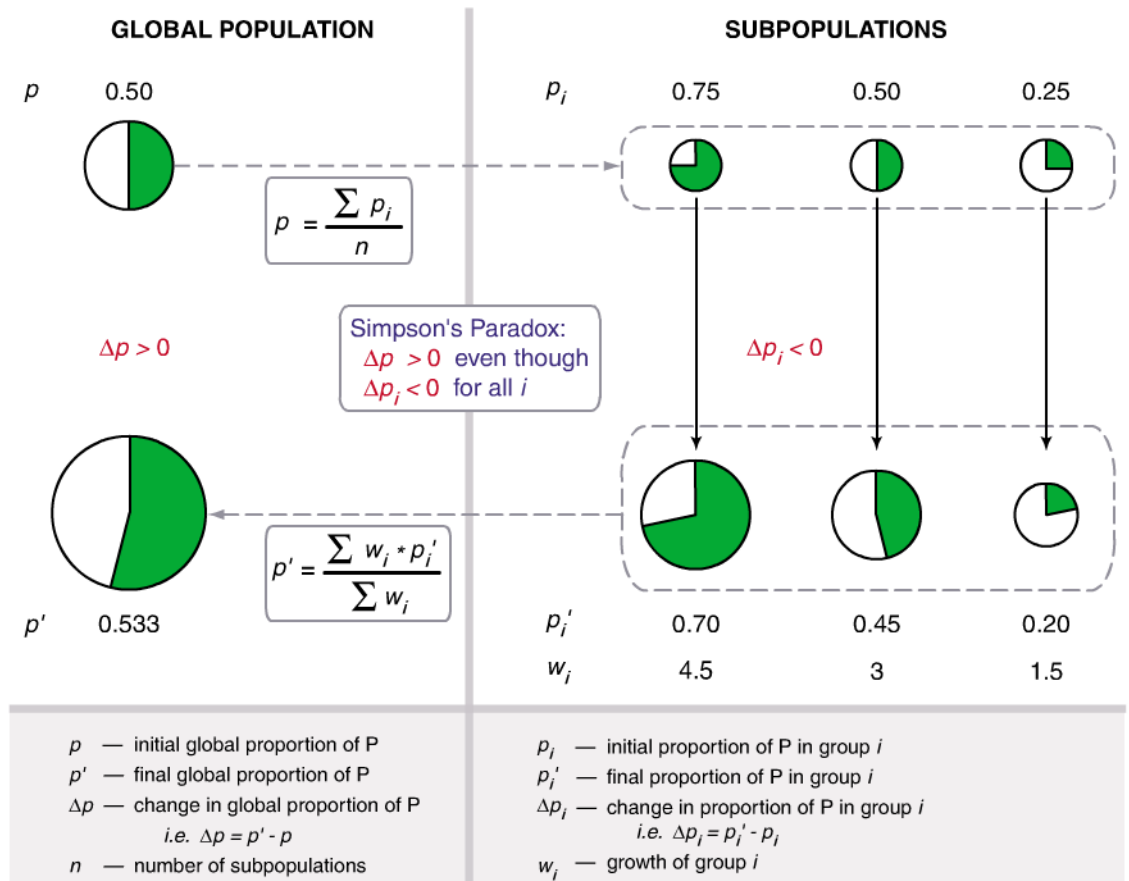
neered to minimize pleiotropic effects, enabling measurement and control of other parameters.

We constructed two *Escherichia coli* strains that recapitulate the interaction of producers and nonproducers (26) (fig. S1). The common good in this system is a membrane-permeable (27) Rhl autoinducer molecule (fig. S1), rewired to activate antibiotic (chloramphenicol; Cm) resistance gene expression. Otherwise isogenic, green fluorescent protein (GFP)-marked producers synthesize the Rhl autoinducer constitutively, whereas nonfluorescent nonproducers do not. The system, denoted *rhl-catLVA* (fig. S1), exhibited the expected properties for public-good producers and nonproducers. First, in antibiotic-containing media, producers grew in a density-dependent manner (fig. S2, left) that was abolished when a synthetic autoinducer was exogenously supplied (fig. S2, right), indicating that autoinducer production was limiting. Second, when started from the same initial density, pure cultures of nonproducers grew slower than pure cultures of producers in antibiotic (fig. S3). However, addition of either synthetic autoinducer or cell-free conditioned medium (containing autoinducer made by producers) increased nonproducer growth in antibiotic-containing media (fig. S3).

When cultures containing preincubated mixtures of producers and nonproducers were diluted into antibiotic-containing medium, both the relative growth of the two strains within a mixture and the growth of the whole mixture depended on the initial proportion of producers (Fig. 2A). In our system, nonproducers proliferated faster than producers within each mixture, independently of the initial composition, as verified by flow cytometry (Fig. 2A). The slower growth of producers can be attributed to the cost of production of the autoinducer, together with the linked GFP reporter. Furthermore, cultures with a higher proportion of producers grew to larger population sizes during the course of the selection phase (12 to 13 hours, 30°C) in antibiotic, and ending subpopulation size was strongly correlated with the initial producer proportion ($r = 0.988$ in 21 trials).

The relative growth advantage of nonproducers versus producers within a mixture, combined with the observed correlation between the overall growth of a mixture and the initial proportion of producers, implied that a situation described by Simpson's paradox could be observed (Fig. 1). To test this, we measured the global proportion of producers in the 10 nonpure cultures

Fig. 1. Principle of Simpson's paradox. Simpson's paradox (5, 19, 20) refers to a situation in which several groups, composed of two types of elements, P and NP, evolve so that the proportion of P elements decreases within each group but nevertheless increases in average overall. The right side shows the evolution of three hypothetical subpopulations represented by pie charts of P (green) and NP (white) slices; the initial and final subpopulations are connected by solid black arrows. The left side shows the corresponding composition of the initial and final global population formed by these three subpopulations (dotted lines). As a whole, the figure illustrates the paradox of P decreasing in each subpopulation ($\Delta p_i < 0$ for every group i) but increasing overall ($\Delta p > 0$). This "paradox" is a purely statistical effect, based on the fact that the global proportion of P is a group size-weighted average that differs from the nonweighted average. In general, if we start from n groups of equal sizes and proportions p_i of P ($i = 1, \dots, n$), whether Simpson's paradox is observed depends on the changes in proportion of P within each group, Δp_i , and on the overall growth of each group, w_i . The global variation of the proportion of P, Δp , satisfies (29) $\langle w_i \rangle \Delta p = \text{cov}(w_i, p_i) + \langle w_i \Delta p_i \rangle$, where $\langle \cdot \rangle$ denotes a non-



weighted average over the groups, $\langle x_i \rangle = (\sum x_i)/n$, and $\text{cov}(w_i, p_i) = \langle w_i p_i \rangle - \langle w_i \rangle \langle p_i \rangle$ represents the covariance between w_i and p_i . Simpson's paradox corresponds to having $\Delta p_i < 0$ for all groups i , but $\Delta p > 0$ globally, and requires sufficient correlation between w_i and p_i , viz, $\text{cov}(w_i, p_i) > -\langle w_i \Delta p_i \rangle$.

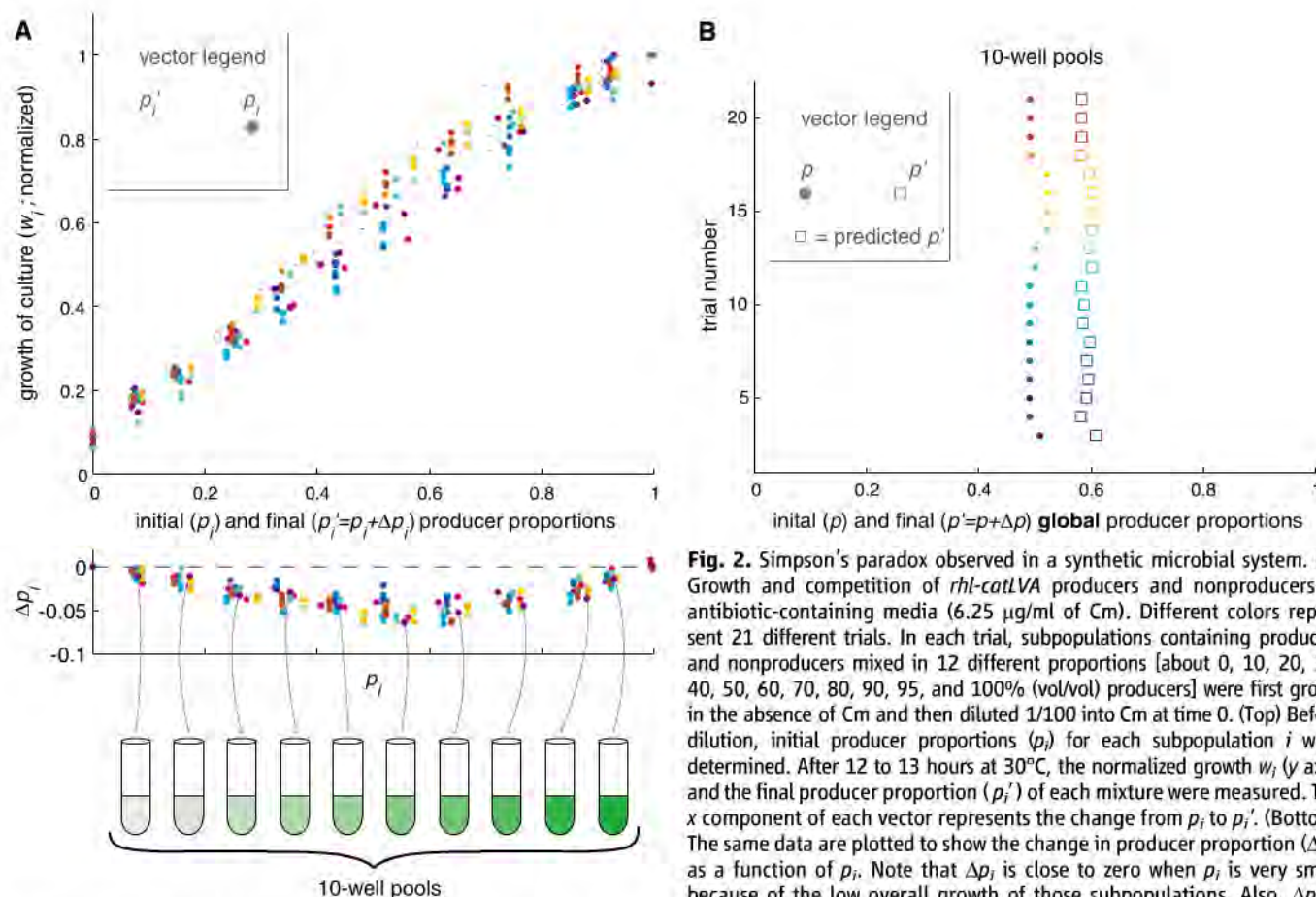


Fig. 2. Simpson's paradox observed in a synthetic microbial system. **(A)** Growth and competition of *rhl-catLVA* producers and nonproducers in antibiotic-containing media (6.25 $\mu\text{g/ml}$ of Cm). Different colors represent 21 different trials. In each trial, subpopulations containing producers and nonproducers mixed in 12 different proportions [about 0, 10, 20, 30, 40, 50, 60, 70, 80, 90, 95, and 100% (vol/vol) producers] were first grown in the absence of Cm and then diluted 1/100 into Cm at time 0. (Top) Before dilution, initial producer proportions (p_i) for each subpopulation i were determined. After 12 to 13 hours at 30°C, the normalized growth w_i (y axis) and the final producer proportion (p_i') of each mixture were measured. The x component of each vector represents the change from p_i to p_i' . (Bottom) The same data are plotted to show the change in producer proportion (Δp_i) as a function of p_i . Note that Δp_i is close to zero when p_i is very small because of the low overall growth of those subpopulations. Also, Δp_i is zero when $p_i = 1$ because those cultures are pure producer populations.

The curved arrows joining purple points and individual test tubes depict how the 10 nonpure subpopulations from each trial were pooled to form the global populations (10-well pools) in (B). **(B)** Simpson's paradox satisfied by *rhl-catLVA* producers and nonproducers. Initial (p) and final (p') global proportions of producers were determined in 19 of the 21 trials from (A) (the first two trials were not measured at a global level). Each vector plots the change from p to p' (mean change = 0.105, SD = 0.011, $n = 19$). Colors indicate the correspondence between each trial of subpopulations in (A) (leftward vectors) and each global pool in (B) (rightward vectors). Square symbols show predicted p' values calculated by using the data from individual subpopulations of (A).

with different initial proportions of producers by mixing equal volumes of these cultures and then determining the composition with flow cytometry. As predicted by straightforward calculations (Fig. 1) based on the data obtained for the growth of independent mixtures (Fig. 2A), the global proportion of producers increased relative to its initial value (Fig. 2B), despite the fact that within each mixture, producers did not increase in proportion (Fig. 2A). These results are an illustration of Simpson's paradox in growing microbial populations.

The question of the maintenance of producers has also been addressed in studies of bacterial quorum-sensing mutants (16) and siderophore nonproducers (12) using simplified laboratory conditions and quantitative measurements. However, in our experiments, there is no direct benefit of being a producer, specifically, no negative frequency dependence ($\Delta p_i > 0$ for lower values of p_i). More importantly, producers and nonproducers are grown here as nonclonal mixtures under selective conditions in which the public good confers an advantage to nonproducers [in contrast, see (18)].

The conditions for observing Simpson's paradox are not only based on the properties of the two strains. First, the time scale of the antibiotic selection phase is important; if cultures are allowed to reach stationary phase, those differing greatly in producer proportion (e.g., 20% compared with 80%) will have comparable group sizes, thus preventing Simpson's paradox from occurring. Second, Simpson's paradox also depends on the variance of initial group composition. Thus, long-term maintenance of producers requires an ecological process that enables repeated formation of new groups with a sufficiently large composition variance (1). The degree of dispersal can be controlled by varying the "spatial scale of competition" (6), that is, the degree to which the groups are mixed at each step. From this point of view, Simpson's paradox corresponds to the observation that "global competition" (complete mixing) may have an effect opposite to "local competition" (no mixing).

Notably, a simple possible mechanism for generating sufficiently large composition variance is an extreme dilution of the group populations (1, 2). Such Poisson dilution gave rise to stochastic fluctuations of group compositions with sufficient-

ly large variances to generate Simpson's paradox. We diluted a 50:50 mixture of producers and nonproducers into 288 wells (three 96-well plates), so that the number of founder cells in these groups was Poisson-distributed with a mean λ (estimated by counting the number of wells with no cells). As before, all founding groups of bacteria were first grown in the absence of antibiotic and then diluted into the antibiotic-containing medium for 12 hours at 30°C. The 288 wells were subsequently pooled together, and the overall proportion of producers was measured. Figure 3A shows the change in producer proportion in a single round: For small enough λ , the generated variance was sufficient to reach the Simpson's paradox regime.

Subsequently, we tested whether this process could be iterated over several rounds, starting with a 10% producer mixture. After each round, the Poisson dilution-antibiotic selection protocol was repeated with use of the pooled population as the new starting mixture for the next round; as a result the overall proportion of producers increased over several consecutive rounds to >95% producers (Fig. 3B). The stochastic fluctuations constitute, therefore, a possible mechanism for

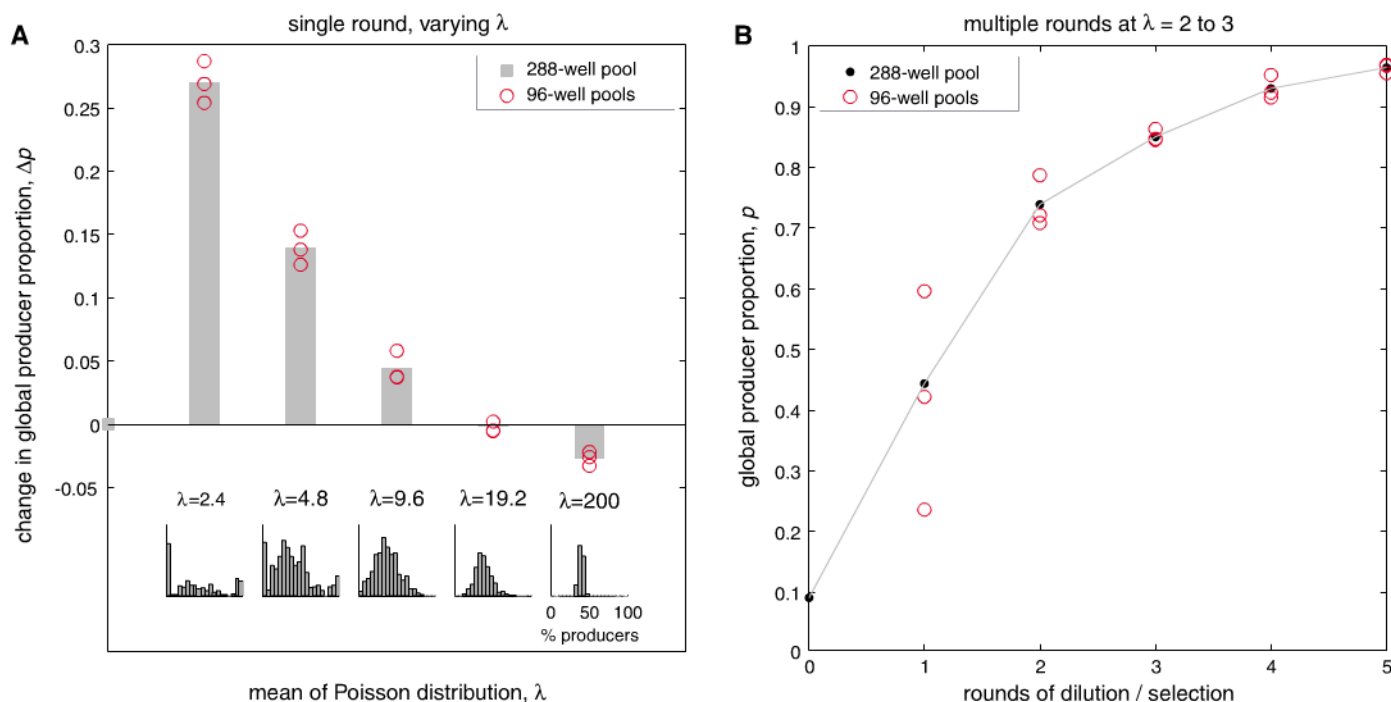


Fig. 3. Poisson dilution conditions can generate sufficient variance to satisfy Simpson's paradox. **(A)** Effect of Poisson mean on the global change in producer proportion. A 50:50 mixture of producers and nonproducers was strongly diluted into three 96-well plates per treatment and first grown without Cm. Then, at time 0, the mixtures were diluted 1/100 into 6.25 $\mu\text{g}/\text{ml}$ of Cm for 12 hours at 30°C. The change (Δp) in producer proportion for the global population (288-well pool) is shown for different dilutions, which resulted in the indicated values of λ , the mean number of founder cells per well. Note that the x axis is not to scale. Red circles, showing the observed change in separate subpools of each of the three individual plates (96-well pools), provide an estimate of the variation arising from pooling smaller

numbers of wells. (Insets) Histogram show the distributions of initial (time 0) producer proportions (p_i) resulting from Poisson dilution conditions. **(B)** Iteration of Poisson dilution conditions and growth in Cm. A 10% producer mixture underwent five successive rounds of the dilution and growth described in (A). After each round, the three 96-well plates were pooled (288-well pool), analyzed for global producer proportion (p), strongly rediluted, and then aliquoted to three new 96-well plates for the subsequent round. The Poisson mean λ ranged from 2 to 3 in each round. Red circles are as described in (A). Resulting from stochastic effects, the larger variation observed in earlier rounds (red circles) is expected because p is small. Note that, in general, the variation also depends on λ and the number of pooled wells.

reversing the direction of selection in growing populations [as noticed in (1) and (2)]. Although others (15) have demonstrated the effects of small group size on producer dynamics within a single population, in this study small founder group size is shown to indirectly favor producers through its effect on population distributions.

From a biological standpoint, our synthetic system provides a simple example of conflicting levels of selection (28): Producer cells are beneficial in terms of growth at the higher level of populations (whether single groups or a set of groups), but they are nevertheless not necessarily favored by natural selection, which primarily operates at the lower level of individuals (producers cells have thus a disadvantage within any single group). Simpson's paradox corresponds to a situation where this conflict is overcome, and the trait beneficial to the population is selected in spite of its individual cost. The synthetic system presented here is amenable to further analysis. For example, both the cost of being a producer and the benefit of receiving the public good could in principle be experimentally manipulated. Our work thus shows that one can analyze quantitatively how the direction of selection can be influenced by a combination of cellular and ecological parameters.

References and Notes

- W. D. Hamilton, *Am. Nat.* **97**, 354 (1963).
- J. B. S. Haldane, *The Causes of Evolution* (Longmans Green, London, 1932).
- W. D. Hamilton, in *ASA Studies 4: Biosocial Anthropology*, R. Fox, Ed. (Malaby, London, 1975), pp. 133–153.
- R. Axelrod, W. D. Hamilton, *Science* **211**, 1390 (1981).
- E. Sober, D. S. Wilson, *Unto Others: The Evolution and Psychology of Unselfish Behavior* (Harvard Univ. Press, Cambridge, MA, 1998).
- S. A. Frank, *Foundations of Social Evolution* (Princeton Univ. Press, Princeton, NJ, 1998).
- P. B. Rainey, A. Buckling, R. Kassen, M. Travisano, *Trends Ecol. Evol.* **15**, 243 (2000).
- B. J. Crespi, *Trends Ecol. Evol.* **16**, 178 (2001).
- L. Lehmann, L. Keller, *J. Evol. Biol.* **19**, 1365 (2006).
- D. C. Queller, E. Ponte, S. Bozzaro, J. E. Strassmann, *Science* **299**, 105 (2003).
- K. R. Foster, G. Shaulsky, J. E. Strassmann, D. C. Queller, C. R. L. Thompson, *Nature* **431**, 693 (2004).
- A. S. Griffin, S. A. West, A. Buckling, *Nature* **430**, 1024 (2004).
- L. Keller, M. G. Surette, *Nat. Rev. Microbiol.* **4**, 249 (2006).
- B. Kerr, C. Neuhauser, B. J. M. Bohannan, A. M. Dean, *Nature* **442**, 75 (2006).
- M. A. Brockhurst, *PLoS One* **2**, e634 (2007).
- S. P. Diggle, A. S. Griffin, G. S. Campbell, S. A. West, *Nature* **450**, 411 (2007).
- K. M. Sandoz, S. M. Mitzimberg, M. Schuster, *Proc. Natl. Acad. Sci. U.S.A.* **104**, 15876 (2007).
- G. M. Dunny, D. J. Brickman, M. Dworkin, *Bioessays* **30**, 296 (2008).
- C. R. Blyth, *J. Am. Stat. Assoc.* **67**, 364 (1972).
- P. J. Bickel, E. A. Hammel, J. W. O'Connell, *Science* **187**, 398 (1975).
- J. W. Chin, *Nat. Chem. Biol.* **2**, 304 (2006).
- W. Weber, M. Daoud-El Baba, M. Fussenegger, *Proc. Natl. Acad. Sci. U.S.A.* **104**, 10435 (2007).
- W. Shou, S. Ram, J. M. G. Vilar, *Proc. Natl. Acad. Sci. U.S.A.* **104**, 1877 (2007).
- K. Brenner, D. K. Karig, R. Weiss, F. H. Arnold, *Proc. Natl. Acad. Sci. U.S.A.* **104**, 17300 (2007).
- F. K. Balagaddé et al., *Mol. Syst. Biol.* **4**, 187 (2008).
- Information on materials and methods is available on Science Online.
- J. P. Pearson, C. Van Delden, B. H. Iglewski, *J. Bacteriol.* **181**, 1203 (1999).
- L. Keller, Ed., *Levels of Selection in Evolution* (Princeton Univ. Press, Princeton, NJ, 1999).
- G. R. Price, *Nature* **227**, 520 (1970).
- We are grateful to C. Bargmann, C. Guet, L. Keller, E. Kussell, R. Losick, and A. Murray for comments on the manuscript and members of our laboratory for advice and discussion. We also thank the Yale Coli Genetic Stock Center and the National BioResource Project (NIG, Japan) for strains and the Rockefeller Flow Cytometry Resource Center for help. J.S.C. was partly supported by a NIH fellowship and O.R. by a Human Frontier Science Program fellowship.

Supporting Online Material

www.sciencemag.org/cgi/content/full/323/5911/272/DC1

Materials and Methods

Figs. S1 to S3

References

9 July 2008; accepted 19 November 2008

10.1126/science.1166739

Mispredicting Affective and Behavioral Responses to Racism

Kerry Kawakami,^{1*} Elizabeth Dunn,² Francine Karmali,¹ John F. Dovidio³

Contemporary race relations are marked by an apparent paradox: Overt prejudice is strongly condemned, yet acts of blatant racism still frequently occur. We propose that one reason for this inconsistency is that people misunderstand how they would feel and behave after witnessing racism. The present research demonstrates that although people predicted that they would be very upset by a racist act, when people actually experienced this event they showed relatively little emotional distress. Furthermore, people overestimated the degree to which a racist comment would provoke social rejection of the racist. These findings suggest that racism may persevere in part because people who anticipate feeling upset and believe that they will take action may actually respond with indifference when faced with an act of racism.

Contemporary race relations are marked by an apparent paradox. On one hand, racism is strongly condemned (1–3), and being labeled a “racist” has become a powerful stigma of its own (4). On the other hand, acts of blatant racism against blacks still occur with alarming regularity. A recent survey (5) found that 67% of blacks indicated that they often face discrimination and prejudice when applying for a job, and 50% reported that they experienced racism when engaging in such common activities as shopping or dining out. For many blacks, derogatory racial comments are a common occurrence, and almost one-third of whites report encountering anti-black slurs in the workplace (6). Why would whites exhibit such overt racism if this behavior was sure to provoke anger and social rejection from others of their own race?

We suggest that social deterrents to racism may be weaker than public rhetoric implies. First, even if people are upset by an act of racism, they may not penalize individuals for violating egalitarian social norms because enforcing such norms can be costly (7–9). Confronting a racist or even confronting someone who does not rebuke racists can consume cognitive and emotional energy. Second, people may be less upset and less likely to take action in response to racism than they themselves would anticipate. This possibility is supported by research demonstrating that people often make inaccurate forecasts related to their emotional responses (10, 11), exhibiting a robust proclivity to overestimate how upset they would feel in bad situations (12–14). This research has focused on affective, and not behavioral, predictions. The primary goal of the present research is to investigate discrepancies between how people imagine they would feel and behave and how they actually feel and behave upon hearing a racist comment.

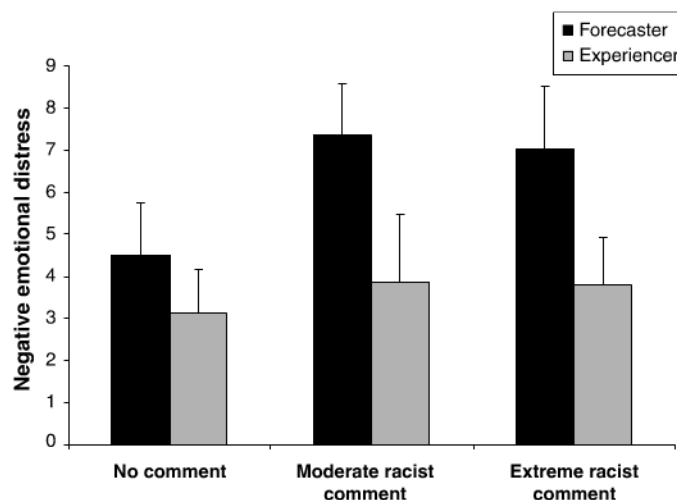
According to aversive racism theory, even individuals who embrace egalitarian beliefs may continue to harbor nonconscious negative feelings toward blacks (15, 16). Recent research demonstrates that, whereas egalitarian beliefs typically guide thoughtful, deliberative responses, lingering negative feelings toward blacks often emerge in the context of more spontaneous responses (1, 3, 17–19). When contemplating their own responses to hypothetical situations, people tend to adopt a relatively deliberative mindset (10, 20), suggesting that people are likely to draw on their conscious egalitarian values in imagining how they would respond to an act of racism (21). Yet, when faced with actual racism, people's spontaneous feelings and behavior may reveal latent bias toward blacks. In accordance with this framework, we hypothesized that people who imagined hearing a racist comment would expect to be more upset and would overestimate the degree to which they would reject the racist compared with people who actually heard the comment.

In an initial study investigating participants' actual and anticipated responses to an anti-black

slur, we assigned 120 participants who self-identified their race/ethnicity (e.g., black, Asian, Pakistani) to the role of “experiencer” or “forecaster” and exposed them to an incident involving no racial slur, a moderate racial slur, or an extreme racial slur. Because our goal was to examine how people who do not belong to the target group respond to racial slurs, black participants were not included in this study (22). Upon entering the laboratory, the experimenter introduced the experiencers to two male confederates—one black and one white—who posed as fellow participants, and then the experimenter exited the room. Shortly thereafter, the black confederate left the room, ostensibly to retrieve his cell phone, and gently bumped the white confederate's knee on his way out. In the control condition, this incident passed without comment. In the moderate slur condition, once the black confederate had left the room, the white confederate remarked, “Typical, I hate it when black people do that.” In the extreme racial slur condition, the white confederate stated, “clumsy ‘N word.’” Within minutes, the black confederate returned, followed by the experimenter, who asked everyone to complete an initial survey, which included items assessing current affect. Next, the experimenter asked the real participant to select one of the confederates as a partner for a subsequent anagram task and to report their choice orally to the experimenter. Finally, all participants completed the anagram task in another room with the person they had selected. In the forecaster condition, participants were presented with a detailed description of the events that experiencers actually encountered. Forecasters were asked to predict in writing how they would feel if they were in the experiencer's position and to predict which confederate they would choose as a partner.

As shown in Fig. 1, forecasters in the extreme and moderate racist comment conditions anticipated being more upset than forecasters in the no comment condition. Experiencers, however,

Fig. 1. Differences in emotional distress [on a scale from 1 (low distress) to 9 (high distress)] as a function of role (forecasters versus experiencers) and comment (extreme racist versus moderate racist versus no comment). Error bars represent SE with $n = 19$ to 21 participants in each condition. The predicted two-way interaction was significant ($F_{2,117} = 7.55$, $P < 0.001$). Forecasters were influenced by the type of comment ($F_{2,57} = 26.62$, $P < 0.001$), but experiencers were not ($F_{2,57} = 1.86$, $P = 0.16$). Simple effects analyses demonstrated that forecasters in the extreme and moderate racist comment conditions anticipated being more upset than in the no comment condition [$t(38 \text{ and } 37) = 5.68$ and 7.31 , $s < 0.001$].



¹Department of Psychology, York University, 4700 Keele Street, Toronto, Ontario, Canada, M3J 1P3. ²Department of Psychology, University of British Columbia, 2136 West Mall, Vancouver, British Columbia, Canada, V6T 1Z4. ³Department of Psychology, Yale University, 2 Hillhouse Avenue, Box 208205, New Haven, CT 06520-8205, USA.

*To whom correspondence should be addressed. E-mail: kawakami@yorku.ca

reported little distress regardless of the type of comment. Likewise, as shown in Fig. 2, role and racist comment conditions influenced the choice of task partner (22). Across the two racist comment conditions, a significant minority of forecasters predicted choosing the white (17%) over the black confederate, whereas in the no comment condition, forecasters showed a nonsignificant preference for the white (68%) over the black confederate. Experiencers were somewhat more likely to choose the white (63%) over the black confederate across the two racist comment conditions, but they did not differ in their choice of the white (53%) versus black confederate in the no comment condition. Additional analyses further demonstrated that, whereas experiencers were significantly more likely to choose the white confederate than forecasters predicted in the racist comment conditions, experiencers' and forecasters' choices did not differ in the absence of a racist comment. In sum, consistent with our hypotheses, forecasters substantially mispredicted the extent to which a racist comment would provoke distress and social rejection.

As expected, distress was unrelated to partner choice in the no comment condition [correlation coefficient $r(36) = -0.24$, $P = 0.14$]. However, participants who felt or expected to feel more distress were less likely to choose or predict choosing the white confederate in the moderate and extreme racist comment conditions [correlation coefficients $r(38 \text{ and } 40) > -0.40$, and P s < 0.01 , respectively]. Furthermore, when role, distress, and their interaction were entered into a logistic regression predicting partner choice in the racist comment conditions, the interaction did not approach significance, logistic regression coefficient $B(1, N = 82 \text{ participants}) = -0.33$, $P = 0.47$, suggesting that affect predicted partner choice in similar ways in both the forecaster and experiencer conditions.

We used standard mediational analysis procedures to examine whether differences in forecasted and experienced affect could statistically explain the observed differences in forecasted and experienced partner choice (23). Specifically, when role and distress were entered into a logistic

regression predicting partner choice in the racist comment conditions, the effect of role was eliminated, whereas distress continued to predict partner choice (22). Although these analyses do not prove causality, the results suggest that people may erroneously believe that they would reject a racist in part because they overestimate the emotional distress that a racist comment would evoke.

One potential alternative interpretation for our partner choice findings is that experiencers' responses may have been driven by a motivation to avoid the black confederate because of concerns about how the black person might respond or feelings of guilt. However, because the black confederate was unaware of the comment and because no differences in partner choice were found between the no comment and racist comment conditions, this explanation does not readily account for the observed results. Furthermore, additional analyses revealed that feelings of guilt and embarrassment did not mediate the participants' partner choice and that participants who felt greater general distress after the comment were more, not less, likely to choose the black confederate (22).

Even though the results from experiment 1 directly supported our hypotheses, the fact that experiencers did not respond negatively to the racist slur is counterintuitive. Consistent with many other studies in the affective forecasting literature (24), forecasters received a full description of the events that transpired, yet they were not presented with the events in the same vivid way as experiencers. To remedy this situation, a second study included a forecaster-video condition in which participants were presented with a video showing a precise enactment of the experimenter condition from the experiencers' visual perspective.

In this study, 76 participants assigned to the experiencer, forecaster-text, or forecaster-video conditions were exposed to the moderate slur utilized in experiment 1. As predicted, after a racist comment, participants in both the forecaster-text and forecaster-video conditions anticipated feeling more emotional distress than experiencers reported [$t(51) = 10.54$, $P < 0.001$, and $t(46) = 6.99$, $P <$

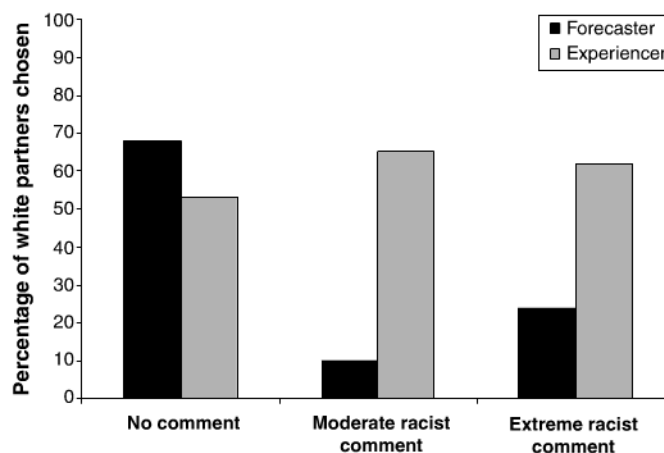
0.001, respectively] (22). In addition, whereas a minority of participants predicted that they would choose the white partner in both the forecaster-text (25%) and forecaster-video (17%) conditions, most experiencers actually preferred the white (71%) over the black confederate [$\chi^2(2, N = 73) = 17.80$, $P < 0.001$]. Replicating experiment 1, mediational analyses suggested that experiencers were less likely to reject the white partner than forecasters anticipated because experiencers were less upset after hearing a racist comment than forecasters imagined.

Another possible difference between forecaster and experiencer conditions is that forecasters may not have perceived the racist situation to have been as real as experiencers who actually encountered the event. Our paradigm, however, mirrors standard affective forecasting procedures that have shown similar forms of misprediction, regardless of whether participants are presented with real or hypothetical events (14, 20, 25). Furthermore, this distinction does not explain why, in the present research, forecasters were more distressed and influenced by the event than experiencers. Conceptually one would assume that the more "real" one perceives the situation, the more impact it will have. Still, to address this issue empirically, we presented forecasters ($N = 40$) with the same moderate slur video used in experiment 2. For half of the participants, the video was described as a real situation with actual students; for the other half, the video was described as a hypothetical situation with actors. Regardless of whether the situation was described as real or hypothetical, forecasters anticipated feeling highly distressed and only a minority predicted that they would choose the white confederate as a partner (22). These findings replicate previous results and suggest that differences between forecasters and experiencers cannot readily be explained by the belief that the situation is real or hypothetical.

Taken together, our findings reveal that people's predictions regarding emotional distress and behavior in response to a racial slur differ drastically from their actual reactions. Whereas participants who imagined themselves in the situation anticipated being very upset and distancing themselves from a person who made a racist comment, those who experienced this event did not differ from control participants who were not exposed to a racist comment. Remarkably, this pattern of results emerged even when the comment included a racial slur widely regarded as one of the most offensive words in the English language (26).

Although previous experimental research has provided some evidence that targets of prejudice may overestimate the anger they would exhibit in response to experiencing harassment (27, 28), the present research sheds light on anticipated and actual responses by individuals who are not part of the target group. Despite an impressive history of social psychological research on intergroup relations (2), theorists are just beginning to understand how lay people react to prejudice toward other groups. Investigating responses by majority

Fig. 2. Percentage of participants who choose the white racist partner as a function of role (forecasters versus experiencers) and comment (extreme racist versus moderate racist versus no comment), with $n = 19$ to 21 participants in each condition. A significant interaction was found between role and comment conditions on choice of task partner [logistic regression coefficient $B(1, N = 120) = 3.48$, $P < 0.01$].



and other groups to overt prejudice against blacks may be critical to understanding the continued existence of racism. Our research suggests that, although people anticipate feeling upset and taking action upon witnessing a racist act against an out-group, they actually respond with indifference. The present findings also suggest a potential link between affective and behavioral responses to racism (29) and complement current theorizing on the role of emotion in prejudice and discrimination (2, 30).

Because of the socially sensitive nature of investigations related to reactions to racism, an alternative explanation for the current findings involves social evaluative concerns and demand characteristics. Participants in the role of forecaster might have readily recognized the social demands dictated by widespread egalitarian norms and responded in ways that they believed were socially or contextually acceptable rather than according to their true inclinations. However, both experiencers and forecasters were assured of the anonymity of their affective responses (which then predicted partner choice), and because partner selection was made publicly by experiencers but privately by forecasters, social evaluative concerns about appearing racist should have made experiencers more likely than forecasters to reject the white partner. Furthermore, additional analyses related to study 3 (22) showed that forecasters' responses were unrelated to individual differences in social evaluative concerns.

It is also important to note that our results dovetail with previous research on less socially sensitive issues that show that people commonly overlook their own ability to reconstrue bad situations in the best possible light (14). In the present context, upon hearing a racist comment, participants may have actively reconstrued it as a joke or harmless remark to stem the tide of negative emotions. In addition, we posit that participants may have mispredicted their emotional responses to witnessing a racist comment because of their own ambivalent racial attitudes. Recent

research suggests that, although forecasters may have relied on their conscious egalitarian attitudes when predicting their future emotions, the actual emotions of experiencers may have been shaped more by nonconscious negative attitudes (1, 10, 20).

Besides providing a conceptual contribution, the present studies also have immediate practical relevance. In particular, despite current egalitarian cultural norms and apparent good intentions, one reason why racism and discrimination remain so prevalent in society may be that people do not respond to overt acts of racism in the way that they anticipate: They fail to censure others who transgress these egalitarian norms. These findings provide important information on actual responses to racism that can help create personal awareness and inform interventions, thereby helping people to be as egalitarian as they think they will be.

References and Notes

1. J. F. Dovidio, K. Kawakami, N. Smoak, S. L. Gaertner, in *Implicit Measures of Attitudes*, R. Petty, R. Fazio, P. Brinol, Eds. (Psychology Press, New York, 2009), pp. 165–192.
2. S. T. Fiske, in *The Handbook of Social Psychology*, vols. 1 and 2, D. T. Gilbert, S. T. Fiske, G. Lindzey, Eds. (McGraw-Hill, New York, 1998), pp. 357–411.
3. K. Kawakami, K. L. Dion, J. F. Dovidio, *Pers. Soc. Psychol. Bull.* **24**, 407 (1998).
4. S. R. Sommers, M. I. Norton, *Group Process. Intergroup Relat.* **9**, 117 (2006).
5. "Blacks See Growing Values Gap Between Poor and Middle Class: Optimism About Black Progress Declines," (Pew Research Centre, Washington, DC, 2007).
6. "One in Three Reports Sexual Remarks in the Workplace," (Novations, Boston, MA, 2007).
7. R. Axelrod, *Am. Polit. Sci. Rev.* **80**, 1095 (1986).
8. T. Kameda, M. Takezawa, R. Hastie, *Pers. Soc. Psychol. Rev.* **7**, 2 (2003).
9. T. Yamagishi, *J. Pers. Soc. Psychol.* **51**, 110 (1986).
10. E. W. Dunn, N. D. Forrin, C. E. Ashton-James, in *The Handbook of Imagination and Mental Simulation*, K. D. Markman, W. M. P. Klein, J. A. Suhr, Eds. (Psychology Press, New York, in press).
11. D. T. Gilbert, *Stumbling on Happiness* (Alfred A. Knopf, New York, 2006), pp. xviii, 277.
12. E. W. Dunn, T. D. Wilson, D. T. Gilbert, *Pers. Soc. Psychol. Bull.* **29**, 1421 (2003).

13. D. T. Gilbert, E. Driver-Linn, T. D. Wilson, in *The Wisdom in Feeling: Psychological Processes in Emotional Intelligence*, L. F. Barrett, P. Salovey, Eds. (Guilford, New York, 2002), pp. 114–143.
14. D. T. Gilbert, E. C. Pinel, T. D. Wilson, S. J. Blumberg, T. P. Wheatley, *J. Pers. Soc. Psychol.* **75**, 617 (1998).
15. J. F. Dovidio, S. L. Gaertner, in *Advances in Experimental Social Psychology*, vol. 36, M. P. Zanna, Ed. (Elsevier, San Diego, CA, 2004), pp. 1–52.
16. S. L. Gaertner, J. F. Dovidio, in *Prejudice, Discrimination, and Racism*, J. F. Dovidio, S. L. Gaertner, Eds. (Academic, Orlando, FL, 1986), pp. 61–89.
17. P. G. Devine, *J. Pers. Soc. Psychol.* **56**, 5 (1989).
18. K. Kawakami, J. F. Dovidio, J. Moll, S. Hermen, A. Russin, *J. Pers. Soc. Psychol.* **78**, 871 (2000).
19. K. Kawakami, C. E. Phillips, J. R. Steele, J. F. Dovidio, *J. Pers. Soc. Psychol.* **92**, 957 (2007).
20. E. W. Dunn, C. Ashton-James, *J. Exp. Soc. Psychol.* **44**, 692 (2008).
21. E. Pronin, in *Advances in Experimental Social Psychology*, M. P. Zanna, Ed. (Elsevier, San Diego, CA, in press).
22. Materials and methods are available as supporting material on Science Online.
23. R. M. Baron, D. A. Kenny, *J. Pers. Soc. Psychol.* **51**, 1173 (1986).
24. T. D. Wilson, D. T. Gilbert, in *Advances in Experimental Social Psychology*, M. Zanna, Ed. (Elsevier, San Diego, CA, 2003), p. 345.
25. T. D. Wilson, T. Wheatley, J. M. Meyers, D. T. Gilbert, D. Axson, *J. Pers. Soc. Psychol.* **78**, 821 (2000).
26. S. Pinker, *The Stuff of Thought: Language as a Window into Human Nature* (Viking, New York, 2007).
27. J. K. Swim, L. L. Hyers, *J. Exp. Soc. Psychol.* **35**, 68 (1999).
28. J. A. Woodzicka, M. LaFrance, *J. Soc. Issues* **57**, 15 (2001).
29. P. G. Devine, M. J. Monteith, in *Affect, Cognition, and Stereotyping: Interactive Processes in Group Perception*, D. M. Mackie, D. L. Hamilton, Eds. (Academic, San Diego, CA, 1993), pp. 317–344.
30. D. M. Mackie, E. R. Smith, *From Prejudice to Intergroup Emotions: Differentiated Reactions to Social Groups* (Psychology Press, New York, 2002).
31. This research was supported by Social Science and Humanities Council of Canada grants to K.K. and E.D.

Supporting Online Material

www.sciencemag.org/cgi/content/full/323/5911/276/DC1

Materials and Methods

SOM Text

References

21 August 2008; accepted 4 November 2008

10.1126/science.1164951

New Products

Photometric Biochemistry Analyzer

The CuBiAn is a fully automated, membrane-free chemical analyzer that measures key parameters in cell culture media, including immunoglobulin G (IgG). The instrument offers high reproducibility with low operating costs in calibration and maintenance. Pipetting, sample predilution, and temperature control are all automated to provide significant assay ranges. The CuBiAn can detect IgG concentrations along with 11 different metabolites in a single sample and sequence. IgG is detected by immunoturbidimetry, while all other molecules are quantified by photometric enzyme assays. A wide measurement range allows for nearly unlimited flexibility for new assay methods. The key parameters measured are IgG, glucose, lactate, ammonia, glutamine, glutamate, inorganic phosphate, lactate dehydrogenase, total protein, sodium, potassium, and chlorine. It requires low sample volumes and can provide 90 results per hour.

Innovatis
For information 800-286-1631
www.innovatis.com

**Vortexer**

The Eppendorf MixMate is the first vortexer available with independently verified data showing the low transfer of hand-arm vibration during operation. The use of a vortexing procedure to mix liquids causes transfer of vibration to the hand and arm, posing a possible risk. The daily maximum dose of exposure incurred with the MixMate was analyzed by the independent British institution, Industrial Noise & Vibration Centre. The results showed that the MixMate's two-dimensional rotating motion not only reduces hand-arm vibration to safe levels, it also provides rapid, reproducible mixing and vortexing for numerous tube and plate formats.

Eppendorf

For information +49-40-53801-0
www.eppendorf.com

Plasmid DNA Kits

The GET Plasmid DNA kits are spin-column purification kits for the isolation of high-quality plasmid from bacterial cultures. The kits are available in three different formats (maxi, medi, and mini) for use with various yields of plasmid. The kits feature an extraction method based on alkaline lysis of bacteria. The easy protocol eliminates toxic phenol/chloroform extractions or ethanol precipitations. The extracted plasmid is ready for further DNA manipulation such as restriction enzyme digestion, ligation, transformations, transfections, and sequencing.

G-Biosciences/Genotech

For information 314-991-6034
www.GBiosciences.com

Mouse Sperm Cryopreservation Service

The Sperm Cryo service provides a simple, cost-effective process to freeze mouse sperm in a way that still achieves high fertilization and recovery rates. The process enables scientists worldwide to manage mouse colonies in a new way, reducing husbandry costs and the number of animals used in biochemical research. The ability to freeze mouse sperm reliably also provides a cost-effective way to safeguard unique and valuable mouse models of human disease. Freezing sperm is an effective way to conserve and distribute genetics in the agricultural industry, but before this process, the

sperm of certain varieties of mice underperformed woefully after being frozen and thawed.

The Jackson Laboratory

For information 207-288-6051
www.jax.org

Ovens

A line of Lab Companion Ovens includes 11 models to satisfy the majority of laboratory applications, including forced convection, natural convection, economy, and vacuum model ovens. The forced convection models have a capacity from 2.1 cubic feet to 5.3 cubic feet with a temperature range from 10°C above ambient to 250°C. The natural convection models range from 1.8 cubic feet to 4.8 cubic feet with a temperature range from 15°C above ambient to 250°C. Two vacuum ovens are available with a chamber size of 1 cubic foot or 2.3 cubic feet. Both offer a temperature range from 5°C above ambient to 250°C.

Jeio Tech

For information 781-376-0700
www.jeiotech.com

Sample Volume Checker

The VolumeCheck is an automated system that enables precise and rapid determination of sample volume in unsealed deep- or shallow-well microplates, tube racks, and high-volume test tube racks. It is available in three configurations: a standard system, a high-speed model capable of scanning a complete 96-well plate in one minute, and a large volume model for test tube volume above 2 ml. The VolumeCheck makes use of proprietary acoustic sensor technology to provide high-accuracy, noncontact measurement. The user simply places a microplate or tube rack onto the input tray, which is automatically retracted into the VolumeCheck. In 60 seconds, measured volumes are displayed graphically for each microplate well or tube in the rack. The volume data are automatically associated with the microplate/tube rack identification and well/tube position and saved to an output file.

Micronic

For information +31-320-277070
www.micronic.com

Electronically submit your new product description or product literature information! Go to www.sciencemag.org/products/newproducts.dtl for more information.

Newly offered instrumentation, apparatus, and laboratory materials of interest to researchers in all disciplines in academic, industrial, and governmental organizations are featured in this space. Emphasis is given to purpose, chief characteristics, and availability of products and materials. Endorsement by *Science* or AAAS of any products or materials mentioned is not implied. Additional information may be obtained from the manufacturer or supplier.

Connecting you
to the world of...
Science

Science Careers Classified Advertising

For full advertising details, go to ScienceCareers.org and click for Advertisers, or call one of our representatives.

UNITED STATES & CANADA

E-mail: advertise@sciencecareers.org
Fax: 202-289-6742

Joribah Able
Industry - US & Canada
Phone: 202-326-6572

Alexis Fleming
Northeast Academic
Phone: 202-326-6578

Tina Burks
Southeast Academic
Phone: 202-326-6577

Daryl Anderson
Midwest/Canada Academic
Phone: 202-326-6543

Nicholas Hintibidze
West Academic
Phone: 202-326-6533

EUROPE & INTERNATIONAL

E-mail: ads@science-int.co.uk
Fax: +44 (0) 1223 326532

Tracy Holmes
Associate Director, *Science Careers*
Phone: +44 (0) 1223 326525

Alex Palmer
Phone: +44 (0) 1223 326527

Dan Pennington
Phone: +44 (0) 1223 326517

Susanne Kharraz Tavakoli
Phone: +44 (0) 1223 326529

Louise Moore
Phone: +44 (0) 1223 326528

JAPAN

Mashy Yoshikawa
Phone: +81 (0) 3 3235 5961
E-mail: myoshikawa@aaas.org

To subscribe to *Science*:
In US/Canada call 202-326-6417 or 1-800-731-4939.
In the rest of the world call +44 (0) 1223 326515.

Science makes every effort to screen its ads for offensive and/or discriminatory language in accordance with US and non-US law. Since we are an international journal, you may see ads from non-US countries that request applications from specific demographic groups. Since US law does not apply to other countries we try to accommodate recruiting practices of other countries. However, we encourage our readers to alert us to any ads that they feel are discriminatory or offensive.

Science Careers

From the journal *Science*



iZumi Bio, Inc., founded in 2007, is conducting research and development to realize the power of induced pluripotent stem (iPS) cells to transform drug discovery and enable the promise of regenerative medicine. We are focused on leveraging and translating stem cell biology into treatments for a broad array of human diseases. iZumi is funded by Kleiner Perkins Caufield and Byers and Highland Capital Partners and is located in the San Francisco Bay Area.

A position at iZumi is an opportunity to join a team of leading scientists and collaborators committed to improving human health.

iZumi is an equal opportunity employer. We are committed to building a workforce that respects individual skills and diversity while embracing teamwork; we demonstrate integrity, passion and scientific excellence. We hire outstanding people and subscribe to a rigorous, fast-paced work ethic where the science leads the business. If you are interested in joining the iZumi team, please submit your resume/CV online at careers@izumibio.com and reference #SC1111 when applying.

Director/Senior Director, Drug Discovery Biology: Leads all activities related to the production of iPS cell lines and their use for pharmaceutical discovery.

Ph.D. or MD; 7-10 years of drug discovery experience in a biotech and/or pharmaceutical company; solid understanding of pre-clinical drug discovery process; expertise in using physiologically relevant cell-based assays along the entire spectrum of drug discovery; drug discovery experience in the following therapeutic areas a plus: diabetes, cardiovascular, neurodegeneration; experience presenting programs to potential partners and investors that result in collaborations and funding opportunities; proven ability to build and lead productive teams; basic knowledge of stem cell biology.

Human Stem Cell Group Leader: Directs an innovative research program using human stem cells to investigate and model developmental and disease mechanisms.

Ph.D. in Developmental Biology; minimum 5 years experience in academic or industrial environment; experience optimizing human ES cell derivation; expert experience with human ES/iPS cell culture, characterization, and differentiation; demonstrated success in technical proficiency, scientific creativity, collaboration with others and independent thought; expert knowledge of scientific principles and concepts, and a reputation as emerging leader in field with sustained performance and accomplishment; generation and culture of mouse or human iPS cells and experience with animal and cellular models of metabolic and neurodegenerative diseases a plus.

Chemical Genomics Group Leader: Implement an innovative research program employing small molecules to probe and manipulate cell function.

Ph.D. in Chemistry, Biochemistry or related science; minimum 5 years experience in academic or industrial environment; proficiency in the development of cell-based assays and the use of small molecules and genomic tools; demonstrated success in technical proficiency, scientific creativity, collaboration with others and independent thought; expert knowledge of scientific principles and concepts and a reputation as emerging leader in field with sustained performance and accomplishment; thorough knowledge in cell-based assays and small molecules as tools.

Tissue Engineer: Develop and optimize methods for iPS cell production and differentiation.

Ph.D. in Bioengineering, Cell Biology, or related field; 3-5 years of hands-on experience establishing primary tissue culture from human samples; experience across a broad variety of biomaterials and tissue engineering techniques including method development for establishing primary cell culture, differentiation, tissue scaffolding; molecular biology and virology experience is a plus.

Cardiovascular Scientist: Differentiate cardiac myocytes and/or vascular endothelial cells from embryonic stem cells.

Ph.D. or MD degree; 3-5 years of postdoctoral experience in an academic setting; knowledge of molecular and genetic pathways that control cardiac myocyte and vascular endothelial cell differentiation; experience in developing mouse and/or human cardiovascular model systems in culture for studying normal physiology and disease; electrophysiology expertise; experience with human embryonic stem cells a plus.

Research Assistant/Associate: Use molecular and cell culture techniques to develop novel cell lines and technologies.

B.S. or M.Sc. degree in Developmental Biology, Molecular Biology, or related discipline; 2+ years full time experience in an academic or biotechnology industry laboratory; knowledge and demonstrated proficiency in a broad range of molecular and cell biological techniques, including preparing DNA/RNA/protein from cells, qRT-PCR, immunocytochemistry, cell culture and cell-based assays; ability to conduct FACS and analysis; impeccable aseptic technique; passion and excitement for conducting both independent and collaborative groundbreaking research in a dynamic, innovative, multidisciplinary company setting; experience tailoring currently accepted protocols; excellent organizational, problem-solving, verbal/written communication; strong working knowledge of human stem cell culture and experience differentiating ES cells preferred.



**Science & Technology
Facilities Council**

The Science and Technology Facilities Council brings strategic leadership and an integrated approach to UK investments in large national and international research facilities, whilst delivering world-class science, technology and people for the UK. The Council is involved in some of the world's most exciting research projects – like the Diamond Light Source, the Large Hadron Collider, and the exploration of the solar system – and will develop new areas of science and technology – with your help.

Director of Space Science and Exploration

£53,000 – £59,000 pa

Reporting to the Director of Science Programmes, you'll be a key member of the UK space science community. You will work within the British National Space Centre partnership which represents UK space activities in international fora. Overall, your aim will be to achieve the maximum science and industrial return within the resources available for space science and exploration in the UK and Europe.

This highly creative and wide-ranging role will involve communicating the UK space agenda to a number of important international bodies involved in the future of European space programme while maintaining close links at Director Level with organisations that invest in space in the UK. You'll take a proactive role in identifying possible improvements in the UK space programme and be responsible for summarising key issues, devising strategies and recommending lines for the UK to adopt at ESA Council. Overall, you'll ensure that UK policy in space science and exploration is clearly communicated to everyone within the European space community and that the UK is influential within the future of the ESA.

To succeed, you'll need to have a thorough understanding of the STFC space science and exploration activities and of the European Space Agency programme within a global context. You will be familiar with spacecraft systems and the engineering of end-to-end space projects. In addition, you'll need proven management, leadership and negotiation skills and extensive experience at a senior level in international space activities, likely including industrial experience and appropriate technical awareness. The post requires a substantial amount of travel to meetings around the UK and overseas.

The UK is growing within the space field and this is your chance to be a part of it.

For an application form and further details, please visit the JRU website to download the application documents – <http://jru.rcuk.ac.uk/AllVacancies/32408.htm>

Alternatively please contact Beccie Callahan via email; jru-recruitment@ssc.rcuk.ac.uk or telephone 01793 416459 quoting the reference number JRU 324/08.

Closing date: 23 January 2009.

www.scitech.ac.uk





KEAN
UNIVERSITY
www.kean.edu

**College of Natural, Applied and
Health Sciences
Open Rank Faculty Position
Sustainability Initiative**

Kean, a comprehensive university, is committed to excellence and access and to developing, maintaining and strengthening interactive ties with the community. Kean University takes pride in its continuing effort to build a multicultural professional community to serve a richly diversified student population of over 14,000.

All faculty are expected to demonstrate a commitment to teaching excellence and an on-going program of research and publication or creative and performance activity. Participation in curriculum development, student advisement and service at the departmental, college and university levels is also expected. Interest or experience in using advanced instructional technologies to improve the teaching/learning process is highly desirable.

Open Rank Faculty Position (10 months) – Full-time, tenure-track faculty position for the Sustainability Initiative within the College of Natural, Applied and Health Sciences (CNAHS). Responsibilities include teaching; coordinating a new Bachelor of Science degree program in Sustainability Science as well as the interdisciplinary Institute of Urban Ecosystem Studies; overall planning, coordination and implementation of the Sustainability Initiative; overseeing the hiring and evaluation of faculty; leadership in program evaluation; budgetary responsibilities; and additional duties as required by the Dean of CNAHS. The anticipated start date is September 1, 2009.

Qualifications: Ph.D. in an environmental field related to sustainability (with emphasis on natural sciences) and experience in resource conservation and sustainability practices. The successful applicant will have demonstrated teaching excellence at the college level, strong written and verbal communication skills, extensive experience coordinating, organizing and implementing programs, a strong record of scholarship, ability to maintain an active research program, as well as administrative and fiscal management abilities and strong leadership/management qualities.

Review of applications will begin immediately and continue until position is filled. Send letter of interest, resume and contact information for three professional references to: **Dr. Jeffrey H. Toney, Dean of the College of Natural, Applied and Health Sciences, Kean University, 1000 Morris Avenue, Union, NJ 07083.** Official transcripts for all degrees and three current letters of recommendation are required before appointment. Salary is competitive and commensurate with qualifications and experience. Comprehensive benefits program included. **Contingent on Budgetary Approval and Appropriated Funding.**

Kean University is an EOE/AA Institution.

**Dean of the School of
Graduate Studies/Vice Dean
of Basic Science Research for
the College of Medicine**

The State University of New York Downstate Medical Center, located in Brooklyn, New York, seeks a dynamic leader to serve as Dean of the School of Graduate Studies and Vice Dean of Basic Science Research for the College of Medicine. The Dean of the School of Graduate Studies will provide leadership and support to approximately 100 faculty and 85 students who participate in three Ph.D. and MD/Ph.D. programs: Molecular and Cellular Biology, Neural and Behavioral Science, and Biomedical Engineering. The Dean will work closely with the faculty to ensure an outstanding education for our students, will spearhead efforts to obtain extramural funding to supplement state support of the graduate school, and will direct the recruitment of students. As Vice Dean for Basic Science Research, he/she will provide support and oversight of the Center's basic research programs, promote basic science and translational research interactions within the institution, and assist faculty in identifying and securing additional extramural funding. Candidates should have a strong track record of sponsored biomedical research and experience training graduate students. Send CV and statement of educational philosophy by February 15 to: **GradSearch@downstate.edu**



**SUNY
DOWNSTATE**
Medical Center
SUNY Downstate is an EOE



大陽陽於市 學研研出屋
A World-class University

Celebrating 25th Anniversary



香港城市大學
City University
of Hong Kong

City University of Hong Kong invites nominations and applications for the following posts. Candidates with applied research achievements will receive very positive consideration. Relevant experience in business and industry will be a definite asset.

**Professor/Associate Professor/Assistant Professor
Department of Physics and Materials Science [Ref. A/559/49]**

The University aspires to be internationally recognized as a leading university in the Asia-Pacific region through excellence in professional education and applied research. The Department of Physics and Materials Science was formed in 1993 as the first of its kind in Hong Kong, and already excels in several fields.

The Department seeks strong candidates in emerging fields that strengthen and expand its existing areas of focus. Particularly strong candidates are welcome in any field. The University places much emphasis in the areas of Energy, Environment and Biomedical Engineering.

Requirements: A PhD in a closely related discipline with a promising research record and a strong teaching ability. The successful candidates are expected to develop new research directions and courses.

Salary and Conditions of Service

Remuneration package will be highly competitive, commensurate with qualifications and experience. Initial appointment will be made on a fixed-term gratuity-bearing contract. Fringe benefits include leave, medical and dental schemes, and housing benefits where applicable. (The remuneration package is currently under review.)

Application and Information

Information concerning the posts and the University is available at <http://www.cityu.edu.hk> or from the Human Resources Office, City University of Hong Kong, Tat Chee Avenue, Kowloon, Hong Kong [Fax : (852) 2788 1154 or (852) 2788 9334/email : hrojob@cityu.edu.hk]. Please send the nomination or application enclosing a current CV with evidence of teaching ability in English, and a concise (up to one page) statement of research interests and teaching philosophy to the Human Resources Office. **Applications will be considered until positions are filled.** Please quote the reference of the post in the application and on the envelope. The University reserves the right to consider late applications and nominations, and not to fill the positions. Personal data provided by applicants will be used for recruitment and other employment-related purposes.



**UNIVERSITY OF
LIVERPOOL**

**School of Biomedical Sciences
Department of Pharmacology**

Chair of Pharmacology

Salary Negotiable

The University of Liverpool invites applications for a Chair of Pharmacology. This is an opportunity for an outstanding individual with a proven research record. The University has been awarded a prestigious MRC Centre for Drug Safety Science.

You will have an established independent research programme which will complement and enhance the existing strengths in Pharmacology and the MRC Centre. Candidates with a research background in Immunopharmacology are of particular interest, but applications from candidates with an established track record in research in Pharmacology or Toxicology will be welcomed. High quality laboratory research space exists, and there is an opportunity to develop further refurbished research laboratories.

Informal enquiries to Professor B K Park, Head of the Department of Pharmacology and Director of the MRC Centre on 0151 794 5450, email: b.k.park@liv.ac.uk

Job Ref: A-508334/S

Closing Date: 20 February 2009

For full details, or to request an application pack, visit
www.liv.ac.uk/working/job_vacancies/ or e-mail jobs@liv.ac.uk
Tel 0151 794 2210 (24 hr answerphone)

Please quote Job Ref in all enquiries.

COMMITTED TO DIVERSITY AND EQUALITY OF OPPORTUNITY

King Abdullah University of Science and Technology (KAUST)

Faculty Positions in Chemical and Biological Engineering

King Abdullah University of Science and Technology (KAUST) is being established in Saudi Arabia as an international graduate-level research university dedicated to inspiring a new age of scientific achievement that will benefit the region and the world. As an independent and merit-based institution and one of the best endowed universities in the world, KAUST intends to become a major new contributor to the global network of collaborative research. It will enable researchers from around the globe to work together to solve challenging scientific and technological problems. The admission of students, the appointment, promotion and retention of faculty and staff, and all the educational, administrative and other activities of the University shall be conducted on the basis of equality, without regard to race, colour, religion or gender.

KAUST is located on the Red Sea at Thuwal (80 km north of Jeddah). Opening in September 2009, KAUST welcomes exceptional researchers, faculty and students from around the world. To be competitive, KAUST will offer very attractive base salaries and a wide range of benefits. Further information about KAUST can be found at <http://www.kaust.edu.sa/>

KAUST invites applications for faculty positions at all ranks (Assistant, Associate or Full Professor) in Chemical and Biological Engineering. Research interests may include areas such as:

- Biological Engineering (biomedical engineering; biotechnology and bioprocess engineering)
- Natural Resource Engineering (energy engineering; environmental engineering)
- Fluids Engineering (fluid mechanics; molecular modelling and thermodynamics)
- Particle and Materials Engineering (complex materials; surfaces and interfaces)
- Process Systems Engineering (methodologies; applications)
- Reaction and Separation Engineering (reaction engineering and catalyst technology; separation engineering and technology)

High priority will be given to the overall originality and promise of the candidate's work rather than the candidate's sub-area of specialisation within Chemical or Biological Engineering. Nevertheless, KAUST is particularly interested in applicants whose research has applications in the fields of catalysis, clean combustion, membranes, solar/alternative energy and water desalination.

An earned PhD in Chemical Engineering or a related Science or Engineering discipline, evidence of the ability to pursue a programme of research, and a strong commitment to graduate teaching are required. Applicants should have at least one year of postdoctoral research experience. A successful candidate will be expected to teach courses at the graduate level and to build and lead a team of graduate students in Master's and PhD research.

Applications (including a curriculum vitae, list of publications, citation report with H-index value, brief statements of research and teaching interests, and the names and contact details of at least 3 referees) should be sent to the Search Committee by electronic mail to kaust.chemeng@imperial.ac.uk. Please note that the Search Committee may also appoint additional referees at its discretion. The review of applications will begin immediately, and applicants are strongly encouraged to submit applications as soon as possible; however, applications will continue to be accepted until December 2009, or until all 10 available positions have been filled.

In 2008 and 2009, as part of an Academic Excellence Alliance agreement between KAUST and Imperial College London, the KAUST Faculty search will be conducted by a committee consisting of Professors from the Faculty of Engineering at Imperial College London. This committee will select the top applicants and nominate them for Faculty positions at KAUST. However, KAUST will be responsible for actual recruiting decisions, appointment offers, and explanations of employment benefits. The recruited Faculty will be employed by KAUST, not by Imperial College London. Faculty members recruited by KAUST before September 2009 will be hosted in Chemical Engineering at Imperial College London as Academic Visitors until KAUST opens in September 2009. At Imperial College London, these Academic Visitors will conduct research with Imperial College London staff and may occasionally teach courses.

Enquiries and applications to: kaust.chemeng@imperial.ac.uk

Valuing diversity and committed to equality of opportunity



Max-Planck-Institute for Medical Research

Department of Biomolecular Mechanisms

The Department of Biomolecular Mechanisms at the Max Planck Institute for Medical Research in Heidelberg invites people interested in the structure and dynamics of macromolecular switches and assemblies to apply for

4 doctoral degree (Ph.D.) positions (reference number 13/2008) and 3 postdoctoral positions (reference number 14/2008)

Our department is an international and interdisciplinary team of four closely interacting groups. Our main research topics are: mRNA processing, chaperone-assisted and unassisted protein folding, and the detailed mechanisms of enzyme-catalysed reactions involving flavin or haem cofactors. We offer a unique environment of top-level scientific research and state-of-the-art technology. For further information, see the groups' web pages at <http://wbmm.mpimf-heidelberg.mpg.de/groups>. The stimulating and productive environment provides young scientists with an ideal starting-point for further career steps. Heidelberg is one of the top centres for biomedical research in Germany, and graduate students have access to several different Ph.D. programmes.

Candidates should have knowledge of and interest in one or more of the fields mentioned (with respect to either the research topic or the techniques employed), an outstanding track record and excellent skills in spoken and written English.

The Max Planck Society is an equal opportunity employer and seeks to increase the percentage of female employees in areas where they are under-represented. Qualified women are strongly encouraged to apply. Furthermore, we are also committed to employ more individuals with disabilities, and therefore actively encourage them to apply.

Candidates should send their formal application before February 28, 2009 to bmm.recruitment@mpimf-heidelberg.mpg.de with the reference number given in the subject line. The e-mail should contain a single Portable Document File (PDF) including

- a brief letter, preferably indicating which of the department's groups would be preferred
- a Curriculum Vitae
- a full list of publications (if applicable)
- a description of past and present research activities (1 page) and
- the names and addresses of referees (two for Ph.D. applicants or three for postdoctoral applicants).

FACULTY POSITIONS DEPARTMENT OF PHYSICS THE UNIVERSITY OF TEXAS AT AUSTIN

The Department of Physics at The University of Texas at Austin is seeking candidates for tenure-track assistant professorship positions in physics starting in September 2009. In special cases, appointments at more senior levels will be considered. Successful candidates will assume full teaching responsibilities for undergraduate and graduate courses in the Department of Physics and are also expected to conduct vigorous research programs. Research areas of current highest priority for the Department are Biophysics Experiment and Fundamental Theory/Cosmology. Outstanding candidates in other areas of departmental focus will also be considered. Excellent English language communication skills are required. Applicants must have a Ph.D. (or equivalent) and a demonstrated potential for excellence in teaching and research.

Interested applicants should send a curriculum vitae, a list of publications, a statement of research interests, a research plan, and should arrange for at least five letters of recommendation to be sent to: **Prof. John T. Markert, Chair, Department of Physics, The University of Texas at Austin, 1 University Station C1600, Austin, TX 78712-0264.** Review of completed applications began in **October, 2008** and is ongoing.

The University of Texas at Austin is an Equal Opportunity/Affirmative Action Employer.



National University of Ireland, Galway
Ollscoil na hÉireann, Gaillimh

Applications are invited for the following post:

PROFESSOR OF FUNDAMENTAL STEM CELL BIOLOGY

Closing date: 27 February, 2009

Further Information:

www.nuigalway.ie/vacancies

Human Resources Office, NUI Galway
T: 353 91 492151 E: hr@nuigalway.ie

National University of Ireland, Galway
is an equal opportunities employer



www.nuigalway.ie

Faculty Positions

Program in Basic and Translational Science Thomas Jefferson University, Kimmel Cancer Center

The Department of Medical Oncology at Thomas Jefferson University, Kimmel Cancer Center, is recruiting Faculty for its Program in Basic and Translational Science, with a focus on Stem Cell Biology and Transplant Medicine. This will also involve a joint appointment in Jefferson's Stem Cell Biology and Regenerative Medicine Center. Applicants with experience in all different areas of Stem Cell Biology are encouraged to apply.

The Department of Medical Oncology is part of an NCI-designated cancer center with outstanding research programs in cancer biology and cancer care. Outstanding partner programs in surgical and radiation oncology also exist at Jefferson. Positions are available for strong academic candidates with a focus on basic, clinical, or translational research. Candidates must demonstrate a strong commitment to independent research and education. Leadership responsibilities in the Kimmel Cancer Center will also be assigned commensurate with level of experience. The candidate should have the academic qualifications for appointment at the level of Assistant, Associate, or Full Professor. A generous start-up package is available for qualified applicants. The Kimmel Cancer Center at Thomas Jefferson University is an NCI-designated Cancer Center and a leader in cancer treatment and research. Thomas Jefferson University is an equal opportunity/affirmative action employer.

Interested individuals should send a CV and the names of two references to: **Michael P. Lisanti, MD-PhD, Director, Division of Basic and Translational Science, Department of Medical Oncology; Director, Jefferson's Stem Cell Biology and Regenerative Medicine Center, c/o Dawn Scardino, Thomas Jefferson University, 834 Chestnut Street, Suite 320, Philadelphia, PA 19107, (email Dawn.Scardino@jefferson.edu).**



Jefferson
University



Thyroid Cancer Research Scholar, Mentored Research Scholar and Postdoctoral Fellows: A Request for Applications

The American Cancer Society announces this **Request for Applications** for the **American Cancer Society MEN2 Thyroid Cancer Consortium**. Up to seven (7) **Research Scholar** and/or **Mentored Research Scholar** grants and up to five (5) **Postdoctoral Fellow** grants will be awarded. The Consortium will be led by a single renowned senior scientist who will be awarded the American Cancer Society MEN2 Thyroid Cancer Professorship and act as leader for the overall program (details at links below). Appropriate areas of investigation include, but are not limited to: understanding signaling pathways associated with RET mutations, broad molecular events underlying the development of thyroid cancer and other MEN2-related tumors, improved animal models of MEN2, new screening and monitoring tools, new imaging approaches, and new pharmacologic and other strategies to blunt the effects of RET and related mutations.

Individuals applying for a **Research Scholar Grant** must have an independent research or faculty position and be within six years of their first independent research or faculty appointment at the time of application. These grants will be awarded for up to \$200,000 a year, direct costs, for 5 years. **Mentored Research Scholar Grants** will be awarded to junior faculty members with a doctoral degree in a clinical or cancer control research discipline (e.g., M.D., and/or Ph.D.) that are within the first four years of a full time faculty appointment or equivalent, and have no more than 4 years of postdoctoral research experience immediately prior to their faculty appointment. The successful applicant is expected to transition into a career as an independent investigator. Awards are for up to five years and for up to \$135,000 per year direct costs.

Applicants for **Postdoctoral Fellowships** must have obtained their doctoral degree prior to activation of the fellowship. Awards are for three years with progressive stipends of \$44,000, \$46,000, and \$48,000 per year, plus a \$4,000 per year institutional allowance. Individuals who have held a PhD or MD for more than 4 years at the time of application are not eligible.

Deadline: Complete applications are due by **April 1, 2009**. Funding will begin January 1, 2010. For information regarding funding policies or to obtain an application, go to <https://proposalcentral.aaltum.com> or refer to the ACS website at www.cancer.org/research: select *Funding Opportunities* followed by *Index of Grants*, scroll down to *Special Initiatives* and select the appropriate RFA for MEN2 Thyroid Cancer. For inquiries, contact **Charles Saxe, PhD** at (404) 929-6919 (charles.saxe@cancer.org).

POSITIONS OPEN



Department of Health and Human Services
National Institutes of Health
National Institute on Aging



Statistical Genetics Director

The National Institute on Aging (NIA), a major research component of the National Institutes of Health (NIH) and Department of Health and Human Services (DHHS), is recruiting for a Staff Scientist (Facility Head) who will serve as the Statistical Genetics Director of the Laboratory of Genetics (LG), Intramural Research Program (IRP), in Baltimore, MD. The incumbent will be responsible for collaborating in and coordinating statistical genetic and epidemiological analyses of aging-related human conditions and diseases. The collaborative research includes the adaptation or development of new analytic programs with participation in an interactive group studying genetic and epidemiological data for selected aging-related phenotypes in the Baltimore Longitudinal Study of Aging; in other outbred populations; and in the Sardinian "founder population".

Accordingly, the duties of this position require the applicant to hold a Ph.D. and have at least 2 years of additional postdoctoral experience in statistical genetics or comparable epidemiological statistics. Applicants must have a record of scientific accomplishments, including excellence in statistical analyses and qualifications to develop, update, and manage statistical staff and analysis software.

Salary is commensurate with experience and accomplishments. The salary range for Staff Scientists is \$82,961 - \$166,430. A full Civil Service package of benefits (including retirement, health, life and long term care insurance, Thrift Savings Plan, etc.) is available. Applicants must send curriculum vitae, bibliography, and three letters of recommendation to: Chair, LG Staff Scientist - Statistical Genetics Search Committee; Vacancy #NIA-IRP-09-02; c/o Peggy Grothe, Intramural Program Specialist; Office of the Scientific Director, National Institute on Aging, 251 Bayview Blvd, Suite 100, Room 04C221 Baltimore, MD 21224. Position will remain open until filled; however, the application review process will begin **February 28, 2009**. If additional information is needed, please call 410-558-8012 or email: grothep@grc.nia.nih.gov.

DHHS and NIH are Equal Opportunity Employers

MONSANTO
imagine[®]



At the vegetable division of Monsanto, world-class talent and technology are at the heart of our research and future.

We have unique opportunities available for highly motivated PhD level candidates within our molecular marker discovery and strategic trait development teams:

- Trait Strategy Lead
- Trait Discovery
- Trait Genetics
- Trait-Marker Discovery
- Marker-Assisted Breeding

These positions will be located at one of the Seminis or De Ruiter R&D sites in Woodland, CA or the Netherlands.

Visit our website today to learn why Monsanto is the scientific employer of choice.

www.seminis.com/careers

www.deruiterseeds.com/jobs/vacature

The world, re-imagined



Science Careers is the window
that displays your vision.



Visit our
ENHANCED
WEBSITE!

Revealing your vision to employers is our job. We're your source for connecting with top employers in industry, academia, and government. We're the experts and entry point to the latest and most relevant career information across the globe.

Our newly designed website offers a set of tools that reveal career opportunities and your personal potential. Whether you're seeking a new job, career advancement in your chosen field, or ways to stay current on industry trends, *Science Careers* is your window to a limitless future.

Improved Website Features:

- » Relevant Job E-mail Alerts
- » Improved Resume Uploading
- » Content Specific Multimedia Section
- » Facebook Profile

Job Search Functionality:

- » Save and Sort Jobs
- » Track Your Activity
- » Search by Geography
- » Enhanced Job Sorting



Your Future Awaits.

Science Careers

From the journal *Science*



ScienceCareers.org

AWARDS

Avant-Garde AWARD

NIDA NATIONAL INSTITUTE
ON DRUG ABUSE

NATIONAL INSTITUTES OF HEALTH

U.S. Department of Health and Human Services

This 5-year, \$2.5M award is designed to support
individual scientists of exceptional
creativity
who propose
cutting-edge
and
transformative
approaches to **major challenges**
in biomedical and behavioral
research on **drug
abuse and HIV/AIDS**
2009

Additional information is available at:
<http://drugabuse.gov/avgp.html>

POSITIONS OPEN



University of Alabama at Birmingham
Faculty Positions in Virology and Immunology

The Department of Microbiology invites applications for up to six tenure-track junior or senior faculty positions in virology and immunology. Successful candidates will have demonstrated records of originality and productivity in research, existing or outstanding potential for consistent extramural research funding, and concerned interest in graduate and medical education. UAB ranks in the top 20 institutions in NIH funding for research and offers an unusually interactive research environment. Collaborations among the basic science disciplines and between basic and clinical faculty are stimulated by the presence of many multidisciplinary Centers, including a leading Center for AIDS Research, a Comprehensive Cancer Center, a Comprehensive Arthritis, Musculoskeletal and Autoimmunity Center, a Comprehensive Diabetes Center, a Center for Clinical and Translational Science, a Center for Emerging Infections and Emergency Preparedness, a Liver Center and a campus-wide Program in Immunology. State-of-the-art BSL3/ABSL3 containment facilities are available.

Current areas of research strength are highlighted on the department web site (<http://www.microbio.uab.edu/interests.html>). Successful applicants can provide expertise in new, complementing areas or can extend existing strengths. Investigators in the areas of tumor virology, HIV, select agent research, cancer immunology, inflammation and cancer, immunology of diabetes, autoimmunity, and transplantation immunology are particularly encouraged to apply.

Review of applications will begin immediately and will continue until the positions are filled. Applicants are asked to submit (preferably electronically) their c.v., a 2-4 page summary of their research accomplishments and future plans, and the names and contact information of three references to: **David D. Chaplin, M.D., Ph.D., c/o Michael Settine, email: msettine@uab.edu; UAB Dept. of Microbiology, 845 19th Street S., Birmingham, AL 35294. Tel: (205) 934-3598.**

*UAB is an Affirmative Action/Equal Opportunity Employer.
Women and minorities under-represented in biomedical research are
encouraged to apply.*

AWARDS

New Phytologist
Tansley Medal
for excellence in plant science



The *New Phytologist* Tansley Medal will be awarded annually in recognition of an outstanding contribution to research in plant science by an individual in the early stages of their career.

Submissions are welcomed from both student and post-doctoral researchers with up to five years experience since gaining their PhD. The winner will receive a prize of £2000 and the successful article will be published in *New Phytologist*, which will be accompanied by a comment from the Editor-in-Chief.

Application process

Submit an extended abstract (1000 words, with 1-2 figures) that describes (1) the research conducted, including the rationale, (2) methods, (3) key results and (4) the main conclusion, including key points of discussion. This abstract should be submitted along with your curriculum vitae, and a supporting statement from a scientist who has agreed to act as a referee for your application.

Successful applicants will be notified by Wednesday July 15th 2009 and asked to submit their work as a full research article no later than August 31st 2009. These articles will be reviewed by members of the *New Phytologist* Editorial board, and the winner announced by December 2009.

Extended abstracts should be received by Monday 15th June 2009. To submit your application online or for further details please visit: <http://www.newphytologist.org/tansleymedal.htm>



New
Phytologist

... promoting plant science



FONDATION BETTENCOURT SCHUELLER

2008 LILIANE BETTENCOURT LIFE SCIENCES AWARD



CAETANO REIS E SOUSA

The 2008 Liliane Bettencourt Life Sciences Award has been awarded to the outstanding immunobiologist Caetano Reis e Sousa from the Cancer Research UK London Research Institute.

A major scientific goal of Caetano Reis e Sousa is to understand the regulation of adaptive immunity by antigen-presenting cells and the innate mechanisms leading to dendritic cell (DC) activation. Among his important contributions is the characterization of several "pattern-recognition pathways" involved in DC activation by potential pathogens such as viruses and fungi. By combining skilled molecular approaches to dissecting ligand-receptor interactions and intracellular signalling with a highly sophisticated expertise in in vitro and in vivo cellular immunology, he has become a world leader in the field of innate immunity and DC biology. This outstanding investigator, first-rate author, excellent public speaker and wonderful mentor has played a leading role in increasing our understanding of the host-pathogen relationship.

The Liliane Bettencourt Life Sciences Award of € 250,000 is an essential part of the Bettencourt Schueller Foundation's commitment to Biomedical Research. It aims to support a top-level European researcher under the age of 45, along with his or her team, to pursue their work in the field of Life Science. The international Jury for the Award is chaired by Professor Pierre Corvol, Administrator of the Collège de France and member of the French Academy of Sciences.

The Bettencourt Schueller Foundation was created in 1987 by Mrs. Liliane Bettencourt, in memory of her father, the late Eugène Schueller, founder of L'Oréal. Its mission is to encourage entrepreneurship in Sciences, Arts and Social Commitment. In 2008, the Foundation has provided more than 60% of its budget in support of scientific research programs.

Fondation
Bettencourt Schueller
27-29, rue des Poissonniers
92522 Neuilly-sur-Seine Cedex
www.fondationbs.org
Contact: mw@fondationbs.org

ROBERT J. AND CLAIRE PASAROW FOUNDATION
22nd Annual
MEDICAL RESEARCH AWARDS
CALL FOR NOMINATIONS
Cancer, Cardiovascular Disease, Neuropsychiatry

The Foundation has established three yearly medical prizes for distinguished accomplishment in research in order to increase public awareness of vital areas of investigation. This is the twenty-second year of the awards program. Each award is for \$50,000, presented directly to the awardee. The three prizes – one in each of the three fields – are given for extraordinary basic and/or clinical or translational research.

Cancer: including basic cellular processes and the various forms of cancer. **Past awardees:** Peter K. Vogt, PhD; Irving L. Weissman, MD; George F. Vande Woude, PhD; Erkki Ruoslahti, MD; Harold N. Weintraub, MD, PhD; Ronald M. Evans, PhD; Stanley J. Korsmeyer, MD; Carlo M. Croce, MD; Alfred G. Knudson, Jr., MD, PhD; Robert A. Weinberg, MD; Eric S. Lander, D.Phil.; Paul L. Modrich, PhD; Anthony S. Fauci, MD; Alexander J. Varshavsky, PhD; Tom Maniatis, PhD; Roger D. Kornberg, PhD; Elizabeth H. Blackburn, PhD; Fred W. Alt, PhD; Bert O'Malley, MD; Tony Hunter, PhD; and Bert Vogelstein, MD

Cardiovascular Disease: including disorders of the heart and vascular system. **Past awardees:** Burton E. Sobel, MD; Harvey Feigenbaum, MD; Bernardo Nadal-Ginard, MD, PhD; Mordecai P. Blaustein, MD; Jonathan Seidman, PhD and Christine Seidman, MD; Glenn A. Langer, MD; Philip Majerus, MD; Jan L. Breslow, MD; Kenneth R. Chien, MD, PhD; Michael A. Gimbrone, Jr., MD; Masashi Yanagisawa, MD, PhD; Mark T. Keating, MD; Eric N. Olson, PhD; Richard P. Lifton, MD, PhD; Robert J. Lefkowitz, MD; Shaun Coughlin, MD, PhD; Judah Folkman, MD; Barry S. Collier, MD; Douglas C. Wallace, PhD; Daniel Steinberg, MD, PhD; and Richard O. Hynes, PhD

Neuropsychiatry: including neurologic and mental disorders. **Past awardees:** Nancy Wexler, PhD; Eric R. Kandel, MD; Floyd E. Bloom, MD; Solomon H. Snyder, MD; Michael E. Phelps, PhD; Patricia S. Goldman-Rakic, PhD; Huda Akil, PhD and Stanley Watson, MD, PhD; Arvid Carlsson, MD, PhD and Philip Seeman, MD, PhD; Stanley B. Prusiner, MD; Joseph T. Coyle, MD; Eric J. Nestler, MD, PhD; Fred H. Gage, PhD; Michael I. Posner, PhD and Marcus E. Raichle, MD; Pasko Rakic, MD, PhD; Seymour Benzer, PhD; Tomas Hökfelt, MD, PhD; Thomas M. Jessell, PhD; Judith L. Rapoport, MD; Bruce McEwen, PhD; Huda Y. Zoghbi, MD; and Aaron T. Beck, MD

The criterion for the Pasarow Medical Research Awards is evidence of extraordinary accomplishment in medical science.

Nominators for the 2008 Award should provide a letter of no more than one page stating the rationale for the nomination and a copy of the nominee's curriculum vitae and bibliography in a two-page NIH format. Applications will be reviewed by the Board of Directors in consultation with various medical scholars. Members of the Board of Directors are **Michael Pasarow**, Chairman; **Anthony H. Pasarow**, Co-Treasurer; **Susan A. Pasarow**, MSW, Co-Treasurer; **Jack D. Barchas**, MD, President; **Shaun Coughlin**, MD, PhD – University of California, San Francisco; **Ronald M. Evans**, PhD – The Salk Institute; **Brian E. Henderson**, MD – University of Southern California; **Joseph P. Van Der Meulen**, MD – University of Southern California, and **Alexander J. Varshavsky**, PhD – CalTech.

Nominations should be sent to: **Robert J. and Claire Pasarow Foundation, c/o Jack D. Barchas, MD; Weill Cornell Medical College, 1300 York Avenue, Box 171, Room F-1231, New York, NY 10065.**

For more information, please contact **Jack D. Barchas, MD** at (212) 746-3770 or **jbarchas@med.cornell.edu**. Nominations should be received by **February 9, 2009**.

CLAIRE PASAROW

Those associated with the Robert J. and Claire Pasarow Foundation, including the Board of Directors, Advisors, and Awardees, extend our heartfelt condolences to the Pasarow Family on the passing of Claire Pasarow. The Pasarows established the Foundation over twenty years ago to celebrate extraordinary achievement, creativity, and distinction in research in three areas of medicine: cancer, cardiovascular disease, and neuropsychiatry. The late Robert Pasarow started a business in which Claire actively participated; she was also a gifted sculptor and artist. Their shared enthusiasm, passion, and enjoyment in learning the stories of the work of the medical researchers who received the Pasarow Awards were deeply appreciated. After the death of Robert, Claire continued as the inspirational source for the work of the Foundation. Claire Pasarow's spirit and love of creative effort was a joy to all of us who knew her.

MAX-PLANCK-INSTITUT FÜR
 BIOPHYSIKALISCHE CHEMIE
 KARL-FRIEDRICH-BONHOEFFER-INSTITUT
 GÖTTINGEN



The research group Electron Paramagnetic Resonance (EPR) spectroscopy at the Max Planck Institute for biophysical Chemistry is offering

Ph.D. and Postdoc Positions
(Code Number 33-08)

in biomolecular EPR spectroscopy. The candidates should have a Master or equivalent degree in Chemistry or Physics. For a postdoc position some experience with magnetic resonance spectroscopy is desired. The laboratory is equipped with Bruker Elexsys X-, Q- and W-band pulse spectrometers with ENDOR and PELDOR capabilities. The EPR methodology is applied to study the structure and function of proteins and enzymes.

The Positions are available from January 1st, 2009. Payment will be according to German TVöD standard or from a scholarship.

The Max Planck Society seeks to increase the number of women in those areas where they are underrepresented and therefore explicitly encourages women to apply. The Max Planck Society is committed to employing more handicapped individuals and especially encourages them to apply.

Please send your application documents per email with reference to the code number to **Marina.Bennati@mpibpc.mpg.de**.

Max Planck Institute for Biophysical Chemistry
RG „Electron Paramagnetic
Resonance Spectroscopy“
Dr. Marina Bennati

Tel.: 0049-551-201-1911



**Your
 career
 is our
 cause.**

**Get help
 from the
 experts.**

**www.
 sciencecareers.org**

- Job Postings
- Job Alerts
- Resume/CV Database
- Career Advice
- Career Forum

Science Careers

From the journal *Science*



Science Careers is the key that opens doors.

Visit our
ENHANCED
WEBSITE!



Opening doors is what we do. We're the key to connecting with the industry's top employers. We're the experts and source for accessing the latest and most relevant career information across the globe.

Our newly designed website offers a set of tools that help you unlock career opportunities and your personal potential. Whether you're seeking a new job, career advancement in your chosen field, or ways to stay current on industry trends, *Science Careers* is your key to a brighter future.

Improved Website Features:

- » Relevant Job E-mail Alerts
- » Improved Resume Uploading
- » Content Specific Multimedia Section
- » Facebook Profile

Job Search Functionality:

- » Save and Sort Jobs
- » Track Your Activity
- » Search by Geography
- » Enhanced Job Sorting



Your Future Awaits.

Science Careers

From the journal *Science*



ScienceCareers.org

POSITIONS OPEN
Visit our enhanced website!

Science Careers

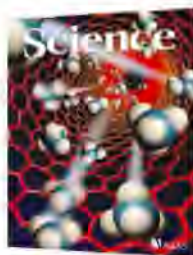
is the catalyst
for your ambition.



Promoting your ambition is what we do. Whether you're seeking career advancement in your chosen field, or a new job in academia or industry, *Science Careers* is your catalyst for an accelerated future.

Improved Website Features:

- » New design for easier navigation
- » More relevant job search results
- » Automated tools for a more effective search



Your Future Awaits.

Science Careers
From the Journal *Science* AAAS
ScienceCareers.org

POSITIONS OPEN



CHAIR of the SCHOOL of CHEMISTRY and BIOCHEMISTRY Georgia Institute of Technology

The Georgia Institute of Technology (Georgia Tech) invites nominations and applications for Chair of the School of Chemistry and Biochemistry. Georgia Tech seeks an individual with an earned Doctorate in chemistry, biochemistry, or a related discipline. Candidates must have demonstrated outstanding leadership and scholarship, and have strong commitments to interdisciplinary research, educational activities, and faculty/staff development.

The School of Chemistry and Biochemistry at Georgia Tech is a dynamic Department with diverse research activities that benefit from a Georgia Tech-wide expansion in the natural sciences. Georgia Tech's commitment to interdisciplinary collaboration is also a major asset that has led to frequent, facile, and fruitful interactions of faculty in the School with other strong programs in science and engineering at the Institute. External research funding in chemistry and biochemistry has tripled in the last six years, with campuswide chemical R&D more than doubling from 2003 to 2006 alone (*C&EN*). The School of Chemistry and Biochemistry offers B.S. degree programs in chemistry and in biochemistry, and M.S. and Ph.D. programs in the fields of biochemistry, analytical, inorganic, organic, physical, and polymer chemistry. The School is comprised of 40 faculty members (a 35 percent increase over the past decade) and is currently ranked (*U.S. News & World Report*) among the top 15 percent of graduate chemistry programs in the United States.

For further information, please refer to the Georgia Tech web page at [website: http://www.chemistry.gatech.edu/](http://www.chemistry.gatech.edu/).

Applications and nominations should be sent to e-mail: science@cos.gatech.edu or by regular mail to: **Chemistry and Biochemistry Chair Search Committee, Dean's Office, College of Sciences, Georgia Institute of Technology, 225 North Avenue, SE, Atlanta, GA 30332-0365 U.S.A.** Applications will be accepted until the position is filled. Applications should include a letter of interest and a current resume that describes the research, teaching, and administrative experience, publications, and names/addresses/telephone numbers of at least five references. *Georgia Institute of Technology, a unit of the University System of Georgia, is an Equal Education and Employment Opportunity Institution.*

ASSISTANT PROFESSOR, ENVIRONMENTAL MICROBIOLOGY. The Department of Microbiology at Oregon State University invites applications for a nine-month, 1.0 full-time equivalent, tenure-track position. The successful candidate will be expected to establish a competitive research program focused on aspects of microbial ecology, metabolism, bioremediation, genomics, and evolution. Areas of particular interest include, but are not limited to, aquatic prokaryotic systems, including subsurface and marine microbiology, and aquatic pathogens. Research programs that could link to local initiatives in computational and genome biology and mass spectrometry are encouraged. The candidate will also teach undergraduate and graduate courses in microbiology. Information at [website: http://microbiology.science.oregonstate.edu/positions](http://microbiology.science.oregonstate.edu/positions). Apply at [website: http://www.oregonstate.edu/jobs](http://www.oregonstate.edu/jobs), posting #0003557. Closing-date is March 16, 2009.

OSU is an Affirmative Action/Equal Opportunity Employer.

POSITIONS OPEN



NEURO-ONCOLOGY FACULTY POSITION

The Dardinger Neuro-Oncology Center at the Ohio State University Medical Center is seeking applicants for a faculty position. The successful candidate will join a well-established Neuro-Oncology Program that is very active in developmental therapeutics and clinical trials for primary and metastatic brain tumors. This position requires a Ph.D. and/or M.D. with postdoctoral experience. The chosen candidate will be asked to set up an independent neuro-oncology laboratory within the Dardinger Neuro-Oncology Center. Academic rank and tenure status will depend on background and preferences of the candidate.

Applicants should submit curriculum vitae, statement of research plans, and arrange to have three letters of reference sent to: **E. Antonio Chiocca, M.D., Ph.D., Professor and Chair, Department of Neurological Surgery, The Ohio State University, N1021 Doan Hall, 410 W. 10th Avenue, Columbus, OH 43210.**

The Ohio State University is an Equal Opportunity, Affirmative Action Employer.

Women and minorities are strongly encouraged to apply.

ASSISTANT/ASSOCIATE/FULL PROFESSOR Autoimmune Diseases University of Wisconsin, Milwaukee

The Health Sciences Department of the College of Health Sciences invites applications for a full-time, nine-month, tenure-track Assistant, Associate, or Full Professor in the health sciences, specifically in regard to autoimmune diseases. Applicable fields of study include virology, immunology, hematology, cell biology, and other work related to autoimmune disease. Candidates should have an active research program with the potential for establishing external funding. This position will support the M.S. and B.S. degrees in clinical laboratory sciences and the interdisciplinary Ph.D. degree in health sciences. The appointment will begin August 24, 2009.

Application procedure: All applicants will need to apply online at [website: http://www.jobs.uwm.edu/applicants/Central?quickFind=50820](http://www.jobs.uwm.edu/applicants/Central?quickFind=50820) and submit electronically curriculum vitae, cover letter, and contact information for three professional references (name, address, telephone, and e-mail). This address also gives more information about the position. Review of applications began December 1, 2008, and will continue until position is filled.

POSTDOCTORAL POSITIONS Antibody-based Therapeutics

Highly motivated individuals with a Ph.D./M.D. and a strong background in molecular/cellular biology and/or physical sciences to work on antibody-based therapeutics in autoimmunity and cancer. Please send curriculum vitae and details of three references to: **Dr. E. Sally Ward (e-mail: wardlab@utsouthwestern.edu), Department of Immunology, University of Texas Southwestern Medical Center, Dallas, TX 75390-9093.** *UT Southwestern is an Equal Opportunity, Affirmative Action Employer.*

MARKETPLACE

For COLLAGEN Detection...
Connect with Cosmo Bio

ELISAs to measure COLLAGENS: Type 1 (hu); Type 2 (hu, ms, rt, +). **ELISAs to measure ANTI-COLLAGEN ANTIBODIES:** Type 1 (hu); Type 2 (hu, ms, rt, +). **SPECIFIC ANTIBODIES:** Types 1, 2, 3, 4, 5, 6, 7, 8, 9, 10, 11, 12, 14.

Research Products from Japan
www.cosmobio.com

COSMO BIO CO., LTD.
Inspiration for Life Sciences

The last word on *Science Signaling*...



....is now even better.

*Science Signaling** now adds peer-reviewed, original research papers. Under the editorial leadership of Chief Scientific Editor, Michael B. Yaffe, M.D., Ph.D., Associate Professor of Biology at MIT, *Science Signaling* will provide the research community with top-notch research accompanied by other insightful features and commentary.

Subscribe Today!

Don't miss an issue. Sign up for a new institutional subscription, or renew your university's site license so all your students and colleagues can take advantage of *Science Signaling*.

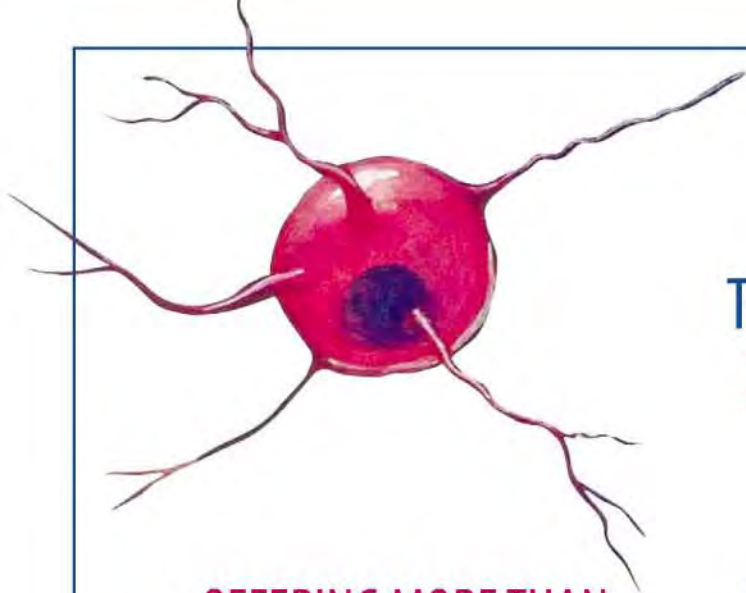
For a free trial go to: www.sciencemag.org/cgi/recommend_subscription

www.ScienceSignaling.org

* Formerly known as *Science's* STKE

Science Signaling





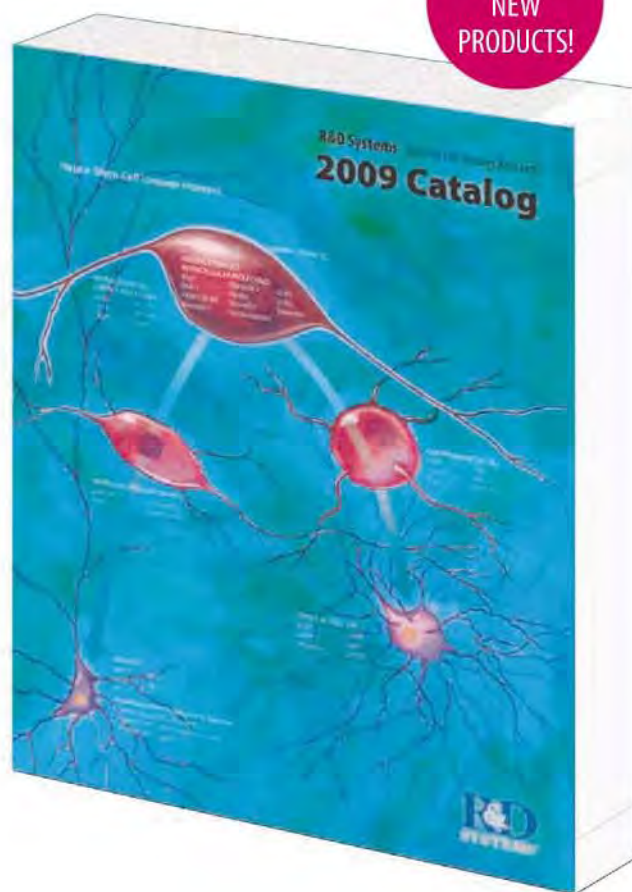
**OFFERING MORE THAN
15,000
QUALITY PRODUCTS
for Cell Biology Research.**

R&D Systems is a leading supplier of cell biology reagents with over 20 years of experience serving the research community. More than 97% of the products supplied by R&D Systems are developed and manufactured at our own facilities. This enables us to maintain strict manufacturing and quality control standards, ensuring that our reagents meet the high levels of performance and consistency expected by our customers.

Request a catalog online:
www.RnDSystems.com/go/Catalog

R&D Systems **Tools for Cell Biology Research™** **2009 Catalog Available Now!**

**OVER 2,000
NEW
PRODUCTS!**



Cancer • Endocrinology • Immunology • Proteases • Neuroscience
Development • Stem Cells • Signal Transduction • Glycobiology

R&D Systems Tools for Cell Biology Research™

USA & Canada R&D Systems, Inc. Tel: (800) 343-7475 info@RnDSystems.com

Europe R&D Systems Europe, Ltd. Tel: +44 (0)1235 529449 info@RnDSystems.co.uk

Selection expanding weekly—visit www.RnDSystems.com/go/request to sign up for weekly new product updates.

